NIRS - M -218

Proceedings of

NIRS-ETOILE

Joint Symposium 2009 on Carbon Ion Radiotherapy

March 16 and 17, 2009

Centre ETOILE, Lyon-France

Organized by

NIRS

National Institute

of Radiological Sciences, Japan

and

Centre ETOILE

Centre National d' Hadronthérapie

par Ions Carbone, France

Chair organizers

H. Tsujii, NIRS & J. Balosso, ETOILE

NIRS-ETOILE Joint Symposium on Carbon Ion Radiotherapy

March 16 - 17, 2009

Valpré-1, chemin de Chalin-69131 Lyon/Ecully-France

Organized by

National Institute of Radiological Sciences, Japan

and

Centre ETOILE, France

NIRS-ETOILE Joint Symposium on Carbon Ion Radiotherapy
Program

Monday, March 16, 2009

Opening remarks

8:30	ETOILE, a national center in Rhône-Alpes	Officials
	Opening remarks by NIRS group	H. Tsujii
	Greetings	Embassy of Japan

Present status of ETOILE project and other plans (Chair : J. Balosso, H. Tsujii)

9:00	Present status of ETOILE Centre development	J. Balosso
9:20	Brief introduction of plans in Japan	H. Tsujii
9:40	ENLIGHT and related programme for carbon ion therapy development	M. Dosanjh
10:00	General discussion	
10:20	Coffee break	

Clinical Experiences at NIRS (Chair: P. Pommier, T. Kamada)

10:45	Overview of the National Institute of Radiological Sciences	S. Ban
10:55	Overview of the carbon ion therapy at HIMAC	H.Tsujii
11:25	Discussion	
11:35	Skull Base Tumor	A. Hasegawa
11:50	Discussion	
12:10	Lunch	
13:40	Head & Neck Tumor	J. Mizoe
13:55	Lung Cancer	N. Yamamoto
14:10	Bone & Soft Tissue Sarcoma	T. Kamada
14:25	Discussion	
14:40	Hepatoma	H. Kato
14:55	Rectal Cancer	S. Yamada
15:10	Pancreas Cancer	H. Imada
15:25	Discussion	
15:40	Coffee break	
16:10	Uterine Cancer	S. Kato
16:25	Prostate Cancer	H. Tsuji
16:40	Discussion	

General Discussion About Particle Clinical Study (Chair : J. Balosso, H. Tsujii)

16:55	HIMAC way	T. Kamada
17:15	ETOILE way	P. Pommier
17:30	GSI delayed results and HIT way	S. Combs
17:50	Discussion	
	Off session discussion about ETOILE-NIRS cooperation	
19:00	End	

Tuesday, March 17, 2009

	Ion Beam Biology (Chair: JM Moreau and R. Okayasu)	
8:30	Radiobiology for a chordoma cell line UCH1	T. Kato
8:45	Molecular mechanisms of tumor cell radioresistance	C. Rodriguez-Lafrasse
9:00	The mechanism behind the effective cell killing by high LET heavy ion irradiation	R. Okayasu
9:15	Discussion	
9:30	Biological effectiveness of mammalian cells exposed to heavy ion beams	Y. Furusawa
9:45	Modelization of the RBE: difficulties and needs for a new model	M. Beuve
10:00	Discussion	
10:15	Coffee break	
	Ion Beam Physics (Chair: JM Lagniel and K. Noda)	
10:45	Current status of treatment delivery at HIMAC	M.Torikoshi
11:05	The project of new treatment facility at HIMAC	K. Noda
11:20	Cryogenic gantry: which problems remain to be solved	F. Kircher
11:35	Discussion	
11:50	New modalities of real-time contrôle imaging for ion therapy	D. Dauvergne
12:05	Analysis of moving target	S. Mori
12:30	Discussion	
12:35	Lunch	
	New Facilities (Chair: M. Dosanjh and J. Mizoe)	
14.05	News from Gunma project - Gunma University at Maebashi	S. Yamada
14:20	News from HIT at Heidelberg	T. Haberer
14:35	News from CNAO at Pavia	S. Rossi
14:50	News from Rhön Klinikum AG - University of Marburg	P. Grübling
15:05	News from MedAustron in Wiener-Neustadt	R. Mayer
15:20	Kiel: advance of a complehensive project of radiotherapy and hadrontherpy	R. Kampf
15:35	Discussion	
	Closing remarks	
15:50	Closing remarks	H. Tsujii
16:05	Closing remarks	J. Balosso
16:20	End	

INDEX

Preface

Carbon ion therapy for treating radioresistant cancers is presently blooming widely around the world, with an ever-increasing number of projects being proposed. Recently, USA and China have joined the group of Japanese and European (Germany and Italy) pioneers. In this field, the Japanese background of up to 14 years of clinical experience stands as the clinical base for the present development of hadrontherapy worldwide.

In France, the national project GCS-ETOILE is going forward through the successive steps of the competition for the final selection of a private partner. This decision is expected to be reached by the end of 2009. Therefore, now is the time for French radiotherapists, oncologists, physicists, researchers and hospital managers to take advantage of this joint symposium co-organized by the National Institute of Radiological Sciences in Chiba, Japan, and the GCS-ETOILE of Lyon, France, to review the present state of the art in clinical hadrontherapy.

This is the Proceedings for the NIRS-ETOILE Joint Symposium held on March 16-17, 2009 in Lyon. During this 2-day joint symposium, the first day consists of a review of the clinical experiences. Detailed presentations will be given on results of the main indications for carbon ion radiotherapy: skull base tumors, head and neck tumors, lung cancer, hepatoma, prostate cancers, bone and soft tissue sarcomas, pelvic rectal recurrences, pancreatic cancers and uterine cancers. The second day will open some cutting-edge scientific topics that will be presented by Japanese and European speakers. Then, to continue a tradition, the progress of opening centers in Germany and Italy will be also presented, along with the status of some projects.

In the present time of economic difficulties, challenging projects such as hadrontherapy centers can be exposed to severe hardship. It is therefore of the utmost importance to make the clinical and scientific results of hadrontherapy as available as possible to support critical decision-making. The major goal of this symposium is to intensify Japanese-French collaboration, and to set the course for further joint initiatives in the future development of ion-beam therapy.

We hope these Proceedings will provide you with interesting and productive information on carbon ion radiotherapy.

H. Tsujii, Chiba
J. Balosso, Lyon

Present Status of ETOILE Centre Development

Jacques Balosso
with Pascal Pommier, Guillaume Wasmer, Stéphanie Patin, Emmanuel Richard, Pauline Bordet, Patrick Gavignet, Chantal Ginestet, Marcel Bajard, Jean Michel Lagniel, Joseph Remillieux, Joël Rochat, Jean Pierre Boissel, Jean Michel Moreau, Annick Bourne-Branchu, Olivier Chapet, Yi Hu, Marie Hélène Baron-Maillot *and* Marianne Tery

GCS-ETOILE, National Center for Hadrontherapy, Lyon, France
e-mail address:jacques.balosso@centre-etoile.org
web site: www.centre-etoile.org

Abstract
The ETOILE project has speed up its development since the beginning of 2007. It gained governmental support and juridical structure as a Health Cooperation Grouping (GCS-ETOILE) with its proper management group chaired by a MD. The call for bids has been released in February 2008 in the frame of a public-private partnership. Three industrial consortia have initiated the competitive dialogue with the GCS-ETOILE in July 2008. This negotiation phase should end at the end of 2009 to give place to the signature of the contract and the launch of the building in 2010. The project is characterized by the parallel course of multiple programmes all together necessary for the final success of the project, namely: i) the application for the health authorities for the validation of the initial core indications; ii) the detail economical modelization to define in close relation with the governmental health services the level of reimbursement for the carbon ions treatments; iii) a new round of epidemiological studies to obtain a real scale figure of the recruitment, and the organization of the national network; iv) the discussion with neighbour countries to attract patients from a larger area than solely France for the early indications; v) the information and the necessary lobbying activities to ascertain the national position of the ETOILE Centre; vi) the necessary financial conditions to gain the state warranties for the loan and the financial security of the project; vii) the researches and technological development to create conditions of an active research centre beside the clinical activities.

Introduction
The ETOILE project became in 2008 the ETOILE Centre as the goal of the GCS-ETOILE, a kind of public joint structure born by the three university hospitals and the two public anti-cancer centers of the Rhône-Alpes Region. This region, having Lyon as main town, is counting about 10% of the French population and has the highest income per inhabitant. ETOILE has much originality that attract attention but that are also sources of difficulties since many questions that have to be solved have never been raised in the recent years. Its original features can be mentioned as : i) to be a unique centre for a whole country for comprehensive hadrontherapy carbon and protons with a dominant offer of carbon ions therapy; ii) to be the first GCS in France aiming at becoming a care provider operating a facilities built and run as a Private-Public Partnership; iii) to be a project that has to set up in the same time at a national scale: the recruitment network, the assessment of the clinical indications, the financial agreement for the reimbursement of the treatments, the construction of a selves standing economical balance with a unique activity after a shortest as possible growing curve; iv) to be a public medical institution managed by a team chaired by a MD which is not the rule in France; v) to be in the same time a research institution in preclinical domains and a care provider connected to the international network of

hadrontherapy centres for active clinical research. To add to the series of natural difficulties of such a project, the present economical crisis is making financial agreement even more difficult.

In this paper the main conditions of the development of the project are described.

The Tendering process and the construction previsions

The tendering process started in February 2008 when the public call for bids has been published for "the conception, the building and the running of a national centre for hadrontherapy" for France to be located in Lyon. The precise position of the future centre is shown on this nearby picture as the large blue volume behind the two modern twin's buildings. Before that point, an official launch of the project has been given by a mission letter of the French health minister in February 2007.

The first year between this event and the call for bids has been used for three important steps, namely:

- to build the juridical structure named as the Health Cooperation Grouping – ETOILE (GCS-ETOILE) and gathering its management team from the earlier members of the ETOILE Project and some new comers;
- to hire the supportive group, called APP, of technical, financial and juridical experts, independently from the members of the GCS to support the "public person" for the tendering process;
- and to fill the very detailed application for the French economy and finance minister to obtain formal clearance to deal with a Private-Public Partnership (PPP) which is considered as an outstanding procedure that needs sound arguments on the financial ground.

ETOILE construction flow-chart

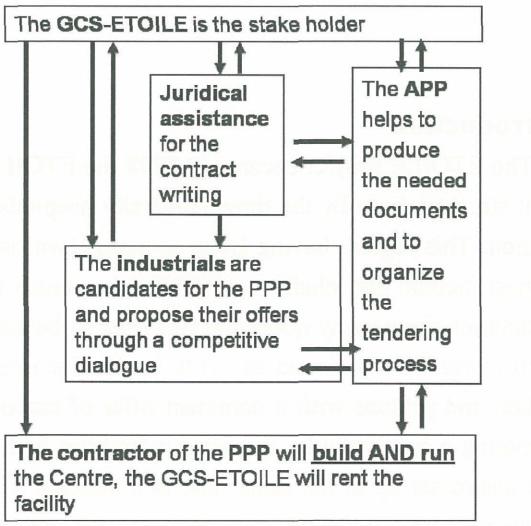

The tendering process in the frame of a PPP has to be a so called "competitive dialogue" organised in three successive rounds. During this process each candidate – consortium presents independently and confidentially its offer according to a frame that goes in deeper and extending details along the successive rounds. Each round is initiated by the release of a specific body of specifications, 2 to 3 months are given to the candidates to make their offer and then a discussion is organised between the Project Group of ETOILE with the support of its APP on one side and the representatives of the candidates in successive and independent sessions for each candidate, on the other side. After each round the GCS-ETOILE has to decide which candidate will continue for the next rounds, elimination are not necessary and all the candidates can be invited to continue for the next round. At the time of the joint symposium NIRS-ETOILE, the process will be at the verge of the discussion sessions of the second round with two of the

three initial candidates, one having retired itself although the invitation of the three candidates by the GCS-ETOILE to participate to the second round.

After the third round the remaining candidates will be invited to submit their final offer including a PPP contract project. This final offer, the only-one having a juridical definitive value, will be assessed by the General Assembly of the GCS-ETOILE and will be accepted or rejected by a formal deliberation. All the offers can be rejected through this process and the competition could end with no winner and no contract. Therefore, the competitive tense of the process is very high and the project retains a rather large uncertainty until its very end.

Hopefully a PPP contract should be signed at the beginning of 2010 then giving way to the preparation of the construction that should start at the end of 2010 giving the possibility to treat the first patients at the ETOILE Centre at the end of 2013 – beginning 2014.

The challenges to meet on the way

At the present state of the project the most important challenges are fourfold.

1. The validation of the medical value of carbon ion therapy by the High Authority for Health (HAS)

The obtaining of a reimbursement rate to make available the carbon ion therapy for any patient covered by health insurance (100% of the French citizens) needs an official recognition of the medical value of the procedure. This is an independent expertise based on a particular application that describes the medical and scientific rational along with an exhaustive review of the literature and a comparison of the results of the state of the art procedure versus the expected results of carbon ion therapy. This application will be completed in March 2009 and the results of the expertise by the HAS will be expected for the middle of the year.

This step is crucial since it is not possible to obtain sufficient support through a totally experimental approach. Therefore, the potential indications of carbon ion therapy as identified by the ETOILE medical project have been divided into two sets: i) a set of "consolidated" indications that encompass the former neutron indications and the most largely investigated indications by the NIRS and the GSI. These "consolidated" indications are therefore those having the highest probability to be readily accepted by HAS. As a whole they have a cumulated incidence of 750 cases per year in France (see the table on the next page). This number could be extended to 1000 cases by the recruitment of patients coming from neighbor countries in EU (Catalonia, Swiss, UK,...). ii) a set of "prospective" indications, more numerous (3000 to 6000 cases per year) but less investigated, will necessitate successful clinical trials to be progressively included in the first set. This second set will not be submitted to the expertise of the HAS at first but will be subject to multicentric prospective clinical trial in the frame of the Hadrontherapy centre network.

As soon as the HAS will have validate some carbon ion therapy indication, an active policy to refer French patients abroad for treatment in already working institutions will be possible.

2. The commitment of the State to support the financial risk of the project

The ETOILE Centre although being a national project, will be built far from the capital and is supported by the 5 members of the GCS which are 3 regional university hospitals and 2 anti-cancer centers that all together have not a financial base strong enough to afford the financial risk of this project. Consequently it is necessary to substitute the warranty of the State to the one of the GCS members. The GCS structure is not adapted to national project and the State has no established policy to give its warranty to such institution. It is therefore an exceptional situation that needs in the same time a strong political and administrative support that is not obvious to obtain.

Beyond the financial risk, the initial years of work when the full activity of the centre will not yet be completed, will be a particular economical burden. Once again, the size of the financial support needed, about

one hundred M€ along four to five years, is out of the possibilities of the GCS members and has to be obtained at a national level. No immediately available solutions exist to this problem either. This point needs also a persistent work out with the national authorities.

Table of the carbon ion indications of the highest priority as defined by the ETOILE medical project

Tumor site	*Detailed definition of the indications*	*Recommended hadrontherapy modality*	*Estimated incidence in France case§/yr*	*Present status of indication**
Salivary gland tumor (parotid-gland)	Unresectable tumor or refusal of surgery or R2 resection or local relapse[#]. All pathologies: adenoid cystic carcinoma, mucoepidermoid carcinoma, adenocarcinoma, acinic cell carcinoma, etc.	Carbon exclusive treatment or carbon boost to a loco-regional photontherapy	≈ 100	Consolidated priority indications for the adults[@]
Paranasal sinuses tumors	Unresectable tumor or refusal of surgery or R2- resection or local relapse. Adenocarcinoma and adenoid cystic carcinoma.	Carbon exclusive at the primitive tumor site.	≈ 250	Consolidated priority indications for the adults
Adenoid cystic carcinoma with extension to the skull base	Unresectable tumor or refusal of surgery or R2- resection or local relapse.	Carbon exclusive at the primitive tumor site.	≈ 10	Consolidated priority indications for the adults
Malignant melanoma of head and neck mucosa	All tumor sites without immediate life threatening metastasis. Tumors, if possible not resected or after R2-resection in emergency or local recurrence without previous irradiation.	Carbon exclusive at the primitive tumor site. Treatment of urgency	≈ 40	Consolidated priority indications for the adults
Chordoma of skull base, spine or sacrum	All clinical forms	Carbone or protons exclusive at the primitive tumor site	≈ 30 à 50	Consolidated priority indications for the adults
Chondrosarcoma of axial skeleton	Skull base	Proton exclusive at the primitive tumor site	≈ 20	Consolidated priority indications for the adults
	Spine and sacrum	Carbon or proton exclusive at the primitive tumor site	< 10	
Soft tissue Sarcoma (retroperitoneal sites excluded)	Low grade and M0, all pathologies, all tumor sites. Unresectable or refusal of surgery or "definitive R2 ": R2 without possible second resection or R2 after second resection or local recurrence after R2 resection.	Carbon exclusive at the primitive tumor site	≈ 100	Priority indications for the adults[£]
	Not life-threatening M+ situation with disabling T or rT.		≈ 80	Priority indications for the adults
Retroperitoneal soft-tissue sarcoma	After local relapse and second resection: "R0" or R1 and M0 (for unresectable T and R2 see previous indication).		≈ 40	Priority indications for the adults
	Initial situation: R1 M0			Prospective indication for the adults[$]
Soft tissue sarcoma of the head and neck, and of the limbs	"Definitive R1": R1 resection without acceptable second resection possibility .		≈ 200	Prospective indication for the adults
Osteosarcoma and chondrosarcoma (all sites except axial skeleton)	Unresected tumors or R2-resection, M0. M+ accepted only for the osteosarcomas. Discussion based on pathologic grade.		≈ 10	Prospective indication for the adults
Tumors of miscellaneous highly functional sites	Disabling locally invasive benign tumor and of high local recurrence potential (Desmoid tumors ...) .	Carbon exclusive	Very rare	Prospective indication for the adults

§ The *estimated annual incidence* correspond to the estimated number of total annual tumor cases that response to the detailed carbon ion indications. It is the maximal potential of recruitment that takes into account neither the feasibility nor the real offer of the treatment. France has a 62 million inhabitant's population.
* *The present status* of the indications expresses more or less the degree of the priority and the potential medical benefit based on clinical studies and the experts' opinions.
# *Local relapse* is defined as the reappearance of the tumor at the same site as the initial one without other regional or metastatic manifestation.
@ The *consolidated indications* represent the indications that either the benefice of the carbon ion have been clearly demonstrated by the clinical studies, or based on the consensual experience of neutron, or on the experts' opinions for the indications that are too rare to be tested in comparative clinical studies. Because of the known efficacy of the carbon ions in these indications, they are priorities.
£ The *priority indications for adults* without the mention 'consolidated' rely on the experts' opinions concerning these specific conditions of high radioresistance and low metastatic potential that theoretically fully justify the use of the carbon ions.
$ The prospective indications of adults correspond to the theoretical carbon ion applications without demonstrated medical evidence yet. It's often about the indications that are sufficiently frequent for future prospective clinical trials.

3. The capacity to recruit the foreseen number of patients with a steep rising curve

Since the very beginning, the patient recruitment of the ETOILE Center will be operated at the national level. The nominal capacity of the centre and the size of the population of patients according to the definition of the initial indications will definitely make possible the treatment of all the French patients having these indications. The capacity will be at the size of the target population and will permit an equal and ethical access for any patient. However, the recruitment will have to by well organized to meet its expected size and will certainly rapidly be extended to neighbor countries to afford the need of the center to reach its economical balance.

To manage the recruitment, a special organization at the national scale is established by the GCS-ETOILE which is called OMéRRIC, Medical Organization of the Recruitment for Carbon Ions Radiotherapy. This organization is based on a National Remote Multidisciplinary Consultation (NRMC), exactly as it is mandatory, at a local scale of course, for any cancer patient before definitive treatment decision in France. To establish OMéRRIC, networking activities are needed to inform the radiotherapists and to diffuse de procedure to participate to the NRMC and how to refer patients. This activity, hopefully, will start when the HAS validation will be obtained to begin to refer patients to the early operating centers, NIRS first, then the German and Italian facilities before the opening of ETOILE. A challenging point will be to maintain a close adaptation between the rising demand of treatment and the offer…

4. The convergence of the acceptable cost and the real cost of the treatments

The successful end of the tendering process will mainly rely on the level of the global cost of the operation of the center and, as a consequence, the cost of the treatments. In any case the ETOILE Centre will be able to meet its objectives, in particular its target level of activities, only if it can reach a very high productivity. The hypothesis for the activity and the calculation of the carbon ions treatments real cost are the following: about 26000 sessions of hadrontherapy (protons or carbon) per year, a rising recruitment of the "consolidated" indications of carbon ions therapy over 5 years to reach the expected 750 cases of carbon ions treatments per year for a cumulated number of about 9750 sessions per year and a complementary activity of 16250 sessions per year of protontherapy allowing to treat about 542 patients by protons (see the activity chart below in the next chapter). According to the fact that the reimbursement rate of the protons is already defined in France, these hypotheses allow to calculate the price of the carbon ions treatments.

To be accepted in the context of the public health organization in France, but it is probably true for any European country, this cost should remain in the limits of the nowadays innovative anti-cancer therapy as the targeted chemotherapy and other highly expensive procedures as bone marrow transplantation, etc. Clearly, if the economical constrains make impossible to fulfill these conditions, it will be concluded that carbon ions therapy is not mature for routine operation yet and certainly the ETOILE project will not succeed.

The buildup of clinical activities: protons and carbon ions

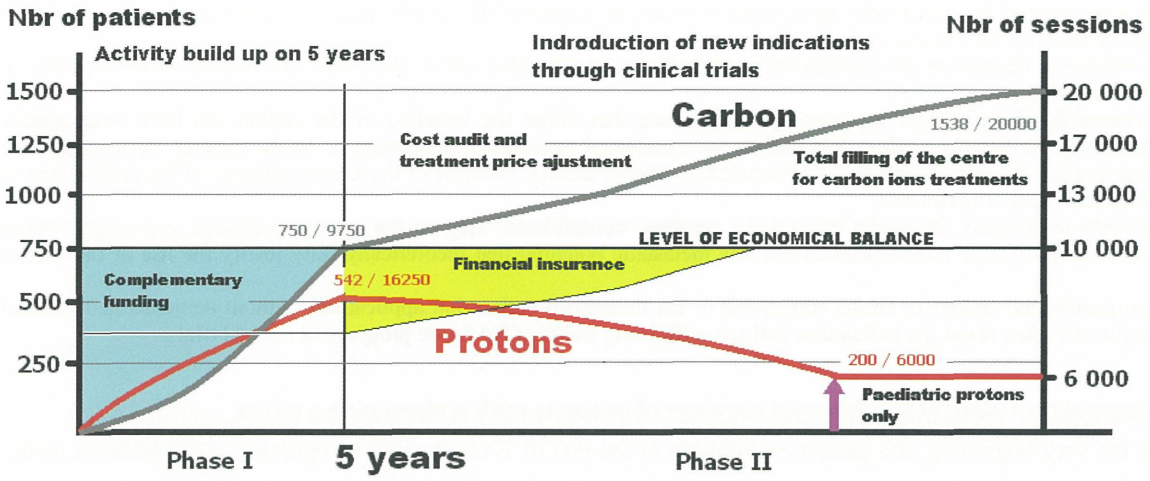

The development of the treatment activities has been modelized as represented on the above chart. This chart shows many details:

- The phase I is the phase of rising activity. It should last 5 years which is rather short if we consider that no centre in the world has reach yet the level of activity which should be reached at the end of this phase.
- The structure of the recruitment with a mixed activity of protons (in red) and carbon ions (in dark grey). The dual activity is absolutely necessary to afford an economical balance compatible with an acceptable cost of the carbon ions treatments. The number of carbon ions treatments to be reached at the end of the phase I is the total number of consolidated indications expected in France per year.
- The phase II is a slowly changing phase during which the activity of carbon ions treatment will be able to increase according to the possibilities to pay for it, either through research credits for prospective and investigative indication in the frame of clinical trials or as new validated indications. Accordingly, the protontherapy activity will decrease to be limited, at the end, to the full time use of a proton gantry for paediatric treatments.
- The State complementary funding beside the reimbursement of the treatments, are also symbolized on this chart: the supportive funding during the phase I are represented in blue and a special provision proposed for insurance purpose in case of deficit due to any reason (but mainly lack of recruitment) is represented in yellow. This provision is one aspect of the State warranty to avoid soliciting the warranty of the GCS members. Noteworthy, the protons activity is necessary during the phase I and during the phase II until carbon ions treatment could fill the whole activity of the centre. Along the same line it is easy to understand that the ETOILE Centre carbon treatments offer will remain enough for France for a number of years.
- The final reduce proton activity for children is a local characteristic of ETOILE Centre due to the local demand of one of the member of the GCS that has a large paediatric recruitment.

The scientific environment of hadrontherapy in France

The ETOILE Project, as detailed many time since its initiation in 1997, has generated a strong scientific environment with specific funding by the Region Rhône-Alpes since 2000. This development was at first closely linked to the development of the project, the same funding being used for the running of the project and for the support of the scientific researches. Many doctoral and post-doctoral positions have been financed thus. Since 2008 the two domains are clearly separated. On one hand, the researches are still supported by dedicated credits from the Region and others local public institutions as the City of Lyon and are pursuing the so called Regional

Programme of Research in Hadrontherapy (PRRH) linked since 2007 to a similar national programme (PNRH). On the other hand, the ETOILE Project, born by the GCS-ETOILE since 2007, is supported by State credits. The research teams involved in the PRRH are in every cases part of established research and teaching institutions as the University or the French Public Research Institutions as INSERM and CNRS. Outside of the medical project, proper ETOILE research teams do not exist as yet. The main topics of research developed in the frame of the hadrontherapy (PRRH) are the following:

1. The medical project

The indications, the epidemiological studies and the projects of protocols are developed under this label with a strong collaboration with the protontherapy centre in Orsay (ICPO Institute Curie - Centre de Protonthérapie d'Orsay).

2. The economic simulations

A large body of studies and simulations are developed to study the recruitment and the flux of patients in relation with the costs, the geography and the epidemiology. Some regional collaborations are specially important for this topics with specialized research teams in particular in Saint-Étienne and Roanne (CERCLH and University of Saint Etienne).

3. The in-silico modelization

It aims at predicting the therapeutic response taking into account the largest possible body of parameters. The ultimate objective is to make possible in the future an optimization of the decision to treat with carbon ion at the individual scale. The main partners for this domain are the Institute of Theoretical Medicine and its partner institutions.

4. The study of the particles generated in the target volume

Starting from the fragmentation phenomenon, this research aims at developing new principles of on line imaging modalities that could allow an immediate quality control of the irradiation in hadrontherapy (mostly carbon). These modalities are based on the positron emitters and the gamma rays generated in the target by the fragmentation process. This very innovative and important topic has given way to a national programme coordinated by the CNRS and the CEA named INNOTEP.

5. Hadron-radiobiology

The understanding of the cellular and the molecular mechanisms of the radio sensitivity and, moreover, the radioresistance in the frame of hadrontherapy are devoted to the optimization of the indication definitions, the calculation of the RBE and in the future the possibility of pharmacomodulation of the responses of the resistant tumours. These researches are developed in collaboration with teams of the GSI in Germany and of the GANIL in France. A project exists to host this research in the ETOILE building itself in the future.

6. Dosimetry and dose deposit simulation

This transdisciplinary topic aims at integrating different physical approaches into a TPS specific for carbon ion therapy.

7. Mobile target and organ motion and distortion

This topic tries to go beyond the current techniques of respiratory gating by the introduction of biomechanical models of organ motion and distortion during the time of the treatment session.

8. New principle of real time control imaging

This topic is closely related to the n°4 above since it is the technological part of the development of new tools to control in real time the quality of the irradiation by some imaging process.

9. Technological developments

Participation and stimulation of technological developments of a superconductive gantry for carbon ions and new modalities of beam control and distributions are parts of this domain along with the TPS development.

These researches are managed in collaborations with many different research teams at a national scale including the CNRS, CEA, GANIL), and could involve industrial collaborations.

Regularly, since 1999, twice a month some of the researchers of the Region Rhône-Alpes involved in these different topics are meeting for seminars. Sometimes a whole day of discussion is organized, and the following picture gathering all the GCS-ETOILE team and most of the researchers involved in the PRRH has been taken during such a meeting in spring 2008.

ETOILE in Europe and in the World

The GCS-ETOILE presently, and the ETOILE Centre in the future, has strong links with the other hadrontherapy centres in the world. First of all, of course, the pioneer centres of the new wave as the NIRS and GSI have strongly inspired the ETOILE Project. However, beyond that, ETOILE is persistently promoting the principle of the multicentric scale for decision making for indications and prospective clinical researches. In fact, the carbon ions indications, at least at the beginning, are multiple sets of small groups of patients making impossible to build evidence based conclusion outside a strong policy of multicentric assessment. European programmes as ULICE are organizing and funding this multicentric approach. A first step could be as much as possible to refer patients from France, selected through the OMéRRIC network, to the early operating centres as NIRS, HIT and CNAO. The same international approach is also true for research. The teams of the PRRH are actively collaborating in the frame of ENLIGHT++ and the PARTNER programme in the frame of the Marie Curie exchange programme.

The GCS-ETOILE is also willing to establish long way collaboration with neighbour regions and countries to welcome patients for treatment at the ETOILE Centre to consolidate its recruitment and increase the value of the prospective follow-up and clinical research for the initial indications.

Conclusion

The ETOILE Project is not any more a project with theoretical concerns, it became since beginning 2008 an emerging reality with multiple realistic challenges that make its advance an extremely complicated process that

has not yet double its no return point. The continuous development worldwide of carbon ions therapy is one of the main supports that could help ETOILE to become definitely a reality in the French landscape of public health.

Overview of Carbon Ion Radiotherapy at NIRS

Hirohiko Tsujii

National Institute of Radiological Sciences, Chiba, Japan
e-mail address: tsujii@nirs.go.jp

Abstract

The world-first clinical center offering carbon ion radiotherapy (C-ion RT) was set to open in 1994 at NIRS, Japan, using HIMAC. Among several types of ion species, carbon ions were chosen for cancer therapy because they were judged to have the most optimal properties in terms of superior physical and biological characteristics. As of January 2009, a total of 4,494 patients have been registered for C-ion RT. Clinical results have shown that C-ion RT has the potential ability to provide a sufficient dose to the tumor, together with acceptable morbidity in the surrounding normal tissues. Tumors that appear to respond favorably to carbon ions include locally advanced tumors as well as those with histologically non-squamous cell types of tumors such as adenocarcinoma, adenoid cystic carcinoma, malignant melanoma, hepatoma, and bone and soft tissue sarcoma. By taking advantage of the unique properties of carbon ions, treatment with small fractions within a short treatment period has been successfully carried out for a variety of tumors.

Introduction

The structural survey of JASTRO has demonstrated that the number of cancer patients undergoing radiotherapy (RT) has increased to a total of 150,000, an equivalent to roughly 28% of all cancer patients in Japan, with forecasts that this number will continue to rise in the future (1). In recent years, the scope of diseases that can be treated with RT has significantly widened in the wake of the diffusion of high precision RT such as stereotactic RT (SRT), intensity-modulated RT (IMRT) and particle beam RT. These approaches permit sparing of normal tissues and administration of a curative dose to the tumor. In this regard, charged particles like protons and carbon ions have come to be clinically effective since R. Wilson first proposed their clinical application in 1946 (2). In the early 1950s, the clinical use of proton beams was initiated at the Lawrence Berkeley National Laboratory (LBNL), paving the way for heavy ion RT starting at the same facility in the 1970s (3-4). At present, particle beam RT is provided at over 20 facilities worldwide, and still many more are under construction or in the planning stage.

In Japan, the decision was made in 1984 to build the Heavy Ion Medical Accelerator in Chiba (HIMAC) at the National Institute of Radiological Sciences (NIRS) as an integral part of the nation's "Overall Ten-year Anti-Cancer Strategy". The accelerator complex took almost a decade to build, being completed by the end of 1993 (Fig. 1). A year later, clinical study with carbon ions for cancer therapy was initiated. Similar to the proton accelerator built at the Loma Linda University in 1990 as the first proton beam accelerator put primarily into therapeutic service, HIMAC can claim to be the world's first facility dedicated to cancer therapy using carbon ion beams. HIMAC has also been operated as a multipurpose facility available for joint use for both cancer treatment, biological research and physical research.

This article reviews the clinical aspects of C-ion RT over the last decade at NIRS.

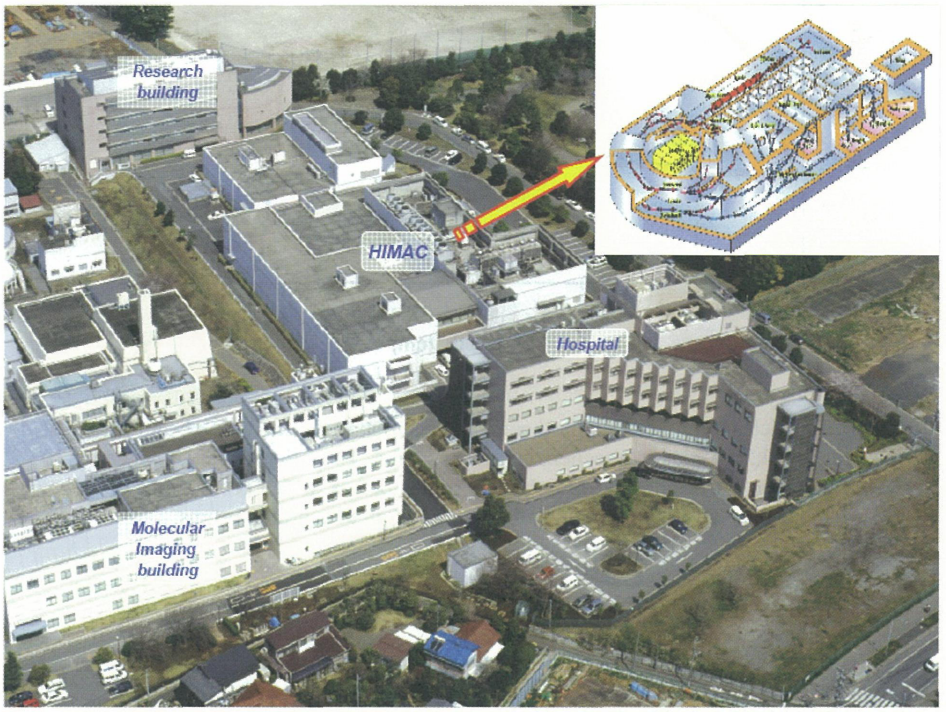

Fig. 1 The HIMAC facility at NIRS.

Characteristics of Carbon Ion Beams

Unlike X-rays, which deposit most of their energy near the skin's surface, carbon ion beams are more effective on tumors in deeper tissues. The particles release the bulk of their energy as they slow down in the last few millimeters of their track, a point called the Bragg peak. The beams also scatter very little, allowing the maximum radiation dose to be precisely targeted to the tumor, thus minimizing damage to surrounding healthy tissues.

Carbon ions also cause a different type of cellular damage from protons and photons, delivering a larger mean energy per unit length (Linear Energy Transfer: LET) of their trajectory in the body (5-7). Carbon ions directly cleave double-stranded DNA at multiple sites without the need for oxygen, so they can tackle hypoxic parts of tumors that are resistant to RT. As a result, carbon ion beams are described as a high-LET radiation similarly to neutron beams. However, in contrast to neutron beams, whose LET remains uniform at any depth in the body, the LET of carbon ion beams increases steadily from the point of incidence in the body with increasing depth to reach a maximum in the peak region (Fig.2). This property is extremely advantageous from a therapeutic viewpoint in terms of biological effect on the tumor. The reason is that carbon ion beams form a large peak in the body, as the physical dose and consequently their biological effectiveness increase as they advance to the more deep-lying parts of the body. This has opened up the promising potential of their highly effective use in the treatment of intractable cancers that are resistant to photon beams.

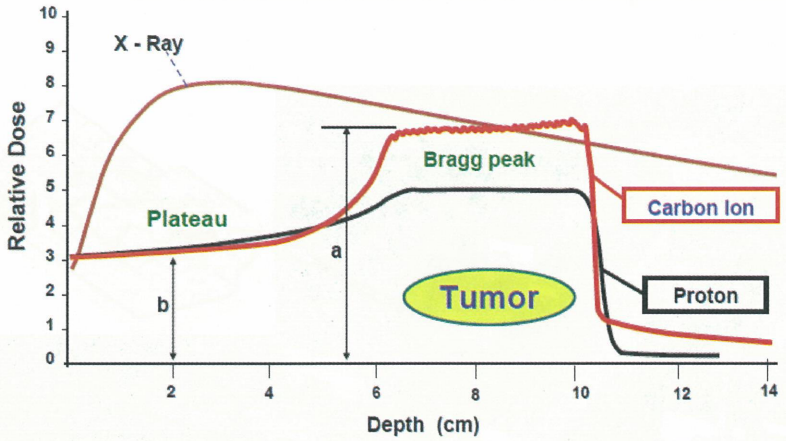

Fig. 2
Charged particles have well-localized energy deposition at the end of the beam path, called the Bragg peak, resulting in excellent dose distribution. The ratio of peak to plateau (a/b) of RBE for carbon ion beams is greater than for proton beams, which is one of the reasons why carbon ion beams have more excellent dose distribution than proton beams.

Carbon Ion Radiotherapy at NIRS

1. Organization for performance of C-ion RT

Consistent efforts have been made from the start to provide C-ion RT on an ethically and scientifically sound basis under the investigative control of Committees headed by the Carbon Ion Radiotherapy Network Committee as the supreme organ. All clinical protocols have been prepared by the Disease-specific Committees, checked by the Ethical Committee, and finally approved by the Network Committee. The Review Committee is appointed to deliberate on the validity of whether individual clinical trials should be continued, and the results of all clinical trials are submitted to the Network Committee whose sessions are invariably held in public.

In November 2003, the Ministry of Health, Labour and Welfare in Japan approved C-ion RT as "Highly Advanced Medical Technology (HAMT)" under the title of "C-ion RT for Solid Cancer". HAMT is designed to respond to the development of new medical technologies and to meet the diversifying needs for advanced treatment. It permits Specific Medical Institutions under the National Health Insurance System to offer advanced medical treatment, thereby enabling them to practice both general and advanced medical treatment within the National Health Insurance System. Under this scheme, care providers are able to charge their patients a special fee for advanced treatment in addition to the ordinary personal share of the medical fee payable by the patient himself under the National Health Insurance System. The treatment fees for HAMT were calculated on the basis of the incidental cost factors, including the construction costs of HIMAC, personnel costs, costs for the materials used for treatment, accelerator operating costs (water, electricity, lighting, etc.) and the expenditures for maintenance and management of running the facility.

2. Patients and treatment techniques

1) Patient characteristics

C-ion RT at NIRS was initiated in June 1994. Up to the present, more than 50 protocols have been established, and phase I/II and II trials have been conducted in an attempt to determine the optimal dose-fractionations and irradiation techniques for each specific tumor (8-11). The number of patients has increased year-by-year, and the facility has meanwhile reached a capacity permitting around 700 patients to be treated each year (Fig. 3). The registration of patients has reached a total of 4,494 (4,717 lesions) as of January

2009 (Fig. 4). The categories of disease which can be treated in the HAMT scheme include skul base tumor, head and neck cancer, lung cancer, prostate cancer, bone and soft-tissue sarcoma, liver cancer, pelvic recurrences of rectal cancer, and uveal melanoma.

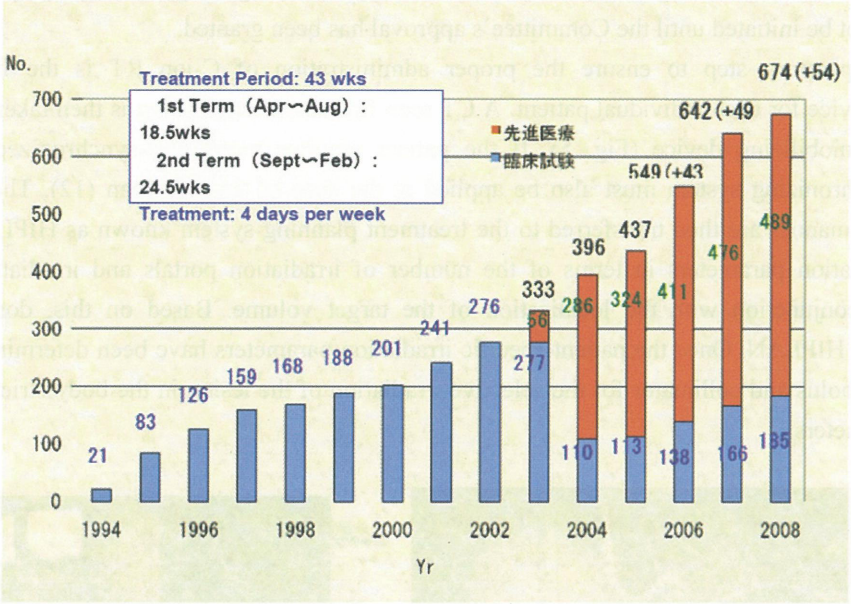

Fig. 3
Annual number of patients treated with carbon ion radiotherapy at NIRS (0994.6.21 – 2009.1.31).
Dark bars indicate the patients treated under HAMT, and the light bars the patients treated in clinical trials.

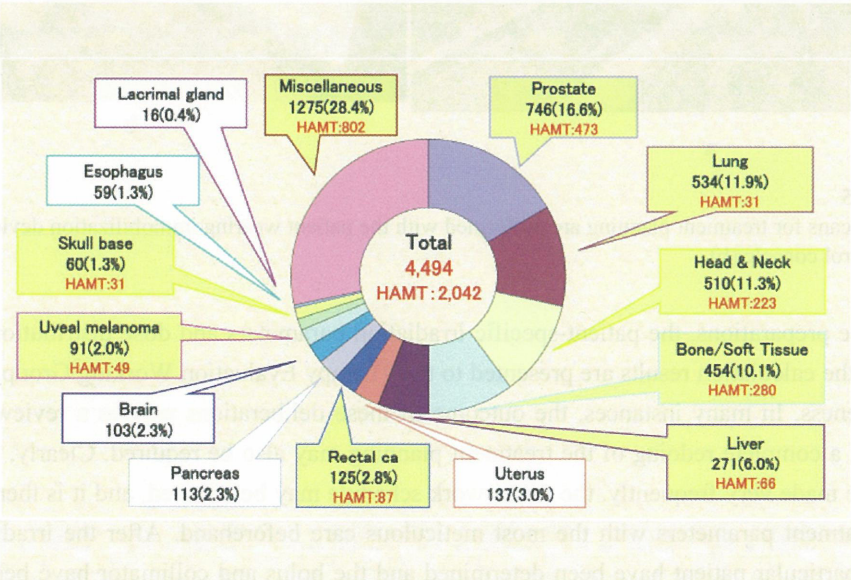

Fig. 4
Distribution of tumor sites treated with carbon ion RT from June 21, 1994 to January 31, 2009. HAMT: Highly Advanced Medical Technology.

2) Irradiation techniques

When the patient is referred to our institute, a preliminary screening process takes place to determine whether or not the particular patient is eligible for C-ion RT under any of the disease-specific protocols. This requires

close coordination and consultation with the referring physician. When the decision has been reached that the criteria for patient eligibility are met, the patient is provided with detailed explanations about the possible side effects of treatment and the prospect of the therapeutic outcome in order to obtain the patient's informed consent. The signed consent form is then submitted to the Ethics Committee together with all other necessary documentation. The Committee thereupon deliberates on patient eligibility, and the preparatory steps for treatment will not be initiated until the Committee's approval has been granted.

The first preparatory step to ensure the proper administration of C-ion RT is the fabrication of an immobilizing device for each individual patient. A CT scan for treatment planning is then taken with the patient wearing the immobilizing device (Fig. 5). If the patient requires respiration-synchronized irradiation, the respiration synchronizing system must also be applied at the time of this CT scan (12). The CT image data obtained in this manner are then transferred to the treatment planning system known as HIPLAN (13). At this stage, the irradiation parameters in terms of the number of irradiation portals and irradiation direction are determined in conjunction with the localization of the target volume. Based on this, dose distribution is calculated using HIPLAN. Once the patient-specific irradiation parameters have been determined, the next step is to design the bolus and collimator for the selective irradiation of the lesion in the body strictly in accordance with these parameters.

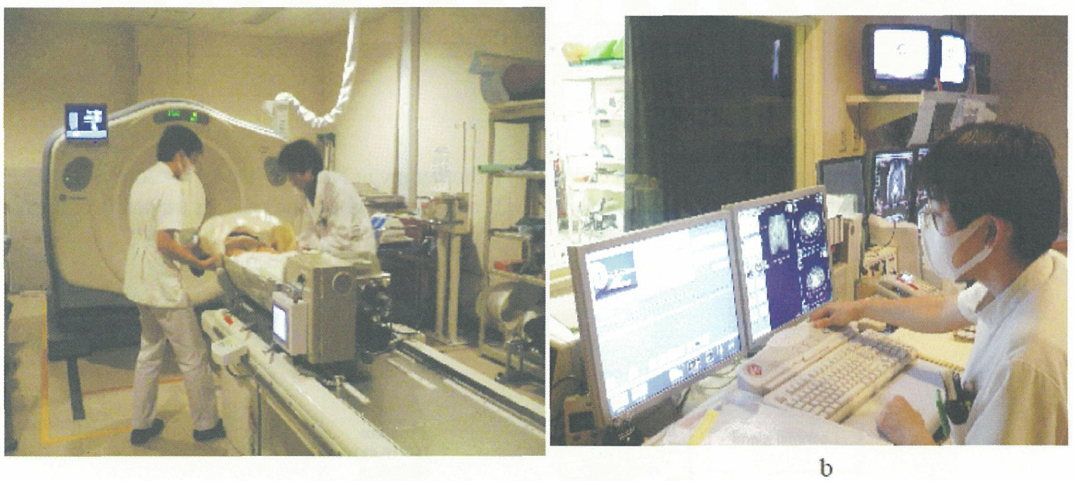

a b

Fig. 5
CT scans for treatment planning are performed with the patient wearing immobilization devices (a). Control console (b).

Based on these preparations, the patient-specific irradiation parameters and dose distribution have now been determined and the calculation results are presented to the Therapy Evaluation Working Group, which examines their appropriateness. In many instances, the outcome of these deliberations will be a review request, and on many occasions, a complete redoing of the treatment planning may also be required. Clearly, if such review or redo requests are made very frequently, the entire work schedule may be affected, and it is therefore essential to examine the treatment parameters with the most meticulous care beforehand. After the irradiation parameters applicable to a particular patient have been determined and the bolus and collimator have been fabricated, the final preparations for therapy can now take place by measuring the radiation dose under the same conditions as for the actual RT session and carrying out a mockup rehearsal, followed by delivery of irradiation (Fig. 6).

Fig. 6 Treatment room

3) Dose prescription

In C-ion RT it is necessary to spread out the narrow peak to fit the target volume. Metal ridge filters are used for producing the spread-out Bragg peak (SOBP), and the shape of the spread-out peak has to be designed so that the tumor cells will be sterilized uniformly within the peak. The practice is to use HSG cells, which are parotid cancer cells, as substitutes of the tumor cells, to design the dose distribution in such a manner that they will be killed uniformly in the spread-out peak (14-15). The dose is indicated in GyE, a unit calculated by multiplying the physical carbon ion dose with the RBE value so as to permit its comparison with photon beams: GyE = Physical dose x RBE. It should be pointed out here that the RBE of the carbon ion beams used for RT is 3.0 at the distal part of the SOBP. This value is identical to the RBE determined for the neutron beam RT previously provided at NIRS (15).

As biological dose distribution is flat within SOBP, once the RBE values have been determined at a given position, they are easily calculated at any position by dividing the biological dose by the physical dose. RBE of carbon ions was estimated to be 2.0∽3.0 along SOBP for acute skin reactions. As seen in Fig. 7, a clinical dose of 2.7 Gy (E) would be given at any position within SOBP; for example, a physical dose of 0.9 Gy carbon ions at the 8-mm upstream position would give an RBE value of 2.7/0.9 = 3.0, whereas 1.13 Gy at the middle of SOBP should bring an RBE value of 2.7/1.13 = 2.4.

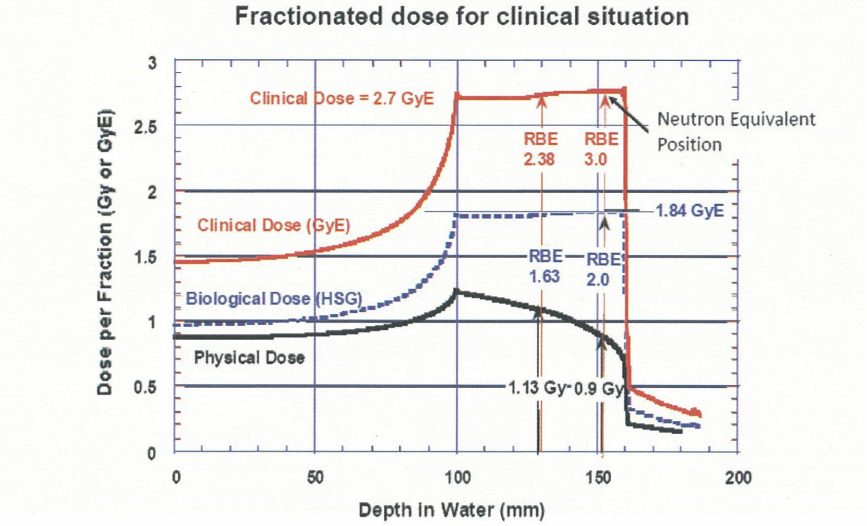

Fig. 7
Experimental and clinical RBE of 290 MeV/u carbon-ion beams with a 6-cm SOBP.

4) Dose fractionation

C-ion RT at NIRS is available four days a week (Tuesday through Friday). In recent years, Monday has become available on a once-a-month basis for tumors treatable in a single fraction, and this also facilitated an increase in the annual patient number load. HIMAC is in principle closed for therapy on weekends as well as on Mondays, when the accelerator is subjected to maintenance or is used for physical-biological experiments.

The radiotherapeutic approach of our treatment has been to fix both the total number of fractions and the overall treatment time for each tumor. In dose escalation studies, we escalated the dose in incremental steps of 5 or 10% at a time. After the recommended dose thus became established in phase I/II trials, the transition to phase II trials was made. Supposing that a fractionation regimen of 16 fractions spread over four weeks had been selected and that a total dose of 57.6 GyE had been increased by 5% to 60.5 GyE, this would have meant that the single-fraction dose would have been stepped up from 3.6 GyE to 3.8 GyE, in light of the fact that the irradiation time and fraction number had been fixed. Once the recommended dose resulting from the dose escalation trial has been decided, phase II trials or Advanced Therapy can then be initiated with this recommended dose.

In view of the unique physical and biological properties of carbon ions, it is theoretically possible to perform hypofractionated RT consisting of only a few irradiation sessions. In contrast, experiments with neutron beams that have the same high-LET components as carbon beams have demonstrated that increasing their fraction dose tended to lower the RBE for both the tumor and normal tissues. In these experiments, however, RBE for normal tissues does not decrease as rapidly as that for the tumor (16). This experimental result substantiates the previous observation that the therapeutic ratio increases rather than decreases even though the fraction dose is increased. Similar results have also been obtained in experiments conducted with carbon ion beams at NIRS (17-18). They have provided biological evidence for the validity of the short-course hypofractionated regimen with C-ion RT.

5) Results of treatment by tumor type

As stated above, carbon ion beams have a therapeutically favorable biological dose distribution. Utilizing these properties makes it possible to complete the therapy in a short time. As is seen in Table 1, progress in dose escalation has already been made on a scale that permits the RT course for stage I lung cancer and liver cancer to be completed in 1 or 2 irradiation sessions, respectively. Even for prostate cancer and bone and soft tissue tumors that require a relatively prolonged irradiation time, it is possible to accomplish the treatment course with carbon ion beams in 16 fractions over 4 weeks, only half the fraction number and time required for x-ray and proton beam therapy. At present, the average number of fractions and the treatment time per patient is 13.5 fractions and 3.5 weeks, respectively. As shown in Fig. 3, the number of registered patients has been steadily increasing year after year. Apart from the fact that the irradiation methods have been firmly established and therapy can be administered without difficulty, this may be ascribed to the significant shortening in the number of fractions and overall treatment time per patient.

Table 1. Dose-Fractionation employed in Carbon ion RT at NIRS

Site		GyE / Fr./ Wk	GyE / fr	BED (α/β=10)	BED (α/β=2.5)
Head & Neck	Adenoca, ACC, MMM	57.6 / 16 / 4	3.6	78.3	140.5
	Sarcoma	70.4 / 16 / 4	4.4	101.4	194.3
Skull base	Chordoma & Chondrosarcoma	57.6 / 16 / 4	3.6	78.3	140.5
Lung	Peripheral	60.0 / 4 / 1	15.0	150.0	420.0
		46.0 / 1 / 1dy	-	-	-
Lung	: Mediastinum	48.0 / 12 / 3	4.0	67.2	124.8
	Hilar : Superficial	54.0 / 9 / 3	6.0	86.4	183.6
	: Bulky	68.4 / 12 / 3	5.7	107.4	224.4
Liver	Hepatocellular ca	42.8 / 2 / 2dys	21.4	134.4	409.2
	Metastasis of Rectal ca	46.0 / 1 / 1dy	-	-	-
Bone & soft tissue	sarcoma	70.4/ 16 / 4	4.4	101.4	193.4
Prostate	Low/Medium/High risk	57.6 /16/ 4	3.6	78.3	140.5
Pancreas	Pre-operative RT	35.2 / 8 / 2	4.4	50.7	97.2
	C-ion+ CDDP 1000mg/m²	45.6 / 12 / 3	3.8	62.9	114.9
Rectum	Post-ope pelvic rec.	73.6 / 16 / 4	4.6	107.5	209.0

Our experience to-date can be summed up by characterizing C-ion RT as follows: 1) By location, it is effective in tumors of the head and neck (including the eye), the base of the skull, lung, liver, prostate, bone and soft tissue, and pelvic recurrence of rectal cancer. 2) By pathological type, it is effective against pathologically non-squamous cell types of tumors for which photon beams are little effective, including adenocarcinoma, adenoid cystic carcinoma, hepatocellular carcinoma, and sarcomas (malignant melanoma, bone and soft-tissue sarcoma, etc.). For certain cancers such as malignant melanoma of the head and neck, it was important to develop methods for preventing distant metastasis so as to improve the survival rate still further. In this context, C-ion RT combined with chemotherapy has been initiated. For intractable cancers such as malignant glioma, cancer of the pancreas, uterine cancer and esophageal cancer, it is necessary to further improve therapeutic outcomes. To this end, clinical trials are being continued.

In terms of toxic reactions (side effects), significant progress has been made, as the toxicities initially associated with dose escalation such as ulceration and perforation of the gastrointestinal tract requiring surgery are no longer encountered in the wake of improvements in irradiation techniques.

The details of the treatment for each tumor are described in the subsequent pages in this volume of the Proceedings.

Summary

The promising aspect of C-ion RT for the treatment of cancer lies in its superior biological dose distribution that makes the carbon ion beam the best-balanced particle beam available. Thus, comparison of the ratio of RBE in the peak region against RBE in the plateau region shows that, of all heavy ion beams, carbon ion beams have the most favorable value.

In the middle of 2009, C-ion RT will reach its 15th anniversary at NIRS. So far, with the support of the many members concerned both inside and outside the Institute, a substantial amount of evidence has been accumulated in terms of the safety and efficacy of C-ion RT for various types of malignant tumors. One of the most important objectives in these endeavors has been to determine, in particular, the validity and limits of hypofractionated, accelerated RT. Furthermore, at the end of 2003, the Institute was successful in obtaining approval for the Highly Advanced Medical Technology (HAMT) from the government. This was an important landmark for widening the scope of diseases corresponding to C-ion RT. In this manner, C-ion RT has meanwhile won for itself a solid place in general medical practice, with the next target being that of obtaining approval for this therapy to be included in general practice under the National Health Insurance scheme.

References

[1] Shibuya H, Tsujii H: The structural characteristics of radiation oncology in Japan in 2003, 27 April 2005. Int J Radiat Oncol Biol Phys. 62: 1472-1476, 2005.

[2] Wilson RR: Radiological use of fast protons. Radiology. 47:487-491, 1946.

[3] Linstadt DE, Castro JR, Phillips TL: Neon ion radiotherapy: results of the phase I/II clinical trial. Int J Radiat Oncol Biol Phys. 20:761-769,1991.

[4] Castro JR: Future research strategy for heavy ion radiotherapy. Progress in Radio-Oncology. (ed. Kogelnik HD), Monduzzi Editore, Italy, pp643-648, 1995.

[5] Raju MR: Heavy particle radiotherapy. Academic Press, New York, 1980.

[6] Chen GTY, Castro JR, Quivey JM: Heavy charged particle radiotherapy. Ann Rev Biophys Bioeng. 10: 499-529, 1981.

[7] Kraft G: Tumor therapy with heavy charged particles. Prog Part Nucl Phys. 45: S473-S544, 2000.

[8] Tsujii H, Morita S, Miyamoto T, et al: Preliminary results of phase I/II carbon-ion therapy at the NIRS. J Brachytherapy Int. 13: 1-8, 1997.

[9] Tsujii H, Mizoe J, Kamada T, et al: Overview of clinical experiences on carbon ion radiotherapy at NIRS. Radiother Oncol. 73(Suppl 2): S41-S49, 2004.

[10] Tsujii H, Mizoe J, Kamada T, et al: Clinical results of carbon ion radiotherapy at NIRS. J Radiat Res. 48 (Suppl A): A1–13, 2007

[11] Tsujii H, Kamada T, Baba M, et al: Clinical advantages of carbon-ion radiotherapy. New J Phys. 10: 1367-2630, 2008.

[12] Minohara S, Kanai T, Endo M, et al: Respiratory gated irradiation system for heavy-ion radiotherapy. Int J Radiat Oncol Biol Phys. 47: 1097-1103, 2000.

[13] Endo M, Koyama-Ito H, Minohara S, et al: HIPLAN - a heavy ion treatment planning system at HIMAC. J Jpn Soc Ther Radiol Oncol. 8: 231-238, 1996.

[14] Kanai T, Furusawa Y, Fukutsu K, et al: Irradiation of mixed beam and design of spread-out bragg peak for heavy-ion radiotherapy. Rad Res. 147: 78-85, 1997.

[15] Kanai T, Endo M, Minohara S, et al: Biophysical characteristics of HIMAC clinical irradiation system for heavy-ion radiation therapy. Int J Radiat Oncol Biol Phys. 44: 201-210, 1999.

[16] Denekamp J, Waites T, Fowler JF: Predicting realistic RBE values for clinically relevant radiotherapy schedules. Int J Radiat Biol. 71: 681-694, 1997.

[17] Koike S, Ando K, Uzawa A, et al: Significance of fractionated irradiation for the biological therapeutic gain of carbon ions. Radiat Prot Dos. 99: 405-408, 2002.
[18] Ando K, Koike S, Uzawa A, et al: Biological gain of carbon-ion radiotherapy for the early response of tumor growth delay and against early response of skin reaction in mice. J Radiat Res. 46:51-57, 2005.

Overview of the National Institute of Radiological Sciences

Sadayuki Ban

Planning and Management Office, Research Center for Charged Particle Therapy,
Planning Office, International Open Laboratory,National Institute of Radiological Sciences, Chiba, Japan
e-mail address: s_ban@nirs.go.jp

Introduction

The National Institute of Radiological Sciences (NIRS) was founded in 1957 as a national research institute under the auspices of the Science and Technology Agency of Japan, and so 2007 was its 50th anniversary.
In April 2001, NIRS became an independent administrative institution, to provide more flexible, high-quality administrative services, and started the first 5-year plan. After the successful first 5-year plan, the organization of NIRS was restructured again in April 2006, and the second 5-year plan for the promotion and development of research was initiated.

Missions

The missions of NIRS are as follows:

(1) Advancing cancer radiotherapy technology
(2) Enhancing radiation safety
(3) Establishing a system to address potential exposure accidents
(4) Domestic and international cooperation and exchanges
(5) Disseminating research results and developing human resource

With these missions, NIRS has conducted a wide range of radiation life-scientific research, from molecular to mammalian and from basic to clinical levels.

Summary of the second 5-year plan

NIRS was reorganized, adopting a more flexible personnel system, in April 2006. NIRS has established four research centers (Research Center for Charged Particle Therapy, Molecular Imaging Center, Research Center for Radiation Protection, and Research Center for Radiation Emergency Medicine). Further, NIRS contains one center that provides administration and support for the total activities of the institute. **The Fundamental Technology Center** performs advanced research and development necessary for the support of NIRS activities. Radiation generators and the quality of radiation fields are maintained by this center. Also, research and development on advanced irradiation technologies and dosimetry technologies are performed by this center. NIRS has many highly advanced facilities that comprise the core for promoting comprehensive research on radiation effects on human health and welfare in Japan. Those include HIMAC, which provides a stable supply of charged particle beams for cancer therapy, the Electrostatic Facilities, which employ a single-particle system for living cells *in vitro*, the Radon Facilities, which have radon measuring systems, and the Low Dose Radiation Effects Research Building. These facilities have been used for joint research with both domestic and overseas research institutions.

In November 2008, the International Open Laboratory was established to promote advanced research at an international level.

(1) Advancing cancer radiotherapy technology:

High LET radiation therapies were found to be more effective against certain cancers than conventional radiation therapies such as X rays and gamma rays, but not against some other cancers. All these radiations are strong near the surface of the human body and became attenuated in deeper areas of tissues. This suggests that when a deep cancer is treated with these types of radiations, normal tissue between the surface and target receives serious damage, and the dose decreases at the tumor. As a result, NIRS has decided to promote the medical application of heavy ions, taking advantage of its accumulated research results, and constructed the world's first heavy ion medical accelerator, HIMAC (Heavy Ion Medical Accelerator in Chiba) in November 1993. **The Research Center for Charged Particle Therapy** has developed heavy-ion therapy for a variety of types of cancer. Charged particle therapy was considered an advanced technology that was designed to reduce side effects and enhance therapeutic results, and was begun in 1994. Because good therapy results were achieved and recognized, carbon-ion therapy was approved as 'Highly Advanced Medical Technology' by the Ministry of Health, Labour and Welfare in October 2003. The number of registered patients has been increased year and year, exceeding 4,000 in June 2008, and is expected to go over 5,000 in 2009.

Molecular imaging is a new field in which target tissues in the living body can be visualized from outside of the body. NIRS has made a long-term investment to establish **The Molecular Imaging Center**. This center has developed new diagnostic techniques using such as PET, SPECT, CT and MRI, as well as clinical applications for them. Main works in this center are tumor imaging studies, mainly using positron emission tomography, basic and clinical studies in patients with psychiatric and neurological diseases such as schizophrenia, depression, and dementia, development of various types of molecular probes to be used in molecular imaging studies, and fundamental and modern research on molecular imaging studies. High-quality diagnostic imaging research is a key project for heavy-ion cancer therapy. In the last year, this center proposed an epoch-making idea of OpenPET, and has constructed the machinery and facility. OpenPET has been expected to make possible conducting diagnosis and therapy simultaneously.

NIRS established **The International Open Laboratory** in November, 2008 with the purpose of creating and maintaining favorable surroundings in which young researchers may engage in advanced research at an international level, with the support of Distinguished Visiting Scientists in strategically important fields such as Radiology, Biology, Physics, Chemistry, and Engineering, thus contributing to the Institution as a whole. This laboratory consists of an Administrative Office, three Research Units, and a Management Office. The management of each unit has been committed to a distinguished foreign scientist. The laboratory has been expected to produce highly evaluated research achievements in the areas of accelerator physics and techniques, heavy ion physics and application, radiation biology and radiation oncology related to charged particle therapy, treatment planning and optimization for radiation therapy, and radiation diagnosis and techniques.

(2) Enhancing radiation safety

The safe and reliable use of radiations depends on regulation and control based on scientific evidence. **The Research Center for Radiation Protection** has investigated how radiation exists in nature and how radioactive substances act on the environments and life, and determines the quantitative relationship between radiation doses and their effects. The major works of this center are the collection and dissemination of scientific evidence about radiation hazards, the investigation of the mechanisms of radiation injury in organisms caused by low-dose radiation, and the development of methods to evaluate the effect of radiation on ecosystems using experimental ecosystems models. The goal of this center is to estimate radiation risks, evaluate low-dose effects on living things, especially on the human body, and protect the environment and life from radiation.

(3) Establishing a system to address potential exposure accidents

NIRS is positioned as a national center for radiation emergency medical preparedness in the nuclear disaster prevention system in Japan, and assumes the role of a specialized radiation emergency hospital to provide advanced radiation emergency medicine. **The Research Center for Radiation Emergency Medicine** keeps the radiation emergency medicine system on standby, and maintains the facilities and devices for emergencies. On the assumption of various radiation accidents, many works have been conducted in this center, such as the diagnosis and treatment of injuries due to radiation exposure, including internal decontamination, and establishment of methods and technologies to evaluate external and internal radiation doses rapidly and accurately in various radiation accidents.

(4) Domestic and international cooperation and exchanges

NIRS promotes cooperation and exchanges with domestic institutes and universities and contributes to scientific and technical cooperation.

Also, NIRS promotes cooperation and exchanges with international organizations and universities, contributes to technical cooperation with radiation workers in developing countries, and makes proposals to the world for the reduction of radiation risks and the peaceful use of radiation (Fig. 1).

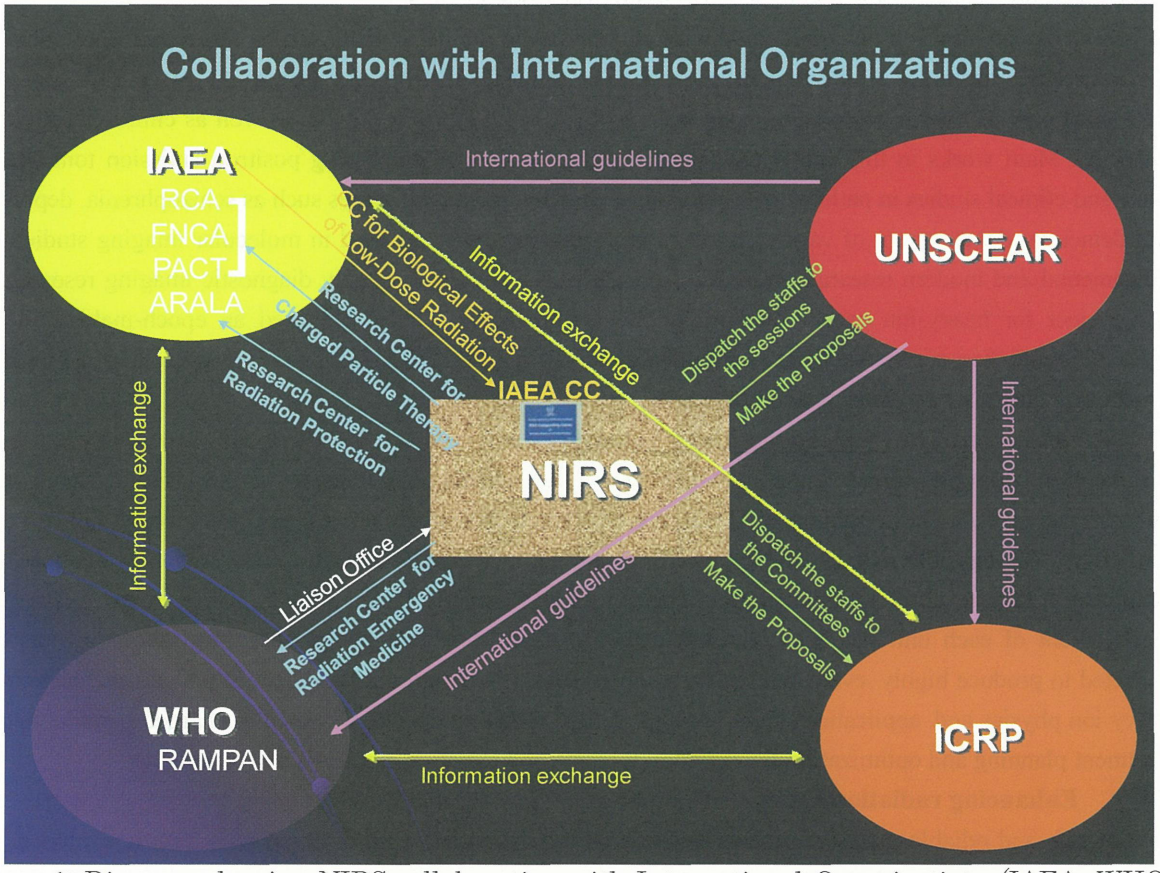

Figure 1: Diagram showing NIRS collaboration with International Organizations (IAEA, WHO, UNSCEAR and ICRP). Through international cooperation and exchanges, NIRS promotes the peaceful use of radiation for the health and welfare of human beings of the world.

NIRS dispatches many of its personnel to the United Nations Scientific Committee on the Effects of Atomic Radiation (UNSCEAR), and to the International Commission on Radiological Protection (ICRP), and makes proposals to these organizations so as to contribute to the development of international guidelines on risk estimation and radiation protection. NIRS has contributed to various activities of the International Atomic Energy Agency (IAEA) in sending the experts to the Regional Cooperative and Training Related to Nuclear

Science and Technology in the Asian Pacific Region (RCA), Forum for Nuclear Cooperation in Asia (FNCA), the Program of Action for Cancer Therapy (PACT), and the As Low As Reasonably Achievable Network (ARALA Network), as well as holding conferences for these organizations. NIRS has also sent experts to the World Health Organization (WHO) and the Nuclear Energy Agency of the Organization for Economic Cooperation and Development (OECD/NEA). NIRS also organizes many international conferences and training courses with the aim of promoting research exchanges and technical cooperation with developing countries. As a result of these activities, in January 2006, NIRS was designated as an IAEA Collaborating Center on the biological effects of low-dose radiation. NIRS has also reached joint-research agreements with a number of overseas research institutes and universities.

(5) Disseminating research results and developing human resources

NIRS gives training sessions in radiation protection and safety to medical workers, disaster prevention workers, researchers and technicians involved in radiation-related work. The training courses are designed with input from instructors both inside and outside NIRS, as well as from external experts, and the content is based on the results of research and development. More than 10,000 persons have received this training and now actively support the safe use of radiation and play a vital role in radiation protection throughout Japan. Also, NIRS provides "Courses for Schoolteachers" and "Informative Seminars" for the general public, aiming at a "More Open Institution". For these purposes, NIRS organizes a "Scientific Camp" of four days and three nights for high-school students and higher professional school students, and a "Super-Science High-School Field Study" for those high-school students taking courses in mathematics, science and technology.

Closing

NIRS is dedicated to the study of comprehensive research and development of radiation-related sciences. Through international and domestic cooperation and exchanges for the peaceful use of radiation, NIRS will contribute to the health and welfare of human beings.

Carbon Ion Radiotherapy for Central Nervous System Tumors

Azusa Hasegawa, Jun-etsu Mizoe, Keiichi Jingu, Hiroki Bessho, Yoshido Kakimoto,
Tadashi Kamada, and Hirohiko Tsujii

Hospital, Research Center for Charged Particle Therapy, National Institute of Radiological Sciences, Chiba, Japan.
E-mail: azusa@nirs.go.jp, j_mizoe@nirs.go.jp

Abstract

To estimate the toxicity and efficacy of a phase I/II or phase II clinical trial for patients with central nervous system (CNS) tumor treated with carbon ion radiotherapy.

One of 2 phase I/II clinical trial for brain tumor was carried out from October 1994 to February 2002, and the diseases treated were low-grade astrocytoma (WHO grade 2), malignant glioma, and metastatic brain tumor. Another phase I/II clinical traial for malignant glioma was carried out from April 2002 and August 2008. A phase I/II dose escalation study for skull base and paracervical tumor was initiated in April 1997. The phase I/II dose escalation trial was performed up to the fourth-stage dose level. From April 2004, a phase II clinical trial for skull base and paracervical tumors was initiated under the Highly Advanced Medical Technology scheme with an irradiation schedule of 60.8 GyE in 16 fractions over four weeks.

At the time of analysis, there was no evidence of any serious acute or late reactions in brain and skull base and paracervical tumors. In the treatment of low-grade astrocytomas with carbon ion radiotherapy alone, the carbon ion dose was escalated to the second stage. There were distinct improvements in Progression free-survival and overall survival in the high-dose group. The result of Combined X-ray radiotherapy, chemotherapy, and carbon ion radiotherapy for malignant gliomas indicate that the survival rate tends to improve with increases in carbon ion dose. For skull base and paracervical tumor, the carbon ion dose in excess of 57.6 GyE improves local control.

I. Brain tumors

I-1. Phase I/II Clinical Trial of Carbon Ion Radiotherapy for Central Nervous System (CNS) Tumors (Protocol 9302)

This protocol (9302) was carried out from October 1994 to February 2002, and the diseases treated were low-grade astrocytoma (WHO grade 2), malignant glioma, and metastatic brain tumor. Eligibility criteria were the presence of histologically proven tumor, patient age ranging from 18 to 80 years, KPS of 60% or more, neurological function of grade I or II, absence of anti-cancer chemotherapy within the previous two weeks, survival expectancy of six months or more, and absence of meningeal dissemination.

I-1-1) Carbon Ion Radiotherapy for Low-Grade Astrocytomas (WHO Grade 2):

Materials and Methods

Carbon ion radiotherapy was administered with a schedule of 24 fractions over 6 weeks. During the trial period, 15 patients were enrolled. One female patient had to be excluded from the study because her symptoms became aggravated in the course of irradiation and her treatment was stopped at a dose of 29.9 GyE in 13 fractions before reaching her scheduled total dose (55.2 GyE). The remaining 14 patients were 9 males and 5

females, aged from 19 to 66 years, with a median of 32.5 years. Tumor location was the front lobe in 6 patients, temporal lobe in 2 patients, basal ganglion in 2 patients, parietal lobe in 1 patient, occipital lobe in 1 patient, pons in 1 patient, and cerebellum in 1 patient. Surgery had been performed prior to carbon radiotherapy by way of gross total resection in 1 patient, partial resection in 7 patients, and biopsy in 6 patients. Radiotherapy was commenced with a carbon ion dose of 50.4 GyE (2.1 GyE/fraction) (9 patients), with a one-step dose escalation to a final dose of 55.2 GyE (2.3 GyE/fraction) (5 patients).

Results and Discussion

Acute reactions were of a minor nature, with only 2 patients (14%) developing grade 2 skin reaction, with the other reactions being grade 1 or less (RTOG). Observable late reactions were also minor, with 2 patients (14%) developing grade 2 brain reaction, with the other reactions being grade 1 or less (RTOG/EORTC).

Local primary control within 6 months was PR for 2, NC for 10, and PD for 2 patients (effectiveness rate, 15%). Fourteen patients were subdivided into two groups according to carbon ion dose; the low-dose group (50.4 GyE) of 9 patients with a median progression free-survival (m-PFS) of 18 months, and the high-dose group (55.2 GyE) of 5 patients with m-PFS time of 91 months. Median survival time (MST) was 28 months for the low-dose group and not ridged (n.r.) for the high-dose group.

In the treatment of low-grade astrocytomas with carbon ion radiotherapy alone, the carbon ion dose was escalated to the second stage. There were distinct improvements in PFS and overall survival (OS) in the high-dose group. Nevertheless, in the wake of the recent advances in x-ray therapy and the significant improvements in the results for low-grade astrocytomas, the decision was made to exclude them from the indication of carbon ion radiotherapy in the future.

I-1-2) Combined X-Ray, Chemotherapy and Carbon Ion Radiotherapy for Malignant Gliomas:

Materials and Methods

In the first step of this clinical study, a total x-ray dose of 50 Gy was delivered in 25 fractions over five weeks to the location with a high signal area on T2-weighted MRI, and ACNU was administered at a dose of 100 mg/m^2 in the first and in the fourth or fifth weeks. After photon radiotherapy, carbon ion followed in 8 fractions over two weeks to the Gd-DTPA-enhanced area on T1-weighted MRI. After confirming that carbon ion irradiation at this dose level was safe for three or more patients with at least 1-year follow-up periods, the carbon ion dose was escalated.

During the trial period, 16 patients with anaplastic astrocytoma (AA) and 36 patients with glioblastoma multiforme (GBM) were enrolled. Four of the GBM patients were not treated with carbon ion radiotherapy and were excluded from the analysis (3 because of symptom deterioration due to tumor progression and 1 for refusing treatment). The remaining 48 analyzed patients, 29 males and 19 females, ranged in age from 18 to 78 years, with an average of 53 years. The predominant tumor locations were the frontal lobe in 22 patients and the temporal lobe in 10 patients. Surgery prior to radiotherapy included 8 patients with gross total resection, 8 with subtotal resection, 27 with partial resection, and 5 with biopsy. Carbon ion radiotherapy administered after x-ray therapy took place by way of dose escalation up to the fifth stage (16.8, 18.4, 20.0, 22.4, and 24.8 GyE), with all patients receiving radiation as scheduled.

Results and Discussion

Acute reactions (RTOG) consisted of serious temporary reactions in bone marrow function due to anti-cancer drug, and were mitigated by the administration of granulocyte colony-stimulating factor (G-CSF). The main reaction shown by many patients was hair loss due to x-ray exposure. Late brain reactions, however, were grade 2 or less (RTOG/EORTC), with no evidence of late reactions of grade 3 or above beyond the target volume for carbon ion irradiation.

The 16 AA patients had m-PFS of 18 months and the 32 GBM patients 7 months ($p=0.1000$). MST was 35 months for the AA patients and 17 months for the GBM patients ($p=0.0044$). The 16 AA patients were

subdivided into two groups according to carbon ion dose; the low-dose group (16.8 - 20.0 GyE) of 6 patients had m-PFS of 15 months while the high-dose group (22.4 - 24.8 GyE) of 10 patients had m-PFS time of 18 months (p=0.8660). MST for the low-dose group was 20 months and for the high-dose group 40 months (p=0.0382). The 32 GBM patients were subdivided into three groups according to carbon ion dose; m-PFS was 4.4 months for the low-dose group (16.8 GyE), 6.6 months for the medium-dose group (18.4 - 22.4 GyE), and 13.7 months for the high-dose group (24.8 GyE) (p=0.0251). Furthermore, MST was 6.9 months for the low-dose group, 19 months for the medium-dose group, and 25.7 months for the high-dose group (p=0.0031).

These findings indicate that the survival rate tends to improve with increases in carbon ion dose, and can be taken as evidence for the effectiveness of carbon ion radiotherapy for the treated diseases. Mizoe *et al.* had reported the results of this analysis in 2005 (3). From the therapeutic results obtained in the treatment of low-grade astrocytomas, skull base tumors and head-and-neck tumors, we could assume the safety of the applied carbon ion dose for normal brain tissues. In view of these findings, it was decided to proceed to the next clinical trial stage consisting of carbon ion radiotherapy alone from April 2002.

Case Description

GBM in the frontal lobe (Fig. 1): Male, 47 years. After x-ray radiotherapy of 50 Gy in 25 fractions over 5 weeks, carbon ion radiotherapy was administered at 18.4 GyE in 8 fractions over 2 weeks. Although 51 months have elapsed since the therapy, the post-treatment course remains favorable, with no evidence of tumor recurrence.

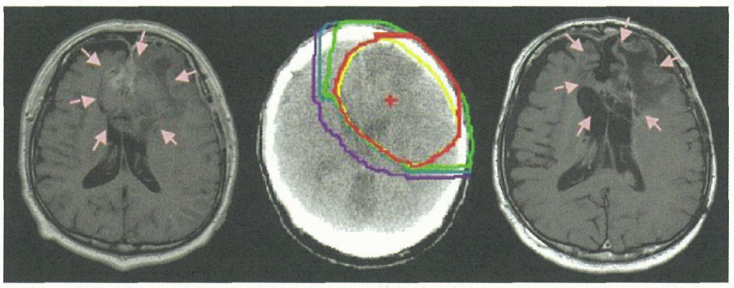

Figure 1. Glioblastoma Multiforme in the Left Frontal Lobe treated with X ray-Chemotherapy-Carbon Ion Radiotherapy
Images of gadolinium-enhanced T1-weighted MRI before treatment, isodose distribution of carbon ions, and 51 months later.
The X ray dose delivered to the hyperintensity area in the T2-weighted images was 50 Gy in 25 fractions over 5 weeks. Continuously, the carbon ion dose delivered to the gadolinium-enhanced area in the T1-weighted images was 18.4 GyE in 8 fractions over 2 weeks.
Isodose level: red = 96%; green = 50%; cyan = 30%; purple = 10%.
Contour: yellow = clinical target volume.

I-1-3) Metastatic Brain Tumors:

Materials and Methods

Carbon ion radiotherapy exclusively was performed by a schedule of 16 fractions over 4 weeks. Four patients, all female, were enrolled in the treatment course. Their ages ranged from 57 to 80 years, with an average of 70. All had single metastatic tumors: 1 in the frontal lobe, 1 in the temporal lobe, 1 in the parietal lobe, and 1 in the vermis cerebelli. Their primary location was the lung, and all of the tumors were adenocarcinoma. Prior to the carbon ion radiotherapy for the brain metastases, 1 of the patients had received surgery, 1 fast neutron radiotherapy, and 2 carbon ion radiotherapy. All patients were treated with a carbon ion dose of 52.6 GyE in 16 fractions over 4 weeks (3.3 GyE per fraction).

Results and Discussion

There was no clear evidence of any acute or late reactions. The maximum tumor reactions within 6 months were PR for 3 and NC for 1 patient (effectiveness rate: 75%). While none of the 4 patients presented with local

recurrence, 3 of them died later of brain metastasis and 1 died of generalized metastasis.

Metastatic tumors are currently treated to a large extent with conventional radiotherapy in the wake of its dramatic progress, including the gamma knife and the x knife. The objective of the protocol used in this study was to identify the tolerance dose in a relatively short time period (16 fractions over 4 weeks), while relevant data can be obtained from other treatment results (skull base and head-and-neck tumors). For these reasons, no further patients were enrolled after the radiotherapy of these 4 patients carried out at the first dose stage only.

I-2. Phase I/II Clinical Trial of Carbon Ion Radiotherapy for Malignant Gliomas (Protocol 0101)

Materials and Methods

The 30 patients treated between April 2002 and August 2008 was included in this clinical trial. Eligibility criteria for this clinical trial were the same as those for the carbon ion radiotherapy trial with concomitant x-ray and anti-cancer chemotherapy. The GTV was based on MRI and included the Gd-DTPA-enhanced volume on T1-weighted and high-intensity volume on T2-weighted images, with a minimum 5-mm margin as the CTV. The CTV was then expanded during the process of this study. The initial CTV for the x-ray dose in the previous protocol was replaced by a carbon ion dose of 30.0 GyE delivered in 12 fractions over 3 weeks, without the use of ACNU. Dose escalation of the carbon ion radiotherapy was performed for the Gd-DTPA-enhanced volume on T1-weighted MRI, and 15 patients (AA: 3 patients; GBM: 12 patients) received 28.0 GyE in 8 fractions over 2 weeks, and 15 patients (AA: 3; GBM: 12 patients) received 32.0 GyE by the same schedule. This phase I/II clinical trial was concluded in August 2008.

Results and Discussion

Analysis was carried out on the 30 patients with a post-radiotherapy observation time of 6 months or longer. Acute skin and brain reactions observed within three months of irradiation consisted of a grade 1 or milder reaction in most patients (RTOG). Nineteen of the 30 patients presented with radiation encephalitis. Nine of them developed grade 2 brain reaction by RTOG/EORTC, and they were treated with steroid medication.

The maximum tumor reactions within 6 months after irradiation were CR or PR for 4 patients (AA: 1 patient), SD for 20 patients (AA: 5 patients), and PD for 6 patients. Three of the 4 CR or PR patients belonged to the second dose escalation stage group (62 GyE). The 6 AA patients had 50% PFS and 100% OS rates at 24 months. The 24 GBM patients were divided into five groups: group A (n=4), a tight field irradiated with 58 GyE, group B (n=8), an intermediate field irradiated with 58 GyE, group C (n=5), a tight field irradiated with 62 GyE, group D (n=3), an intermediate field irradiated with 62 GyE, group E (n=4), a wide field irradiated with 62 GyE. M-PFS was 5.2 months for group A, 9.5 months for group B, 8 months for group C, 7.5 months for group D, and 9.7 months for group E. MST was 10.1 months for group A, 12.9 months for group B, 10 months for group C, 10 months for group D, and 11.5 months for group E. In the treatment of malignant gliomas with carbon ion radiotherapy alone, the carbon ion dose was escalated to the second stage. There was distinct improvement in PFS in the high dose groups, but many cases of grade 2 radiation encephalitis developed in the high dose and extended field groups compared with the low dose and tight field groups. In view of these findings, it was decided to proceed to the next clinical trial with a combination protocol of Temozolomide and carbon ion radiotherapy from April 2009.

Case Description

AA in the temporal lobe (Fig. 2): female, 41 years. Carbon ion radiotherapy of 62 GyE was administered by a schedule of 20 fractions over 6 weeks. Although 24 months have elapsed since therapy, the post-treatment course remains favorable, with no evidence of tumor recurrence.

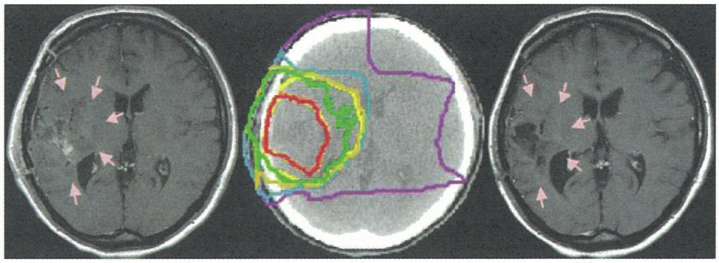

Figure 2. Anaplastic Astrocytoma in the Right Temporal Lobe treated with Carbon Ion Radiotherapy Only
Images of gadolinium-enhanced T1-weighted MRI before carbon ion radiotherapy, isodose distribution, and 6 months later. The dose delivered to the clinical target volume was 62 GyE in 20 fractions over 5 weeks.
Isodose level: red = 96%; orange = 90%; green = 50%; cyan = 30%; purple = 10%.
Contour: yellow = clinical target volume.

II. Skull base and Paracervical Tumors

Phase I/II Clinical Trial of Carbon Ion Radiotherapy for Skull Base and Paracervical Tumors (Protocol 9601)

Introduction

The limiting factor for photon radiotherapy conventionally applied to the skull base and paracervical tumors is the adjacent normal tissue, seeing that photon radiotherapy has poor local control. On the other hand, proton radiotherapy with its superior physical-spatial distribution has provided a major improvement in local control in view of the possibility of dose escalation. It has been pointed out, however, that in certain patient groups it is difficult to achieve local control with proton radiotherapy even at elevated doses. It has thus been recognized that 1) chordoma patients offer a worse prognosis than chondrosarcoma patients, 2) among chordoma patients, the prognosis for paracervical chordoma patients is worse than for skull base chordoma, it is worse for non-chondroid patients than for chondroid ones, and it is worse for females than for males, and 3) for meningeal tumors, the prognosis for the atypical or malignant types is worse than for the benign type, and the prognosis for the age group of 60 and above is poorer than for those under 60. Therefore, the high RBE of carbon ion radiotherapy has a promising potential for these intractable skull base and paracervical tumors.

Materials and Methods

Prior to this protocol, a pilot study using 48 GyE in 16 fractions over 4 weeks with 8 patients was carried out starting in May 1995. Then, a phase I/II clinical trial (Protocol 9601) was initiated in April 1997. In the meantime, the carbon ion dose was escalated in successive stages: 48.0 GyE (4 patients), 52.8 GyE (6 patients), 57.6 GyE (10 patients) and 60.8 GyE (9 patients). The phase I/II clinical trial was concluded in February 2004, and in April 2004 a phase II clinical trial was initiated under the Highly Advanced Medical Technology scheme with an irradiation schedule of 60.8 GyE in 16 fractions over 4 weeks. Twenty-five patients had been enrolled into this trial up to August 2008.

Results and Discussion

The 54 patients included in the analysis between May 1995 and August 2008 consisted of 25 males and 29 females. One female patient with chondrosarcoma had to be excluded because she was treated with surgery for metastasis and her diagnosis was changed to malignant melanoma. She was treated with 57.6 GyE. The age range of the 53 patients was from 16 to 78, with a median of 49 years. Histologically, 31 patients had chordoma, 10 chondrosarcoma, 6 malignant meningioma, 5 olfactory neuroblastoma and 1 giant cell carcinoma.

Acute reactions were of a minor nature, as 1 patient of the 48 GyE group showed a grade 3 skin reaction and

1 patient of the 57.6 GyE group showed a grade 3 mucosal reaction. A late grade 2 brain reaction was detected in 2 patients, but no other adverse reactions were discovered. At the time of analysis, there was no evidence of any serious acute or late reactions.

The tumor effect remains mostly as stable disease (SD) within six months after carbon ion radiotherapy, and there were in most cases no changes in tumor size during the follow-up periods. Local control was defined as showing no evidence of tumor regrowth by MRI, CT, physical examination, or biopsy. The five-year LC rates according to prescribed tumor dose were 75% at 48 GyE (n=4), 67% at 52.8 GyE (n=6), 78% at 57.6 GyE (n=9) and 95% at 60.8 GE (n=34) (Fig. 3). The five-year OS rates were 50% at 48 GyE, 100% at 52.8 GyE, 100% at 57.6 GyE and 77% at 60.8 GyE (Fig. 4). Four of 34 patients irradiated with a dose of 60.8 GyE died of interrupted pneumonia, distant metastasis, hepatic failure, and marginal failure. Local tumor control was achieved in these cases. The five-year LC rates according to histological types were 78% for chordomas (n=31), 100% for chondrosarcomas (n=10), 80% for malignant meningiomas (n=6), and 100% for olfactory neuroblastomas (n=5). The five-year OS rate was 85% for chordomas, 64% for chondrosarcomas, 83% for malignant meningiomas, and 100% for olfactory neuroblastomas. Two of the six malignant meningioma patients died because of distant metastasis 23 months, and local recurrence 85 months, respectively, after carbon ion radiotherapy. This local recurrence patient had had a postoperative recurrence and received low-dose carbon ion radiotherapy of 52.8 GyE.

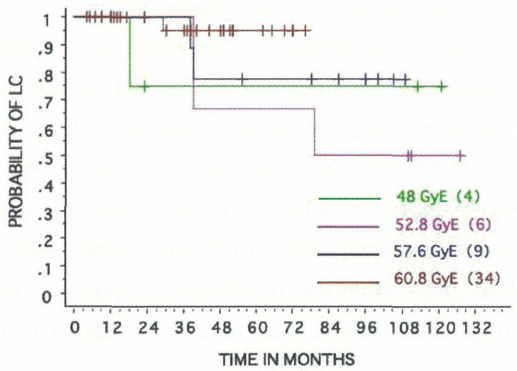

Figure 3. Local Control Curve for Skull Base Tumor (Apr 97~Aug 08)

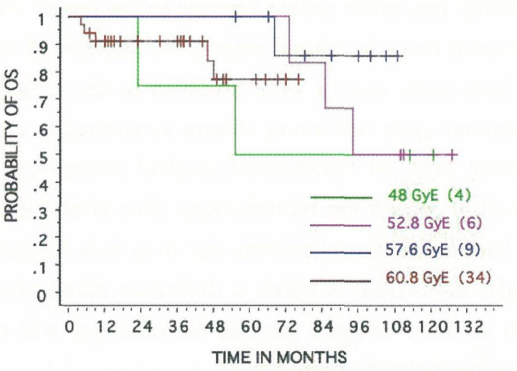

Figure 4. Overall Survival Curve for Skull Base Tumor (Apr 97~Aug 08)

The 31 chordoma patients were divided into two groups, a low-dose group (n=10) irradiated with doses ranging from 48 to 57.8 GyE and a high-dose group (n=21) irradiated with 60.8 GyE. The five-year LC rates were 60% for the low-dose group and 93% for the high-dose group. One patient of the high-dose group developed marginal failure 29 months later. The five-year OS rates were 90% for the low-dose group and 84% for the high-dose group. Two patients from the high-dose group died due to hepatic failure and marginal failure. Figure 5 shows LC and OS curves for 21 chordomas irradiated with 60.8 GyE.

In this phase I/II clinical study for skull base and paracervical tumors, dose escalation trials were performed up to the fourth-stage dose level. Because dose escalation is implemented after checking the reactions of the important adjacent organs – the brain and spinal chord – the scheduled enrollment period was exceeded and therapy was commenced under the Highly Advanced Medical Technology scheme for these patients in April 2004 with a dose fractionation regimen of 60.8 GyE in 16 fractions over 4 weeks. No tumor regression was seen in most cases regardless of carbon ion dose. The lower dose groups (48.0 and 52.7 GyE) showed local recurrence in two chordoma and one malignant meningioma. The third-stage dose escalation group (57.6 GyE) showed local recurrence in two chordoma and one chondrosarcoma. The fourth-stage dose escalation group (60.8 GyE) showed local recurrence in one chordoma.

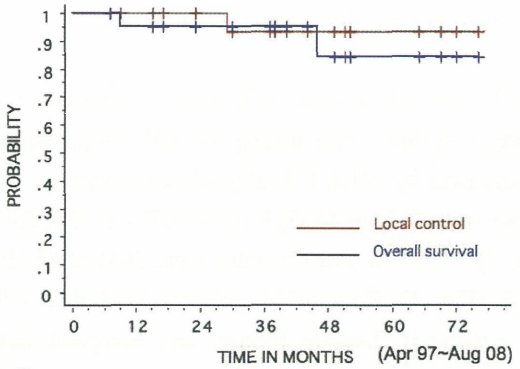

Figure 5.
Local Control and Overall Survival for 21 Chordomas irradiated with 60.8 GyE

Conclusion

The carbon ion dose in excess of 57.6 GyE improves local control. Additionally, we did not observe severe toxicity to critical organs such as the brainstem, spinal cord and optic nerves. From April 2004, carbon ion radiotherapy was initiated under the Highly Advanced Medical Technology scheme with an irradiation schedule of 60.8 GyE in 16 fractions over 4 weeks.

High LET charged particles such as carbon ions have excellent dose localizing properties, and this potentiality can cause severe damage to the tumor while lessening the effects on normal tissue. When the tumor was located close to critical organs, delineation of the CTV was done with efforts to spare them. In particular, when both optic nerves were involved in the high-dose area, treatment planning was performed to spare the contralateral optic nerve and chiasm according to our previous dose criteria. For tumors close to the brainstem and spinal cord, we recommend surgical resection to create a space between the tumor and brainstem or spinal cord before carbon ion radiotherapy. This allows the prevention of severe toxicity to the brainstem and spinal cord. Tumors such as chordoma can thus only be judged on the results of long-term prognosis. Consequently, it will take more time to reach a definitive conclusion. It is clear that carbon ion radiotherapy compared with photon or other charged particle radiotherapy will deliver a high local control rates with low toxicity to the surrounding normal tissues.

Case Description

Postoperative recurrence of chordoma in the left parapharyngeal space (Fig. 6): Female, 63 year. Sixty-six months have elapsed since carbon ion radiotherapy by a regimen of 52.8 GyE in 16 fractions over 4 weeks. The tumor has virtually disappeared and the post-treatment course remains favorable, with no evidence of tumor recurrence.

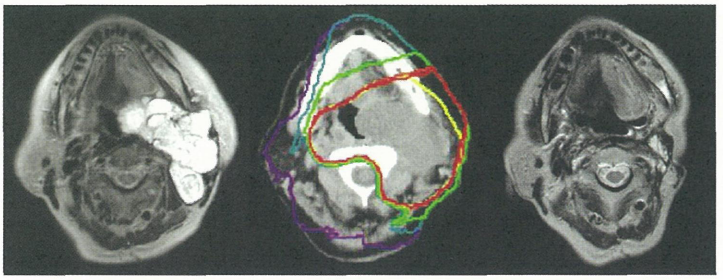

Figure 6. Postoperative Recurrence of Chordoma in the Left Parapharyngeal Space treated with Carbon Ion Radiotherapy
Images of T2-weighted MRI before carbon ion radiotherapy, isodose distribution, and 66 months later. The dose delivered to the clinical target volume was 52.8 GyE in 16 fractions over 4 weeks.
Isodose level: red = 96%; orange = 90%; green = 50%; cyan = 30%; purple = 10%.
Contour: yellow = clinical target volume.

References

[1] Tsujii H, Mizoe J, Kamada T, *et al.* Overview of clinical experiences on carbon ion radiotherapy at NIRS. *Radiother Oncol* 2004;73:41–49.

[2] Tsujii H, Mizoe J, Kamada T, *et al.* Clinical results of carbon ion radiotherapy at NIRS. *Radiat Res* 2007;48:A1–13.

[3] Mizoe J, Tsujii H, Hasegawa A, *et al.* Carbon ion radiotherapy for malignant gliomas. *Neuro-oncol.* 2005; 7; 389.

[4] Hasegawa A, Mizoe J, Mizota A, Tsujii H. Outcomes of visual acuity in carbon ion radiotherapy: analysis of dose–volume histograms and prognostic factors. *Int J Radiat Oncol Biol Phys*, 2006; 64 (2): 396-401.

[5] Mizoe J, Tsujii H, Hasegawa A, Yanagi T, Takagi R, Kamada T, Tsuji H, Takakura K: Phase I/II clinical trial of carbon ion radiotherapy for malignant gliomas: combined x-ray radiotherapy, chemotherapy, and carbon ion radiotherapy. *Int J Radiat Oncol Biol Phys,* 2007; 69 (2): 390-396.

[6] Mizoe J, Hasegawa A, Takagi R, Bessho H, Onda T, Tsujii H: Carbon ion radiotherapy for skull base chordoma. *Skull Base,* 2008; 17: in print.

Head and Neck Tumors

Jun-etsu Mizoe, Azusa Hasegawa, Hiroki Bessho, Kenichi Jingu and Yoshido Kakimoto

Hospital, Research Center for Charged Particle Therapy, National Institute of Radiological Sciences, Chiba, Japan
e-mail address: j_mizoe@nirs.go.jp

Introduction

Clinical trial with carbon ion radiotherapy for the head and neck tumors was conducted under "the Phase I/II Clinical Trial (Protocol 9301) on Heavy Particle Radiotherapy for Malignant Head and Neck Tumors", that was initiated in June 1994 by way of a dose escalation study on a fractionation method of 18 fractions over 6 weeks. This trial was followed by a next dose fractionation and dose escalation study commenced in June 1996 under "the Phase I/II Clinical Trial (Protocol 9504) on Heavy Particle Radiotherapy for Malignant Head and Neck Tumors" using a fractionation method of 16 fractions over 4 weeks. The results of these two trials were published in 1994 [1]. Following the outcome of these two studies, the "Phase II Clinical Trial on Heavy Particle Radiotherapy for Malignant Head and Neck Tumors (Protocol 9602)" was initiated on a 64.0GyE/16 fractions/4 weeks fractionation method (or 57.6 GyE/16 fractions/4 weeks when the wide-range of the skin was included in the target volume) in April 1997.

Based on the results of preliminary analysis of the 9602 protocol, two protocol were derived with effect from April 2001 into 1) the "Phase I/II Clinical Trial of Carbon Ion Radiotherapy for Bone and Soft Tissue Tumors of the Head and Neck (Protocol 0006)" designed as a dose escalation study for bone and soft-tissue tumors, and 2) the "Phase II Clinical Trial of Carbon Ion Radiotherapy Combined with Chemotherapy for Mucosal Malignant Melanoma of the Head and Neck (Protocol 0007)" for the treatment of malignant melanoma with concomitant chemotherapy. The 9602 and 0007 protocols have been carried out since November 2003 under the Highly Advanced Medical Technology.

Phase II Clinical Trial on Heavy Particle Radiotherapy for Malignant Head and Neck Tumors (Protocol 9602)

The eligibility criteria for enrollment in this Clinical Study were the presence of histologically proven malignancy, measurable tumor in the head and neck region including NOMO in principle, with no co-existent malignant active tumor, no distant metastasis to other parts, an age range from 15 to 80 years and a prospective prognosis of at least 6 months or longer. The candidates were also required to have a K.I. of 60% or more and to give their written informed consent for inclusion in this Clinical Study. A further requirement was the absence of prior radiotherapy for the carbon treated area, the absence of intractable inflammatory lesion and no interval time less than four weeks from the completion of last chemotherapy.

The clinical trial was commenced in April 1997, and by August 2008 a total of 330 patients corresponding to 333 lesions was registered (for three patients, a second lesion was treated in the same patient). Five of the 330 patients were excluded from the analysis because of 1) that carbon ion radiotherapy had to be cancelled for two patient with malignant melanoma due to a deterioration of the symptoms, 2) that another patient with lacrimal gland tumor was diagnosed as a metastasis from the thyroid gland before carbon ion radiotherapy, 3) that the

amelblastoma of a further patient was diagnosed as a benign tumor after histological re-examination and 4) that the histological confirmation was done by cytology only. The data for 328 lesions of 325 patients treated until August 2008 are recorded as follows: Patient age ranged from 16 to 80, averaging 57 years of age, with 165 male and 163 female. Their K.I. ranged from 60% to 100%, with the median value being 90%. The sites of disease are consisted of 85 lesions with paranasal sinus, 68 with nasal cavity, 40 with salivary gland, 39 with oral cavity, 37 with orbita, 33 with pharynx, 11 with thyroid gland, 8 with auricula and 7 with tumors in other sites. Histologically, the tumors are classified as follows: 107 with adenoid cystic carcinoma, 100 with malignant melanoma, 38 with adenocarcinoma, 19 with squamous cell carcinoma, 13 with papillary adenocarcinoma, 11 with mucoepidermoid carcinoma, 6 with osteosarcoma, 5 with acinic cell carcinoma, 5 with unfifferentiated carcinoma and 24 with other histological types of tumor. There were five cases of stage I, 24 of stage II, 47 of stage III, 141 of stage IV, 74 of post operative, 27 of post chemotherapy, 9 of post operative and post chemotherapy and one of post carbon ion radiotherapy. Carbon ion radiotherapy was given on a fractionation method of 16 fractions/4 weeks. The 328 lesions were irradiated with a dose of 57.6GyE in 241 and with one of 64.0GyE in 87 cases.

Early reactions of the normal tissues of the 328 lesions which were treated until the August of 2008 included grade 3 skin reactions in 15 patients (5%) and in the mucosa in 45 patients (14%), and no reactions worse than grade 3 were observed. Late toxic reactions comprised grade 2 skin reaction in 7 patients (2%) and mucosa reactions in 8 patients (3%), with no evidence of toxicities worse than these.

The tumor reaction at six months after treating the 328 lesions was CR for 40 lesions, PR for 148 lesions, NC for 135 lesions and PD for 5 lesions, with the effective rate (CR+PR) being 57%. The five-year local control rate was 70% and five-year overall survival was 48% (Fig. 1). Five-year local control rate by histological type was 81% for the 38 adenocarcinoma, 74% for the 107 adenoid cystic carcinoma, 74% for the 100 malignant melanoma and 70% for the 19 squamous cell carcinoma (Fig. 2). The five-year survival rate was 68% for adenoid cystic carcinoma and 56% for adenocarcinoma (Fig. 3).

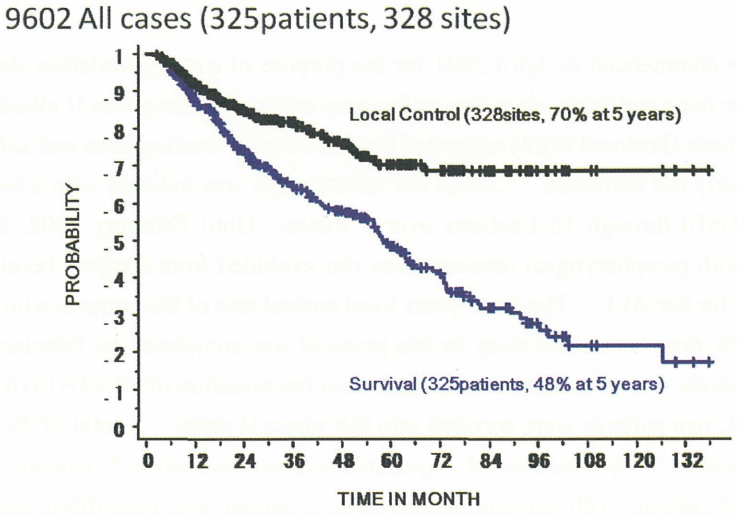

Fig.1: Local control and survival curves of the H&N cancer (9602)

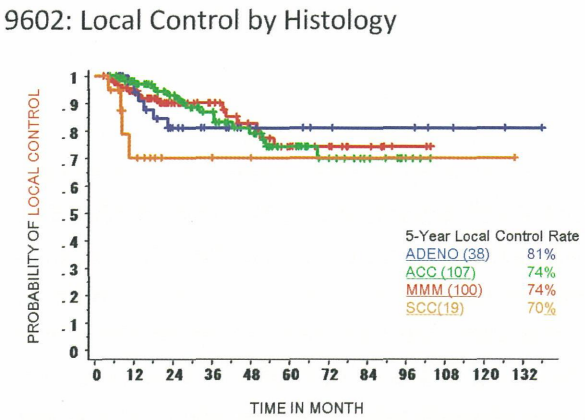

Fig. 2: Local control curves by histology (9602)

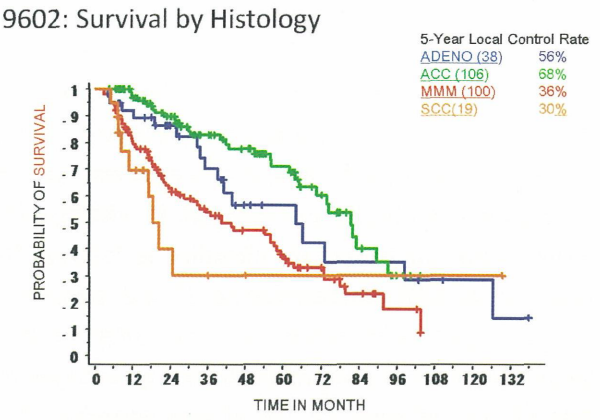

Fig. 3: Survival curves by histology (9602)

Although the reactions in normal tissues included early grade 3 skin and mucosal reactions in approximately 10% of the subjects, the late reactions were grade 2 or less. This therapy can therefore be described as presenting no clinical problems. The overall local control rate was 70% at 5 years. The therapeutic effectiveness of the therapy was particularly outstanding for non-squamous cell carcinoma, a tumor intractable to photon radiotherapy. Treatment results of combined surgery and radiotherapy ranged from 49% to 98% of five-year local control and from 40% to 80% of five year over all survival. Recommended treatment is surgery with or without radiotherapy [2]. When they were treated by radiotherapy alone, it's local control is 20~25% [3,4]. In our series of 9602, the local control rate was 70% eve if there included 141 cases (43%) of T4 and 110 cases (34%) of recurrence of post operative and/or post chemotherapy. Therefore the local control of carbon ion radiotherapy is promising for locally advanced head and neck cancer.

Phase I/II and II Clinical Trials of Carbon Ion Radiotherapy for Bone and Soft Tissue Tumors of the Head and Neck (Protocol 0006)

Phase I/II protocol was commenced in April 2001 for the purpose of a dose escalation study against bone and soft-tissue tumors in the head and neck, since the preliminary analysis of the phase II clinical trial for malignant tumors in the head and neck (Protocol 9602) suggested that the dose for treating bone and soft-tissue tumors in the head and neck was clearly not sufficient. Carbon ion radiotherapy was initiated with a total dose of 70.4 GyE (fraction dose of 4.4 GyE) through 16 fractions over 4 weeks. Until February 2008, 28 patients had been enrolled. One patient with parapharyngeal osteosarcoma was excluded from analysis because of past history of whole body irradiation for her ALL. The three years local control rate of the patients who were treated by 70.4 GyE was exceeded 90%, dose escalation study in this protocol was completed on February 2008. From April 2008, phase II clinical study was commenced with same dose fractionation of 70.4 GyE/16 fractions/4 weeks. Till the August of 2008, two patients were enrolled into this phase II study. A total of 29 patients of phase I/II and II study were analyzed. They consisted of 10 patients with osteosarcoma, 5 patients with MFH, 2 patients with chondrosarcoma, 2 patients with hemangiopericytoma, 2 patient with myxofibrosarcoma, 2 patients with leimyosarcoma, and each one patient with fibrosarcoma, angiosarcoma, small round cell sarcoma, spindle cell sarcoma, PNET and rhabdomyosarcoma. The irradiated dose was 70.4 GyE for all patients.

Preliminary analysis of the 29 patients who had follow-up period for over six months showed that early skin reactions were grade 2 or less and that only one patient presented an early grade 3 mucosal reaction. All late skin and mucosal reactions were grade 1 or less. The tumor reactions consisted of CR (4), PR (5) and SD (20). The

effectiveness rate was 31%. The three-year local control rate was 92% and their three-year overall survival rate was 75% (Fig. 4).

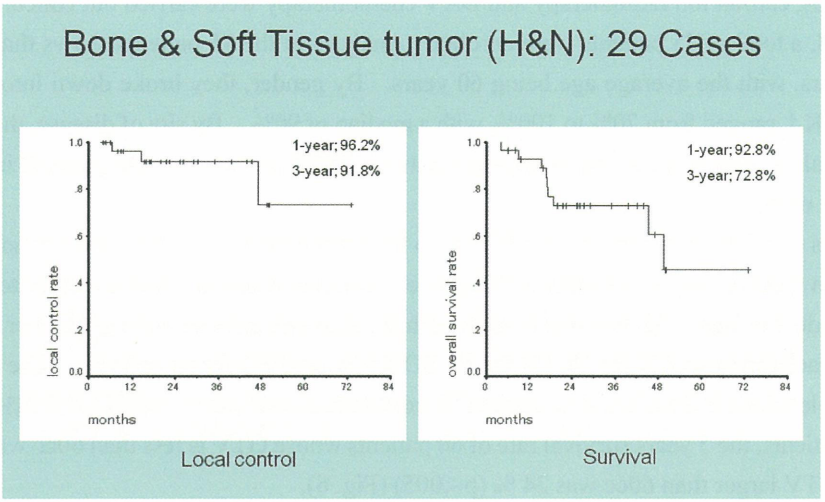

Fig. 4: Local control curve and survival curve of bone and soft tissue tumor in H&N (0006)

Bone and soft-tissue tumor in the head and neck is a rare disease. Willers et. al. said; "Wide resection margins are anatomically difficult to achieve, and the delivery of high radiation dose can be limited by the vicinity of critical normal tissue structures (spinal cord, brain stem, optic chiasm, eyes). Accordingly, local control rates for head and neck sarcomas are lower compared to the extremities." [5] Five years local control rate of combined surgery and radiotherapy is 60 – 70% with five years over all survival of 60%. Local control of surgery alone is around 54% and that of radiotherapy alone is 43 – 50% [6]. Radiotherapy with a total dose less than 65 Gy showed no local control [7,8,9]. Results of carbon ion radiotherapy in our previous study (9602) for bone and soft tissue tumors, in which study patients were treated by 64.0 or 57.6 GyE/16 fraction, showed 24% of five years local control and 36% of overall survival. On the other hand, the three-year local control rate of this study (0006) was 92% and their three-year overall survival rate was 75%. The results showed improved tendency of 0006 study in both local control and overall survival.

Although the number of osteosarcoma patients had been anticipated to be particularly increased in this study, it is evident that the observation time was not adequate because the registration period was only within three years. Clinical study will therefore be continued with the dose of 70.4 GyE because the high local control rate achieved with this dose.

Phase II Clinical Trial for Mucosal Malignant Melanoma of the Head and Neck Combined with Chemotherapy (Protocol 0007)

Although the phase II Clinical Study for the Head and Neck tumors (Protocol 9602) had achieved a satisfactory local control rate for the malignant melanoma, the survival rate was not commensurate with the favorable local control rate of the malignant melanoma. In view of this, this protocol was commenced in April 2001 for the purpose of prophylactic therapy against distant metastasis, the major cause of death in malignant melanoma of the head and neck region.

Carbon ion radiotherapy was administered on a fractionation method of 57.6 GyE/16 fractions/4 weeks. Concomitant chemotherapy (DAV: Day 1: DTIC 120mg/m2 + ACU 70mg/m2 + VCR 0.7mg/m2; Days 2 - 5: DTIC 120mg/m2, 4 weeks' interval, a total of 5 courses) was administered at a rate of two courses before, and three courses after carbon ion radiotherapy. The results for the seven patients treated until February 2002 show

that at the time of completion of the two courses of DAV chemotherapy prior to carbon ion radiotherapy, there were 2 PR, 2 NC and 3 PD patients, necessitating the early commencement of carbon ion radiotherapy. From April 2002 onwards, carbon ion radiotherapy and DAV chemotherapy were carried out concurrently.

Until August 2008, a total of 75 patients were enrolled Analysis of the 75 patients shows that their age ranged from 26 to 74 years, with the average age being 60 years. By gender, they broke down into 29 males and 46 females, and their K.I. ranged from 70% to 100%, with a median of 90%. By site of disease, they consisted of 61 patients in the nasal cavity and paranasal sinus, eight patients in the oral cavity, four patients in the pharynx and two patients in the orbit.

The early reactions of 57 patients who have a follow up time more than 6 months were consisted of one patient with a grade 3 skin reaction and 11 patients with a grade 3 mucosal reaction while the other toxicities that were observed were grade 2 or less. All late reactions in both the skin and mucosa were grade 1 or less.

The local tumor reactions show CR for 18, PR for 33, SD for 24, and PD for no patients. The effective rate was 68%. The 5-year local control and survival rates of 57 concomitant patients were 85% and 58% (Fig.5). Of these 57 concomitant patients, the 5 years survival rate of 60 patients whose GTV is less than 60cc was 68% and one of 15 patients with GTV larger than 60cc was 24 % ($p<.005$) (Fig. 6).

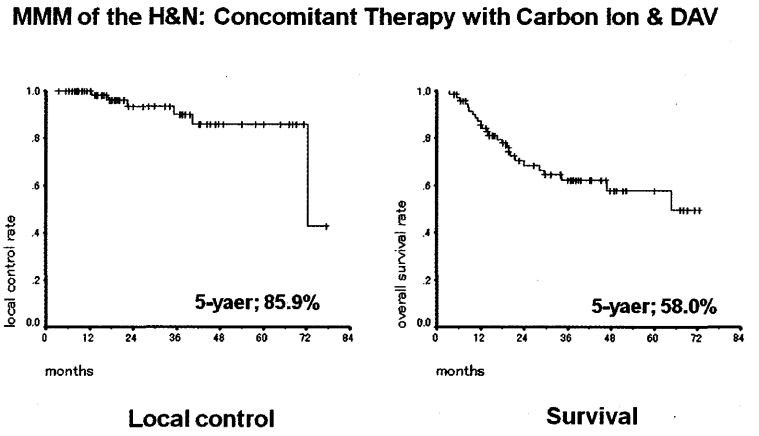

Fig. 5: Local control curve and survival curve of mucosal malignant melanoma (0007)

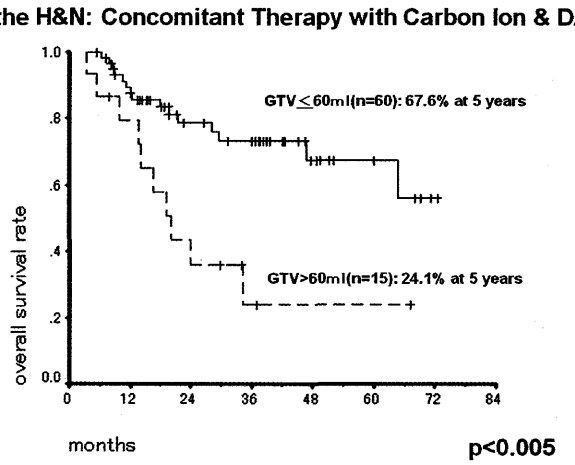

Fig. 6: Survival curves of mucosal malignant melanoma subdivided by GTV at 60 cm^3 (0007)

The reported local failure of systemic therapy including surgery, operation and chemotherapy is very high (45~54%) [9,10]. Five years local control of carbon ion radiotherapy showed 74% in 9602 protocol and 85% in 0007 protocol. These results will show an effectiveness of carbon ion radiotherapy for the local control of mucosal malignant melanoma of the head and neck. The review article by Lengyel E., et. al. reported 5-year survival rates of 17~48%, which is attributed mainly to a haematogenous dissemination [11]. Overall 5 years survival rate of carbon ion radiotherapy showed 36% in 9602 and 58% in 0007 protocol. There will be some tendency of improving result in combined therapy (0007).

Conclusion

Malignant tumors in the head and neck region are therapeutically very diverse because of the many important organs present in this region and the great variety of tissue types. Carbon ion radiotherapy also requires considerable versatility in terms of the use of a specific radiation dose suited for the particular histological type and the application of concomitant chemotherapy and radiotherapy. At present, efforts are being made to increase the patient numbers in order to produce results that can provide cogent clinical evidence.

References

[1] Mizoe JE, Tsujii H, Kamada T, et al. Dose escalation study of carbon ion radiotherapy for locally advanced head-and-neck cancer. Int J Radiat Oncol Biol Phys. 2004;60:358-64.

[2] TERHAARD CHJ, LUBSEN H, RASCH CRN, et al. THE ROLE OF RADIOTHERAPY IN THE TREATMENT OF MALIGNANT SALIVARY GLAND TUMORS Int. J. Radiation Oncology Biol. Phys. 2005;61:103–111.

[3] Mendenhall WM, Morris CG, Amdur RJ, et al. Radiotherapy alone or combined with surgery for salivary gland carcinoma. Cancer. 2005;103:2544-50.

[4] Schulz-Ertner D, Nikoghosyan A, Didinger B, et al. Therapy strategies for locally advanced adenoid cystic carcinomas using modern radiation therapy techniques. Cancer. 2005;104:338-44.

[5] Willers H, Hug EB, Spiro IJ, et al. Adult soft tissue sarcomas of the head and neck treated by radiation and surgery or radiation alone: patterns of failure and prognostic factors. Int J Radiat Oncol Biol Phys. 1995;33:585-93.

[6] Mendenhall WM, Mendenhall CM, Werning JW, et al. Adult head and neck soft tissue sarcomas. Head Neck. 2005:27:916-22.

[7] Le QT, Fu KK, Kroll S, et al. Prognostic factors in adult soft-tissue sarcomas of the head and neck. Int J Radiat Oncol Biol Phys. 1997;37:975-84.

[8] Barker JL Jr, Paulino AC, Feeney S, et al. Locoregional treatment for adult soft tissue sarcomas of the head and neck: an institutional review. Cancer J. 2003;9:49-57.

[9] Chen SA, Morris CG, Amdur RJ, et al. Adult head and neck soft tissue sarcomas. Am J Clin Oncol. 2005;28:259-63.

[10] Mendenhall WM, Amdur RJ, Hinerman RW, et al. Head and neck mucosal melanoma. Am J Clin Oncol. 2005;28:626-30.

[11] LENGYEL E, GILDE K, REMENÁR E, et al. Malignant Mucosal Melanoma of the Head and Neck -a Review-. Pathology Oncology Research. 2003;9:7-12.

Carbon Ion Radiotherapy in Hypofraction Regimen for Stage I Non-Small Cell Lung Cancer

Masayuki Baba, Naoyoshi Yamamoto, Mio Nakajima, Kyosan Yoshikawa, Reiko Imai, Naruhiro Matsufuji, Shinichi Minohara, Tada-aki Miyamoto, Hiroshi Tsuji, Tadashi Kamada, Jun-etsu Mizoe, and Hirohiko Tsujii

Hospital, Research Center for Charged Particle Therapy, National Institute of Radiological Sciences, Chiba, Japan
e-mail address: baba@nirs.go.jp

Abstract

From 1994 to 1999, we conducted a phase I/II clinical trial for stage I non-small cell lung cancer (NSCLC) by using carbon ion beams alone, demonstrating optimal doses of 90.0GyE in 18 fractions over 6 weeks (Protocol #9303) and 72.0GyE in 9 fractions over 3 weeks (Protocol #9701) for achieving more than 95% local control with minimal pulmonary damage. In the present study, the total dose was fixed at 72.0GyE in 9 fractions over 3 weeks (Protocol #9802), and at 52.8GyE for stage IA and 60.0GyE for stage 1B in 4 fractions in 1 week (Protocol #0001). Following this schedule, we conducted a phase II clinical trial for stage I NSCLC from 1999 to 2003. We also conducted a phase I/II single fractionation clinical trial (Protocol #0201), a dose escalation study. The total dose was initially 28.0GyE in 2003, and it was raised to 44.0GyE in 2007. This article describes the intermediate steps. Most targets were irradiated from four oblique directions. A respiratory-gated irradiation system was used for all sessions. Local control and survival were assessed by Kaplan-Meier method. For statistical testing, the Log-rank test was used.

The local control rate for all patients (#9802 and #0001) was 91.5%, and those for T1 and T2 tumors were 96.3% and 84.7%, respectively. While there was a significant difference (p=0.0156) in tumor control rate between T1 and T2, there was no significant difference (P=0.1516) between squamous cell carcinomas and non-squamous cell carcinomas. The 5-year cause-specific survival rate was 67.0% (IA: 84.4, IB: 43.7), and overall survival was 45.3% (IA: 53.9, 1B: 34.2). No adverse effects greater than grade 2 occurred in the lung.

In a single fractionation trial, the local control rate for all 72 patients was 89.3%, and the control rates for T1 and T2 tumors were 94.6% and 78.7%, respectively. No adverse effects greater than grade 3 occurred in the lung.

Carbon beam radiotherapy, an excellent new modality in terms of high QOL and ADL, was proven to be a valid alternative to surgery for stage I cancer, especially for elderly and inoperable patients.

Introduction

In 1998, lung cancer became the leading cause of cancer-related death in Japan, as it had done in Western countries. Surgery plays a pivotal role in the curative treatment for non-small cell lung cancer (NSCLC), but it is not necessarily the best treatment for elderly persons and/or patients with cardiovascular and pulmonary complications. Conventional radiotherapy as an alternative, however, produces a five-year survival rate in merely 10-30% of the patients due to poor control of the primary tumor. Dose escalation is essential to improve the effectiveness of radiotherapy, but this involves increasing risk of pulmonary toxicity. Carbon ion radiotherapy (CIRT) is a promising modality because of its excellent dose localization and high biological effect

on the tumor. Our clinical trials led us to conclude that irradiation with heavy particle beams, notably carbon ion beams, offers a significant potential for improving tumor control without increasing toxicity risks.

Between 1994 and 1999, a phase I/II study of the treatment of stage I NSCLC by CIRT was first conducted using a dose escalation method to determine the optimal dose. An additional purpose was to develop correct, reliable and safe irradiation techniques for CIRT. As reported in our phase I/II study [1], the following results (Table 1) were obtained: 1) The local control rate was dose-dependent, reaching more than 90% at 90.0GyE with a regimen of 18 fractions over 6 weeks and at 72.0GyE with 9 fractions over 3 weeks. Both doses were determined to be optimal. It was found that setting the provisional target by allowing for the difference with the CT value can prevent marginal recurrence [2]. 2) Damage to the lung was minimal, with grade 3 radiation pneumonitis occurring in 2.7% of the cases. Respiratory-gated and 4-portal oblique irradiation directions excluding opposed ports proved successful in reducing the incidence of radiation pneumonitis. 3) Survival was strongly influenced by local control and tumor size of the primary lesion. The early detection of nodal and intralobar metastasis followed by irradiation with carbon beams can prevent the survival rate from decreasing further. Local failure, distant metastasis and malignant pleurisy were responsible for decreases in survival.

Adverse reactions in lung
1) minimum damage to lung (grade 3 radiation pneumonitis was 2.7%)
2) influenced by dose, respiration movement, and port direction and number
Local control
1) dose-dependent, but less dependent on tumor size and histological type
2) more than 90% by optimal dose and demonstrated by pathological CR
Survival
1) influenced by local control state and tumor size
2) less decreased by nodal and intralobar metastasis but more by local failure, malignant pleurisy and distant metastasis

Table 1 Results of phase I/II study on carbon beam radiotherapy for stage I non-small cell lung cancer

In the present study, a phase II clinical trial and a phase I/II dose escalation clinical trial are reported. In the phase II clinical trial, the total dose was fixed at 72.0GyE in 9 fractions over 3 weeks [3], and at 52.8GyE for stage IA NSCLC and 60.0GyE for stage IB NSCLC in 4 fractions in one week [4]. Using this optimal schedule, the phase II clinical trial was initiated in April in 1999 and closed in December in 2003, accruing a total number of 127 patients.

The phase I/II dose escalation clinical trial was initiated in April 2003. The initial total dose was 28.0GyE administered in a single fraction using respiratory-gated and 4-portal oblique irradiation directions, with the total irradiation dose being escalated in increments of 2.0GyE each, up to 44.0GyE. This clinical trial is still in progress. This article describes the intermediate steps of the phase I/II clinical trial and the preliminary results of the phase II clinical trial in terms of local control and survival after CIRT.

Materials and Methods

[Phase II clinical trial]

One hundred and twenty-nine patients with 131 primary lesions were treated with CIRT. Fifty-one primary tumors of 50 patients were treated by carbon ion beam irradiation alone using a fixed total dose of 72GyE in 9 fractions over 3 weeks (#9802 protocol [3]). The remaining 79 patients had 80 stage I tumors (#0001 protocol [4]) For survival, 127 patients were evaluated, as 2 patients had been treated twice, one in the first protocol

#9802, and one in the second protocol #0001. The IA and IB stage tumors were treated with fixed doses of 52.8GyE and 60.0GyE in 4 fractions in one week, respectively. Mean age was 74.5 years, and gender breakdown was 92 males and 37 females. The tumors were 72 T1 and 59 T2. Mean tumor size was 31.5 mm in diameter. By type, there were 85 adenocarcinomas, 43 squamous cell carcinomas, 2 large cell carcinomas and 1 adenosquamous cell carcinoma. Medical inoperability stood at 76%.

[Phase I/II clinical trial (single fractionation)]

Seventy-two patients were treated in this clinical trial between April 2003 and August 2007. As mentioned above, the intermediate steps of this still ongoing phase I/II clinical trial included a total dose of 36.0GyE or more, the follow-up time was 6 months or more after CIRT, and the local control ratio of T1 tumors (≦30mm in diameter) was as high as 90% at the total dose of 36.0GyE. The 72 primary tumors of the 72 patients were treated by carbon ion beam irradiation alone using a total dose of 36.0GyE (n=18), 38.0GyE (n=14), 40.0GyE (n=15), 42.0GyE (n=15), or 44.0GyE (n=10) per single fractionation. Mean age was 75 years, and gender breakdown was 23 females and 49 males. The tumors were 47 T1 and 25 T2. Mean tumor size was 27.7 mm in diameter. By type (cancer type was determined by biopsy), there were 45 adenocarcinomas, 26 squamous cell carcinomas, and one large cell carcinoma. Medical inoperability was 65% (Table 2).

Age (mean)		46-87 (75)
Gender	Female	23
	Male	49
PS	0	45
	1	26
	2	1
Tumor size (mean)		10-62 (27.7)*
Stage	IA	47
	IB	25
Histology	Adenoca.	45
	Sq cell ca.	26
	Large cell ca.	1
Reason of poor candidate for surgery		
	Refusal	25 (35)**
	Medically inope.	47 (65)**
Total dose (GyE)		
	36.0	18
	38.0	14
	40.0	15
	42.0	15
	44.0	10
*mm, **percent		Aug. 31, 2007

Table 2 Treatment & characteristics of 72 patients with stage I NSCLC

[Carbon ion beam irradiation]

The same system of carbon ion beam irradiation was used in both phase II and phase I/II clinical trials. The targets were usually irradiated from four oblique directions without prophylactic elective nodal irradiation (ENI). A greater than 10-mm margin was set outside the gross target volume (GTV) to determine the clinical target volume (CTV). The planning target volume (PTV) was established by adding an internal margin (IM) to the CTV. The IM was determined by extending the target margin in the head and tail direction by a width of 5 mm, leading to a successful prevention of marginal recurrence possibly resulting from respiration movement [2]. Fig. 1 shows the dose distribution maps for a representative case. A respiratory-gated irradiation system was used in

all irradiation sessions. Fig. 2 shows the CIRT room. We used vertical or horizontal beams in 2 oblique positions including 4 directions-irradiation totally.

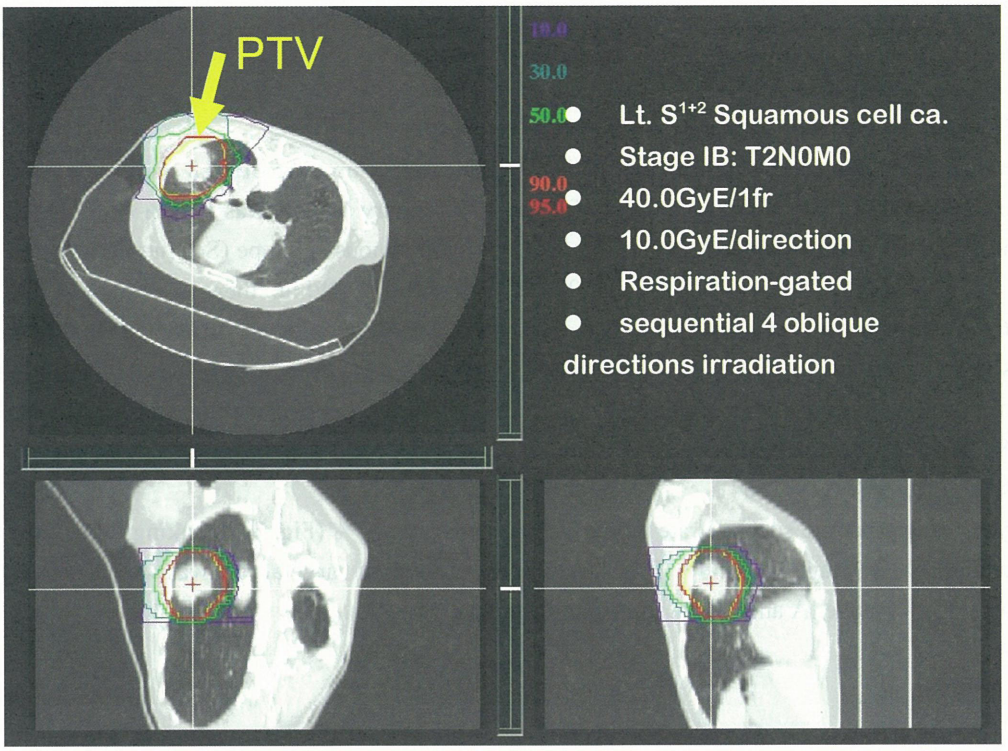

Fig. 1 Dose distribution maps of a 71-yr-old female)

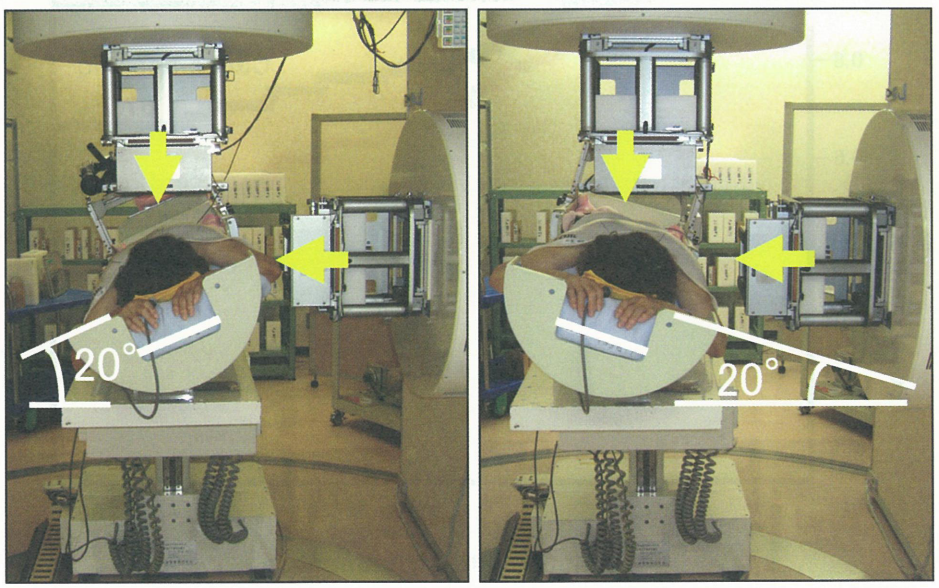

Fig. 2 Treatment room

[Statistical analysis]

Local control and survival were assessed by Kaplan-Meier method. For statistical testing, the Log-rank test was used.

Results

[Phase II clinical trial (#9802, #0001)]

All patients were followed up until death, with a median follow-up time of 50.8 months, ranging from 2.5 months to 70.0 months. The local control rate for the 131 primary lesions was 91.5% (Fig. 3), those for T1 (n=72) and T2 (n=59) tumors were 96.3% and 84.7% and for squamous cell type (Sq) (n=43) and non-squamous cell type (Non-Sq) (n=88) were 87.1% and 93.8%, respectively. While there was significant difference (p=0.0156) in tumor control rate between T1 and T2, there was no significant difference (P=0.1516) between squamous and non-squamous in T1+T1, nor between T1 and T2. However, with respect to squamous cell type cancer, local control was 100% for T1 (n=17) and 78.0% for T2 (n=26), with a near-significant difference (p=0.0518). The local control of non-squamous tumors was 95.3% for T1 (n=55) and 91.0% for T2 (n=33), with no significant difference (p=0.3364).

The 5-year cause-specific survival rate of the 127 patients was 67% (Fig. 3), breaking down into 84.8% for stage IA and 43.7% for stage IB tumors (Fig. 4A). The 5-year overall survival rate was 45.3% (Fig. 3), breaking down into 53.9% for stage IA and 34.2% for stage IB tumors (Fig. 4B).

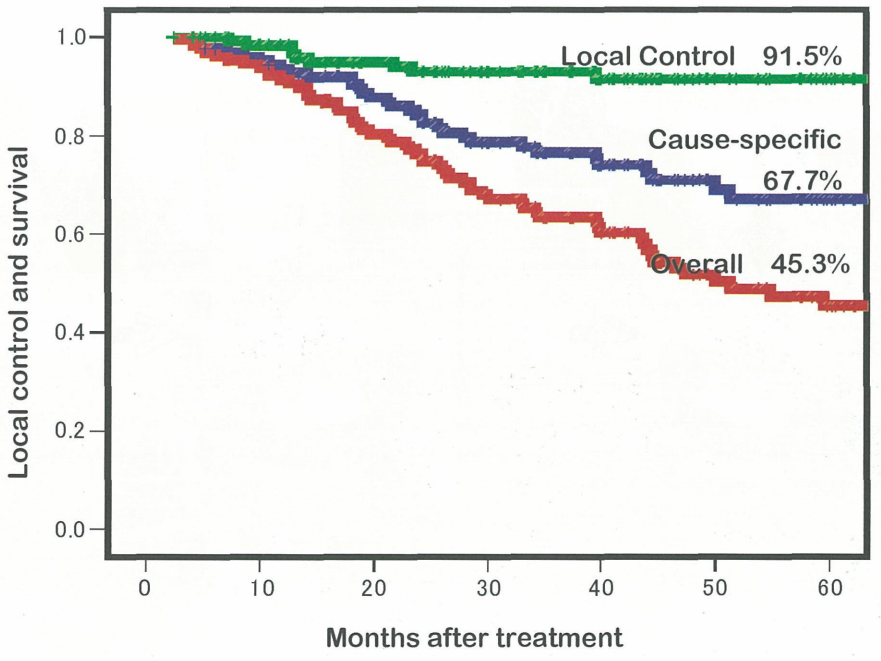

Fig. 3 Local control (n=131) and survivals (n=127) by CIRT

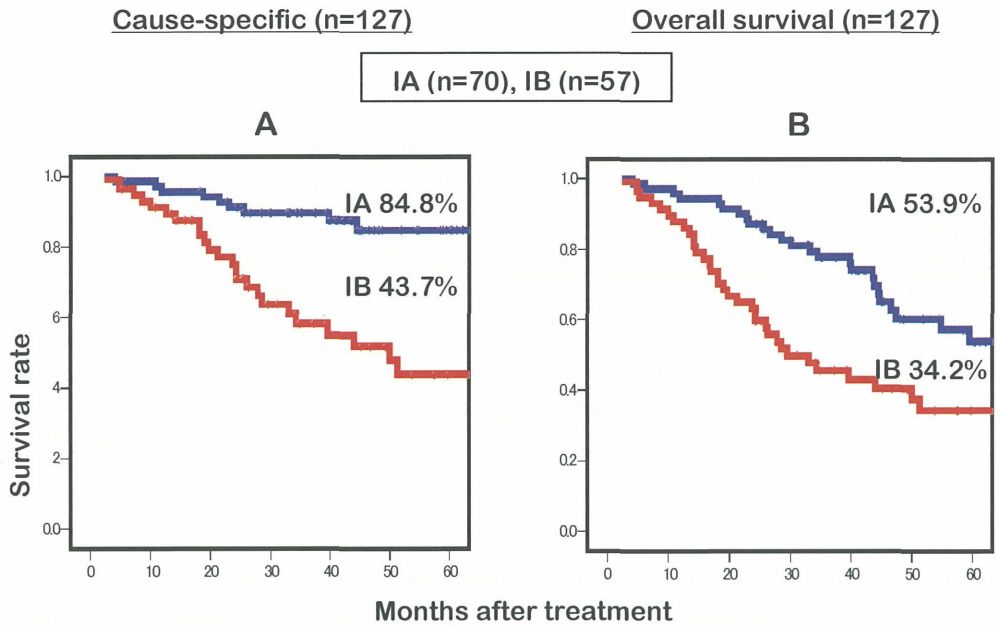

Fig. 4 Survivals of patients by stage IA and stage IB

Toxicities to the skin and lung caused by CIRT were assessed according to RTOG (early) and RTOG/EOTRC (late) as shown in Tables 3, 4. Early skin reactions were assessed for 131 lesions and late skin reactions for 128 lesions. Of the early reaction lesions, 125 were grade 1 and 6 were grade 2. Among the late reaction lesions, 126 were grade 1, 1 was grade 2, and 1 was grade 3. Lung reaction was clinically assessed in the total 129 patients. One hundred twenty-seven had grade 0 and 2 had grade 2 in early reaction. Late effects werefollowed up in 126 patients: 7 patients had grade 0, 116 patients had grade 1, and 3 patients had grade 2. No higher than a single grade 2 reaction was observed.

Skin		Early reaction (RTOG)						Late reaction (RTOG)					
		Lesion No.	Grade					Lesion No.	Grade				
			0	1	2	3	4=<		0	1	2	3	4=<
	#9802	51	0	50	1	0	0	51	0	49	1	1	0
	#0001	80	0	75	5	0	0	77*	0	77	0	0	0
	Total	131	0	125	6	0	0	128	0	126	1	1	0

* 3 cases were not observed due to early death

Table 3 Adverse skin reactions by CIRT

Fifty-three of the 127 patients (41.7%) had recurrence, all occurring between 1 and 54 months (median, 10.5 months) after the commencement of therapy. No occurrence was observed in the other 74 patients (58.3%). The 9 primary recurrences (7.1%) and 11 regional metastases (8.7%) consisting of 7 regional nodes (5.5%), one

intrabronchial (0.8%), and 3 intralobar metastases (PM1) (2.4%) occurred in the loco-regional site. In one patient primary recurrence was seen at the margin, while in another it occurred in-field.

Lung		Early reaction (RTOG)						Late reaction (RTOG)					
		Lesion	Grade					Lesion	Grade				
		No.	0	1	2	3	4=<	No.	0	1	2	3	4=<
	#9802	50	49	0	1	0	0	50	0	48	2	0	0
	#0001	79	78	0	1	0	0	76*	7	68	1	0	0
	Total	129	127	0	2	0	0	126	0	116	3	0	0

* 3 cases were not observed due to early death

Table 4 Adverse lung reactions by CIRT

By sub-stage classification, the incidence of loco-regional recurrence, pleural dissemination, and distant metastasis for stage IB (63%) was much higher than for IA (24%). The total incidence of first recurrence for stage IB (63%) tended to be higher than for stage IA (24%). Verification by χ^2 test showed no significant difference (χ^2=1.63).

The cause of death was as follows: 62 out of the 127 patients (48.8%) died, half of disease progression. Among the patients with recurrence, 5 of 9 with primary recurrence (55%) died from disease progression. Ten of the 11 patients with regional metastases were re-treated, 9 with CIRT and 1 with photons. Seven of these patients, although they had no further recurrence, died due to intercurrent disease, and 1 with node metastasis but no re-treatment died of disease progression. Eight of the 11 patients with regional metastases (72%) died, and 9 of the 10 patients (90%) with malignant pleurisy and 17 of the 23 patients (74%) with distant metastases died of disease progression. Five of them died due to primary recurrence, and 26 due to metastasis and dissemination. For the remaining 31 patients, intercurrent diseases were the cause of death [3, 4].

[Phase I/II clinical trial (single fractionation)]

All patients were followed up until death, with a median follow-up time of 16.1 months, ranging from 1.6 months to 21.6 months. The overall local control rate for the 72 primary lesions was 89.3%, and those for the T1 (n=47) and T2 (n=25) tumors were 94.6% and 78.7%, respectively (Fig. 5). The 28-month overall survival rate was 85.4% and the cause-specific survival rate was 98.0%.

Toxicities of CIRT to the skin and lung were assessed according to NCI-CTC (early) and RTOG/EOTRC (late) as shown in Tables 5 and 6. Early skin reactions were assessed for 72 lesions and late skin reactions for 69 lesions. Of the early reaction lesions, 69 were grade 1 and one was grade 2. Among the late reaction lesions, 65 were grade 1 and one was grade 2. Lung reactions were clinically assessed in the 72 patients. Forty-five had grade 0, and 27 had grade 1 among early reactions. Late reactions were followed up in 69 patients, with 12 showing grade 0 and 57 grade 1. The clinical course of a 71-year-old female is shown in Fig. 6 and Fig. 7. Tumor shrinkage and slight lung fibrosis is apparent, and grade 1 skin reaction was observed.

Discussion

In the present study, local control, cause-specific, and overall survival rates for the 127 patients in the phase II clinical trial were 91.5%, 67.0%, and 45.3%, respectively. Also, overall local control, local control in T1 tumor, and local control in T2 tumor were 89.3%, 94.6%, and 78.7%, respectively, by single fractionation. Local control

in T1 tumor has successfully been raised more than 94% using single fractionation. Toxicities to skin, lung and bone were minimal.

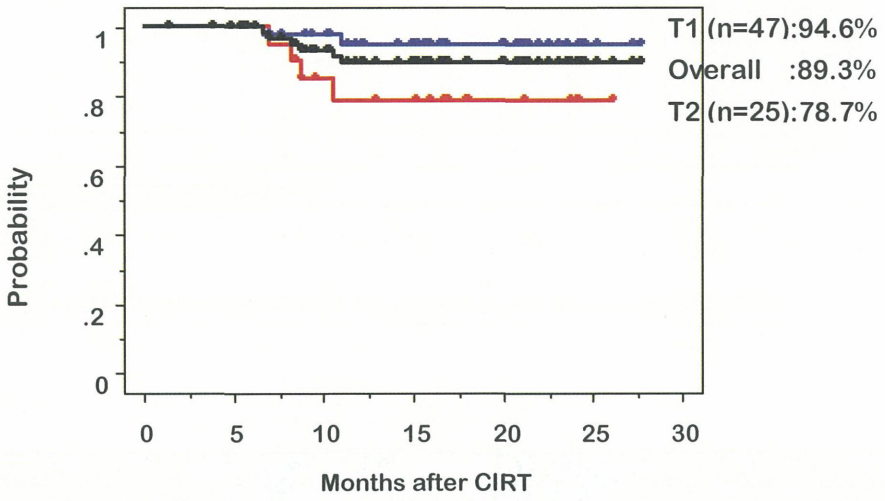

Fig. 5 Tumor control rates after ICRT using single fractionation

Skin	Total dose (GyE)	Early reaction (NCI-CTC)						Late reaction (RTOG/EORTC)					
		No. of Case	Grade					No. of Case	Grade				
			0	1	2	3	4=<		0	1	2	3	4=<
	36.0	18	0	18	0	0	0	17*	0	17	0	0	0
	38.0	14	0	14	0	0	0	13*	0	13	0	0	0
	40.0	15	1	13	1	0	0	15	2	12	1	0	0
	42.0	15	0	15	0	0	0	14*	0	14	0	0	0
	44.0	10	1	9	0	0	0	10	1	9	0	0	0
	Total	7	2	69	1	0	0	69	3	65	1	0	0

*One case was not observed in each group

Table 5 Adverse skin reaction after CIRT using single fractionation

Lung	Total dose (GyE)	Early reaction (NCI-CTC)						Late reaction (RTOG/EORTC)					
		No. of Case	Grade					No. of Case	Grade				
			0	1	2	3	4=<		0	1	2	3	4=<
	36.0	18	12	6	0	0	0	17*	3	14	0	0	0
	38.0	14	9	5	0	0	0	13*	2	11	0	0	0
	40.0	15	11	4	0	0	0	15	4	11	0	0	0
	42.0	15	9	6	0	0	0	14*	1	13	0	0	0
	44.0	10	4	6	0	0	0	10	2	8	0	0	0
	Total	72	45	27	0	0	0	69	12	57	0	0	0

*One case was not observed in each group

Table 6 Adverse lung reaction after CIRT using single fractionation

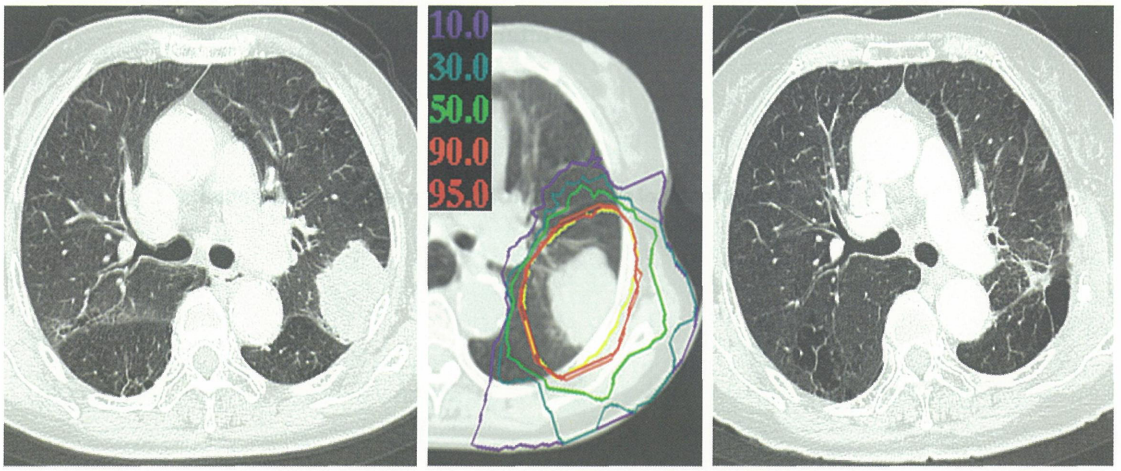

Fig. 6 Clinical course of 71-year-old female (T2N0M0 squamous cell carcinoma) after CIRT (40GyE/ single fractionation). CT (A), dose distribution map (B), and CT (C) at18 months after CIRT are shown. Apparent tumor shrinkage was observed without severe lung fibrosis.

Out of the 131 primary cancers of 127 patients, local occurrence occurred in 9 patients (6.8%). The average recurrence time was 17.2 months, ranging from 7 to 39 months. According to our previous study, the observation period required to determine local control of the irradiated lesions was at least 3 years post therapy [1]. However, the present study suggested the need for a longer observation period. It is self-evident that prolonged survival guarantees more reliable observation of local control results.

For the correct assessment of local control of patients who could not be observed for such a long duration because of death resulting from metastasis/dissemination or intercurrent disease, a histological approach based on repeated bronchoscopy was used, providing evidence of the absence of viable tumor cells in the collected specimens [3].

Furthermore, definite tumor control was also confirmed by the autopsies of CIRT-treated patients and in cases treated by surgery [5]. Such high and definite tumor control appears to be an outstanding feature of CIRT. Presumably, this is primarily due to the radiobiological nature of the high LET beams, which may account for the higher survival rate of stage I NSCLC. On the other hand, the failure of local control for primary tumors directly affects the poor survival of stage I NSCLC patients [1, 3]. Among our cases, 5 of 9 patients with primary recurrence (55%) died due to disease progression.

Eleven regional recurrences occurred. This incidence was close to that of surgery (7.5% [6], 11% [7]). Eight of them (72%) died. Only one patient, with no retreatment, died due to disease progression. The other 7 retreated patients died due to intercurrent death. Martini et al. [6] reported that any resection less than lobectomy and no lymph node dissection had adverse effects on recurrence and survival. In contrast, our treatment strategy for regional recurrence is thought to have gained validity as the standard surgical procedure for stage I NSCLC.

Nine of the 10 patients (90%) with malignant pleurisy and 17 of the 23 patients (74%) with distant metastasis died of disease progression. The poor prognosis of stage IB cases was based on the high incidence of pleural and distant metastasis.

Fig. 7 Skin reaction after CIRT (40.0GyE/1fr). Grade 1 reactions were observed.

With clinical stage I NSCLC, our 5-year overall survival results were somewhat inferior to the surgical ones [3, 5]. This difference may be due to the significant age gap between the two groups. The incidence of death due to recurrence in the surgical groups was 29% or 36%, whereas that due to intercurrent diseases was 19% or a few % [6, 7]. In contrast, our patients showed a higher incidence of death due to intercurrent diseases (60%) than death due to recurrence (40%). Comparison of stage IA with stage IB revealed a large difference in stage IA between overall (53.9%) and cause-specific (84.8%) survival, while there was a smaller difference in stage IB between overall (34.2%) and cause-specific (43.7%) survival. Such large and small survival differences in the two stage I subgroups might well be explained by the low incidence of recurrence death in stage IA (24%) and its high incidence in stage IB (63%). Generally, such a high frequency of intercurrrent death might be related to the advanced age of our patients, as they were on average 10 years older than the surgical patients [6, 7]. As we have reported, elderly patients 80 years and older can be treated safely by CIRT [8].

Compared with pulmonary damage reported in stereotactic radiotherapy for stage I NSCLC [9-11], the incidence and severity in our patients seem to be remarkably low. These lesser adverse effects on the lung were achieved as a result of the small volume irradiated. This advantage is a result of the excellent dose distribution property unique to carbon ion beams and lies in the formation of a Bragg peak in contrast to X-ray as a permeating beam.

Conclusions

One hundred twenty-seven stage I NSCLC patients with 131 primary tumors were treated with CIRT using a total dose of 72GyE in a regimen of 9 fractions over 3 weeks, and 52.8GyE for stage IA and 60GyE for stage IB at 4 fractions in one week. In addition, 54 stage I NSCLC patients with 54 primary tumors were treated with single-fraction CIRT using total doses ranging from 38.0GyE to 44.4GyE.

1. The local control rate of 131 primary lesions was 91.5%. There was statistical difference between the local control rates for T1 and T2, and near significance between squamous cell carcinoma and non-squamous cell carcinoma of T2.
2. Five-year overall and cause-specific survival rates of 127 patients were 45.3% and 67.0%, respectively.
3. Five-year overall survival rates of the patients with stage IA and stage IB were 53.9% and 34.2%, while five-year cause-specific survival rates with stage IA and stage IB were 84.8% and 43.7%, respectively.
4. There was high incidence of intercurrent death due to advanced age and related complications.
5. Adverse effects on skin and lung were minimal, indicating the safety of the modality. Carbon beam radiotherapy, which is an excellent new modality in terms of a high QOL and ADL, is a valid alternative to surgery for stage I cancer, especially for elderly and inoperable patients.
6. In CIRT using single fractionation with a total dose range from 36.0GyE to 44.0GyE, the local control rate for the 72 primary lesions was 89.3%, and those for the T1 (n=47) and T2 (n=25) tumors were 94.6% and 78.7%, respectively.
7. CIRT using single fractionation is very effective, viewed at an intermediate step, and is a safe modality for stage I NSCLC.

References

[1] Miyamoto T, Yamamoto N, Nishimura H, et al. Carbon ion radiotherapy for stage I non-small cell lung cancer. Radiother Oncol 2003;66:127-140.

[2] Koto M, Miyamoto T, Yamamoto N, et al. Local control and recurrence of stage I non-small cell lung cancer after carbon ion radiotherapy. Radiother Oncol 2004;71:147-156.

[3] Miyamoto T, Baba M, Yamamoto N, et al. Curative treatment of stage I non-small cell lung cancer with carbon ion beams using a hypo-fractionated regimen. Int J Radiat Oncol Biol Phys 2007;67:750-8.

[4] Miyamoto T, Baba M, Sugane T, et al. Carbon ion radiotherapy for stage I non-small cell lung cancer using a regimen of four fractions during 1 week. J Thorac Oncol 2007;2:916-26.

[5] Yamamoto N, Miyamoto T, Nishimura H, et al. Preoperative carbon ion radiotherapy for non-small cell lung cancer with chest wall invasion - pathological findings concerning tumor response and radiation induced lung injury in the resected organs. Lung Cancer 2003;42:87-95.

[6] Harpole DH, Herndon JE, Yung WG, et al. Stage I nonsmall cell lung cancer. A multivariate analysis of treatment methods and patterns of recurrence. Cancer 1995;76:787-796.

[7] Martini N, Bains MS, Burt ME, et al. Incidence of local recurrence and second primary tumors in resected stage I lung cancer. J Thorac Cardiovasc Surg 1995;109:120-129.

[8] Sugane T, Baba M, Imai R, et al. Carbon ion radiotherapy for elderly patients 80 years and older with stage I non-small cell lung cancer. Lung Cancer (2008), doi:10.1016/j.lungcan.2008.07.007.

[9] Nagata Y, Takayama K, Matsuo Y, et al. Clinical outcomes of a phase I/II study of 48Gy of stereotactic body radiotherapy in 4 fractions for primary lung cancer using a stereotactic body frame. Int J Radiat Oncol Biol Phys 2005;63:1427-1431.

[10] Onishi H, Shirato H, Nagata Y, et al. Hypofractionated stereotactic radiotherapy (HypoFXSRT) for stage I non-small cell lung cancer: updated results of 257 patients in a Japanese multi-institutional study. J Thorac Oncol 2007;2 (7 Suppl 3):S94-100

[11] Timmerman R, McGarry R, Yiannoutsos C, et al. Excessive toxicity when treating central tumors in a phase II study of stereotactic body radiation therapy for medically inoperable early-stage lung cancer. J Clin Oncol 2006;24:4833-4839

Carbon Ion Radiotherapy in Bone and Soft Tissue Sarcomas

Tadashi Kamada, Shinji Sugawara, Hiroshi Tsuji, Itsuko Serizawa, Reiko Imai, Toru Okada, and Hirohiko Tsujii

Research Center for Charged Particle Therapy, National Institute of Radiological Sciences, Chiba, Japan
e-mail address: t_kamada@nirs.go.jp

Abstract

The Heavy Ion Medical Accelerator in Chiba (HIMAC) is the world's first heavy ion accelerator complex dedicated to medical use in a hospital environment. Heavy ions have superior depth-dose distribution and greater cell-killing capability. In June 1996, clinical research for the treatment of bone and soft tissue sarcomas was begun using carbon ions generated by the HIMAC. As of August 2008, a total of 421 patients with bone and soft tissue sarcoma were enrolled into the clinical trials. Most of the patients had locally advanced and/or medically inoperable sarcomas. The clinical trial revealed that carbon ion radiotherapy provided definite local control and offered a survival advantage without unacceptable morbidity in bone and soft tissue sarcomas that were hard to cure with other modalities.

1. Introduction

Tumors arising from bones, muscles, and vessels are referred to as bone and soft tissue sarcomas. While the incidence of these tumors is extremely low, they are capable of occurring ubiquitously throughout the body. For this reason, they are occasionally detected too late or their accurate diagnosis presents difficulty and incomplete treatment is administered on the false recognition of their being benign.

While tumor resection is the most common treatment modality for such bone and soft tissue sarcomas, major progress has been made in their management, thanks to the development of combined therapy modalities in recent years, in the wake of surgical advancements. These methods combine chemotherapy and radiotherapy with new imaging diagnostics such as MR, CT, and PET. Among these tumors, osteosarcoma originating in the limbs accounts for the majority of malignant bone tumors, and limb-sparing surgery not requiring arm or leg amputation has become possible through a combination of surgical resection with chemotherapy. The therapeutic results have also recorded a dramatic improvement in recent years: Whereas the five-year survival rate was only 10-20% in the 1970s, the latest data are up to as high as 50 - 80%. Similarly, soft tissue sarcomas developing in muscle or other soft tissues have meanwhile come to be treated by combined chemo-radiotherapy modalities and functional preservation operations achieving a five-year survival rate in excess of 70%. In the case of tumors that have developed in or near the spinal cord or in the pelvis, as well as advanced limb tumors and postoperative recurrent tumors, however, chemotherapy may often not be very effective and curative surgery may be difficult to perform. Moreover, most bone and soft tissue sarcomas are known to be resistant to conventional radiation. Thus, despite the significant progress seen in the treatment of bone and soft tissue sarcomas in recent years, patients judged intractable to surgery still face the harsh reality of being less likely to find an effective treatment option. In this regard, carbon ion radiation with its superior dose conformity and its potent biological effect holds out much promise for also achieving outstanding results with radio-resistant bone and soft tissue sarcomas. This

article presents our experiences with carbon ion radiotherapy using the Heavy Ion Medical Accelerator in Chiba (HIMAC) at NIRS.

2. Patients and Methods

A dose escalation trial (phase I/II trial) using carbon ion beams was carried out on 64 lesions of 57 bone or soft tissue sarcoma patients during the period from June 1996 until February 2000 [1]. A fixed-dose phase II trial was then initiated in April 2000, and records as of August 2008 show that 377 lesions of 358 patients have been treated. Both of these trials included bone or soft tissue sarcoma patients for whom surgical resection was contra-indicated. The main eligibility criteria are listed in Table 1. While the phase II trial included patients with radiation-associated sarcoma, it did exclude patients with intravascular tumor embolus. Three hundred and eighty-eight patients (414 lesions) in these 2 trials have been followed for 6 months or longer after carbon ion treatment as of August 2008. Their clinical characteristics are summarized in Table 2. There were 230 males and 158 females, and their age ranged from 12 to 85 years, with a median of 52 years. Tumor locations were as follows: 89 lesions in the spine or paraspinal region; 298 in the pelvis, and 27 in the extremities and other sites. The tumors were categorized as 304 primary bone and 84 primary soft tissue sarcomas. Histological classification showed that chordoma was the most frequent tumor, accounting for 126 patients, followed by osteosarcoma in 66 patients, chondrosarcoma in 63 patients, MFH (including 14 bone primaries) in 30 patients and Ewing/PNET in 28 patients (including 5 soft tissue primaries). For pathological confirmation, central pathological review of surgical or biopsy specimen was carried out. All patients enrolled in the trials gave their written informed consent.

Table 1. Eligibility

- Histologically confirmed bone or soft tissue sarcomas
- Unresectable or declines surgery
- Gross measurable lesion
- Lesion size <15cm in maximum diameter
- KPS 60~100%
- No prior radiotherapy to the lesion
- Signs informed consent statement

Abbreviations: KPS, Karnofsky performance status

Table 2. Patient characteristics

Characteristic		No. (N = 388)
Age, years		
Median (range)		52 (12~85)
Sex		
Female/ Male		158/230
Tumor sites (414 lesions)		
Pelvis		298
Spine/para-spine		89
Extremities etc		27
Histology		
	Bone	304
	Chordoma	126
	Osteosarcoma	66
	Chondrosarcoma	63
	PNET	23
	MFH	14
	Others	12
	Soft tissue	84
	MFH	16
	MPNST	15
	Synovial sarcoma	8
	Liposarcoma	8
	PNET	5
	Leiomyosarcoma	5
	Rhabdomyosarcoma	4
	Others	23
Clinical target volume, cm^3		
Mean (range)		489 (16~2900)

Abbreviations: PNET, primitive neuroectodermal tumor; MFH, malignant fibrous histiocytoma; MPNST, malignant peripheral nerve sheath tumor

The features of the Heavy Ion Medical Accelerator in Chiba (HIMAC) and the carbon ion beam have been previously described. In brief, the accelerated carbon ion beam energies were 290, 350, and 400 MeV. The range of the beams was a depth of 15− 25 cm in water. An appropriately sized ridge filter corresponding to the tumor size was selected to form the spread-out Bragg peak (SOBP). A compensation bolus was fabricated for each patient to make the distal configuration of the SOBP similar to the shape of the target volume. A multi-leaf collimator defined the margins of the target volume. Patients were placed in customized cradles and immobilized with a low-temperature thermoplastic sheet. A set of 5-mm-thick CT images was taken for the treatment planning. Three-dimensional treatment planning was performed with HIPLAN software (National Institute of Radiologic Sciences, Chiba, Japan) for the planning of carbon ion therapy. A margin of 5 mm was usually added to the clinical target volume to create the planning target volume. When the tumor was located close to critical organs such as the spinal cord, skin or bowel, the margin was reduced accordingly. The clinical target volume was covered by at least 90% of the prescribed dose. Dose was calculated for the target volume and any nearby critical structures and expressed in Gray-Equivalent (GyE = carbon physical dose (Gy) x Relative Biological Effectiveness {RBE}). Carbon ion radiotherapy was given once daily, 4 days a week (Tuesday to Friday), for a fixed 16 fractions in 4 weeks. Patients were treated with two to eight irregularly shaped ports (median, 3 ports).

One port was used in each session. At every treatment session, the patient's position was verified with a computer-aided on-line positioning system. The patient was positioned on the treatment couch with the immobilization devices, and digital orthogonal X-ray TV images in that position were taken and transferred to the positioning computer. They were compared with the reference image on the computer screen and the differences were measured. The treatment couch was then moved to the matching position until the largest deviation from the field edge and the isocenter position was less than 2 mm. For all of these patients, a total dose ranging from 52.8 GyE to 73.6 GyE was administered by a fractionation regimen of 16 fractions over four weeks (with single radiation doses of 3.3 - 4.6 GyE).

3. Results

A dose escalation trial (phase I/II trial) with a total dose ranging from 52.8 GyE to 73.6 GyE administered in 16 fractions over four weeks (single radiation doses of 3.3 - 4.6 GyE) was carried out on 64 lesions of 57 bone and soft tissue sarcoma patients between June 1996 and February 2000. As 7 of the 17 patients treated with 73.6 GyE were found to have grade 3 RTOG acute reactions (skin), dose escalation was halted at this dose level. No other grade 3 or worse acute reactions were detected. These findings made it clear that with a fractionation regimen of 16 fractions over four weeks, a total dose of 70.4 GyE was the maximum applicable dose in cases in which skin presented a problem, and a total dose of 73.6 GyE was possible in other cases. The overall local control rate was 89% at 1 year, 63% at 3 years, and 63% at 5 years. A significant difference was found between the local control rates achieved with a total dose of 57.6 GyE or less and those with 64.0 GyE or more. The median survival period was 31 months (2-96 months), and the 1-, 3- and 5-year survival rates were 82%, 47%, and 37%, respectively. A fixed-dose phase II trial was then initiated in April 2000, and as of August 2008, 362 patients have been enrolled for treatment. The number of lesions and patients analyzed six months or longer after therapy stands at 350 lesions of 331 patients, with 10 of these lesions having been treated with a dose of 73.6 GyE (4.6 GyE per fraction), 19 with 64 GyE (4.0 GyE per fraction) and 21 with 67.2 GyE (4.2 GyE per fraction). The remaining 299 lesions were treated with a dose of 70.4 GyE (4.4 GyE per fraction). As of the present, the 2- and 5-year local control rates are 88% and 79%, and similarly, the overall survival rates are 79% and 57%, respectively (Figure 1).

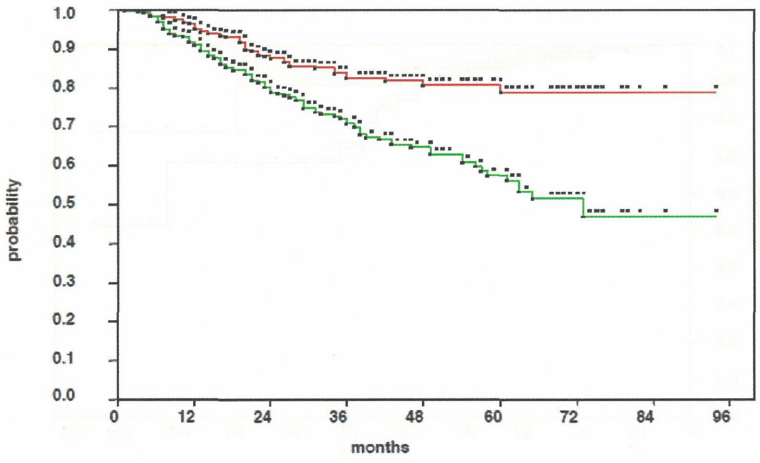

Figure 1. Actuarial local control and overall survival in the 331 phase II study patients with bone or soft tissue sarcomas. Local control rate at 5 years was 79%, and overall survival rate at 5 years was 57%.

Radiation morbidities are summarized in Table 3. Grade 3 or worse toxic reactions included 2 patients with acute skin toxicities (grade 3) and 7 patients with late skin toxicities (grade 3: 6 patients; grade 4: 1 patient).

These late skin reactions suggest that the following may be risk factors in addition to the total dose: 1) subcutaneous tumor invasion, 2) tumor volume, 3) sacrum, 4) previous surgery, 5) additional chemotherapy, and 6) irradiation from two portals. It was possible, however, to prevent these reactions by aiming for a standard dose of 70.4 GyE and by modifying the irradiation method that may include irradiation from three portals, in order to reduce the dose delivered to the skin.

The entire evaluable population for both the above clinical trials amounted to 414 lesions of 388 patients, and their aggregate 5-year local control rate presently stands at 76% and their 5-year overall survival rate at 54% (Figure 2). The 126 chordoma patients (excluding patients with the base of the skull primaries) of this total have a 5-year local control rate of 89% and a 5-year overall survival rate of 85% (Figure 3) (A report on the 30 sacral chordoma patients who were observed for a period of two years or longer was published in the Clinical Cancer Research [2]).

The 5-year local control rate and 5-year overall survival rate for the 65 patients with osteosarcoma of the trunk were 62% and 28% (Figure 4) and for the 63 chondrosarcoma patients 65% and 59%, respectively. (Figure5)

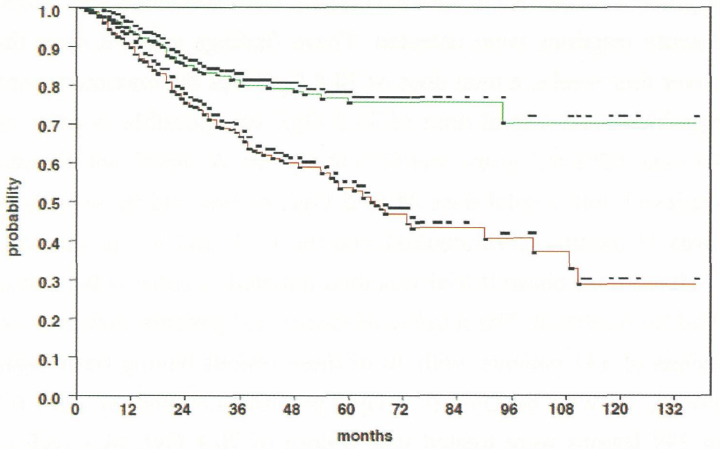

Figure 2. Actuarial local control and overall survival in the 388 patients with bone or soft tissue sarcomas. Local control rate at 5 years was 76%, and overall survival rate at 5 years was 54%.

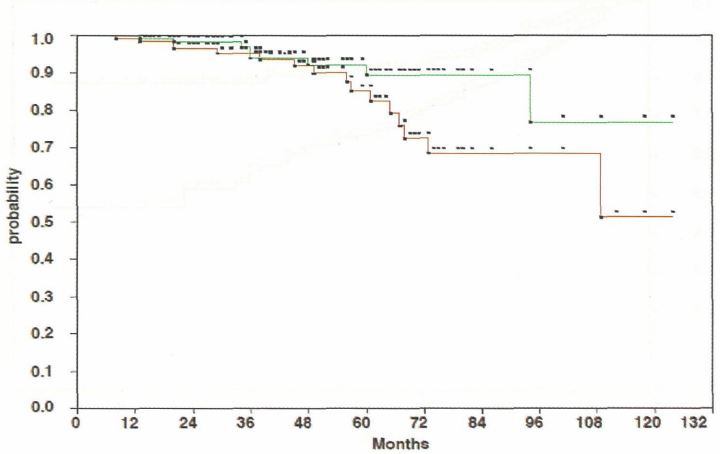

Figure 3. Actuarial local control and overall survival in the 126 patients with chordoma. Local control rate at 5-years was 89 %, and overall survival rate at 5-years was 85%.

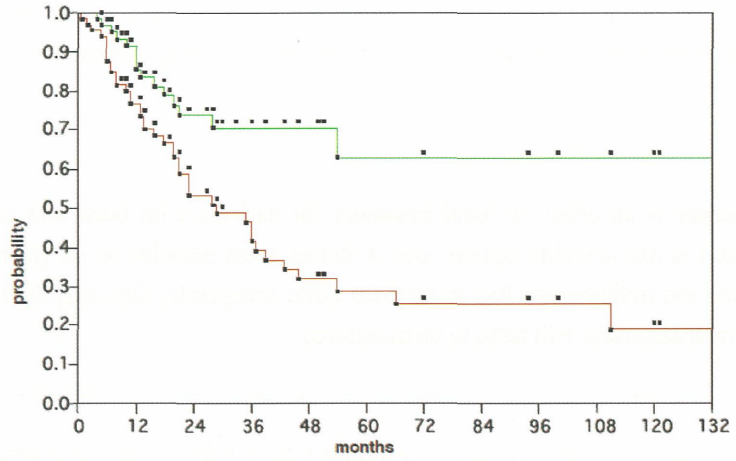

Figure 4. Actuarial local control and overall survival in the 65 patients with osteosarcoma of the trunk. Local control rate at 5 years was 62%, and overall survival rate at 5 years was 28%.

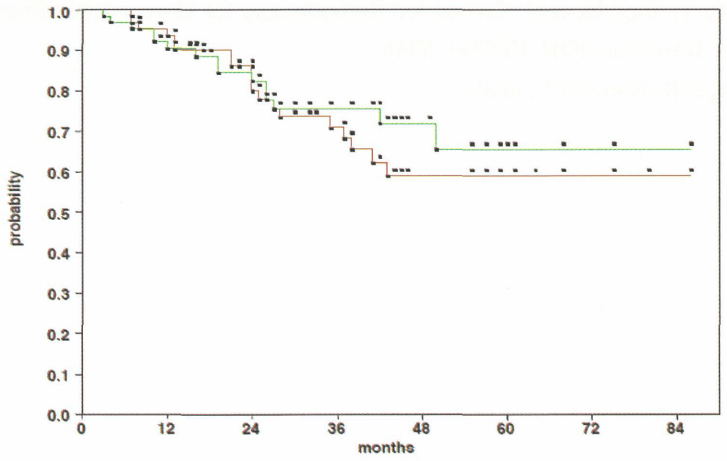

Figure 5. Actuarial local control and overall survival in the 63 patients with chondrosarcoma. Local control rate at 5 years was 65%, and overall survival rate at 5 years was 59%.

4. Discussion

In this study, carbon ion radiotherapy was well tolerated and demonstrated substantial activity against sarcomas. These results were obtained in patients with advanced and/or chemo-resistant gross lesions not suited for surgical resection and located mainly in the trunk. Irradiation with a total dose ranging from 64 to 73.4 GyE in 16 fractions over four weeks resulted in a local control rate of 80% or more for bone and soft tissue sarcomas disqualified from surgery. Although treatment results after carbon ion radiotherapy have so far been quite satisfactory, it is imperative to continue with long-term follow-up observation and carry out further analyses to assess local control, toxicities, survival rate and QOL as a function of such criteria as histological type, location, tumor size, irradiation field and dose to achieve a safe and effective therapy regimen. For small lesions, in particular, the possibilities of a shorter irradiation regimen should be explored. Systematic analyses will be essential to determine the optimum dose and irradiation field setting in accordance with the patient's histological type and tumor location and to shed light on the problems involved. Research will also be needed to clarify the role of heavy particle radiotherapy in the context of combined therapy modalities for bone and soft tissue sarcomas. Not only for patients disqualified from surgery but also for elderly patients and patients with major functional loss consequent to surgical resection, carbon ion radiotherapy is seen as a valid alternative to surgery.

While previous experience with carbon ion radiotherapy to the extremities has so far been rather limited, the combination of carbon ion radiation and surgery could offer a promising potential for patients intractable to limb-sparing surgery as a modality for widening the scope of limb-retaining therapy.

5. Conclusion

Carbon ion radiotherapy is an effective local treatment for patients with bone and soft tissue sarcomas for whom surgical resection is not a viable option, and it shows great promise as an alternative to surgery. The morbidity rate of carbon ion radiotherapy has so far been quite acceptable, although the long-term safety of this approach for patients with sarcomas will need to be monitored.

References

[1] Kamada T, Tsujii H, Tsuji H, et al. Efficacy and Safety of Carbon Ion Radiotherapy in Bone and Soft Tissue Sarcomas. Journal of Clinical Oncology. 2002;20:4466-4471.

[2] Imai R, Kamada T, Tsuji H, et al. Carbon Ion Radiotherapy for Unresectable Sacral Chordomas. Clinical Cancer Research. 2004;10:5741-5746.

[3] Serizawa I, Kagei K, Kamada T, et al.

Carbon Ion Radiotherapy for Hepatocellular Carcinoma

Hirotoshi Kato, Shigeo Yasuda, Takeshi Yanagi, Hiroshi Imada, Shigeru Yamada, Jun-etsu Mizoe, Tadashi Kamada, and Hirohiko Tsujii

Hospital, Research Center for Charged Particle Therapy, National Institute of Radiation Sciences, Chiba, Japan
e-mail address: h_kato@nirs.go.jp

Abstract

The objective of this paper is to present a summary explanation of the clinical study on carbon ion radiotherapy for hepatocellular carcinoma (HCC) conducted from April 1995 to August 2005 at the Research Center for Charged Particle Therapy, National Institute of Radiation Sciences, Japan. A total of 193 patients with HCC were enrolled in the clinical trials with carbon ion beams. In the first and second phase I/II clinical trials, dose escalation experiments were carried out in incremental steps of 10%, resulting in the confirmation of both the safety and the effectiveness in short-course regimens of 12, 8 and 4 fractions. Based on the results, a phase II clinical study with fixed fractionation, that is, 52.8 GyE/4 fractions, was performed, where 47 patients were treated with low toxicity, attaining a high local control rate of 95% at 5 years. The last clinical study was conducted from April 2003 to August 2005 with an even more hypofractionated regime of 2 fractions/2 days, in which 36 patients were safely treated within a dose escalation range from 32.0 GyE to 38.8 GyE. The 2-fraction therapy protocol is continuing under the license of Highly Advanced Medical Technology. There have been no therapy-related deaths and no severe adverse events until now.We can conclude that because of the low toxicity and high local control rate, carbon ion radiotherapy has a promising potential as a new, radical, and minimally invasive therapeutic option for HCC.

Introduction

Hepatocellular carcinoma (HCC) is one of the most common malignant tumors with the third highest annual mortality of 598,000 throughout the world (2002), especially in Asia, Africa, as well as a number of countries in Europe, including Spain, Italy, Greece, and France. Worldwide, some 626,000 new cases were reported in 2002. In recent years, the incidence of HCC has shown an increasing trend in Australia, India, Israel, Canada, Italy, Spain, Finland and USA. HCC is associated with liver cirrhosis in 80% of the total HCC patients. This disease is thus a very advanced form of hepatic disorder resulting from hepatitis C or B viral infection. The overall 5-year survival rate for all patients with HCC has remained steady at 3 to 5%. HCC patients often require repeated therapies owing to the multicentric nature of carcinogenesis in the cirrhotic liver. Therefore, both radical effect and minimal invasiveness are essential for the treatment of HCC. A variety of therapies are currently available for the treatment of HCC, but each of them has its specific limitations. None has so far been brought on the market that satisfies the above two essential requirements of radicality and minimal invasiveness in the treatment of tumors of any size encountered in practice.

Methods and Materials

1. Outline of carbon ion radiotherapy for HCC -Clinical Trials to Medical Treatment – (Table 1)

Clinical trials with carbon ion radiotherapy for HCC were initiated in April 1995 (1). A total of 193 patients with HCC were enrolled into the trials. In the first and second phase I/II clinical trials, dose escalation experiments were carried out in incremental steps of 10% each in order to find the optimum dose. In the first of these trials, 24 patients were treated with a 15-fraction regimen at a total dose range of 49.5-79.5 GyE. In the second trial, 86 patients were treated with short-course regimens, at total dose ranges of 54.0-69.6 GyE in 12 fractions, 48.0-52.8 GyE in 8 fractions, and 48.0-52.8 GyE in 4 fractions. Based on the results of these studies, a third protocol was established to implement a phase II clinical trial using a fixed total dose of 52.8 GyE spread over 4 fractions of 13.2 GyE each (2). The fourth protocol, a phase I/II clinical study, was performed using an even more hypofractionated regime of 2 fractions/2 days at total dose levels ranging from 32.0 GyE to 38.8 GyE (3). Most of the subjects enrolled under these four protocols had been judged as not amenable to, or as having had recurrence after, other treatments, or as having no prospect of an adequate treatment effect with any of the existing therapies. This 2-fraction therapy is currently ongoing according to guidelines allowing careful step-wise dose escalations at a 5% increase rate under the license of Highly Advanced Medical Technology.

2. Carbon ion radiotherapy

2-1. Preparation for treatment

One or two metal markers (0.5 × 3 mm) made of iridium wire were inserted near the tumor under ultrasound imaging guidance as landmarks for target volume localization. The irradiation fields were established with a three-dimensional therapy plan based on 5-mm-thick CT images. CT planning was performed using the HIPLAN, which was originally developed for 3D treatment planning (4). The clinical target volume was defined according to the shape of the tumor plus a 1.0-1.5-cm margin. The median target volume was 159 ml (range: 37-1466 ml). Double right-angled field geometry was used for irradiation in most patients (double right-angled field: 77%, double oblique field: 7%, 3-field: 14%, 4-field: 2%). Supine or prone position was selected according to the location of the tumor. Respiration gating was employed in the CT scan planning and irradiation stages (5).

2-2. Verification of patient position and target volume localization

To accurately reproduce the patient position, a low-temperature thermoplastic sheet and a customized cradle were used. Patients were immobilized on a rotating couch to permit either vertical or horizontal beam irradiation from any angle. To assess the accuracy of patient position and target volume localization, orthogonal fluoroscopy and radiography were used immediately prior to each treatment session.

Results

The clinical trial results up to the 4-fraction regimen for which observation has been continued for 5 years or longer are described below. The 2-fraction therapy was not included in this analysis due to its continuation and the as yet short observation time.

1. Toxicities

Not a single therapy-related death occurred. Using the Child-Pugh score, an international standard for assessing the degree of hepatic insufficiency, on a rating scale from 5 to 15 points, with the score increasing with deterioration of hepatic function, post-therapy changes were investigated in order to evaluate the effect of carbon ion radiotherapy on liver function. An increase in score count associated with carbon ion radiotherapy remained within one point or below in many patients in the early (within 3 months of the start of radiotherapy) and late phases (after 3 months) (Fig. 1). This demonstrated that changes in liver function remained minor after carbon ion radiotherapy was initiated. The number of cases reported with a score increase of 2 points or more in

the late phase, which is of particular clinical significance, tended to be smaller with decreasing fraction numbers.

No serious adverse effects were noted either in the skin or digestive organs. All toxicities were judged to be tolerable.

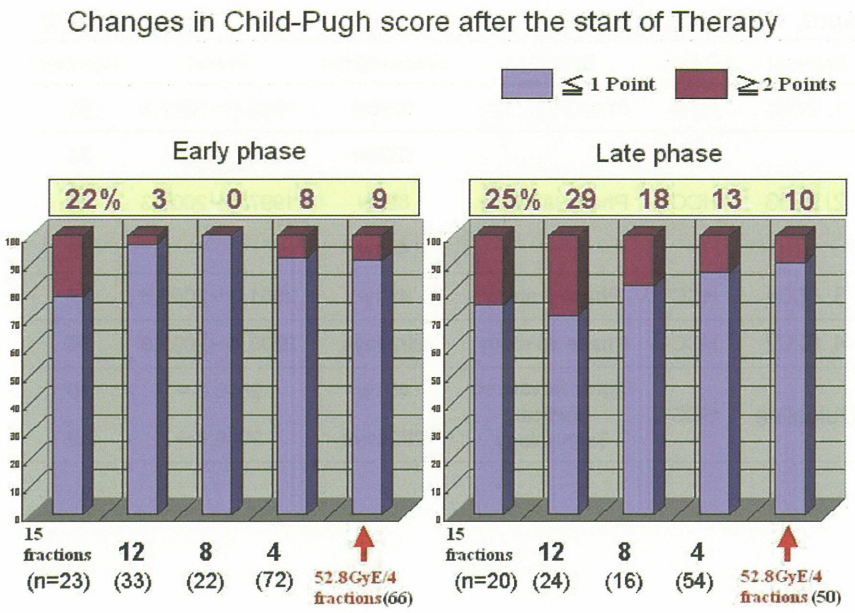

Fig. 1: Changes in Child-Pugh score before and after carbon ion radiotherapy

Variations in Child-Pugh score, an international standard to assess the degree of hepatic insufficiency changes before and after irradiation, were studied. Degrees of hepatic insufficiency can be evaluated with the Child-Pugh score on a scale from 5 to 15 points. The score point increases as the degree of hepatic insufficiency deteriorates.

The increase in score associated with carbon ion radiotherapy remained within one point or below in many patients in the early (within 3 months of start of radiotherapy) and late phases (after 3 months).

2. Anti-tumor effect

HCC develops in a successive manner, fostered by the underlying cirrhosis of the liver. Patient survival is therefore determined by the overall results, including the treatment of recurrent lesions and also the treatment of hepatic insufficiency in case of a decline in liver function. As a result, the survival rate does not reflect the effectiveness of any particular treatment alone. In comparing the effectiveness of the different therapies for HCC, it is therefore easier to make a judgment on the basis of the local control rate rather than the survival rate. In the present clinical trials, other treatments proved ineffective or led to recurrence in 57% of the patients, and as the phase I/II trials were conducted as dose escalation studies to determine the recommendable dose, there is a possibility that some of the patients may have been treated with a smaller than optimum dose. It is therefore not possible to make a simple comparison of the survival rates achieved in these clinical trials with other treatments.

In this study, only patients with an observation period of 3 years or more after the commencement of carbon ion radiotherapy were eligible for analysis and the local control rates for the analyzed lesions are shown separately according to protocol and fractionation regimen (Table 2). There were no significant differences in control rate among the different fractionation schedules.

Table 1. Outline of carbon ion radiotherapy for HCC

Carbon Ion Radiotherapy for HCC

April, 1995～August, 2008 **Total n=252**

Protocol	Disease	Category	Fractionation	Period	Number
1. 9401	HCC	Phase I/II study	15f/5w	1995.4～1997.3	24
2. 9603	HCC	Phase I/II study	12f/3w	1997.4～2001.3	34
			8f/2w		24
			4f/1w		28
3. 0004	HCC	Phase II study	4f/1w	2001.3～2003.3	47
4. 0202	HCC	Phase I/II study	2f/2days	2003.4～2005.8	36
Guideline	HCC	Highly Advanced Medical Technology	4f/1w	2005.9～	10
			2f/2days	2006.4～	49

Table 2. Results of clinical trials for HCC with carbon ion beams

Trial		Phase I/II	Phase I/II			Phase II		52.8GyE/4f
Number of fractions		15	12	8	4	4		4
Total dose (GyE)		49.5-79.5	54.0-69.6	48.0-58.0	48.0-52.8	52.8		52.8
Number of lesions		24	34	24	28	47		69
Maximum tumor diameter (cm)	Median	5.0	3.7	3.1	4.6	3.7		4.0
	Range	2.1-8.5	1.5-7.2	1.2-12.0	2.2-12.0	1.2-7.5		1.2-12.0
Recurrent Tumor	yes	18 (75%)	18 (53%)	16 (67%)	18 (64%)	20 (43%)		35 (51%)
	no	6 (25%)	16 (47%)	8 (33%)	10 (36%)	27 (57%)		34 (49%)
1-year local control (%)		92	97	91	89	96		94
3-year local control (%)		81	86	86	89	96		94
5-year local control (%)		81	86	86	89	96		94

Discussion

1. Standard therapies for HCC

The standard therapies for HCC are hepatectomy, transcatheter arterial embolization (TAE), percutaneous ethanol injection (PEI), and radio-frequency ablation (RFA). According to the Survey and Follow-up Study of Primary Liver Cancer in Japan, the relative shares of these therapies in the total treatment records for the two-year period from January 1, 2002 through December 31, 2003 were: hepatectomy 34%, TAE 30%, and percutaneous local therapy involving PEI, percutaneous microwave coagulation therapy (PMCT), and RFA 31%. The respective merits and demerits of each of these procedures can be summed up by saying that, while they

remove the cancer cells with the greatest degree of certainty by hepatectomy, they are also stressful on the liver and the body as a whole. TAE is clinically useful and has a relatively low degree of invasiveness but is of limited radicality. PEI and RFA, on the other hand, are simple procedures offering a high degree of radicality but their effect is limited to comparatively small tumors (3 cm or smaller in diameter). The use of radiotherapy for HCC has been considered difficult in view of the problems of radiation-induced hepatic insufficiency (6,7). Progress in the development of irradiation devices in recent years, however, has made it possible to achieve highly localized irradiation. This has spurred advances in radiotherapy research for liver cancer (8-15).

2. Optimal candidates for carbon ion radiotherapy

For patients with extensive infiltration and those with multiple lesions it is difficult to achieve radicality with carbon ion radiotherapy alone. Carbon ion radiotherapy is indicated, however, for patients with few restrictions concerning liver function, a level of liver function corresponding to medium or better (Child-Pugh grade A or B). For small lesions 3 cm or less, however, minimal invasiveness, high local control rate, and low-cost therapies such as PEI and RFA are available. In contrast, large lesions 3 cm or above are difficult to treat with PEI or RFA alone, making them ideal targets for carbon ion radiotherapy. Especially for patients with locally concentrated lesions over 3 cm and up to 5 cm, the local control rate was 90% at one to five years, and the cumulative survival rate was 95% at one year, 71% at three years, and 67% at five years. In addition, with relatively good liver function of Child-Pugh grade A, the cumulative survival rate was 94% at one year, 81% at three years and 75% at five years (Fig. 2). These outcomes seem superior to those achieved with other therapies, for example, hepatectomy, for which cumulative survival rates of 91% at one year, 74% at three years, and 59% at five years for a single lesion, and those of 91% at one year, 73% at three years, and 56% at five years for tumors 2 to 5 cm in diameter, have been reported (16). This evidence suggests that patients with locally concentrated lesions over 3 cm, up to 5 cm, are most eligible for carbon ion radiotherapy.

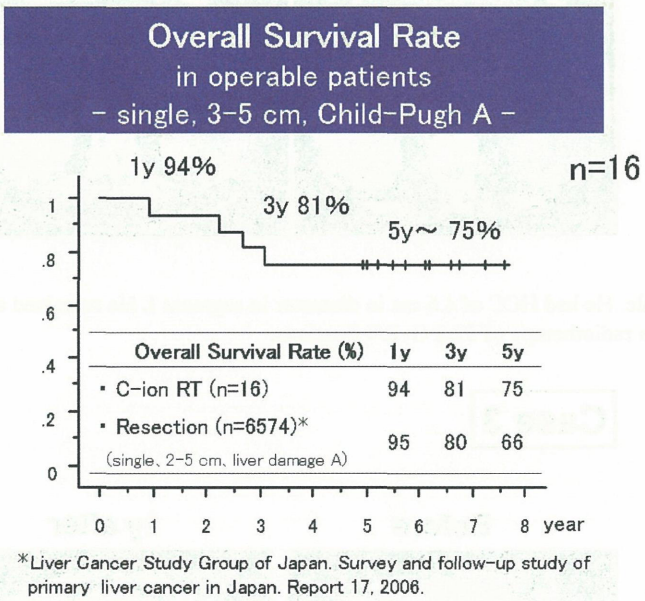

Fig. 2: Overall survival rate in operable patients

3. Future prospects

Hospitalization for HCC carbon ion radiotherapy now totals only 5 days, 3 days for preparation and 2 days for irradiation. The future goal will be to further reduce the number of days of hospitalization and to perform almost all processes on an outpatient basis. In fact, several cases have already received outpatient therapy with carbon ion beams.

Conclusion

Although carbon ion radiotherapy is safe and effective, and it seems to have promising potential as a new, radical, and minimally invasive therapeutic option for HCC, further careful follow-up is still needed to confirm its clinical efficacy in practical medicine. A future goal will be to minimize the number of days of hospitalization and to perform almost all processes on an outpatient basis.

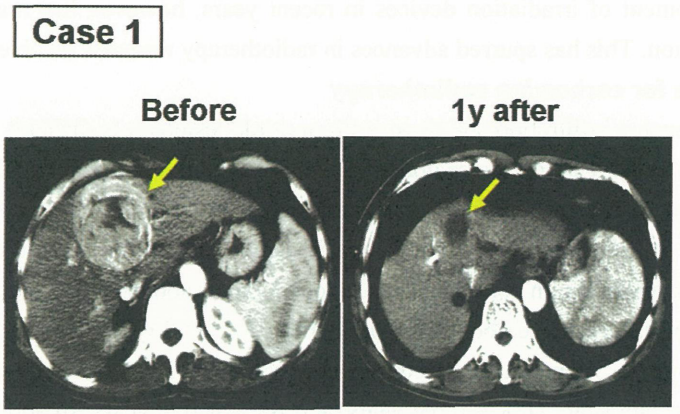

Fig. 3: Case 1
67-year-old male. He had HCC of 7 cm in diameter in segment IV. He survived for 5 years after carbon ion radiotherapy of 72.0 GyE/15 fractions.

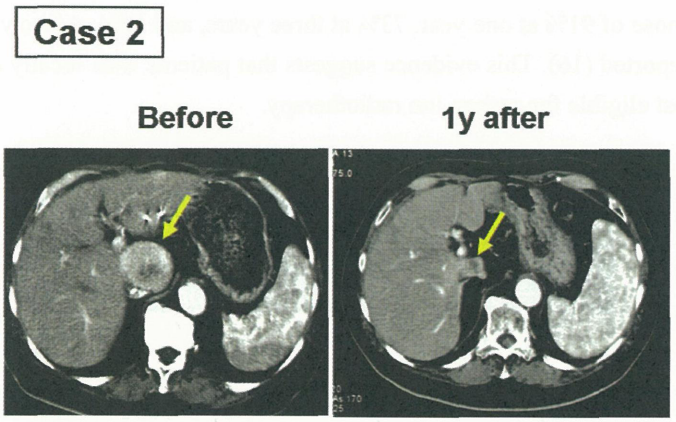

Fig. 4: Case 2
72-year-old male. He had HCC of 4.6 cm in diameter in segment I. He remained alive for 8.0 years after carbon ion radiotherapy of 52.8 GyE/4 fractions.

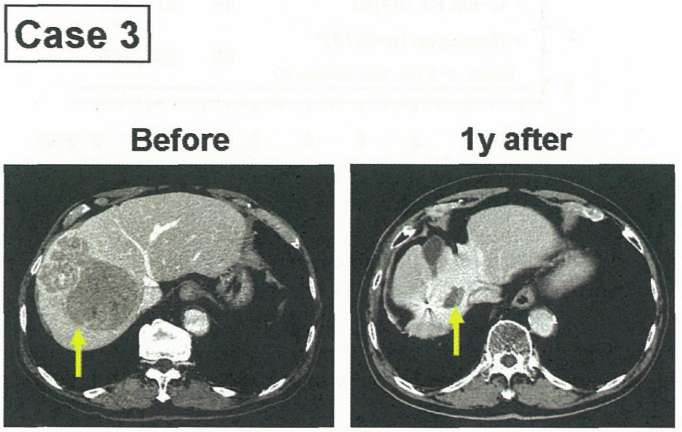

Fig. 5: Case 3
77-year-old man. He had HCC of 10.5×7.7 cm in the right hepatic lobe. He remained alive for 2.0 years after carbon ion radiotherapy of 38.8 GyE/2 fractions.

References

[1] Hirotoshi Kato, Hirohiko Tsujii, Tadaaki Miyamoto, et al. Results of the first prospective study of carbon ion radiotherapy for HCC with liver cirrhosis. Int J Radiat Oncol Biol Phys 2004; 59: 1468-1476.

[2] Hirotoshi Kato, Shigeru Yamada, Shigeo Yasuda, et al. Phase II study of short-course carbon ion radiotherapy (52.8GyE/4-fraction/1-week) for HCC. HEPATOLOGY 2005;42,Suppl.1:381A.

[3] Hirotoshi Kato, Shigeru Yamada, Shigeo Yasuda, et al. Two-fraction carbon ion radiotherapy for HCC: Preliminary results of a phase I/II clinical trial. J Clin Oncol 2005;23,Suppl.:338s.

[4] Endo M, Koyama-Ito H, Minohara S, et al. HIPLAN-A HEAVY ION TREATMENT PLANNING SYSTEM AT HIMAC. J. Jpn. Soc. Ther. Radiol. Oncol. 1996; 8: 231-238.

[5] Minohara S, Kanai T, Endo M, et al. Respiratory gated irradiation system for heavy-ion radiotherapy. Int J Radiat Oncol Biol Phys 2000;47: 1097-1103.

[6] Ingold DK, Reed GB, Kaplan HS, et al. Radiation hepatitis. Am J Roentgenol 1965;93:200-208.

[7] Phillips R, Murikami K. Primary neoplasms of the liver. Results of radiation therapy. Cancer 1960;13:714-720.

[8] Ohto M, Ebara M, Yoshikawa M, et al. Radiation therapy and percutaneous ethanol injection for the treatment of HCC. In: Okuda K, Ishak KG, editors. Neoplasm of the Liver. Tokyo: Springer-Verlag; 1987. p. 335-341.

[9] Robertson JM, Lawrence TS, Dworzanin LM, et al. Treatment of primary hepatobiliary cancers with conformal radiation therapy and regional chemotherapy. J Clin Oncol 1993;11:1286-1293.

[10] Yasuda S, Ito H, Yoshikawa M, et al. Radiotherapy for large HCC combined with transcatheter arterial embolization and percutaneous ethanol injection therapy. Int J Oncol 1999;15:467-473.

[11] Cheng J C-H, Chuang VP, Cheng SH, et al. Local radiotherapy with or without transcatheter arterial chemoembolization for patients with unresectable HCC. Int J Radiat Oncol Biol Phys 2000;47:435-442.

[12] Guo W-J, Yu E-X. Evaluation of combined therapy with chemoembolization and irradiation for large HCC. Br J Radiol 2000;73:1091-1097.

[13] Matsuzaki Y, Osuga T, Saito Y, et al. A New, Effective, and Safe Therapeutic Option Using Proton Irradiation for HCC. GASTROENTEROLOGY 1994;106:1032-1041.

[14] Kawashima M, Furuse J, Nishio T, et al. Phase II Study of Radiotherapy Employing Proton Beam for HCC. J Clin Oncol 2005;23: 1839-1846.

[15] Chiba T, Tokuue K, Matsuzaki Y, et al. Proton Beam Therapy for HCC: A Retrospective Review of 162 Patients. CCR 2005;11:3799-3805.

[16] Liver Cancer Study Group of Japan. Survey and follow-up study of primary liver cancer in Japan. Report 17. Kyoto: Shinko-Insatsu; 2006

Carbon Ion Therapy for Patients with Locally Recurrent Rectal Cancer

Shigeru Yamada, Tsuyoshi Yanagi, Shigeo Yasuda, Hiroshi Imada, Hirotoshi Kato, Tadashi Kamada, Hirohiko Tsujii, Hiroshi Tsuji, Masayuki Baba, Jun-etsu Mizoe, Riwa Kishimoto, Kyousan Yoshikawa, Susumu Kandatsu, and Takenori Ochiai for the Working Group for Locally Recurrent Rectal Cancer

Hospital, Research Center for Charged Particle Therapy, National Institute of Radiological Sciences, Chiba, Japan, Chiba University Graduate School of Medicine, Chiba, Japan.

e-mail: s_yamada@nirs.go.jp

Abstract

Purpose: To evaluate the tolerance for and effectiveness of carbon ion radiotherapy in patients with locally recurrent rectal cancer.

Patients and Methods: We conducted a phase I/II dose escalation study of carbon ion radiotherapy. One hundred patients with 105 sites of locally recurrent cancer receiving carbon ion radiotherapy were analyzed. Forty-eight relapses originated in the presacral region, 28 in the pelvic sidewalls, 16 in the perineal region and 8 in the colorectal anastomosis. The total dose ranged from 67.2 to 73.6 gray equivalent (GyE) and was administered in 16 fixed fractions over 4 weeks (4.2 to 4.6 GyE/fraction).

Results: None of 75 patients treated with the highest total dose of 73.6 GyE experienced National Cancer Institute - Common Toxicity Criteria grade 3 to 5 acute reactions. The local control rate in patients treated with 73.6 GyE in the present study was 97% at one year and 92% at 3 years. Dose escalation was then halted at this level. The median survival time in patients treated with 73.6 GyE was 54 months (range, 7 to 65 months), and the 1- and 3-year overall survival rates were 71% at 3 years and 39% at 5 years, respectively.

Conclusion: Carbon ion radiotherapy seems to be a safe and effective modality in the management of locally recurrent rectal cancer, providing good local control and offering a survival advantage without unacceptable morbidity.

Introduction

The major recurrence patterns after surgery for rectal cancer include liver metastasis and local recurrence, with the rate of local recurrence (LR) for rectal cancer ranging from 10 to 40% [1-3]. Although the use of pre- or postoperative radiation therapy has reduced the incidence of LR, 10-15% of patients still develop recurrence. Patients with locally recurrent rectal cancer have low rates of subsequent local control and overall survival. Surgical resection remains the only potentially curative treatment. Curative surgery of LR is technically difficult and the rates of complications and operative mortality are relatively high. In fact, surgery of LR is seldom feasible, and most patients are referred for radiotherapy. External-beam radiation therapy is generally considered a palliative treatment. LR is resistant to conventional radiotherapy and is located close to critical organs.

The carbon ion beam possesses unique physical and biologic properties [4,5]. It has a well-defined range and insignificant scatter in tissues, and the energy release is enormous at the end of its range. This well-localized energy deposition (high-dose peak) at the end of the beam path, called the Bragg peak, is a unique physical characteristic of charged particle beams, as is the induction of more cell cycle- and oxygenation-independent,

irreversible cell damage than that observed with low-LET radiation. To improve long-term local control and survival of locally recurrent rectal cancer, we have initiated a radiation dose-escalation trial using carbon ion beams.

Patients and Methods

Patient Eligibility

Patients were included in the study if they were confirmed with locally recurrent rectal cancer without distant metastasis by computed tomography (CT), magnetic resonance imaging (MRI), and carbon-11methionine positron emission tomography (PET) findings, had adenocarcinoma of the rectum and had a potentially curative resection of the primary tumor and regional lymph nodes performed with neither gross nor microscopic residual disease. Patients who had undergone chemotherapy within 4 weeks before carbon ion radiotherapy or those who had prior radiation therapy at the same site were excluded from the study. The tumor had to be grossly measurable, but the size could not exceed 15 cm. Eligibility criteria included a Karnofsky performance status score higher than 60 and estimated life expectancy of at least 6 months. Exclusion criteria were having another primary tumor, and infection at the tumor site and digestive tract in contact with the clinical target volume. A complete history was obtained and a physical examination was performed before registration, including CT, MRI and PET to determine the extent and size of the tumor. Chest and upper abdominal CT scans were mandatory at the time of entry into the trial. All patients signed an informed consent form approved by the local institutional review board.

Carbon Ion Radiotherapy

The Heavy Ion Medical Accelerator in Chiba is the world's first heavy ion accelerator complex dedicated to medical use in a hospital environment. The features of the accelerator and carbon ion beam have previously been described [6,7]. In brief, carbon ion radiotherapy was given once daily, 4 days a week (Tuesday to Friday), for fixed 16 fractions in 4 weeks. Patients were treated with two to five irregularly shaped ports (median, three ports). The clinical target volume (CTV) was determined by setting the margin 5mm outside the gross tumor volume (GTV) and included the regional lymph nodes (LN). The LN areas that should be considered part of the target volume include the internal iliac, external iliac and presacral nodes. Dose constraints of the maximum dose for the intestine and bladder were 30 GyE in 9 fractions and 60 GyE in 16 fractions, respectively. Nodal areas of risk are usually prophylactically treated with 37.8-41.4 GyE in 9 fractions of 4.2-4.6 GyE before irradiation field are reduced in size.

Dose Escalation and Toxicity Criteria

At least three patients were treated at the same dose level, and then a 10% escalation of the total dose was carried out after careful observation of normal tissue responses using to NCI-CTC (National Cancer Institute - Common Toxicity Criteria Version 2.0). Dose adjustment was planned if there was any acute RTOG grade 3 or higher toxicity. We followed the standard phase I dose escalation methods. If no dose-limiting toxicity (DLT) was observed in any of the three patients at a given dose level, the dose level was escalated for the next cohort. If DLT was observed in no more than one in three patients, then three more patients were treated at the same dose level. If no further cases of DLT were seen in the additional patients, then the dose level was escalated for the next cohort. Otherwise, dose escalation was stopped. Three patients at any dose level of each site had to be followed up for at least 3 months before a subsequent dose escalation. We used 67.2 GyE in 16 fractions, 4.2 GyE/fraction as the starting dose. For late reactions, the Late Effects of Normal Tissues/Subjective, Objective, Management, and Analytic scoring system was used in addition to the RTOG/European Organization for Research and Treatment of Cancer late scoring system. Scores for late reactions were the highest observed 3

months or later after carbon ion radiotherapy.

Toxicity

Toxicity on organs such as the skin, bladder and digestive tract was assessed according to NCI-CTC Version 2.0 (April 30, 1999) and RTOG/EOTRC (late) classification.

Tumor Response and Local Control Criteria

Tumor response was defined as the maximum tumor response observed by the RECIST scoring system during the first 6 months after the initiation of carbon ion radiotherapy. Complete response (CR) was defined as the disappearance of all measurable tumor in the treatment volume. Partial response (PR) meant a 30% or greater decrease in tumor size (longest diameter). Stable disease was that with a less than 30% decrease or a less than 20% increase in tumor size. Progressive disease was defined as a 20% or greater increase in tumor size. The absence of local failure in the treatment volume based on CT, MRI, and PET scans was described as local control. Local recurrence was defined in terms of lesions occurring in the tumor bed.

Follow-Up

All patients were seen on a regular basis during follow-up. Initial evaluation of tumors using CT, MRI, and PET scans was performed within 1 month after the completion of carbon ion radiotherapy. Thereafter, the patients were followed up by CT or MRI every 1 or 2 months for the next 6 months, and then the intervals between imaging and follow-up were extended to 3 to 6 months. PET was not performed regularly after the initial evaluation.

Statistics

Survival time and local control time were defined as the interval between the initiation of carbon ion radiotherapy and the date of death or the date of diagnosis of local failure, respectively. The survival and local control curves were generated by Kaplan-Meier method and the log-rank test was used for comparisons. Results were considered significant at $P < 0.05$.

Results

Patient Characteristics

Between April 2001 and February 2008, 103 patients (108 lesions) were enrolled into this study. One patient was excluded because of subarachnoid hemorrhage before treatment. Thus, 102 patients of 103 eligible patients were treated with carbon ion radiotherapy. Two more patients were excluded because of peritoneal dissemination or lymph node metastasis of the mediastinum. Thus, 105 lesions in 100 patients (65 men and 35 women) were treated with carbon ion radiotherapy. Patient characteristics are summarized in Table 1. Median age was 62.5 years (range 27 to 83 years). All patients presented with adenocarcinoma at initial surgery. Abdominoperineal resection had been performed in 56 patients, anterior resection in 42, and Hartmann's resection in two. Forty-eight relapses originated in the presacral region, 28 in the pelvic sidewalls, 16 in the perineal region, and 8 in the colorectal anastomosis. Carbon beams of 290, 350 and 400 MeV/nucleon energy were generated by the HIMAC synchrotron. Carbon ion therapy was given once daily, 4 days a week, for fixed 16 fractions in 4 weeks. The dose was set at 67.2 GyE (4.2 GyE per fraction) and escalated to 73.6 GyE (4.6 GyE) at 5% increments.

Toxicity

Toxicities in the 102 patients (107 lesions) receiving carbon ion therapy are listed in Table 2. They were relatively few and mild in these patients. All patients completed the scheduled treatment course. No grade 3 to 5

acute toxicity was observed. Two grade 3 late skin and one gastrointestinal reactions were observed among the 107 lesions.

Table 1. Patient Characteristic

Characteristics	No. of Pts. (N=100)
Age, years	
Median	62.5
Range	27-83
Female/Male	65/35
Primary tumor operation	
abdominoperineal excision	56
low anterior resection	42
Hartmann's resection	2
Tumor sites (n=59)	
presacral	48 (+1)
lymph nodes	28 (+2)
perineal	16 (+1)
anastomotic	8 (+1)

Table 2. Acute and Late Toxicities by NCI-CTC and RTOG/EORTC Scoring System

	Acute (NCI-CTC)						Late (RTOG/EORTC)					
	No. of lesions	Gr0	Gr1	Gr2	Gr3	Gr4	No. of lesions	Gr0	Gr1	Gr2	Gr3	Gr4
Skin	107	24	76	7	0	0	107	54	50	1	2	0
Gastrointestinal	107	105	1	1	0	0	107	105	0	1	1	0
Urinary	107	106	1	0	0	0	107	105	0	2	0	0

The maximum tolerated dose(MTD) of 73.6 GyE had been indicated for patients with bone and soft-tissue sarcomas in the pelvis by a phase I/II dose escalation study of carbon ion radiotherapy. The local control rate in patients treated with 73.6 GyE in the present study was 97% at one year and 92% at 3 years, significantly better than the hitherto reported local control rates. The patients in our series had been considered mostly to have tumors for which there were no other effective local treatments. Despite such dire conditions, patients experienced good tumor control and a relatively low incidence of complications with carbon ion radiotherapy. To confirm these findings, a phase II clinical trial using 73.6 GyE is warranted.

Despite the fact that various types of chemotherapies were applied before or after carbon ion radiotherapy, there were no obvious effects of chemotherapy on the incidence of toxicities in this series.

Tumor Response

Evaluation of tumor response was not considered the primary endpoint of this study. Tumor response was evaluated in 105 lesions. One patient was excluded from tumor response analysis because of difficulty in imaging evaluation. CR was observed in 14 lesions and PR in 31 (Table 3). Sixty lesions remained stable. The overall tumor response rate (CR+PR) was 47%. Remarkable anti-tumor effects were observed.

Table 3. Tumor Response of 105 Lesions

Total dose (GyE)	No. of lesions	CR	PR	SD	PD
67.2	10	4	1	5	0
70.4	20	0	8	12	0
73.6	75	10	22	43	0

The overall actuarial local control rates at five years were 35%, 89% and 93% at 67.2 GyE, 70.4 GyE and 73.6 GyE, respectively. Ten in-field recurrences were observed among the recurrent patients (Fig.1).

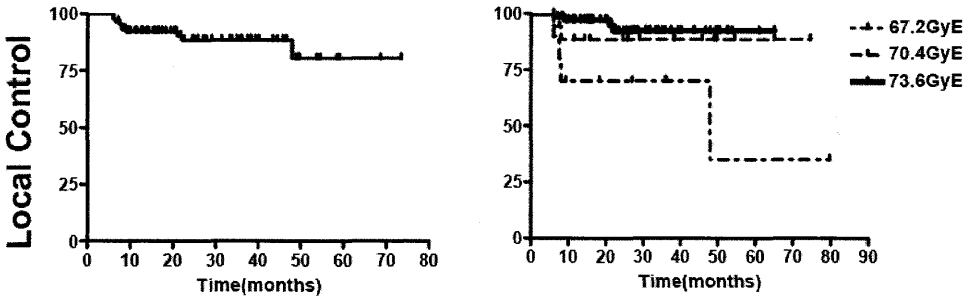

(a) (b)

Fig. 1. Local control rates a) in all 105 analyzed lesions, b) by total dose

In terms of symptomatic response within 3 months after treatment, pain improved in 97% of the symptomatic

The overall survival estimates for the 100 analyzed patients are shown in Fig 2. The three-year and five-year cases. Pain relief was maintained at one year in 67%, 91% and 100% of the patients treated with 67.2GyE, 70.4GyE and 73.6GyE, respectively. In general, symptoms tended to improve during the course of radiation rather than worsen. While most authors agree that irradiation is frequently an effective therapy for symptomatic pelvic tumors, it has also been established that the response usually persists for only about 3-6 months. Symptomatic response rates range from 50% to 94%. overall survival rates were 62% and 39%, respectively. The overall survival rates at three years were 36% at 67.2 GyE, 55% at 70.4 GyE, and 67% at 73.6 GyE. There was a clear correlation between overall survival rates and total dose.

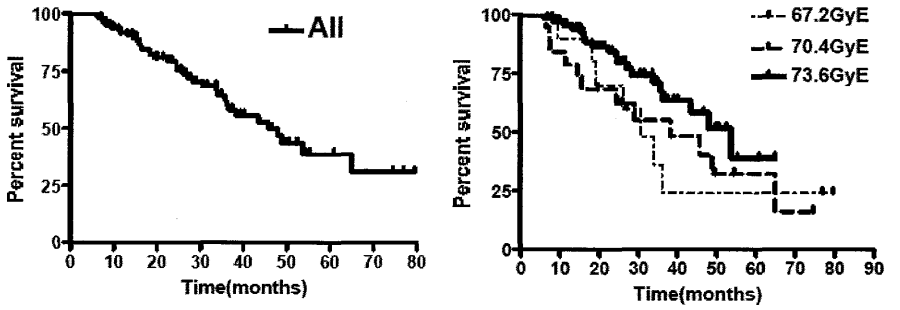

(a) (b)

Fig. 2. Overall survival rates a) in all 100 analyzed patients, b) by total dose

Our survival rate data are nearly the same as those associated with surgical resection.

The above results substantiate the superior usefulness of heavy ion radiotherapy in the treatment of recurrent rectal cancer to conventional photon radiotherapy or combinations with chemotherapy.

Discussion

In this study, carbon ion radiotherapy was well tolerated and demonstrated substantial activity against locally recurrent rectal cancer. These results were obtained in patients with advanced and/or chemoresistant gross lesions not suited for surgical resection.

We found a dose-response relationship for local control at each year. The rate of actuarial local control increased as the total dose increased from 67.2 to 73.6 GyE, reaching more than 90% in patients treated with 73.6 GyE at one year. The 3-year local control rate for patients receiving either 70.4 GyE or 73.6 GyE was very similar at 89 or 92%, significantly better than that for those receiving 67.2 GyE (Fig. 3). Surgery is considered the standard treatment for recurrent rectal cancer patients, but it is in actuality only possible in a very small number of cases. Curative surgery for recurrent rectal cancer has resulted in higher than 50% long-term local control rate [8,9]. However, most patients must be referred to radiotherapy. There have been several attempts to improve the duration and quality of response in advanced cancers by combining radiation treatment with chemotherapy [10-13]. Previous studies reported local control rates in patients with locally recurrent rectal cancer treated by all types of radiotherapy including other particle beams of less than 50% [14,15]. The local control rate of our 73.6 GyE group could be among the best achieved without surgical resection.

Although the focus of this study was not directed at survival duration, nonetheless, it is noteworthy that improved local control resulted in better survival. We found a dose-response relationship for the survival rate. The 2-year overall survival rate increased as the total dose increased from 67.2 to 73.6 GyE, reaching 93% in patients treated with 73.6 GyE. The 2- and 5-year overall actuarial survival rates were 84% and 39% respectively; in the literature, the reported 2-year survival rate for patients with locally recurrent rectal cancer treated by external-beam radiation was 45% or less [15]. External-beam radiation therapy alone or in combination with chemotherapy provides palliation and modest prolongation of life but has only a minimal curative potential in patients with locally recurrent rectal cancer. The reported 2- year and 5-year overall survival rate in patients with locally recurrent rectal cancer treated by curative surgery were 62-82% and 31-46% respectively. This level of survival rate achieved with carbon ion RT can be considered as equivalent to or better than surgical resection.

Wendling has clearly shown that the oxygenation of differential rectal adenocarcinoma is distinctly lower than that of the normal rectal mucosa, and tissue hypoxia or even anoxia are common features of these tumors [16]. Furthermore, Hockel showed that there is significantly greater hypoxia in pelvic recurrence than in primary tumors [17]. Improvements in tumor response and control have been sought through efforts to overcome the radioresistance of the hypoxic tumor cells identifiable in rectal cancers. These aspects might give high-LET particles a particular advantage, no matter whether this is due to a lower oxygen enhancement ratio (OER) or other intrinsic factors. Therefore, high-LET particle radiotherapy such as carbon ion or neutron seems to be effective against recurrent tumor, which is hypoxic. Twenty patients with recurrent rectal cancer were treated using the d,T generator in Munster by combined neutron-radiotherapy [18]. The radiation schedule most often used for palliation involves giving 40 Gy photon and 10 Gy neutron doses (14 MeV). Initiation of pain relief seems to occur faster with neutrons than with photons alone. Pain relief was achieved in 11 of 15 patients (73%), and the probability for a pain-free period is 46% for 9 months. It remains to be proven if the frequency of pain relief is higher and the pain-free period as well as the progression-free period last longer than with photons. The incidence of acute toxicity was 30% and late toxicity 10%. All toxicity was seen at the skin. A higher neutron dose will give better results, but may cause local radiation side-effects.

Carbon ion therapy offers the potential advantages of improved dose localization and enhanced biological effect [19]. Our results have shown that carbon ion therapy has the promising potential of delivering a sufficient dose to the tumor with acceptable morbidity in the surrounding normal tissues. Tumors that appear to respond favorably to carbon ions include locally advanced tumors with a non-squamous histology such as adenocarcinoma [20,21]. Carbon ion therapy may very well improve tumor control of recurrent rectal cancer.

In conclusion, carbon ion radiotherapy is an effective local treatment for patients with locally recurrent rectal cancer, and it seems to represent a promising alternative to surgery. The morbidity rate of carbon ion radiotherapy has so far been quite acceptable, although the long-term safety of this approach for patients with sarcomas will still need to be monitored.

References

[1] Kapiteijin E, Marijnen CAM, Colenbrander AC et al. Local recurrence in patients with rectal cancer diagnosed between 1988 and 1992. Eur J Surg Oncol 24:528-535, 1998

[2] Galandiuk S, Wieand HS, Moertel CG, et al. Patterns of recurrence after curative resection of carcinoma of the colon and rectum. Surg Gynecol Obstet 174: 27-32, 1992

[3] Bozzetti F, Mariani L, Micel R, et al. Cancer of the low and middle rectum: local and distant recurrence and survival in 350 radically resected patients. J Surg Oncol 62: 207-213, 1992

[4] Blakely EA, Ngo FQH, Curtis SB, et al. Heavy ion radiobiology: Cellular studies. Adv Radiat Biol 11:295-378, 1984

[5] Hall EJ. Radiobiology for the Radiologist. Philadelphia, PA, JB Lippincott, 1988, pp 281-291

[6] Sato K, Yamada H, Ogawa K, et al. Performance of HIMAC. Nuclear Physics A 588:229-234, 1995

[7] Kanai T, Endo M, Minohara S, et al. Biophysical characteristics of HIMAC clinical irradiation system for heavy-ion radiation therapy. Int J Radiat Oncol Biol Phys 44:201-210, 1999

[8] Lopez-Kostner F, Fazio VW, Rybicki LA et al. Locally recurrent rectal cancer: Predictors and success of salvage surgery. Dis Colon Rectum 44: 173-178, 2001

[9] Wanebo HJ, Antoniuk P, Koness RJ et al. Pelvic resection of recurrent rectal cancer. Dis Colon Rectum 42: 1438-1448, 1999

[10] Ciatt S, Pacini P. Radiation therapy of recurrences of carcinoma of the rectum and sigmoid after surgery. Acta Radiol Oncol 21: 105-109, 1082

[11] O'Connel MJ, Child DS, Moertel CG. A prospective controlled evaluation of combined pelvic radiotherapy and methanol extraction residue of BCG for locally unresectable or recurrent rectal cancer. Int J Radiat Oncol Biol Phys 8: 1115-1119, 1982

[12] Wong CS, Cummings BJ, Keane TJ. Combined radiation therapy, mitomycin C, and 5-Fluorouracil for locally recurrent rectal carcinoma. Int J Radiat Oncol Biol Phys 21: 1291-1296, 1991

[13] Lybeert MLM, Martijin H, De Neve W. Radiotherapy for locoregional relapses of rectal carcinoma after initial radical surgery. Int J Radiat Oncol Biol Phys 24:241-246,1992

[14] Knol HP, Hanssens J, Rutten HJT. Effect of radiation therapy alone or in combination with surgery and/or chemotherapy on tumor and symptom control of recurrent rectal cancer. Strahlenther Onkol 173: 43-49, 1997

[15] Murata T, Fujii I, Yoshino M. Radiation therapy with or without chemotherapy and hyperthermia for recurrent rectal cancer. J Jpn Soc Ther Radiol Oncol 9: 63-71, 1997

[16] Wendling P, Manz R, Thews G, et al. Heterogeneous oxygenation of rectal carcinomas in humans. Advan Exp Med Biol 180: 293-300, 1984

[17] Hockel M, Schlenger K, Hockel S. Tumor hypoxia in pelvic recurrences of cervical cancer. Int J Cancer 79, 365-369, 1998

[18] Eising E, Potter R, Haverkamp U. Neutron therapy for recurrence of rectal cancer Strahlenther. Onkol 166: 90-94, 1990

[19] Ando K, Koike S, Ohira C, et al. Accelerated reoxygenation of a murine fibrosarcoma after carbon-ion radiation. Int J Radiat Biol 75: 505-512, 1999

[20] Kamada T, Tsujii H, Tsuji H, et al. Efficacy and safety of carbon ion radiotherapy in bone and soft tissue sarcomas. J Clin Oncol 20: 4466-4471, 2002

[21] Miyamoto T, Yamamoto N, Nishimura H, et al. Carbon ion radiotherapy for stage I non-small cell lung cancer. Radiother Oncol 66: 127-140, 2003

Pancreas Cancer

Shigeru Yamada, Tsuyoshi Yanagi, Hiroshi Imada, Hirotoshi Kato, Shigeo Yasuda, Tadashi Kamada, Hirohiko Tsujii, Hiroshi Tsuji, Masayuki Baba, Jun-etsu Mizoe, Tadaaki Miyamoto, Kyousan Yoshikawa, Susumu Kandatsu, and Hiromitsu Saisho for the Working Group for Pancreas Cancer

Hospital, Research Center for Charged Particle Therapy, National Institute of Radiological Sciences, Chiba, Japan, Clinic of Medicine and Digestive Diseases, Kaken Hospital., Chiba, Japan.

e-mail: s_yamada@nirs.go.jp.

Adenocarcinoma of the pancreas continues to be a significant source of cancer mortality in Japan, resulting in approximately 19,000 deaths a year. It is the fifth leading cause of cancer-related deaths in Japan, with a less than 5% 5-year expected survival rate[1]. About 70-75% of patients with pancreas cancer present with locally advanced disease or distant metastases and have a median survival time of only 6 months. For unresectable pancreas cancer, the median survival time with external beam radiation (EBRT) was better than with surgical bypass[2] or stents alone[3]. The median survival of EBRT alone was 4 to 7 months[4]. The median survival with combined EBRT and chemotherapy for locally unresectable tumor was 8 to 10 months[5], better than with EBRT alone.

Local failure of these combined therapies was still 26 to 48%. On the other hand, surgery with curative intent is undertaken in 15-20% of patients. Even after resection, the predicted 5-year survival rates are still less than 20%[1]. Local recurrence in the pancreatic bed is seen in 50% of the patients undergoing presumed curative resection[6].

We examined the effect of carbon ion therapy in terms of reducing the rate of local recurrence in patients with locally advanced adenocarcinoma of the pancreas or undergoing resection for adenocarcinoma of the pancreas.

Carbon ion therapy

A Phase I/II Clinical Trial of Carbon-ion Therapy for patients with preoperative pancreas cancer (9906) was carried out on surgically resectable patients from June 2000 through February 2003. This was followed by a Phase I/II Clinical Trial of Short-course Carbon-ion Therapy for patients with preoperative pancreas cancer (0203), commencing in April 2003 for similarly surgically resectable patients, with a fractionation regimen from 16 (4 weeks) to 8 (2 weeks) fractions. Concurrently, a Phase I/II Clinical Trial of Carbon-ion Therapy for patients with locally advanced pancreas cancer (0204) was conducted for surgically non-resectable patients with local progressive disease without distant metastasis from April 2003 through February 2007. This was followed by a Phase I/II Clinical Trial of Gemcitabine Combined with Carbon-ion Therapy for patients with locally advanced pancreas cancer.

A. Preoperative pancreas cancer (Protocol 9906, 16 fractions/4 weeks)

Purpose: We examined the effect of preoperative carbon ion therapy in terms of reducing the rate of local recurrence in patients undergoing resection for adenocarcinoma of the pancreas.

Patients and Methods: Twenty-two patients were enrolled into this trial. Median age was 63 years. Carbon ion therapy was given once daily, 4 days a week, for a fixed 16 fractions in 4 weeks. The dose was set at 44.8 GyE and escalated to 48.0 GyE at 5% increments.

Results: All patients completed the scheduled treatment course. Three grade 3 acute reactions and two grade 3 late

reactions occurred among 16 of the patients treated with a total dose of 48.0 GyE. The two grade 3 late reactions were estimated to be caused by carbon ion therapy. Of the 22 patients, 15 (68%) had resection. All tumor specimens pathologically revealed evidence of grade 2 treatment effects with significant fibrosis, hyalinization, and necrosis (pathological grade 2 is defined as less than 33% active cancer cells). Remarkable antitumor effects were observed. The overall local control rates were 100% and 87% at 1 year and 2 years of follow-up, respectively. No local failure was observed in any of the 22 enrolled patients.
Conclusion: Carbon ion radiotherapy seems to be a safe and effective modality in the management of resectable pancreatic carcinoma, providing good local control and offering a survival advantage without unacceptable morbidity.

Patients and Methods

Patient Eligibility

Between April 2000 and February 2003, 22 patients judged according to the staging criteria of the Japanese Committee on Cancer as being at clinical stages I, II, III or IVa, equivalent stages I, II or III by the TNM staging criteria, were enrolled into this trial. Criteria for trial eligibility were pathologic confirmation of ductal adenocarcinoma, age of 18 years or more, ECOG performance score 0, 1, or 2, and adequate hematologic, hepatic, renal, and cardiopulmonary function to allow pancreatectomy. Exclusion criteria were having another primary tumor and infection at the tumor site. Patients who had undergone chemotherapy before carbon ion radiotherapy or those who had prior radiation therapy at the same site were excluded from the study. The tumor had to be grossly measurable, but its size could not exceed 15 cm, and the patients were evaluated by surgical consultation with three surgical investigators as to the resectability of the lesion. Chest and upper abdominal CT scans were mandatory at the time of entry into the trial. All patients signed an informed consent form approved by the local institutional review board.

Carbon Ion Radiotherapy

The features of the accelerator and the carbon ion beam have previously been described[7,8].
Carbon ion therapy was given once daily, 4 days a week, for a fixed 16 fractions over 4 weeks. The dose was set at 44.8 GyE and escalated to 48.0 GyE at 5% increments. The protocol specifications for carbon ion radiotherapy were as follows. The target volumes were established by CT scan. Field arrangements were generally designed using a 3-field or 4-field plan. The clinical target volume (CTV) included the gross tumor volume (GTV) and regional lymph nodes, which included the celiac, superior mesenteric, peri-pancreatic, portal and para-aortic (celiac-IMA) nodes for pancreatic head cancer and splenic nodes for pancreatic body and tail cancer. The CTV was defined as the gross volume plus 1.0 cm or 0.5 cm (in contact with the gut). At least 50% of the functioning renal parenchyma was limited to 15 GyE or less. The spinal cord dose was limited to 30 GyE or less.

Surgery

Surgical resection was to be performed 2 to 4 weeks after the completion of carbon ion radiotherapy if there was no disease progression to an unresectable status as determined by repeated abdominal CT scans, a prohibitive decline in performance status, or other evidence of metastatic disease. Median time from the last day of carbon ion radiotherapy to surgical resection was 21 days (range, 20 - 26 days).

Tumor Response and Local Control Criteria

Tumor response was defined as the maximum tumor response observed by the RECIST scoring system during the first 6 months after the initiation of carbon ion radiotherapy. Complete response (CR) was defined as the disappearance of all measurable tumor in the treatment volume. Partial response (PR) meant a 30% or greater

decrease in tumor size (longest diameter). Stable disease was that with a less than 30% decrease or a less than 20% increase in tumor size. Progressive disease was defined as a 20% or greater increase in tumor size. Local recurrence was defined in terms of lesions occurring in the treatment volume based on CT, MRI, and PET scans. The development of a new, low-density mass in the region of the pancreatic bed was considered evidence of local recurrence even in the absence of symptoms, and cytologic or histologic confirmation of recurrent disease was not required. The absence of local recurrence was described as local control.

Histologic evaluation of the effects of carbon ion therapy included assessment of cytologic changes in conjunction with quantification of the amount of viable residual carcinoma cells (Table 1). Upon completion of specimen analysis, all cases were reviewed by the same histopathologist.

Table 1. Grading system for radiation treatment effects

Grading system for radiation treatment effects

Grade	Histological appearance
0	No tumor cell destruction evident
1	Less than two-thirds of tumor cells are destroyed
2	More than two-thirds of tumor cells are destroyed
3	No viable tumor cells present

Statistics

Survival time and local control time were defined as the interval between the initiation of carbon ion radiotherapy and the date of death or the date of diagnosis of local failure, respectively.

Results

Patient Characteristics

None of the 22 patients initially registered into this trial was excluded from the analysis. The patients consisted of 14 males and 8 females. Median age was 63 years (range, 42 - 77 years). Thirty cancers originated in the head of the pancreas, 8 were in the body of the pancreas, and one was in both the head and body (Table 2).

Table 2. Patient Characteristics

Characteristics		Number of patients
Age (years)	median(range)	63 (42-77)
Gender	male	14
	female	8
ECOG performance score	0	18
	1	4
Tumor location	head	13
	body-tai	8
	head and body	1
Stage(preoperative, TNM))		
	T3N0	4
	T3N1	18

Toxicity

The toxicities in the 22 patients receiving carbon ion therapy are listed in Table 3. The toxicities were relatively few and mild. All patients completed the scheduled treatment course. Three grade 3 acute reactions and two grade 3 late reactions occurred among 12 of the patients treated with a dose of 48.0 GyE. One patient had cholangitis, easily resolved by radiologic stent change and antimicrobials. Two were postoperative complications: one patient had leakage at the choledochojejunostomy, requiring percutaneous drainage, and the other had gastrojejunostomy leakage, requiring percutaneous drainage. Both leakages occurred outside of the treatment fields and were considered to likely not be related to the carbon ion therapy. There was no grade 3 to 5 blood or bone marrow reaction. Both two grade 3 late reactions were post-surgery portal vein stenoses, and both underwent portal vein resections.

Table 3. Acute and Late toxicities by NCI-CTC and RTOG/EORTC Scoring System

	Acute(NCI-CTC)						Late(RTOG/EORTC)					
	No. of patients	Gr0	Gr1	Gr2	Gr3	Gr4	No. of patients	Gr0	Gr1	Gr2	Gr3	Gr4
Skin	22	22	0	0	0	0	20	20	0	0	0	0
Gastrointestinal	22	18	3	1	0	0	20	20	0	0	0	0
Bile duct	22	20	0	1	1	0	20	20	0	0	0	0
Portal vein	22	20	0	2	0	0	20	18	0	0	2	0
Leakage	22	20	0	0	2	0	20	20	0	0	0	0

Tumor Response

Evaluation of tumor response was not considered the primary endpoint of this study.

All 22 patients had CT scans before registration and 2-4 weeks after completion of the carbon ion radiotherapy. On the basis of the CT scans, only one patient showed complete response, and one also showed partial response. Twenty patients (91%) had stable disease, but none had local tumor progression.

Surgical Results

Of 22 patients, 15 (68%) had resection. One of the 22 eligible patients did not undergo surgery. CT scan restaging after carbon ion radiotherapy revealed new liver metastases in this patient. Of the 21 patients undergoing exploratory celiotomy, 5 had no resection. Two had metastases to the liver and three to the peritoneum. Fifteen eligible patients had pancreatic resection; 10 modified Child procedures, two total pancreatectomies, and three distal pancreatectomies were performed. In addition, one patient also underwent solitary liver resection for a small isolated liver metastasis discovered intraoperatively after pancreaticoduodenectomy. This patient, who had pancreatectomy that was not considered potentially curative resection, was included in this analysis. The median time from completion of carbon ion radiotherapy to surgery was 22 days (range, 13 - 29).

Pathological Results of Resected Specimens

The pathological characteristics of the 15 resected specimens are listed in Table 4. All tumor specimens revealed evidence of grade 2 treatment effects with significant fibrosis, hyalinization and necrosis, meaning more than two-thirds of the tumor cells were destroyed. The resection margins were examined in all specimens. No patient had a grossly or microscopically positive resection margin.

Table 4. The pathologic response of the 15 resected specimens

Total dose(GyE)	No. of patients	Grade0	Grade1	Grade2	Grade3
44.8	5	0	0	5	0
48.0	10	0	0	10	0

Patient Outcome

The overall local control rates were 100% at 1 year and 87% at 2 years of follow-up, respectively (Fig.1). One local failure was observed in the residual pancreas at 18 months after pancreaticoduodenectomy. There was no local and regional recurrence within the treatment fields. The 1-year overall survival rates were 62% for all patients and 90% in the resected patients, and median survivals were 13.4 months and 21 months, respectively, with a median follow-up of 13 months (range, 3.3 - 51 months) (Fig.2). Two patients are currently alive without evidence of disease. Twenty patients are dead and 19 patients had metastatic relapse or carcinomatosis. In the nonresected patients, the 1-year overall survival rate and median survival were 30% and 6.3 months.

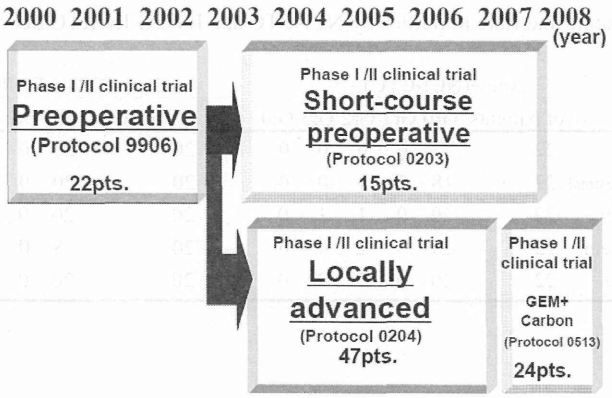

Fig.1 NIRS Sequencing Trial: Schema

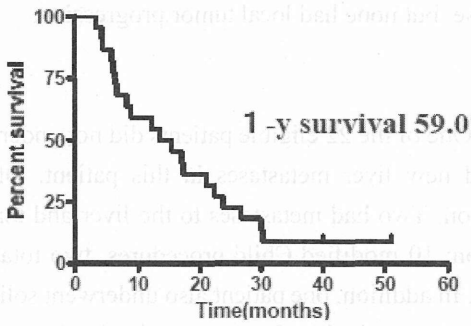

Fig.2 Overall survival for all 22 patients

B. Short-course (8 fractions/2 weeks) preoperative pancreas cancer (Protocol 0203)

The phase I/II trial of preoperative carbon ion radiotherapy (8 fractions/2 weeks) for pancreas cancer prior to surgery was performed with the purpose of establishing the safety of carbon ion radiotherapy, determining the recommended dose, and substantiating its preoperative effectiveness.

At present, patient enrollment in the trial is in progress, and the outcomes are pending. The early data indicate the same high level of local control as the 9906 protocol. However, the histological effect is showing a tendency of being somewhat inferior to the 9906 protocol, suggesting that the dose is not adequate. In view of the reports in the literature on drugs with a sensitizing effect in conjunction with heavy particle beams, further studies are scheduled in search for an even more effective treatment modality.

C. Locally advanced pancreas cancer (Protocol 0204, 12 fractions/3 weeks)

The phase I/II trial of carbon ion radiotherapy (12 fractions/3 weeks) for locally advanced pancreas cancer was performed so as to establish the safety of carbon ion radiotherapy, determine the recommended dose, and confirm its efficacy.

Patients and Methods

Between April 2003 and February 2007, 47 patients judged according to the staging criteria of the Japanese Committee on Cancer as being clinical stages IVa or IVb without distant metastasis were enrolled into this trial. As one patient was excluded because of receiving chemotherapy before treatment, 46 patients were eligible for this analysis. Patients eligible for study entry had been histologically or cytologically confirmed with locally advanced unresectable pancreas ductal carcinoma. Eligibility criteria were: confirmation of ductal carcinoma by CT findings, age of 80 years or younger, ECOG performance score 0, 1, or 2, and hepatic, renal and cardiopulmonary function sufficient for undergoing surgery. The criteria of the CT findings for non-resectability of the tumor included tumor encasement of the celiac trunk and/or superior mesenteric artery. Carbon ion therapy was given once daily, 4 days a week, for a fixed 12 fractions over 3 weeks. The dose was set at 38.4 GyE and escalated to 52.8 GyE at 5% increments.

Results

Toxicity on organs such as skin, bladder and digestive tract was assessed according to the NCI-CTC (acute) and RTOG/EOTRC (late) classifications. Tumor response was defined by the RECIST scoring system as the maximum tumor response observed during the first 6 months after the initiation of carbon ion radiotherapy. Local recurrence was defined in terms of lesions occurring in the tumor bed.

Survival was calculated as the time from the initiation of carbon ion therapy until death. Survival curves were estimated by the Kaplan-Meier method.

All toxicities in the 46 patients receiving carbon ion therapy are listed in Table 5. All patients completed the scheduled treatment course. Seven grade 3 acute and one grade 3 late toxicities were observed. Six of the 7 grade 3 acute toxicities were anorexia and one was cholangitis. Tumor response was evaluated in 46 lesions. CR was observed in one lesion, PR in 7, SD in 37, and PD in one. The local control rate at 1 year in the 46 analyzed patients and in the patients receiving 45.6 GyE or more was 76% and 95%, respectively. The overall survival estimates for the 46 analyzed patients are shown in Fig. 3. One-year overall survival was 43%.

Table 5: Acute and Late toxicities by NCI-CTC and RTOG/EORTC Scoring System

	Acute(NCI-CTC)						Late(RTOG/EORTC)					
	No. of pat.	Gr0	Gr1	Gr2	Gr3	Gr4	No. of pat.	Gr0	Gr1	Gr2	Gr3	Gr4
Skin	46	29	17	0	0	0	46	40	6	0	0	0
G.I.	46	7	14	19	6 *	0	46	33	10	1	2***	0
Bile duct	46	32	0	3	1**	0	46	30	0	0	0	0
Liver	46	46	0	0	0	0	46	30	0	0	0	0
Portal vein	46	46	0	0	0	0	46	30	0	0	0	0

*Appetite loss, **Cholangitis, ***GI bleeding

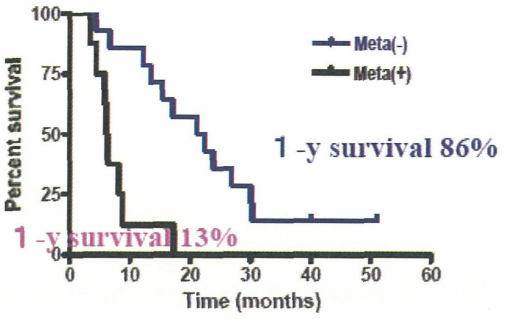

Fig. 3 Overall survival for patients with or without distant metastases

The maximum acute reaction of grade 3 was observed in two-thirds of the patients (67%) at 52.8 GyE. From these results, we concluded that the maximum tolerance dose of carbon ions is 52.8 GyE/12 fractions/3 weeks.

On the basis of the literature on drugs with a sensitizing effect in conjunction with heavy particle beams, further studies were scheduled in an effort to find even more effective treatment modalities based on a combination of chemo- and radiotherapy. We started a Phase I/II Clinical Trial of Gemcitabine Combined with Carbon-ion Therapy for patients with local advanced pancreas cancer from April 2007.

D Gemcitabine Combined with Carbon-ion Therapy (Protocol 0513, 12 fractions/3 weeks)

From the results of the 0204 clinical study, carbon ion radiotherapy considerably improved tumor control of locally advanced pancreas cancer with acceptable morbidity in the surrounding normal tissues, but sufficient survival benefit could not be achieved. On the basis of the literature on drugs with a sensitizing effect in conjunction with heavy particle beams, further studies were scheduled in an effort to find even more effective treatment modalities based on a combination of chemo- and radiotherapy. We started a Phase I/II Clinical Trial of Gemcitabine Combined with Carbon-ion Therapy for patients with locally advanced pancreas cancer from April 2007.

The dose escalation schedule of Gemcitabine combined with carbon ion radiotherapy is shown in Fig.4. First the dose of carbon ion radiation was fixed at 43.2 GyE and the dose of gemcitabine was escalated from 400 mg to 1000 mg; then the dose of gemcitabine was fixed at 1000 mg and the dose of carbon ion radiation was escalated from 45.6 Gye to 50.4 GyE. Carbon ion therapy was given once daily, 4 days a week, for a fixed 12 fractions over 3 weeks. Gemcitabine was given once weekly (Fig.5).

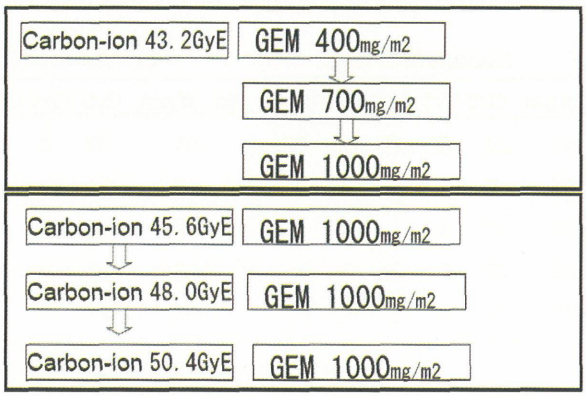

Fig 4. Dose Escalation Schedule(0513)

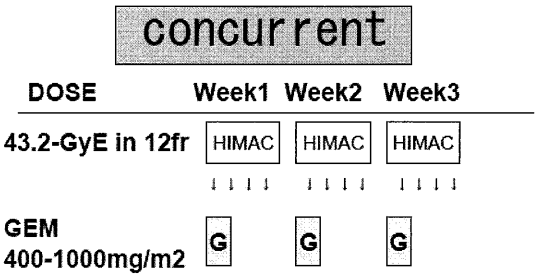

Fig.5 Treatment schema for combination of Gemcitabine and Carbon-ion therapy

At present we are trying to give 1000 mg/m^2 combined with 43.2 GyE of carbon ions. All patients completed the scheduled treatment course. This trial is still ongoing. Gemcitabine combined with carbon ion radiotherapy may be well tolerated by patients with pancreas cancer.

Reference

[1] Registration committee of pancreatic cancer. Annual Report of Nationwide Survey of Pancreatic Cancer. J of Jpn Panc Surg. 18: 101-169, 2003

[2] Lillemoe KD, Cameron JL, Hardacre JM et al. Is prophylactic gastrojejunostomy indicated for unresectable periampullary cancer? Ann Surg. 230: 322-330, 1999

[3] Prat F, Chapat O, Ducot B et al. A randomized trial of endoscopic drainage methods for inoperable malignant stricture of the common bile duct. Gastrointest Endosc. 47: 1-7, 1998

[4] Roldan GE, Gunderson LL, Nagorney DM et al. External beam versus intraoperative and extrabeam irradiation for locally advanced pancreatic cancer: Cancer. 61:1110-1116, 1988

[5] Moertel CG, Gundeson LL, Mailliard JA et al. Early evaluation of combined fluorouracil and leucovorin as a radiation enhancer for locally unresectable, residual, or recurrent gastrointestinal carcinoma. J Clin Oncol. 12:21-27, 1994

[6] Griffin JF, Smalley SR, Jewell W et al. Patterns of failure after curative resection of pancreatic carcinoma. Cancer. 66: 56-61, 1990

[7] Sato K, Yamada H, Ogawa K, et al. Performance of HIMAC. Nuclear Physics A. 588:229-234, 1995

[8] Kanai T, Endo M, Minohara S, et al. Biophysical characteristics of HIMAC clinical irradiation system for heavy-ion radiation therapy. Int J Radiat Oncol Biol Phys. 44:201-210, 1999

Carbon Ion Radiotherapy for Locally Advanced Adenocarcinoma of the Uterine Cervix

Shingo Kato, Hiroki Kiyohara, Hirohiko Tsujii, and Michiya Suzuki, for the Working Group of the Gynecological Tumor

Hospital, Research Center for Charged Particle Therapy, National Institute of Radiological Sciences, Chiba, Japan
e-mail address: s_kato@nirs.go.jp

Abstract

Purpose: To evaluate the toxicity and efficacy of carbon ion radiotherapy (CIRT) for locally advanced cervical adenocarcinoma by phase I/II dose-escalation study.

Methods and Materials: Between April 1998 and August 2008, 45 patients with cervical adenocarcinoma were treated with CIRT. Histologically, 36 patients had adenocarcinomas and 9 had adenosquamous carcinomas. Fifteen patients had stage IIB, 28 had stage IIIB, and 2 had stage IVA disease. The dose of the whole pelvic irradiation was fixed at 36.0 gray equivalent (GyE) in 12 fractions, and an additional dose of 26.4-38.4 GyE in 8 fractions was delivered to the cervical tumor (total dose: 62.4-74.4 GyE). The dose to the GI tracts was limited to less than 60 GyE. The median follow-up duration for all patients was 23 months (range, 6-93 months).

Results: No patient developed severe acute toxicity. No patient developed major late complications except for one patient with a rectovaginal fistula. Local control was obtained in 4 of the 7 patients receiving a total of 62.4-64.8 GyE, in 6 of the 9 patients receiving 68.0 GyE, in 13 of the 19 patients receiving 71.2GyE, and in all of 7 patients receiving 74.4 GyE. The 5-year local control and overall survival rates for stage IIIB or IVA patients who received $\geq$ 68.0 GyE were 64% and 46%, respectively.

Conclusions: Although the number of patients was small, the results have suggested that CIRT provided favorable local tumor control and overall survival with acceptable rates of late complications in the treatment of locally advanced cervical adenocarcinoma.

Introduction

The incidence of adenocarcinoma of the uterine cervix has been increasing over the past few decades (1). Currently, cervical adenocarcinoma accounts for 10-24% of all cervical carcinomas (1, 2).

There have been only a few reports that described the treatment outcomes of patients with cervical adenocarcinoma (3-8). According to these reports, locally advanced adenocarcinomas have a poorer prognosis than squamous cell carcinomas because of a poorer local control rate and higher rate of distant metastasis.

Several randomized phase III clinical trials in the 1990s and meta-analyses demonstrated that the combination of cisplatin-based chemotherapy and radiotherapy improved local control and overall survival in patients with locally advanced cervical cancer compared to radiotherapy alone (9-12). Based on the results, concurrent chemoradiotherapy has become the standard treatment for this disease. However, the majority of the patients included in these studies had squamous cell histology; adenocarcinomas represented approximately 10% of the registered patients. Therefore, the efficacy of concurrent chemoradiotherapy for locally advanced cervical adenocarcinoma has not been thoroughly evaluated clinically.

Carbon ion beams have improved dose localization properties, and this potentiality can produce great effects on tumors while minimizing normal tissue damage. Moreover, carbon ion radiotherapy (CIRT) has various biological advantages in terms of high linear energy transfer (LET) radiation, including a decreased oxygen enhancement ratio, a diminished capacity for sublethal and potentially lethal damage repairs, and diminished cell cycle-dependent radiosensitivity compared to those observed with low LET radiation. Several reports have demonstrated favorable results of CIRT in the treatment of malignant tumors, including head and neck cancer (13), non-small cell lung cancer (14), hepatocellular carcinoma (15), prostate cancer (16), and bone and soft tissue sarcomas (17).

In order to evaluate the efficacy and toxicity of CIRT for locally advanced cervical adenocarcinoma, a phase I/II dose-escalation study has been conducted.

Methods and Materials

1. Patient eligibility

Patients were enrolled into the study if they had medically inoperable adenocarcinoma or adenosquamous carcinoma of the uterine cervix with International Federation of Gynecology and Obstetrics (FIGO) stage IIB, III, or IVA disease (except for rectal invasion). The tumor had to be grossly measurable. Other eligibility criteria included World Health Organization performance status ≤ 3, and estimated life expectancy of ≥ 6 months. Patients who had histories of prior chemotherapy, and surgery or radiotherapy to the pelvis, were excluded from the study. Patients were also excluded if they had severe pelvic infection, severe psychological illness, or active double cancer.

Pretreatment evaluation consisted of an assessment of the patient's history, physical and pelvic examinations by gynecologists and radiation oncologists, cervical biopsy, routine blood cell counts, chemistry profile, chest X-ray, intravenous urography, cystoscopy, and rectoscopy. Computed tomography (CT) scans of the abdomen and pelvis, magnetic resonance imaging (MRI) of the pelvis, and ^{11}C methionine positron emission tomography (PET) scans were also performed for all patients. Patients were staged according to the FIGO staging system, but patients with para-aortic lymph nodes > 1 cm in minimum diameter on CT images were excluded from the study (18). Patients with enlarged pelvic lymph nodes only were included in the study. Tumor size was assessed by both pelvic examination and MRI, and dimensions of the cervical tumor were measured based on T2-weighted MRI images (18). ^{11}C methionine PET scans were supplementally used for detecting distant metastasis. Tumor specimens were reviewed by pathologists of the working group. All patients gave written informed consent according to the institutional regulations.

2. Carbon ion radiotherapy

The treatment consisted of whole pelvic irradiation and local boost, with the target volume being shrunk in three steps so that the highly concentrated dose could be delivered to the tumor without increasing the dose to normal structures. The clinical target volume (CTV) for whole pelvic irradiation (CTV-1) included all areas of gross and potentially microscopic disease, consisting of the primary tumor, uterus, parametrium, at least the upper half of the vagina, and pelvic lymph nodes. Because non-enlarged lymph nodes are poorly visualized on CT, nodal regions were defined by encompassing the pelvic vessels with a 5-10-mm margin. After completing whole pelvic irradiation, local boost irradiation was performed. First, CTV included the gross tumor volume (GTV) and surrounding tissues, such as the parametrium, uterine body, upper vagina, and adjacent lymph nodes (CTV-2). Next, CTV was further shrunk to GTV only, and the intestines and bladder were completely excluded from the target volume (CTV-3). A margin of 5 mm was usually added to the CTV to create the planning target volume (PTV). When the tumor was located close to critical organs such as the bowel or bladder, the margin was reduced accordingly. CTV was covered by at least 90% of the prescribed dose. The dose to the bowel was

limited to < 60 GyE. A spacer was inserted into the vaginal canal to provide a safe distance between the tumor and the rectum (Fig. 1).

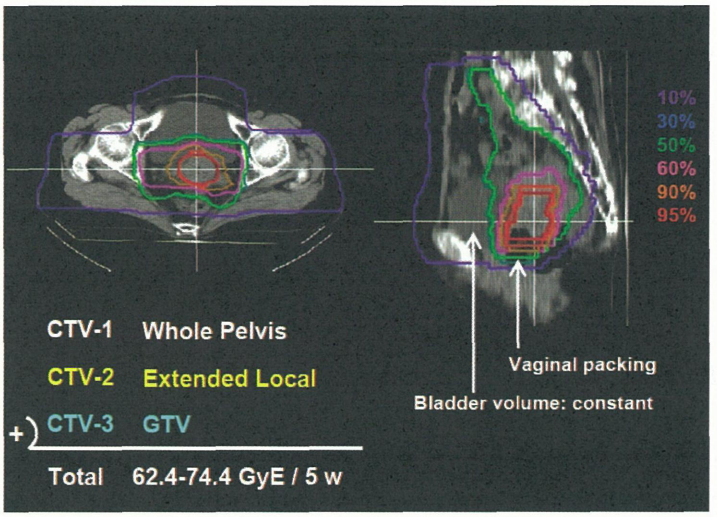

Fig. 1. Carbon ion radiotherapy (CIRT) for locally advanced cervical adenocarcinoma. Isodose curves of CIRT are superimposed on axial and sagittal CT images.

Carbon ion radiotherapy was given once daily, 4 days per week, for a fixed 20 fractions in 5 weeks. The dose to PTV was fixed at 36 GyE/12 fractions. A dose escalation study was planned in the local boost session with an initial dose of 26.4 GyE for 8 fractions (3.3 GyE/fraction) up to 38.4 GyE (4.8 GyE/fraction) by 10% increments. At every treatment session, the patient was positioned on a treatment couch with immobilization devices, and the patient's position was verified using a computer-aided, on-line positioning system. In order to minimize internal target positional uncertainty, 100 ml of normal saline was infused into the bladder. Patients were also encouraged to use laxatives, if necessary, to prevent constipation throughout the treatment period.

3. Assessment of toxicity and efficacy

Acute toxicity was graded according to the Radiation Therapy Oncology Group (RTOG) acute radiation morbidity scoring system, with the highest toxicity within 3 months from the initiation of CIRT. Late toxicity was graded according to the RTOG/European Organization for Research and Treatment of Cancer (EORTC) late radiation morbidity scoring scheme (19). The effect of the treatment was evaluated in terms of local control and overall survival. Local control was defined as showing no evidence of tumor regrowth or recurrence in the treatment volume based on physical examinations, CT, MRI, PET, and/or biopsy. Local control and overall survival rates were calculated by the Kaplan-Meier method.

Results

Between April 1998 and August 2008, a total of 45 patients with cervical adenocarcinoma or adenosquamous carcinoma were treated with CIRT. Patient characteristics are summarized in Table 1. Mean age was 60 years. Histologically, 36 had adenocarcinomas and 9 had adenosquamous carcinomas. Fifteen patients had stage IIb, 28 had IIIb, and 2 had stage IVA disease. Eighteen patients had enlarged lymph nodes in the pelvis. All patients had bulky tumors measuring 3.0-11.0 cm in maximum diameter and a median diameter of 5.5 cm. All patients were subjected to periodic follow-up. The median follow-up duration for all patients was 23 months. In the dose-escalation study, 3 patients received a total dose of 62.4 GyE, 4 received 64.8 GyE, 10 received 68.0 GyE, 21 received 71.2 GyE, and 7 received 74.4GyE (Table 2).

Table 1. Patient characteristics

No. of patients	45
Follow-up, range (median) (mo)	6-93 (23)
Age, range (mean) (yrs)	37-85 (60)
Histology	
Adenocarcinoma	36
Adenosquamous carcinoma	9
FIGO Stage	
IIb	15
IIIb	28
IVa	2
Lymph node status	
Negative	27
Positive	18
Tumor size	
3-6 cm	23
6-8 cm	18
8 cm-	3

Table 2. Dose escalation study of CIRT

(n=45)

Whole pelvis (fixed)	Local boost (dose escalation)	Total dose	No. of patients
3.0 GyE x 12 (36.0 GyE)	3.3 GyE x 8	62.4 GyE	3
	3.6 GyE x 8	64.8 GyE	4
	4.0 GyE x 8	68.0 GyE	10
	4.4 GyE x 8	71.2 GyE	21
	4.8 GyE x 8	74.4 GyE	7

1. Toxicity

No patient developed severe acute toxicities in the skin, gastrointestinal (GI), or genitourinary (GU) tract (Table 3). Seven (16%) patients developed late complications in the skin, GI or GU tract. Almost all of the complications were classified as grade 1, but one patient developed Grade 4 late GI toxicity (Table 4). She had a stage IIb cervical adenocarcinoma, measuring 7 cm in maximum diameter. She received a total of 68.0 GyE to her primary tumor. Fourteen months after CIRT, she developed a rectovaginal fistula. She has been alive without disease and intestinal problems for 73 months after receiving a colostomy. She had uncontrolled diabetes mellitus, which may have contributed to her complication. No other patients receiving 68.0-74.4 GyE developed major late GI toxicity (Table 5).

Table 3. Acute toxicities by RTOG scoring system

Site	No. of Patients	RTOG Grade			
		Gr. 0	Gr. 1	Gr. 2	Gr. 3
Skin	45	38	7	0	0
GI tract	45	29	15	1	0
GU tract	45	38	7	0	0

Table 4. Late toxicities by RTOG/EORTC scoring scheme

Site	No. of Patients	RTOG/EORTC Grade				
		Gr. 0	Gr. 1	Gr. 2	Gr. 3	Gr. 4
Skin	45	44	1	0	0	0
GI tract	45	41	3	0	0	1
GU tract	45	40	2	3	0	0

Table 5. Late GI toxicities by carbon ion dose

Total dose (GyE)	No. of Patients	Follow-up (median) (mo)	RTOG/EORTC Grade				
			G0	G1	G2	G3	G4
62.4	3	8-20 (15)	3	0	0	0	0
64.8	4	10-93 (65)	2	2	0	0	0
68.0	10	13-80 (66)	8	1	0	0	1*
71.2	21	9-53 (23)	21	0	0	0	0
74.4	7	6-15 (11)	7	0	0	0	0

* recto-vaginal fistula

2. Local control and survival

The relationship between carbon ion dose and local control is shown in Fig. 2. Three patients with marginal recurrences were excluded from this analysis. Local control was obtained in 4 of the 7 patients (57%) receiving 62.4-64.8 GyE, in 6 of the 9 patients (67%) receiving 68.0 GyE, in 13 of the 19 patients (68%) receiving 71.2GyE, and in all of the 7 patients receiving 74.4GyE.

The actuarial local control and overall survival curves for all patients are shown in Fig. 3. The 3- and 5-year local control rates were 63% and 57%, respectively. Three patients who had developed local recurrences were surgically salvaged, bringing the 5-year local control rate, including the salvage surgery, to 70%. Twenty-four of the 45 patients (53%) developed distant metastases, including 11 patients to the paraaortic lymph nodes, and they subsequently received photon radiotherapy and/or chemotherapy. The 3- and 5-year overall survival rates were 57% and 42%, respectively. With regard to the stage III or IVA patients who received 68.0-74.4 GyE of CIRT, the 5-year local control and overall survival rates were 64% and 46%, respectively (Fig. 4).

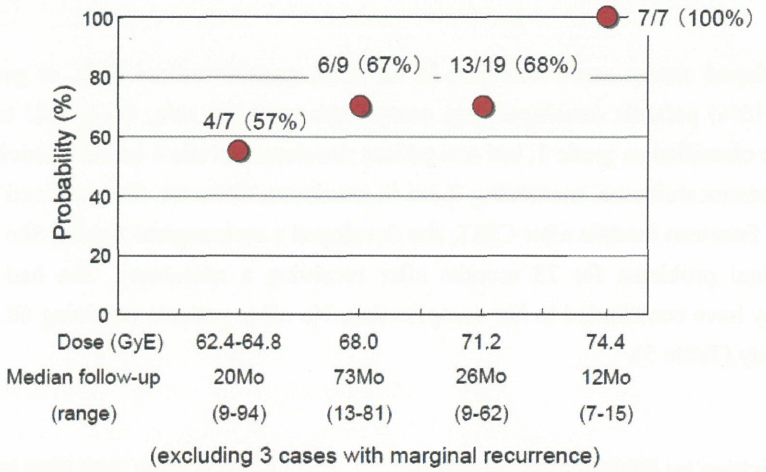

Fig. 2. Dose response relationship between carbon ion dose and local control.

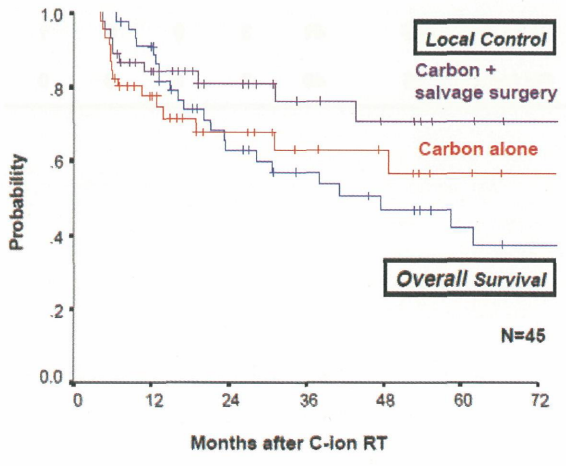

Fig. 3. Overall survival and local control curves in patients with cervical adenocarcinoma treated with CIRT.

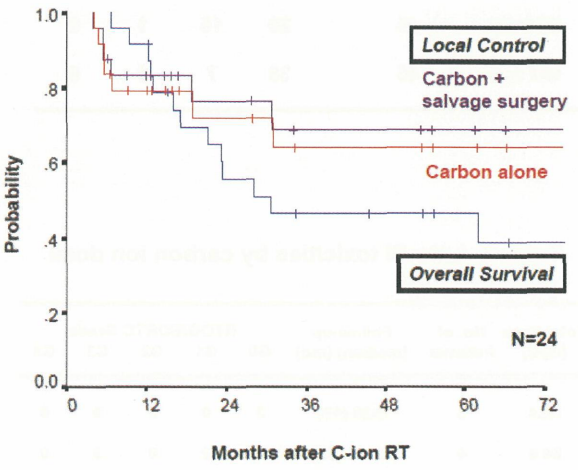

Fig. 4. Overall survival and local control curves in stage IIIb-IVa patients treated with a dose of 68-74.4GyE of CIRT.

Discussion

Two phase I/II clinical studies of CIRT for locally advanced cervical cancer were carried out before this study (20). The following results were obtained from those studies: 1) doses of 35.2-48.0 GyE in 16 fractions (2.2-3.0 GyE/fraction) over 4 weeks could be delivered safely to the whole pelvis, 2) a dose $\geq$ 60 GyE to the GI tract may have caused severe late complications. Based on the results, the dose to the whole pelvis was fixed at 36.0 GyE for 12 fractions (3.0 GyE/fraction) over 3 weeks in the present protocol, which was assumed to be equivalent to 40 Gy of conventional photon radiotherapy. An additional dose of 13.2-19.2 GyE for 4 fractions (3.3-4.8 GyE/fraction) was delivered to the cervical tumor and surrounding tissues including the parametrium, uterine body, upper vagina, and adjacent lymph nodes, where tumor infiltration was highly suspected. Consequently, these lesions were given a total of 49.2-55.2 GyE. Following this, the PTV was shrunk to the GTV only, and the GI tracts were completely excluded from the PTV. The GTV received a total of 62.4-74.4 GyE, whereas the dose to the GI tracts was limited to < 60 GyE (Fig. 1).

The incidence and severity of late complications in this study were significantly lower than those in the previous studies (20). Only one (2%) of the 45 patients developed a major rectal complication (Table 4, 5). The anatomical location of her cervical tumor was in close proximity to the rectum, making it somewhat difficult to exclude the rectum from the PTV-3. She developed a rectovaginal fistula after 3 months of local infection. Because she had uncontrolled diabetes mellitus, this concomitant disease may have had some involvement with this complication. The lower incidence of late GI complications was considered to be attributable to the strict dose constraint to the GI tract.

Variations in bladder and rectal filling may cause displacement of the uterus and upper vagina, leading to systematic errors throughout the course of treatment (20, 21). Our clinical experience using repeated MRI or CT scans during treatment also suggested that the target position might change according to the bladder volume. To decrease such positional uncertainties, we infused a fixed volume (usually 100 ml) of normal saline into the bladder throughout the treatment. Patients were also encouraged to use laxatives, if considered necessary, to prevent constipation during treatment.

If a treatment plan is generated based on the single time-point assessment of the target position, tumor volume shrinkage may also result in systematic errors throughout the treatment course (20, 22). In our past studies, we performed treatment planning twice during the course of CIRT. However, the CTV for local boost may not have conformed to the real tumor volume because of tumor shrinkage, and a large volume of the GI tract may have been involved in the CTV (20). In this study, we performed treatment planning three times in accordance with tumor shrinkage, so that CTV-3 encompassed the GTV only. This repeated treatment planning may have minimized the internal target positional uncertainty and lessened the incidence of late GI toxicity (20).

The crude local control rates for patients receiving 62.4-64.8 GyE, 68.0 GyE, 71.2 GyE, and 74.4 GyE were 57%, 67%, 68%, and 100%, respectively (Fig. 2). This result may indicate that there is a dose-response relationship in CIRT for cervical adenocarcinoma and that a high local tumor control may be obtained with a dose $\geq$ 71.2 GyE. However, longer follow-up periods will certainly be necessary to confirm such a conclusion, because the follow-up period of the patients who received 74.4 GyE was still short.

Several reports have described poorer treatment outcomes for patients with locally advanced cervical adenocarcinomas compared with those for patients with squamous carcinomas. Lea et al. treated 83 patients with stage IIb-IVb cervical adenocarcinoma by radiotherapy or chemoradiotherapy and reported 5-year survival rates of 30% for stage IIb and 0% for stage III-IV (6). Eifel et al. in their large series of radiotherapy reported 5-year survival rates of 28% for stage IIb and 26% for stage III (4). In contrast, Grigsby et al. analyzed prognostic factors by multivariate analysis and found that adenocarcinoma was not a significant prognostic factor. However, when comparing the treatment outcomes among patients with stage III disease, the 5-year survival rate of 25% for adenocarcinoma was lower than that of 36.7% for squamous carcinoma (7).

When comparing our treatment results with those of the previous reports, our 5-year overall survival rate of

46% for stage IIIB-IVA patients receiving 68.0 GyE or more seemed favorable (Table 6). Only a few studies have described failure patterns in patients with stage III cervical adenocarcinoma treated by radiotherapy (4, 7). According to those reports, local failure was observed in 39-67%. In contrast, 5-year local control of our stage III-IVA patients was 64% (Fig. 4). Therefore, the favorable survival rate achieved in our study may have been attributable to the high local tumor control achieved by CIRT. Nonetheless, further study will be needed to confirm the efficacy of CIRT in local management, as our patient number was rather small.

Table 6. Outcomes of RT/CRT and C-ion RT for patients with locally advanced cervical adenocarcinoma.

No.	Author	Year	No.	Stage	Therapy	5y OS	Follow-up
1)	Baalbergen A	2004	22	III	RT (+HT)	-	61Mo. (mean)
2)	Lea JS	2002	24	III	RT/CRT	0%	33Mo. (median)
3)	Hopkins MP	1991	25	III	RT	8%	80Mo. (median)
4)	Eifel PJ	1990	46	III	RT	26%	87Mo. (median)
5)	Quin MA	2006	135	IIIB	RT/CRT	24%	NA
6)	NIRS	2008	29	IIIB-IVA	RT/CRT	19%	38Mo. (median)
7)	NIRS	2009	24	IIIB-IVA	C-ion RT (68GyE-)	46%	26Mo. (median)

All published studies included patients with adenosquamous cell carcinoma.

1) Gynecol Oncol 92:262-267,2004. 2) Gynecol Oncol 84:115-119,2002.
3) Obstet Gynecol 72: 789-795,1991. 4) Cancer 65:2507-2514,1990.
5) Int J Gynecol Obstetr 95, suppl 1: 43-103, 2006. (26th FIGO annual report)

In spite of the higher local tumor control, distant metastasis frequently occurred, and the survival rate was still unsatisfactory (Fig. 3, 4). Several studies also described a high rate of distant metastasis, resulting in poor survival (3-7). To improve the survival rate, the use of chemotherapy in combination with CIRT should be explored.

Conclusions

Although the number of patients was small, our results have strongly suggested that CIRT provided favorable local tumor control and overall survival with acceptable rates of late complications in the treatment of locally advanced cervical adenocarcinoma. Further study is needed to confirm the efficacy of CIRT in the local management of locally advanced cervical adenocarcinoma. The use of chemotherapy in combination with CIRT should also be considered to improve the survival rate.

References

[1] Smith HO, Tiffany MF, Qualls CR, Keys CR. The rising incidence of adenocarcinomas relative to squamous cell carcinomas of the uterine cervix - a 24-year population based study. Gynecol Oncol 2000; 78:97-105.

[2] Benedet JL, Odicino F, Maisonneuve P, et al. Carcinoma of the cervix uteri. (In) Journal of Epidemiology and Biostatistics, FIGO Annual Report on the Results of Treatment in Gynaecological Cancer. 6: P7-43, 2001.

[3] Baalbergen A, Ewing-Graham PC, Hop WC, Struijk P, Helmerhorst TJ. Prognostic factors in

adenocarcinoma of the uterine cervix. Gynecol Oncol 2004; 92:262-267.

[4] Eifel PJ, Morris M, Oswald MJ, Wharton JT, Delcos L. Adenocarcinoma of the uterine cervix. Prognosis and patterns of failure in 367 cases. Cancer 1990; 65:2507-2514.

[5] Hopkins MP, Morley GW. A comparison of adenocarcinoma and squamous cell carcinoma of the cervix. Obstet Gynecol 1991; 77:912-918.

[6] Lea JS, Sheets EE, Wenham RM, et al. Stage IIB-IVB cervical adenocarcinoma: Prognostic factors and survival. Gynecol Oncol 2002; 84:115-119.

[7] Grigsby PW, Perez CA, Kuske RR, et al. Adenocarcinoma of the uterine cervix: Lack of evidence for a poor prognosis. Radiother Oncol 1988; 12:289-296.

[8] Kilgore LC, Soong SJ, Gore H, Shingleton HM, Hatch KD, Partridge EE. Analysis of prognostic factors in adenocarcinoma of the cervix. Gynecol Oncol 1988; 31:137-148.

[9] Eifel PJ, Winter K, Morris M, et al. Pelvic irradiation with concurrent chemotherapy versus pelvic and para-aortic irradiation for high-risk cervical cancer: An update of Radiation Therapy Oncology Group Trial (RTOG) 90-01. J Clin Oncol 2004; 22: 872-880.

[10] Rose PG, Bundy BN, Watkins EB, et al. Concurrent cisplatin-based radiotherapy and chemotherapy for locally advanced cervical cancer. N Engl J Med 1999; 340: 1144-1153.

[11] Whitney CW, Sause W, Brundy BN, et al. A randomized comparison of fluorouracil plus cisplatin versus hydroxyurea as an adjuvant to radiation therapy in stages IIB-IVA carcinoma of the cervix with negative para-aortic lymph nodes: A Gynecologic Oncology Group and Southwest Oncology Group study. J Clin Oncol 1999; 17: 1339-1348.

[12] Green JA, Kirwan JM, Tierney JF, et al. Survival and recurrence after concomitant chemotherapy and radiotherapy for cancer of the uterine cervix: a systematic review and meta-analysis. Lancet 2001; 358: 781-786.

[13] Mizoe J, Tsujii H, Kamada T, et al. Dose escalation study of CIRT for locally advanced head and neck cancer. Int J Radiat Oncol Biol Phys 2004; 60: 358-364.

[14] Miyamoto T, Yamamoto N, Nishimura H, et al. CIRT for stage I non-small cell lung cancer. Radiother Oncol 2003; 66: 127-140.

[15] Kato H, Tsujii H, Miyamoto T, et al. Results of the first prospective study of CIRT for hepatocellular carcinoma with liver cirrhosis. Int J Radiat Oncol Biol Phys 2004; 59: 1468-1476.

[16] Tsuji H, Yanagi T, Ishikawa H, et al. Hypofractionated radiotherapy with carbon ion beams for prostate cancer. Int J Radiat Oncol Biol Phys 2005; 63: 1153-1160.

[17] Kamada T, Tsujii H, Tsuji H, et al. Efficacy and safety of CIRT in bone and soft tissue sarcomas. J Clin Oncol 2002; 20: 4466-4471.

[18] Ascher SM, Imaoka I, Hricak H. Diagnostic imaging techniques in gynecologic oncology. In Hoskins WJ, Perez CA, Young RC ed: Principles and practice of gynecologic oncology, 3rd ed. P629-668, Lippincott Williams and Wilkins, Philadelphia, 2000.

[19] Cox JD, Stetz J, Pajak TF. Toxicity criteria of the Radiation Therapy Oncology Group (RTOG) and the European Organization for Research and Treatment of Cancer (EORTC). Int J Radiat Oncol Biol Phys 1995; 31: 1341-1346.

[20] Kato S, Ohno T, Tsujii H, et al. Dose escalation study of carbon ion radiotherapy for locally advanced carcinoma of the uterine cervix. Int J Radiat Oncol Biol Phys 2006; 31: 1341-1346.

[21] Ahmad A, D'Souza W, Salehpour M, et al. Intensity-modulated radiation therapy after hysterectomy: Comparison with conventional treatment and sensitivity of the normal-tissue-sparing effect to margin size. Int J Radiat Oncol Biol Phys 2005; 62: 1117-1124.

[22] Kavanagh BD, Schefter TE, Wu Q, et al. Clinical application of intensity-modulated radiotherapy for locally advanced cervical cancer. Semin Rad Oncol 2002; 12: 260-271.

Carbon Ion Radiotherapy for Prostate Cancer

Hiroshi Tsuji, Tohru Okada, Shinji Sugahara, Itsuko Serizawa, Hiroyuki Kato, Hitoshi Ishikawa, Tadashi Kamada, Jun-etsu Mizoe, Tatsuaki Kanai, Hirohiko Tsujii, and the Working Group for Genitourinary Tumors

Hospital, Research Center for Charged Particle Therapy, National Institute of Radiological Sciences, Chiba, Japan
e-mail address: h_tsuji@nirs.go.jp

Abstract

Purpose: Analysis of the results of hypofractionated conformal carbon ion radiotherapy (C-ion RT) for localized prostate cancer was performed, with regard to normal tissue morbidity, biochemical relapse-free rate (bNED), and patient survival. Methods and Materials: Five hundreds and forty-two prostate cancer patients who received C-ion RT established through two preceding dose-escalation studies were analyzed in regard to toxicity, survival, and bNED. Results: Concerning radiation morbidity, no grade 3 or higher toxicities were observed either in the rectum or genitourinary system (GU), and the incidences of grade 2 rectum and GU morbidity were only 2.3% and 4.8%, respectively. The incidence of late GU toxicity in patients treated with 16 fractions of C-ion RT was lower than that of 20 fractions. Overall bNED at 5 years was 88.9%, with only four local recurrences. bNED of 16 fractions of C-ion RT was comparable to that of 20 fractions. Gleason's score, T-stage, and initial PSA were significant prognostic factors for bNED, and T-stage was also a significant prognostic factor for overall survival rate. The duration of hormonal therapy also had an impact on biochemical control in high-risk patients, but it appeared possible to apply C-ion RT with short-course hormonal therapy to intermediate-risk patients. Conclusion: C-ion RT with the established dose fractionation regimen yielded satisfactory bNED with very few local recurrences, and with minimal morbidity. C-ion RT of 16 fractions could offer even lower incidence of GU toxicity than that of 20 fractions.

Introduction

Prostate cancer is a slow-growing tumor occurring in advanced-age male patients, but incidence and mortality rate are both rapidly increasing in Asian as well as in Western countries. Radiotherapy is one of the treatments of choice for localized or locally advanced tumor of the prostate. In order to obtain satisfactory results, sufficient radiation effect with desirable dose concentration is required. This tumor is relatively radio-resistant, and severe damage to adjacent normal tissues will have deleterious effects on the post-treatment quality of life.

Carbon ion radiotherapy (C-ion RT) may be the ideal radiation treatment for prostate cancer because of the unique physical and biological advantages of carbon ion beams [1]. The successful results obtained with novel conformal radiotherapy techniques, such as three-dimensional conformal radiotherapy (3DCRT) and intensity modulated radiotherapy (IMRT) [2-4], are evidence that dose conformity confers clear advantages to the radiotherapy of prostate cancer. Carbon ion beams offer superior dose conformity in the treatment of deep-seated tumors compared to the state-of the-art techniques of X-ray therapy, and therefore C-ion RT possesses a greater potential of further improving the treatment outcome of prostate cancer [1].

In this respect, high-linear energy transfer (LET) radiation therapy with fast neutrons was found to yield an excellent tumor control rate. Its unacceptably high toxicity [5,6], however, has stood in the way of this therapy coming into wider use. The high incidence of morbidity associated with fast neutron therapy was mainly due to an inferior dose concentration of neutron beams. This problem, however, can be solved by the use of heavy charged particle beams, such as carbon ions, without foregoing the radiobiological advantages of high LET radiation.

To establish an appropriate dose fractionation regimen for C-ion RT, two phase I/II clinical studies have been performed [7-9] at the National Institute of Radiological Sciences (NIRS), Chiba, Japan since 1994, using carbon ion beams generated by the Heavy Ion Medical Accelerator in Chiba (HIMAC). A phase II clinical study was then started in April 2000, using the established treatment method of hypofractionated C-ion RT with the recommended dose of 66.0GyE in 20 fractions over 5 weeks that had been proved effective in the phase I/II studies [10,11]. The safety and efficacy of this treatment strategy of C-ion RT was further confirmed with this phase II study, and approval for its use as a highly advanced medical technology was obtained in November 2003 [9-11]. This article presents the methods and updated outcomes of this established C-ion RT, and also describes its future prospects at NIRS.

Materials and Methods

1. Protocols

So far, a total of 690 patients have been enrolled, 97 patients in the first two phase I/II studies, 176 in the phase II study, and 417 after official approval for the application of the procedure as a highly advanced medical technology (Table 1). Of this total, 542 patients received the established treatment of C-ion RT, and were followed up for at least 6 months and analyzed. Another 97 patients, who could not be enrolled in the studies because of prolonged neoadjuvant hormone therapy and receiving 16 fractions of C-ion RT, were added into the analysis of toxicity for the sake of evaluating the effect of altered fractionation on toxicity.

Table 1. Clinical studies of C-ion RT for prostate cancer at NIRS

Protocol	Study Design	T-stage	Period	Total Dose (GyE/20 fr.)	Hormone therapy	Number of patients
9402	Phase I / II Dose escalation	T2b~T3	95.6~ 97.12	54.0~ 72.0	(+)	35
9703	Phase I / II Dose escalation	T1~T2a	98.1~ 00.2	60.0~ 66.0	(-)	20
	Fixed dose	T2b~T3		66.0	(+)	42
9904	Phase II Fixed dose	T1~T3	00.4~ 03.11	66.0	High*(+) Low* (-)	176
		T1~T3	03.12~ 08.7	66.0, 63.0	High* >24m Interm* =6m Low* (-)	417
Total			95.6 ~ 08.7			690

*Stratified by risk factors: clinical stage, initial PSA, and Gleason score

Patients were eligible if they had histologically proven prostatic adenocarcinoma, that is, stage T1, T2 or T3 primary tumors [12] without radiologically detectable distant metastasis (M0), involvement of regional lymph nodes (N0, pN0), or solitary, non-fixed involvement of regional lymph nodes diagnosed by staging pelvic lymphadenectomy (pN1). Eligible patients were required not to have undergone previous treatment for prostate cancer except for hormone therapy. All patients signed an informed consent form approved by the local institutional review board. Pathological specimens were reviewed centrally before registration, and those of the phase I/II studies were reviewed retrospectively.

Until September 2005, patients were stratified into two subgroups, high-risk and low-risk groups, according to T-staging, Gleason's score (GS), and initial serum PSA. Thereafter, the high-risk group was further divided into two groups — an intermediate-risk group and a true high-risk group. For the true high-risk group patients, namely, patients with T3 primary tumor, GS ≥ 8 or a serum PSA value ≥ 20 ng/ml, long-term (≥ 24 months) hormonal therapy was applied in combination with C-ion RT. Patients in the low-risk group, that is, T1/T2a patients with GS < 7 and serum PSA < 20 ng/ml, received only C-ion RT. For the intermediate-risk group patients, consisting of those with a serum PSA value < 20 ng/ml and T2b primary tumor or GS of 7, combined treatment of C-ion RT and short-course (6 months) hormonal therapy was performed (Fig.1).

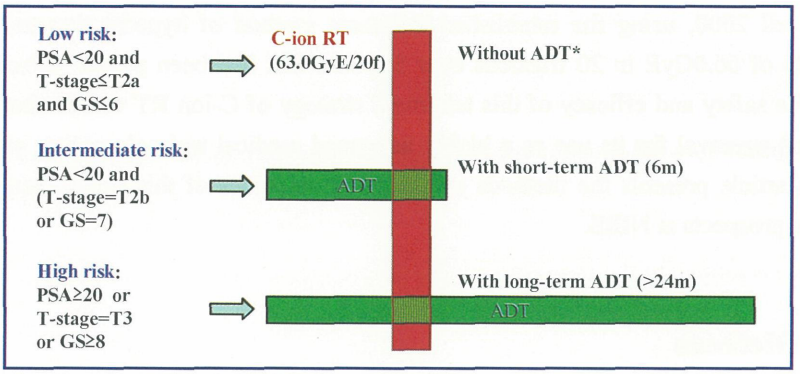

*ADT: Androgen Deprivation Therapy

Figure 1

Fig. 1 Current treatment strategy for prostate cancer at NIRS
Patients were divided into three risk groups of high, intermediate, and low, according to their T-stage, initial PSA, and Gleason score.

2. Carbon Ion Radiotherapy

1) Treatment techniques

In order to make good use of the excellent dose concentration of carbon ion beam, it is extremely important to keep high precision and sufficient reproducibility in patient positioning and the field. The techniques applied were:

a) Rigid immobilization
b) Volume control of the rectum and bladder
c) Precise field-localization with bony structure

a) Rigid immobilization

The head and feet of the patients were positioned in the customized cradles (Moldcare; Alcare, Tokyo, Japan), and the pelvis was immobilized with a low-temperature thermoplastic of 3-mm thickness (Shellfitter; Keraray Co, Ltd, Osaka, Japan). A relatively thick body-shell can exert mild pressure against the lower abdominal wall and reduce organ motion in the pelvis. With this method of immobilization, intra-fractional motion of the prostate was evaluated as less than 2 mm and, therefore, respiratory gating was not used.

b) Volume control of the rectum and bladder

The bladder was filled with 100 ml of sterilized water both at the time of CT acquisition and at each treatment session in the case of beam irradiation in the vertical direction. The patient was instructed to empty the rectum as much as possible just before the treatment, and a laxative or enema was used if necessary. The amount of gas in the rectum was carefully observed by positioning images and the set-up was repeated unless the rectum was sufficiently empty.

c) Precise field-localization with bony structure

At every treatment session, the patient's position was verified with a computer-aided, on-line positioning system. The patient was positioned on the treatment couch with the immobilization devices, and digital

orthogonal x-ray television images were taken in that position and transferred to the positioning computer. The positioning images were compared with reference images, which were checked to confirm their match with the digitally reconstructed radiograph (DRR). Any differences found were measured. The treatment couch was then moved to the matching position until the largest deviation of all measured points was less than 2 mm.

2) Treatment Planning

A set of 2.5-mm-thick CT images was taken for treatment planning, with the patient placed in immobilization devices. Three-dimensional treatment planning was performed using HIPLAN software (National Institute of Radiological Sciences, Chiba, Japan) [13]. Clinical target volume (CTV) was defined as consisting of the prostate and the seminal vesicle (SV) demonstrated by CT images, irrespective of T-stage or other risk factors. MRI was also taken in all patients and used as a reference for defining CTV. However, in the case of patients with a low risk, the whole SV should not always be included in the CTV. Thus, for example, the CTV of the patients staged as T1 or T2a did not cover the SV tips. Further, anterior and lateral safety margins of 10 mm and a posterior margin of 5 mm were added to the CTV to create the initial planning target volume (PTV-1). In order to reduce the dose to the anterior rectal wall, a rectum-sparing target volume (PTV-2) was used for the latter half of C-ion RT, where the posterior margin was reduced to the anterior boundary of the rectum. Evaluation of the plan was routinely performed at the case conferences before the actual treatment, using dose-volume histograms (DVH) for the CTV, PTV-1, PTV-2, and the rectum. Particularly, the DVH of the rectum was evaluated by comparing the reference DVH that was obtained from analysis using actual DVH data of preceding dose-escalation studies. If the rectal DVH of the new patient was beyond the reference DVH at the high dose area, the treatment planning was revised.

C-ion RT was given once a day, 4 days a week (Tuesday to Friday). One port was used in each session. Patients were treated from 5 irregularly shaped ports, one anterior-posterior port and a pair of lateral ports for PTV-1 and another pair of lateral ports for the PTV-2. 100% of the prescribed dose was given at the maximum dose point of each portal. PTV-2 was covered by at least 90% of the prescribed dose, and the minimum dose of PTV-1 was more than 50% of the maximum dose and depended on the volume spared by PTV-2.

Dose was expressed in Gray-Equivalent (GyE = physical carbon ion dose (Gy) x Relative Biological Effectiveness {RBE}). Irrespective of the size of the Spread-Out Bragg Peak (SOBP), the RBE value for carbon ions was estimated to be =3.0 at the distal part of the SOBP. The compensation bolus was fabricated for each patient to make the distal configuration of the SOBP similar to the PTV. A multi-leaf collimator or a customized brass collimator defined the margins of the PTV. Fig. 2 shows the representative dose distribution.

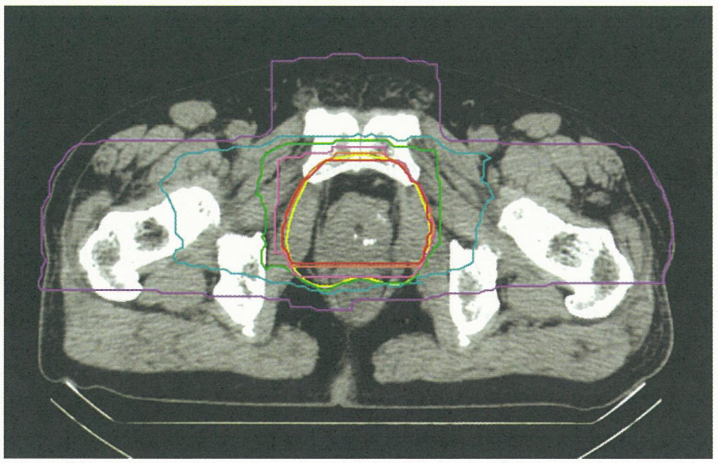

Figure 2

Fig. 2 Typical dose distribution of carbon ion radiotherapy

The irradiated dose was fixed at 63.0GyE or 66.0GyE/20fractions as the recommended dose fractionation schedule established in the two previous phase I/II studies involving dose escalation from the initial dose of 54.0GyE/20fractions to 72.0GyE/20f in 10% increments [11]. In addition, a more hypofractionated schedule of 57.6GyE/16fractionas was applied since September 2007. This newly applied fractionation had been tested in another patient group who could not be enrolled in the clinical studies because of prolonged neoadjuvant hormonal therapy since April 2003.

3. Androgen Deprivation Therapy (ADT)

Before C-ion RT, neoadjuvant androgen deprivation therapy (ADT) such as medical or surgical castration with or without antiandrogen was applied for 2 to 6 months to the patients of the high-risk and intermediate-risk groups. Adjuvant ADT was continued for a duration of 6 months for the intermediate-risk patients and for more than 24 months for the high-risk patients. The median duration of ADT of 445 patients receiving combined treatment was 24.1 months. The remaining 97 patients received C-ion RT only.

Results

Of the 542 analyzed patients, 320 (59.0%) were categorized as high-risk, 125 (23.1%) as intermediate-risk, and 97 (17.9%) as low-risk according to our definition of risk grouping. The average pretreatment PSA value was 25.9 ng/ml, with a median of 13.5 ng/ml and a range of 3.4 - 810.0 ng/ml. One hundred and ninety-seven (36.3%) patients had an initial PSA value of more than or equal to 20 ng/ml. One hundred and seventy-four (32.1%) patients had T3 primary tumors and the remaining 368 (67.9%) had T1 or T2 tumors. One hundred and forty-three (26.4%) patients had GS of less than, or equal to 6, 239 (44.1%) had GS of 7, and 160 (29.5%) had GS of more than, or equal to 8. Median follow-up period was 37.0 months at the time of analysis.

1. Toxicity

The cumulative incidence and status on the last follow-up date for late rectum and genitourinary morbidities in the 563 patients treated with either of 20 fractions or 16 fractions and followed up more than 12 months are summarized in Table 2. None of the patients had developed grade 3 or higher morbidities up to the latest follow-up. Grade 2 morbidities of the genitourinary system and rectum were observed in 4.8% and 2.3% of the patients, respectively. Regarding the effect of alteration in dose fractionation, both the rectal and GU toxicity at 66.0GyE/20f were a little more frequent than those at 63.0GyE/20f or 57.6Gy/16f. The incidences of rectal toxicity at 63.0GyE/20f and 57.6GyE/16f were comparable, whereas the incidence of GU toxicity at 57.6GyE/16f was even lower that that at 63.0GyE/20f.

Table 2. Late gastrointestinal and genitourinary morbidity after C-ion RT in patients followed up more than 12 months

Dose GyE/f.	No.pts.	Rectum				Bladder/urethra			
		Grade0	G1	G2	G3	Grade0	G1	G2	G3
66.0/20	250	199	44	7	0	76	154	20	0
	(%)	(79.6)	(17.6)	(2.8)	(0)	(30.4)	(61.6)	(8.0)	(0)
63.0/20	216	193	19	4	0	127	83	6	0
	(%)	(89.4)	(8.8)	(1.9)	(0)	(58.8)	(38.4)	(2.8)	(0)
57.6/16	97	85	10	2	0	60	36	1	0
	(%)	(87.6)	(10.3)	(2.1)	(0)	(61.9)	(37.1)	(1.0)	(0)
Total	563	477	73	13	0	263	273	27	0
	(%)	(84.7)	(13.0)	(2.3)	(0)	(46.7)	(48.5)	(4.8)	(0)

2. Survival and Tumor Control

The Kaplan-Meier estimates of overall and cause-specific survivals for the 542 patients at five years were 95.1% and 98.7%, respectively (Fig.3). By the date of analysis, 15 patients had died, 4 of metastasis from the prostate, and 11 of other malignancies or intercurrent diseases. So far, no patient belonging to the low-risk and intermediate-risk groups has died of prostate cancer.

Figure 4 shows the local control curve and biochemical relapse-free (bNED) curves. Five-year local control and bNED rates were recorded as 97.5% and 88.9%, respectively. A total of four patients, three presenting with slowly elevated PSA and positive biopsies at 24 months, 38 months, and 48 months after C-ion RT, and one with apparent growth of tumor on MRI images, were judged as having local recurrence. By the date of the analysis, 33 patients met the Phoenix criteria of biochemical failure: more than 2.0 ng/ml rise of PSA from the nadir. Of these 33 patients, 13 patients were diagnosed as having metastasis – 5 in bone and 8 in paraaortic lymph nodes – 2 to 62 months after biochemical relapse, 4 were judged as having local recurrence, and the remaining 16 patients had no clinical evidence of recurrent lesions at the date of analysis. The 5-year bNED rates of 222 low- or intermediate-risk patients and 320 high-risk patients were 94.6% and 85.0%, respectively, and the difference between these two groups was statistically significant.

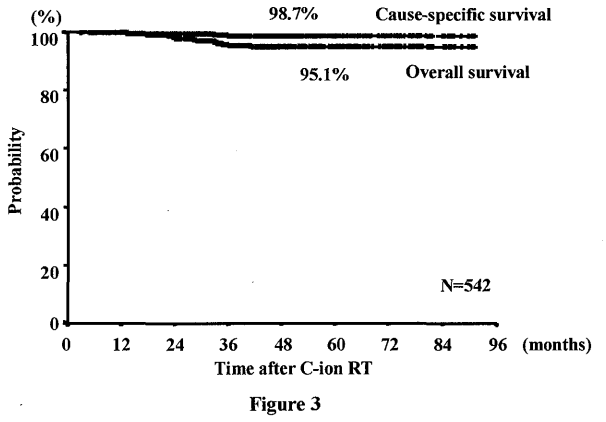

Fig. 3 Overall and cause-specific survival curves of all analyzed patients
Figure indicates 5-year rate of each curve.

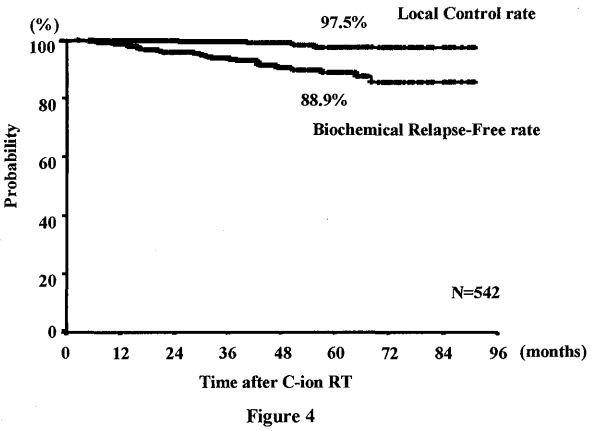

Fig.4 Local control and biochemical relapse-free survival (bNED) curves

3.Prognostic factors

Additional analysis was carried out to evaluate the influence of several prognostic factors on bNED and overall survival (OS), such as pretreatment serum PSA, GS, clinical stage, dose fractionation and the duration of hormone therapy. As a result, initial PSA of more than or equal to 50.0 ng/ml was a significant factor for lower bNED but not for OS. Five-year bNED and OS in T1/2 patients were significantly better than those in T3 patients. However, the 5-year bNED of 91.5% was remarkably high compared to other radiotherapy series for T3 patients. The centrally reviewed GS also had significant influence on bNED, as 5-year bNED of the patient subgroup with GS $\geq$ 8 was significantly lower than those of the subgroups with GS $\leq$ 6 and GS = 7, though OS was not significantly different (Table 3). Regarding the effect of altered fractionation on bNED, there was no difference among the patients treated with 20 fractions and those with 16 fractions (Fig. 5). On the basis of these results of bNED and toxicity, that is, relatively low toxicity with comparable bNED in 16 fractions, we started to treat all new patients with a dose fractionation of 57.6GyE/16f in September 2007.

Table 3. Biochemical relapse-free rate (bNED) and overall survival rate (OS) according to risk factors

			5-year rates (%)			
		No.pts.	bNED	p-value	OS	p-value
All		542	88.9		95.1	
Stage	T1/2	368	93.3	0.0001	97.2	0.0428
	T3	174	80.7		91.5	
PSA	< 20	345	91.5		96.9	
	20~50	126	89.4	0.0470	94.2	n.s.
	50 ≤	71	77.9		90.3	
Gleason score	≤ 6	143	92.9	0.0023	95.6	
	7	239	94.4	0.0003	96.2	n.s.
	8 ≤	160	72.6		92.0	

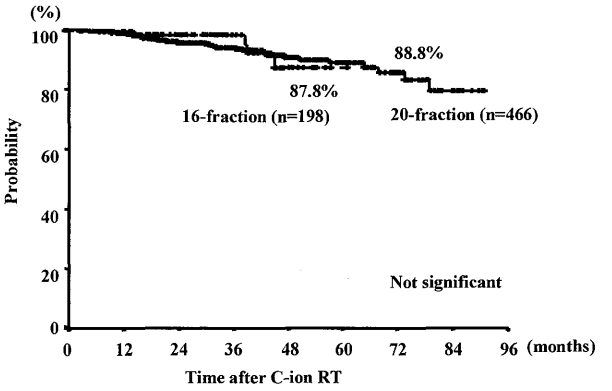

Figure 5

Fig. 5 bNED according to altered fractionation of carbon ion radiotherapy

Of the 320 high-risk patients treated with hormones and carbon ions, 160 finished adjuvant hormone therapy and were analyzed in regard to the influence of the duration of hormonal therapy on biochemical control. The 5-year bNED rate of the 57 patients (77.7%) receiving hormone therapy for less than 24 months was significantly lower than that of the 103 patients (92.1%, p=0.0089) receiving hormone therapy for more than 24 months. Among the patients at intermediate risk, however, biochemical failure occurred only in 2 patients and no significant influence of the duration of hormone therapy was observed. On the basis of these results, we are currently applying short-term hormone therapy to intermediate-risk patients and long-term hormone therapy to high-risk patients in combination with C-ion RT.

Discussion

In this article, the patients treated with the carbon ion radiotherapy (C-ion RT) procedure established in our phase I/II clinical studies were analyzed. The results have demonstrated that C-ion RT achieves a very high biochemical control rate with a relatively low morbidity. A high rate of biochemical control was achieved as a result of the excellent dose concentration associated with C-ion RT and the efficient application of hormonal

therapy. A number of studies using radiation therapy in combination with hormonal therapy have also indicated a high rate of biochemical control [13-14]. Comparing bNED and survival rates of our series with the studies in the literature, both were even better than those of the combinations of hormone therapy and conventional photon radiotherapy (Table 4). We presume this to be due to the positive impact of carbon ion beams on local control.

Table 4. Comparing bNED and survival rate of C-ion RT with other studies of combined treatment of hormone therapy and radiotherapy

Studies	No. pts.	Stage	Dose (Gy/fr.)	Hormone	bNED (%)	Survival (%)
EORTC* Phase III	208	T2-4	70/35	(-)	43	62
	207			(+)	81	79
RTOG** 8531Phase III	468	T1-3	65-70/35	(-)	20	71
	477			(+)	53	75
Carbon Phase I/II & II	320	High risk	66(GyE)/20	(+)	85	94

EORTC: European Organization for Research and Treatment of Cancer; N Eng J Med 1997; 337: 295-300, Bolla M. et al
RTOG: Radiation Therapy Oncology Group; IJROBP 2000; 47(3): 617-627, Mack Toach III et al

In photon radiotherapy, the rate of local recurrence can be affected by the actual volume or pathological differentiation of tumor tissue. However, high LET radiation can be expected to be more effective for large-volume, poorly differentiated tumors compared to photon irradiation, and, in fact, very few local recurrences were actually observed in our series, even in the T3 tumors with high GS. Although the evaluation of local control after radiotherapy of prostate cancer is a controversial issue, it is clear that high bNED cannot be achieved without sufficient local tumor control. The very high bNED attained in the patients of the intermediate-risk group indicated that biochemical failure occurred only in patients with high risk factors for metastasis, such as high PSA, T3, or poorly differentiated histology. This strongly suggests that eradication of cancer tissues in the prostate was achieved by C-ion RT in most patients.

A very low incidence of rectum morbidity was recorded, and this is ascribable to the physical properties of heavy charged particles in terms of dose conformity. This also substantiates the validity of our methods of patient positioning and target setting, and of our irradiation techniques. In addition, the acceptable incidence of genitourinary morbidity and the very high efficacy against local tumors confirm the accuracy of our dose calculation, the biological advantage of carbon ion beams, and the effect of a relatively high dose by a hypofractionated schedule.

A further move in the direction toward a more hypofractionated regimen of 16 fractions over 4 weeks has already been made. In 97 patients treated with a C-ion dose of 57.6 GyE in 16 fractions, bNED was comparable to that of 66.0GyE/20f or 63.0GyE/20f, and the incidence of GU toxicity was even lower. Therefore, this new dose fractionation is now applied to all new patients at NIRS.

Conclusions

In conclusion, carbon ion radiotherapy administered by hypofractionated schedule is an effective and safe option in the treatment of locally confined prostate cancer. With an appropriate use of hormonal therapy, satisfactory biochemical control can be achieved even in high-risk patients. Trials with greater hypofractions have started at NIRS with the aim of establishing even more sophisticated methods of C-ion RT.

References

[1] Nikoghosyan A, Schulz-Ertner D, Didinger B, et al: Evaluation of therapeutic potential of heavy ion therapy for patients with locally advanced prostate cancer. Int J Radiat Oncol Biol Phys 58(1): 89-97, 2004

[2] Perez CA, Michalski J: Outcome of external-beam radiation therapy for localized carcinoma of the prostate (stages T1b, T2, and T3). In: Greco C, Zelefsky MJ, editors. Radiotherapy of prostate cancer. Amsterdam: Harwood Academic Publishers; p.155-184, 2000

[3] Hanks GE, Hanlon AL, Pinover WH, et al: Dose escalation for prostate cancer patients based on dose comparison and dose response studies. Int J Radiat Oncol Biol Phys 2000; 46: 823-832.

[4] Zelefsky MJ, Fuks Z, Hunt M, et al: High-dose intensity modulated radiation therapy for prostate cancer: Early toxicity and biochemical outcome in 772 patients. Int J Radiat Oncol Biol Phys 2002; 53: 1111-1116.

[5] Laramore GE, Krall JM, Thomas FJ, et al: Fast neutron radiotherapy for locally advanced prostate cancer: final report of a Radiation Therapy Oncology Group randomized clinical trial. Am J Clin Oncol 1993; 16: 164-167.

[6] Haraf DJ, Rubin SJ, Sweeney P, et al: Photon neutron mixed-beam radiotherapy of locally advanced prostate cancer. Int J Radiat Oncol Biol Phys 1995; 33: 3-14.

[7] Tsujii H, Morita S, Miyamoto T, et al: Preliminary results of phase I/II carbon-ion therapy at the National Institute of Radiological Sciences. J Brachytherapy Int 1997; 13: 1-8.

[8] Akakura K, Tsujii H, Morita S, et al: Phase I/II clinical trials of carbon ion therapy for prostate cancer. Prostate 2004; 58: 252-258.

[9] Tsuji H, Yanagi T, Ishikawa H, et al: Hypofractionated radiotherapy with carbon ion beams for prostate cancer. Int J Radiat Oncol Biol Phys 2005; 63(4): 1153-1160.

[10] Ishikawa H, Tsuji H, Kamada T, et al; A phase II trial using carbon ion radiotherapy (C-ion RT) for prostate cancer. JCO 23(16) part 1 Supple. 2005; 410S-410S.

[11] Ishikawa H, Tsuji H, Kamada T, et al: Carbon Ion Radiation Therapy for Prostate Cancer: Results of a Prospective Phase II Study. Radiother Oncol in press.

[12] International Union Against Cancer (UICC). TNM Classification of Malignant Tumours, 5th ed. New York: Wiley-Liss, Inc. 1997; p 170-173.

[13] Bolla M, Gonzalez D, Warde P, et al: Improved survival in patients with locally advanced prostate cancer treated with radiotherapy and goserelin. N Engl J Med 1997; 337: 295-300.

[14] Roach MIII, Lu J, Pilepich MV, et al: Predicting long-term survival, and the need for hormonal therapy: a meta-analysis of RTOG prostate cancer trials. Int J Radiat Oncol Biol Phys 2000; 47: 617-627.

Carbon Ion Radiotherapy: Clinical Study The Japanese Way

Tadashi Kamada, Hirohiko Tsujii

Research Center for Charged Particle Therapy, National Institute of Radiological Sciences, Chiba, Japan
e-mail address: t_kamada@nirs.go.jp

Introduction

The pioneering work in carbon ion radiotherapy by Japanese and European investigators has generated great enthusiasm. However, as a particle therapy center is certain to be an extremely complex and expensive medical facility, it may become a source of disagreement in the radiation oncology community.

The paradigm of drug development in medical oncology from phase I to phase II to phase III trials remains unaltered, but this is not the case in radiation oncology.

According to the presentations at the NCI "Workshop on Advanced Technologies in Radiation Oncology" in December 2006, there were only a few level-I trials of implemented new technologies in radiation oncology. [1] For protons, the physical proof of better depth dose characteristics, virtually identical biological effects compared with X-rays, and the fact that decreased doses to normal tissues always result in decreased toxicity, argue against conducting phase III trials comparing protons with X-rays. [2]

Radiation oncology has not, until this decade, seen such dramatic changes in technological innovations, and they give rise to new and complicated issues. What kind of studies should be carried out to sort out the indications, advantages, and disadvantages? In this presentation, the issue of the evaluation of the clinical results of carbon ion radiotherapy and their comparison with other modalities will be discussed.

Carbon Ion Radiotherapy Clinical Trial at HIMAC

The carbon ion radiotherapy program was initiated based on the rationale of exploiting the high physical selectivity of carbon ions, as well as their high LET, with the attendant potential radiobiological advantage for selected tumor types. From the beginning all carbon ion radiotherapies were carried out as prospective phase I/II and II clinical trials in an attempt to identify tumor sites suitable for this treatment, including radio-resistant tumors, and to determine optimal dose-fractionation, and especially for hypo-fractionation, in common cancers. Our ultimate goal is to prove the efficacy and safety of carbon ion radiotherapy in cancer treatment.

Conducted carbon ion radiotherapy protocols and their time lines are summarized in Table 1. A total of 46 protocols have been conducted. The number of patients receiving carbon ion radiotherapy has already reached more than 4,000, and in the year 2008 more than 700 patients were treated in such protocols at NIRS.

Clinical studies revealed that intractable cancers such as advanced head and neck cancer, large skull base tumors, pelvic recurrence of operated rectal cancer, and inoperable sarcomas can be cured, and cancers in the lung, liver, and prostate can be cured safely with a shorter treatment period. [3]

Should Carbon Ion Radiotherapy be Subjected to Randomized Clinical Trials?

When comparing various therapies, the results of randomized controlled studies provide the strongest evidence. Dr. Lawrence, the chief editor of the Journal of Clinical Oncology, has made the following statement about the need for phase III (randomized controlled studies) when comparing different therapies, or different

types of therapeutic equipment, in the field of radiation oncology: "*In medical oncology, there is a need to compare drug treatment A to drug treatment B. It is not possible to determine which is better without carrying out a randomized trial. In radiation oncology, one can know, based on physics, that protons deliver a better dose distribution than photons or that IMRT is superior to three-dimensional conformal therapy. If treatment planning and delivery are carried out using consistent methodology, there is no debate; this is a matter of physics. The big question is: is any observed difference clinically meaningful enough to justify the added expense? What kind of trial needs to be designed to answer this question? Would it be difficult to run a randomized trial in the United States asking whether a treatment that is superior based on physics translates into superior patient survival and/or quality of life? Would patients permit themselves to be randomly assigned to the standard but less expensive therapy?*" [(4)]

Progress in radiation oncology is inextricably linked to the development of treatment facilities, but almost no randomized controlled study has been conducted for the purpose of the introduction of any new modality. In fact, no randomized controlled study was conducted in the shift from cobalt to LINAC, but if there had been there would have been little difference between cobalt and LINAC in the treatment results in patients with early glottic cancer. Cobalt irradiation has advantages in terms of both cost and equipment maintenance, and the results of LINAC may be poor unless a suitable energy is selected. Cobalt is sufficient to treat laryngeal cancer, and it may be unnecessary to introduce LINAC to achieve successful treatment for this cancer. In recent years, however, treatments with cobalt have been significantly reduced in developed countries. The distribution of the very-high-energy x-rays of LINAC allows safer treatment of deeply situated targets, and the design of a study to determine the difference between cobalt and LINAC in patients with glottic cancer is itself a problem.

In any case, the question remains "Should Carbon Ion Therapy be Subjected to Randomized Clinical Trials?" What must be seen in a phase II study to justify moving to phase III? No matter how exciting the laboratory technique and how great the improvement in animal models, there must be evidence that the method is transferable to humans and that successes in the laboratory can be reproduced in humans. Further, there must be real promise of improvement in phase II studies in human tumors. There is real promise of improvement in our carbon ion radiotherapy results presented at this meeting, and it justifies the move to phase III.

From Phase II Clinical Trials to Randomized Clinical Trials (RCT)

However, before moving to a phase III study, several questions are raised. First, are there comparable phase II results in other modalities? If the answer to the first question is yes, do those modalities use the same eligibility criteria? And third, how do we recruit the patients for the phase III trial? Our patients often travel long distances to Chiba seeking carbon therapy. Finally, we charge patients more than $30,000 USD for carbon ion therapy; how do we fund such a trial? Carbon ion radiotherapy is successful in advanced head and neck cancer, large skull base tumors, recurrent rectal cancer and inoperable sarcomas that are not treatable by other means. For these intractable diseases, it is clear that there are no ample data with other modalities. Therefore, for these diseases, there is little knowledge about how to conduct a phase III study and to obtain consent from patients. Hence, the answer to the question, should carbon ion therapy be subjected to randomized trials, is "No" in these intractable diseases. In lung, liver, and prostate cancer, promising results have been obtained with carbon ion radiotherapy. A randomized controlled study might be possible in these rather common cancers. However, as described above, patients are traveling long distances to Chiba to obtain carbon ion therapy. It will be very hard to obtain consent from these patients for a randomized trial. Thus, our answer to the question is that it is untenable. RCT provides the firmest evidence in various clinical settings, but it is too difficult to conduct RCT for assessment of new radiation therapy technologies.

Methodologies for Critical Assessment of New Health Technologies

Radiation oncology researchers need to develop new methodologies for critical assessment of new health technologies as a complement to RCT. Possible future comparative studies of carbon ion radiotherapy may include the following: 1) multi-institutional prospective clinical studies using the same protocols that can be applied to other therapies (non-randomized concurrent clinical trial), 2) matched-pair controlled studies in subjects matched to those receiving other therapies, and 3) RCT between carbon ion and proton or other high-tech radiotherapies.

Comparative studies, feasible at present, to further clarify the usefulness of carbon ion radiotherapy at various indications, include those in which the same protocol applied to other therapies is followed, the backgrounds of the subjects are matched, and the treatment desired by the study participants is performed. In this case, consent from study participants can be easily obtained, the study cost is low, and an agreement among the participating facilities is relatively easily obtained, as the treatment desired by the patients is provided by the co-operating institutions. For realizing this type of comparative study, a project team has been organized to conduct a multi-institutional prospective prostate cancer study in all particle therapy facilities in operation in Japan. This study is expected to start within 1 or 2 years. This could represent a new methodology for the assessment of new radiotherapy technologies. Another method would be to determine the inclusion criteria for patients already treated and then to comparatively analyze the therapeutic results in a matched-pair study. This is feasible if consent is obtained from the institutions that performed the treatments being compared. We conducted a matched-pair study of sacral chordoma with patients treated at the Massachusetts General Hospital in Boston with proton therapy.[5] However, there were only a few matched cases in the two institutions, and the comparison could not be carried out. Nonetheless, this can be retried with other institutions or performed with more common cancers.

Summary

At present, most of the patients receiving carbon ion radiotherapy at NIRS visit the clinic seeking this specific modality, and it is difficult to obtain consent for a randomized controlled study from these patients and it may be unnecessary to conduct a phase III trial. However, in selected tumors where the high-LET benefit could be appreciated, we can participate in randomized studies. Finally, studies aimed at clarifying the usefulness of carbon ion radiotherapy and elucidating any advantages from hypo-fractionation should be considered. A multi-institutional prospective non-randomized concurrent phase II clinical trial is one such new approach, and it will be proposed not only to the Japanese, but also to the international community of particle therapy and radiation oncology.

References

[1] http://www3.cancer.gov/rrp/workshop/2006AdvancedRadiationTech/presentations.html

[2] Goitein M, Cox JD: Should randomized clinical trial be required for proton radiotherapy? J Clin Oncol 26:175-176(2008)

[3] Tsujii H, Mizoe J, Kamada T et al: Clinical results of carbon ion radiotherapy at NIRS. J Radiat Res 48: Suppl., A1-A13 (2007)

[4] Lawrence TS, Petrelli NJ, Li BD, Galvin JM: Think globally, act locally. J Clin Oncol 25:924-930(2007)

[5] Park L, Delaney TF, Liebsch NJ et al: Sacral chordomas: Impact of high-dose proton/photon-beam radiation therapy combined with or without surgery for primary versus recurrent tumor. Int J Radiat Oncol Biol Phys 65: 1514-1521(2006)

Carbon Ion Radiotherapy Using Intensity-Controlled Active Rasterscanning – The Heidelberg Results

Stephanie E. Combs, Anna Nikoghosyan, Thomas Haberer, Oliver Jäkel, Christian P. Karger, Marc Münter, and Jürgen Debus

Department of Radiation Oncology, University of Heidelberg, Heidelberg, Germany
Heidelberg Ion Therapy (HIT), Heidelberg, Germany

Over recent years, high precision radiotherapy has been implemented widely into clinical routine. Modern techniques such as fractionated steretoactic radiotherapy (FSRT) and intensity modulated radiotherapy (IMRT) have enabled the Radiation Oncologist to apply high doses of radiation to defined target volumes while sparing normal tissues, especially organs at risk. This is especially important in regions were tumor volumes and sensitive normal tissue are in close proximity, such as in the skull base. Thus, is was possible to increase the total tumor dose and subsequently increase local control rates, while the risk for radiation induced side effects can be minimized.

However, in certain tumor entities, overall treatment results still remain unsatisfying.

Therefore, particle therapy seems to be a promising alternative.

One main benefit of particle therapy is the inverted dose profile, resulting in low RT doses in the entry channel and behind the defined target volume, while the required dose can be directed into the target area. With carbon ion radiotherapy, this physical privilege is accompanied by distinct radiobiological effects within the tissue, resulting in a higher relative biological effectiveness (RBE). Therefore, an increase in local tumor control and subsequently improvement of overall survival can be expected.

We have shown in a number of studies that radioresistant tumors such as chordomas, chondrosarcomas and adenoidcystic carcinomas certainly benefit from carbon ion RT. Other extracranial tumors including sacral chordomas, lung cancer and sarcomas have been treated with carbon ion RT effectively.

Carbon ion therapy is currently available in few centers in Japan. At the University of Heidelberg we perform treatment with carbon ions at the Gesellschaft für Schwerionenforschung (GSI) in Heidelberg. In this setting, we have treated over 400 patients, mainly with chordomas and chondrosarcomas of the skull base, adenoid cystic carcinomas and prostate cancer.

In Heidelberg, the Heidelberg Ion Therapy Center (HIT) has been built offering Carbon ion and Proton radiotherapy for over 1300 patients per year. The facility offers three treatment rooms, two equipped with horizontal beamlines, and one with a carbon ion gantry. The facility is directly attached to the exsisting Department of Radiation Oncology, and offers the unique possibility to perform pre-clinical as well as clinical studies.

Radiobiology for Chordoma Cell Line UCH1

Takamitsu Kato[1], Akihisa Tsuda[1, 2], Mitsuru Uesaka[2], Akira Fujimori[1], Tadashi Kamada[1], Hirohiko Tujii[1] and Ryuichi Okayasu[1]

1. Research Center for Charged Particle Therapy, National Institute of Radiological Sciences, Chiba, Japan
2. Nuclear Professional School, University of Tokyo, Tokyo, Japan
e-mail address:tkato@nirs.go.jp

Abstract

The aim of this study is to investigate the cellular radiosensitivity of a chordoma cell line, U-CH1. U-CH1 was compared with two different cancer lines, the glioblastoma cell line U87-MG and the cervical cancer cell line HeLa, to understand their phenotypes. We analyzed cell doubling times, DNA contents, and cell cycle distributions to characterize these cell lines and determined radiosensitivities by colony formation assay. Cell doubling time for U-CH1 was 3 days, which was much longer than the other tumor cell lines. The doubling times for U87-MG and HeLa cells were 24 hours and 18 hours, respectively. U-CH1 had the most DNA content among the three cell lines and was near tetraploid. UCH-1 and U87-MG were more sensitive to x-irradiation than HeLa cells. Heavy ion particle irradiation efficiently killed all cell lines compared to x-ray exposure. Relative biological effectiveness (RBE) at 10% survival of glioblastoma and HeLa cells was about 2.5 for LET 70keV/μm carbon ions and 3 for LET 200keV/μm iron beams, while for U-CH1 it was 2.5 for LET 70keV/μm carbon ions and 4 for LET200keV/μm iron beams.

Introduction

Chordoma is a rare malignant bone tumor accounting for only 1 to 4% of all primary malignant bone tumors [1]. Chordoma originates from notochordal remnants and has slower local growth and metastasizes less frequently than other bone and soft tissue malignant tumors [2]. Chordoma is not easy to control because of its anatomic location and propensity for spreading extensively. Complete radical resection produces better local control compared with subtotal resection and chemotherapy [3;4]. Some studies have reported that photon and charged particle carbon radiotherapy may possible delay recurrence after incomplete resection and may also be able to control the tumor [5-9].

Despite the accumulation of data from the medical side, there is a scarcity of information from the biology side because of limited availability of chordoma cell lines for biologists. It is essential to obtain more biological data to archive better tumor control of chordoma. A chordoma cell line, U-CH1, isolated by a German group, presented a long cell doubling time and chromosome instability and rearrangement [10]. This study is the first to report the measurement of the cellular radiosensitivity and heavy-ion biological effectiveness for a sacral chordoma cell line.

Materials and Methods

1. Cell lines and culture conditions

The chordoma cell line U-CH1 was kindly supplied by the Chordoma Foundation in Greensboro, NC, USA. U87-MG and HeLa cell lines were obtained from ATCC, USA. Cells were cultured in MEM-alpha (Gibco, Japan) supplemented with 10% fetal bovine serum (FBS, Sigma, Japan) and antibiotics and antimicotics (Gibco, Japan), and they were maintained at 37℃ in a humidified atmosphere of 5% CO2 in air.

2. Irradiation

X-rays were given by TITAN x-ray irradiator (Shimadzu, Japan). Heavy ions were beamed by HIMAC (Heavy Ion Medical Accelerator in Chiba). The ions used in this study were carbon ions (LET 13keV/μm and LET 70keV/μm) and iron ions (LET 200keV/μm). Asynchronously dividing cells were irradiated at room temperature.

3. Cell doubling time

Original U-CH1 cells had 7 days as their doubling time in Iscove/RPMI (4:1) medium with 10% FBS in collagen-coated flasks. To achieve a convenient cell biological study, we adapted U-CH1 in alpha-MEM 10% FBS with normal flask condition, similar to the other two cell lines. To measure cell doubling time, cells were seeded at 5000 cells in T12.5 flasks, and their number was counted later.

4. Flow Cytometry

Randomly dividing sample cultures were fixed in 70% ethanol and kept at -20°C until analysis. PI-stained 10.000 cells were analyzed by BD FACSCalibur to obtain the DNA content histogram. Cell cycle was analyzed by Modifit program on Mac OS 9.

5. Colony formation assay

Log growing cells were irradiated with photon or heavy-charged particles (Table 1), and then cells were trypsinized and plated onto 100mm cell culture dish for colony formation. HeLa and U87-MG cells were cultured for 10 to 14 days, and U-CH1 cells were kept in an incubator for 3 weeks. After colonies were formed, cells were fixed with 100% ethanol and stained with crystal violet solution. Colonies containing more than 50 cells were counted as survivors.

Table 1. Initial energy and LET for photon and heavy-charged particles

Irradiation	Initial Energy	LET
X-ray	250kVp	2 keV/um
Carbon	290MeV/n	13 keV/um
Carbon	290MeV/n	70 keV/um
Iron	500MeV/n	200 keV/um

Results

1. Cellular doubling time

Chordoma is known as a slow-growing tumor. The original U-CH1 cell line had a 7-day doubling time in the original isolated culture medium and conditions. We used the same cell culture conditions for all three different tumor cell lines to avoid complexities arising from different growth conditions among them.

The doubling time for U-CH1 was about three and half days rather than the original 7 days, but is still longer than 21.5 hours for U87-MG and 18 hours for HeLa cells (Figure 1). This shortened doubling time for U-CH1

enables us to carry out radiation biological experiments like the colony formation assay to determine cell survival.

Figure 1. Growth curves for three cell lines

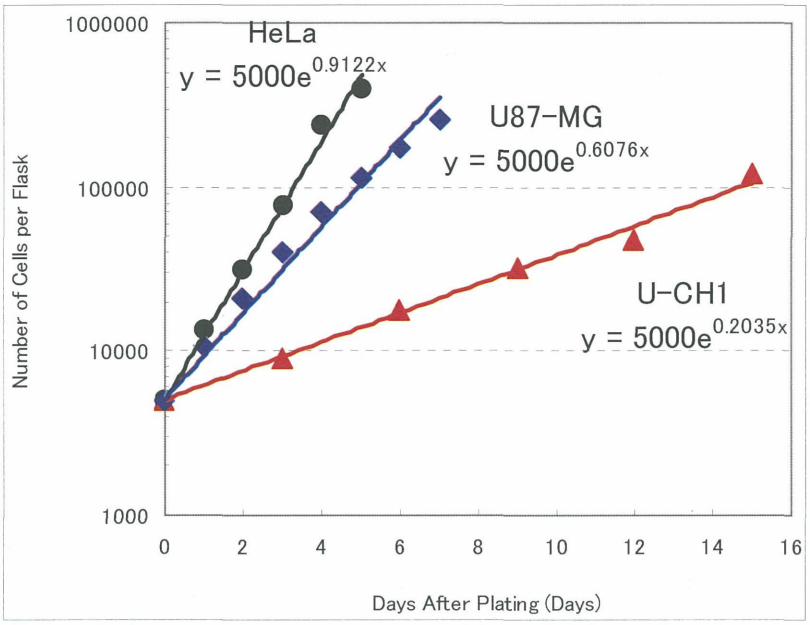

2. Cell Cycle Distribution and DNA Content

Both cell cycle distribution and DNA contents of the three cell lines were measured by BD FACSCalibur machine. DNA contents of U-CH1 and HeLa were near tetraploid (about 100 and 90, respectively) compared with almost normal diploid DNA content (about 60) in U87-MG. Cell cycle distribution in chordoma was overly G1- and G2-phases, and it was very different from the DNA profile patterns of the other two cell lines. The slow growth speed of U-CH1 may have a relationship with the long resting time before DNA synthesis in G1-phase or before cytokinesis in G2-phase.

Table 2. Cell cycle distribution and DNA contents of three cell lines

Name	Doubling Time	G1-phase	S-phase	G2/M-phase	DNA content*
HeLa	18 hours	52.1%	30.3%	17.6%	~90
U87-MG	21.5 hours	64.7%	23.0%	12.3%	~60
U-CH1	81.7 hours	75.0%	13.3%	11.7%	~100

*arbitrary unit, a standard DNA content in normal diploid CHO cells (2n, G1-phase) is equal to 50.

3. Cellular Radiosensitivity and Relative Biological Effectiveness

It is sometimes difficult to perform complete radical resection of chordoma tumors depending on anatomic location or tumor spreading grade. Because of the lower effectiveness of chemotherapy, radiotherapy is a useful treatment tool, and information about cellular radiosensitivities to photon and charged particles is needed. Randomly growing cell cultures were irradiated with various ionizing radiations as listed in Table 1. p53 mutated HeLa cells were the most resistant to any kind of ionizing radiation. U87-MG and U-CH1 had almost the same sensitivities to radiation exposure (Figure 2). D_{10} values, dose to kill 90% of irradiated cells, of each cell line, and ionizing radiation are summarized in Table 3. From these D_{10} values, we calculated the RBE of heavy charged particles compared to x-rays. Although all cell lines had no noticeable differences in LET-RBE curves from LET 13 to 70keV/μm, chordoma had a very high RBE value of 4 at LET 200keV/μm.

Figure 2. Cell survival curves for HeLa, U87-MG, and U-CH1 cells

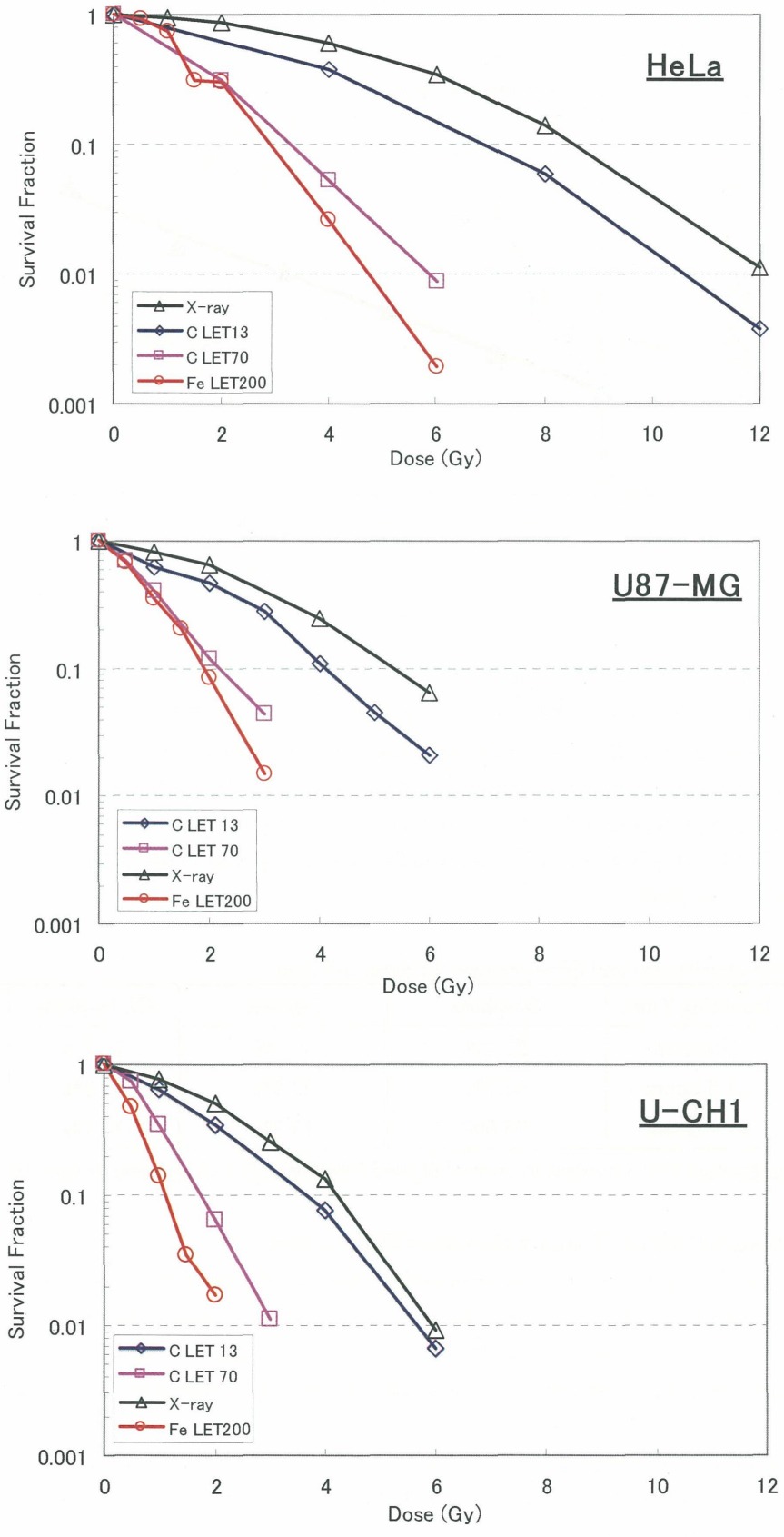

Table 3. D_{10} values in each cell line and ionizing radiation exposure

Name	X-ray	C LET 13keV/μm	C LET 70keV/μm	Fe LET 200keV/μm
HeLa	8.7	7.0	3.3	2.9
U87-MG	5.4	4.1	2.2	1.9
U-CH1	4.3	3.7	1.8	1.1

Figure 3. LET and RBE curves for three cell lines. RBE values were calculated from 10% survival points.

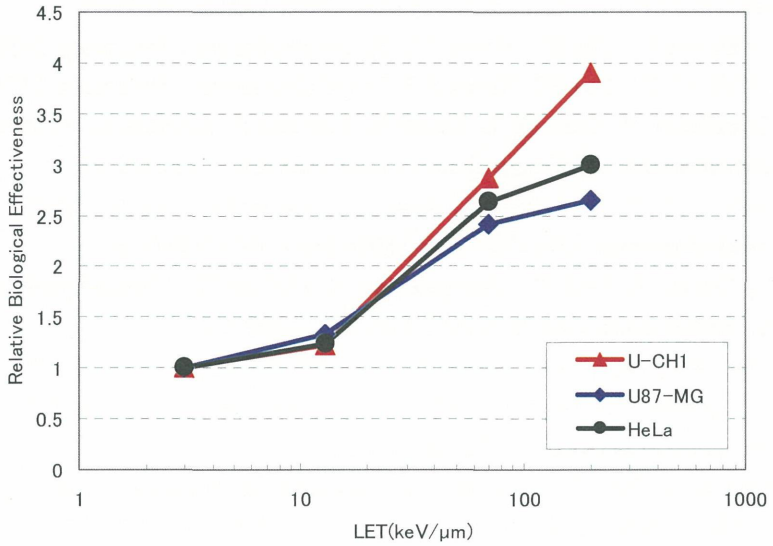

Discussion

Chordoma is a rare tumor and information about its cellular and radiological biology is still lacking. This study surprisingly revealed that the chordoma cell line U-CH1 was not as radioresistant as expected. We also examined the sensitivity to bleomycin, which produces DNA double-strand breaks as ionizing radiation does, and U-CH1 was the most sensitive to this chemical agent among the three cell lines (data not shown). Usually, p53 mutation changes cellular radiosensitivity to become more resistant because of less apoptosis induction by the inactivated p53 pathway [11-13]. Radioresistant HeLa cells have p53 mutation, while U87-MG cells have wild-type p53 and are sensitive to radiation. We suspect that the U-CH1 cell line may have wild-type p53. We checked p53 induction and its downstream protein p21 induction after x-ray exposure by Western blotting (data not shown), and U-CH1 had ionizing radiation exposure-dependent p21 and p53 induction. We conclude that U-CH1 has normal sensitivity to radiation exposure because of the normal expression and function of p53 protein.

Then, if U-CH1 belongs to the non-radioresistant group as we claimed, it may not be difficult to control tumors by regular photon radiation therapy. But U-CH1 cells have a very high RBE value at high LET radiation exposure compared with other two tumor cell lines. This means that charged particle irradiation can provide better biological control with the same dose of x- or gamma-rays. Another advantage for the use of heavy charged particles is the oxygen effect [14]. High LET exposure can almost ignore low oxygen concentrations that lead to radioresistance in tumor populations and can control tumors with better efficiency. Chordoma tumors tend to be very large when they are diagnosed. It may be reasonable to consider that chordoma tumors contain a

large fraction with low oxygen concentrations. Therefore, with high RBE for tumor control and the reduced oxygen effect, chordoma becomes a very attractive target for heavy charged particle therapy.

This study used only one chordoma cell line, so far available in the world, U-CH1. However, we need to test more cell lines to verify our results. This is the first report to present the *in vitro* cellular radiosensitivity of the chordoma cell line and the RBE value for high LET irradiation.

Reference

[1] Azzarelli A, Quagliuolo V, Cerasoli S, Zucali R, Bignami P, Mazzaferro V, et al. Chordoma: natural history and treatment results in 33 cases. J Surg Oncol 1988 Mar;37(3):185-91.

[2] Sundaresan N, Galicich JH, Chu FC, Huvos AG. Spinal chordomas. J Neurosurg 1979 Mar;50(3):312-9.

[3] Sundaresan N, Galicich JH, Chu FC, Huvos AG. Spinal chordomas. J Neurosurg 1979 Mar;50(3):312-9.

[4] Azzarelli A, Quagliuolo V, Cerasoli S, Zucali R, Bignami P, Mazzaferro V, et al. Chordoma: natural history and treatment results in 33 cases. J Surg Oncol 1988 Mar;37(3):185-91.

[5] Imai R, Kamada T, Tsuji H, Yanagi T, Baba M, Miyamoto T, et al. Carbon ion radiotherapy for unresectable sacral chordomas. Clin Cancer Res 2004 Sep 1;10(17):5741-6.

[6] Schoenthaler R, Castro JR, Petti PL, Baken-Brown K, Phillips TL. Charged particle irradiation of sacral chordomas. Int J Radiat Oncol Biol Phys 1993 May 20;26(2):291-8.

[7] Magrini SM, Papi MG, Marletta F, Tomaselli S, Cellai E, Mungai V, et al. Chordoma-natural history, treatment and prognosis. The Florence Radiotherapy Department experience (1956-1990) and a critical review of the literature. Acta Oncol 1992;31(8):847-51.

[8] Catton C, O'Sullivan B, Bell R, Laperriere N, Cummings B, Fornasier V, et al. Chordoma: long-term follow-up after radical photon irradiation. Radiother Oncol 1996 Oct;41(1):67-72.

[9] Cheng EY, Ozerdemoglu RA, Transfeldt EE, Thompson RC, Jr. Lumbosacral chordoma. Prognostic factors and treatment. Spine 1999 Aug 15;24(16):1639-45.

[10] Scheil S, Bruderlein S, Liehr T, Starke H, Herms J, Schulte M, et al. Genome-wide analysis of sixteen chordomas by comparative genomic hybridization and cytogenetics of the first human chordoma cell line, U-CH1. Genes Chromosomes Cancer 2001 Nov;32(3):203-11.

[11] Canman CE, Kastan MB. Role of p53 in apoptosis. Adv Pharmacol 1997;41:429-60.

[12] Canman CE, Wolff AC, Chen CY, Fornace AJ, Jr., Kastan MB. The p53-dependent G1 cell cycle checkpoint pathway and ataxia-telangiectasia. Cancer Res 1994 Oct 1;54(19):5054-8.

[13] Gueven N, Becherel OJ, Birrell G, Chen P, DelSal G, Carney JP, et al. Defective p53 response and apoptosis associated with an ataxia-telangiectasia-like phenotype. Cancer Res 2006 Mar 15;66(6):2907-12.

[14] Davis MA, Little JB. RBE and OER of the heavy ionizing particles released during 10beta-neutron capture therapy. Rev Latinoam Microbiol Parasitol (Mex) 1968 Apr;10(2):207.

Molecular Mechanisms of Tumor Cell Radioresistance in Head and Neck Squamous Cell Carcinomas

Claire Rodriguez-Lafrasse

Laboratory of Molecular and Cellular Radiobiology, EA3738, Lyon, France
e-mail address:claire.rodriguez@sante.univ-lyon1.fr

This work results from collaboration between the biologists of the Laboratory of Molecular and Cellular Radiobiology (Mira Maalouf, Gersende Alphonse, Priscilla Battiston-Montagne) and of the Gesellschaft für SchwerIonenforschung (Cladia Fournier, Gisela Taucher-Scholz) and the physicists of IPNL, LIRIS (Michael Beuve, Anthony Colliaux, Marcel Bajard).

Abstract

It is now well-established that heavy ion radiotherapy can offer some potential merits over conventional radiotherapy. The advantage of this new method of treatment lies in the physical and biological properties of carbon ions. With the growing interest in hadrontherapy, it is highly important to investigate the mechanisms of the action of carbon ions, in order to improve the results of this therapy. Thus, we initiated studies on the mechanisms of cell death in two p53-mutated head and neck squamous cell carcinoma (HNSCC) with opposite radiosensitivity following carbon ion and X-ray exposure, since recent clinical trials had shown that the local treatment of HNSCC by carbon hadrontherapy was much less efficient than that of other radioresistant cancers. We first showed that carbon ion irradiation does not modify the type of death involved, but amplifies it. In the radiosensitive SCC61 cell line, early apoptotic cell death triggered by ceramide production occurred after irradiation. In contrast, the radioresistant SQ20B cells underwent G2/M arrest associated with Chk1 activation and Cdc2 phosphorylation. Furthermore, 5 days after carbon ion irradiation, SQ20B cells bypassed the G2/M arrest and underwent cell death by mitotic catastrophe. However, a subpopulation of SQ20B cells was able to escape mitotic catastrophe and continued to proliferate. These results may explain the moderate tumor control observed in HNSCC patients treated by hadrontherapy.

Introduction

Hadrontherapy offers several advantages over conventional radiotherapy due to the physical and biological properties of carbon particles. Carbon ion irradiation provides good dose localization (Bragg peak) in critical cancer tissue and gives higher relative biological effectiveness (RBE) in cell killing. Taking advantage of these clinically relevant properties, a high number of patients have been treated with carbon ions, and the results have been found to be very promising (1).

Several studies have investigated the biological effectiveness of carbon ions and confirmed that high linear energy transfer (LET) ions are more effective than X-ray in tumor cell killing (2,3). Nevertheless, only a few studies have been performed on the mechanisms of cell death involved in the response to carbon ion exposure, most of them focusing only on apoptosis (4,5). Conversely, different types of cell death have been well characterized in response to X-rays. Premature-senescence, mitotic catastrophe and necrosis are alternative

processes of proliferative inhibition or cell death described in cancer cells (6,7). However, the individual contribution of each cell death modality in response to carbon ion irradiation has not been investigated and needs clarifying.

Moreover, one of the key proteins that acts to preserve genetic stability following DNA damage is the p53 tumor suppressor. TP53 plays a pivotal role in the pathway which controls apoptosis, cell growth and cell proliferation. Mutation of its gene is a common feature observed in more than 50% of human cancers. Although mutations in the p53 gene can lead to resistance to radiotherapy, high linear energy transfer (LET) radiation appears to induce apoptosis regardless of p53 gene status in cancer cells (3,4). However the mechanisms involved in high LET radiation-induced apoptosis in p53 mutated cells are still not defined. Our laboratory and others (8,9) have demonstrated that ceramide generation is a key and determining event in X-ray radiation induced apoptosis and is correlated to radiosensitivity. Conversely nothing is known about the putative implication of this lipid second messenger in high LET ion- induced cell death.

Carbon ion radiotherapy was applied, among others, to patients with head and neck cancers, at the Heavy Ion Medical Accelerator in Chiba, Japan. The treatment results obtained were very promising and showed a very favorable local control rate in adenoid cystic carcinoma (90% at 5 years) and malignant melanoma (100%) (10). However, an unexplained lower control rate at 5 years of 34% was observed in HNSCC patients who developed locoregional recurrence (11) To improve our understanding of the biological effectiveness of carbon ions, we aimed to characterize the different types of cell death and the pathways involved in Head and Neck Squamous Cell Carcinoma (HNSCC) cell lines by using two p53-mutated HNSCC (SCC61 and SQ20B) cell lines with opposite sensitivity to X-rays. This research will contribute to the comprehension of the mechanisms leading to resistance to conventional or carbon radiotherapy.

Materials And Methods

Cell culture

The radiosensitive p53-/- SCC61 cell line was established from a patient with a cancer of the tongue sensitive to radiotherapy. The resistant p53 -/- SQ20B cell line was established from a patient with a recurrent squamous cell carcinoma of the larynx after radiation therapy. Cells were cultured as previously described (8).

Irradiation procedures

X-ray irradiation (6MV) was performed in Lyon (France) using a Clinac CD linear accelerator. Irradiation with 75MeV/n carbon ions (LET 33.6keV/μm; typically occurring in the tissue surrounding the tumor) was performed at GANIL (Caen, France). Irradiation with 9.8MeV/n carbon ions (LET 184keV/μm, typically occurring in the tumor volume) was performed at the UNILAC accelerator, GSI (Darmstadt, Germany).

Clonogenic survival curves

Clonogenic cell survival was assessed by the standard colony formation assay as described in Beuve et al. (12).

Cell cycle distribution

The percentage of cells in each phase of the cell cycle was quantified using propidium iodide labeling. Adherent and floating cells were pooled and, after washes with PBS, fixed in 70% ice-cold-ethanol for at least 24h. Cells were then washed and resuspended in RNase 250μg/ml and propidium iodide 250μg/ml. Analyses were performed with a Coulter-Epixs or Partec flow cytometer.

Beta-galactosidase assay

At the indicated times, cells were washed with PBS, fixed with 2% formaldehyde and 0.2% glutaraldehyde, and stained overnight in X-gal staining solution at pH6. A minimum of 500 cells were counted and the ratio β-gal positive cells/β-gal negative cells established.

DAPI staining

Cell morphology was identified by nuclear staining with the fluorescent dye, DAPI. After irradiation and incubation over varying periods, cells were washed in PBS, fixed with 4% formaldehyde and washed again with PBS. DAPI solution was added to the fixed cells for 1h. Apoptotic, giant or multinucleated cells were identified by fluorescence microscopy.

Ceramide quantification

Ceramide was quantified by high-performance liquid chromatography with fluorimetric detection (8).

Cellular proliferation

The proliferative capacity of cells was determined using 5-Bromo-2'-deoxy-uridine labeling with Detection Kit (Roche, Penzberg, Germany) according to the manufacturer's instructions.

Results

Clonogenic cell survival

We first investigated the clonogenic cell death of SCC61 and SQ20B cell lines following X-ray or carbon ion irradiation. The high LET carbon ions induced a higher level of clonogenic cell death compared to low LET ions and X-rays in both cell lines. Nevertheless, SQ20B cells were systematically less sensitive than SCC61 cells, even in response to high LET carbon ions. The RBE at 10% survival was 1.5 (carbon 33.6 keV/μm) and 4.2 (carbon 184 keV/μm) for SCC61 cells compared to 2.1 and 2.8 for SQ20B cells, respectively.

Apoptotic cell death induced after low and high LET irradiation

In order to investigate the cellular basis of the higher RBE levels, the contribution of apoptotic cell death was studied in both cell lines after 10Gy of high and low LET irradiation. The size of the sub-G1 population corresponding to the number of cells with less than diploid DNA content, was taken as indicative of the amount of apoptotic cells.

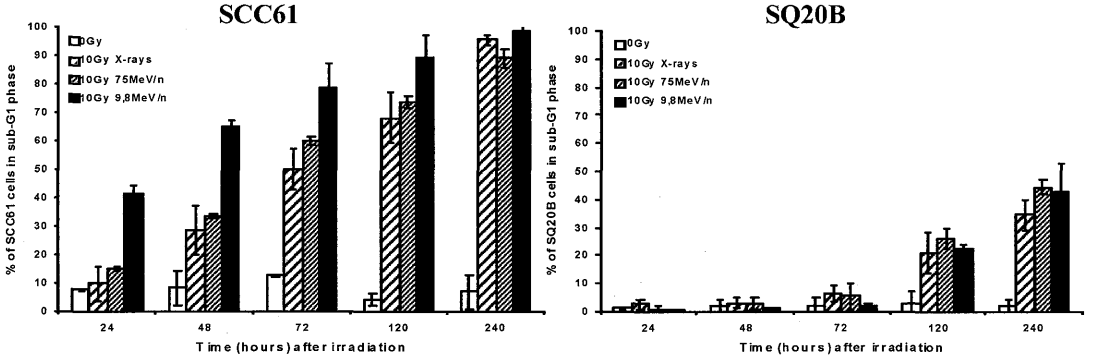

Figure 1 : Apoptosis induction in SCC61 and SQ20B cells after high or low-LET irradiation.

As shown in Figure 2A, in the radiosensitive SCC61 cells a time-dependent increase of apoptotic cells was observed following low and high LET irradiation. After X-ray exposure the percentage of sub-G1 cells reached 50.3±7.2 % at 72h whereas it reached 60.1±1.3% for 75MeV/n carbon and 78.4±8.7% for 9.8MeV/n carbon irradiation. However, with increasing time, the differences between carbon ion beams and X-ray exposure became smaller and the number of apoptotic cells reached a maximum of 95% at 240h for all types of irradiation. On the contrary, no significant apoptosis induction was observed during the first 72h following low or high LET irradiation in the SQ20B radioresistant cells. However, a progressive increase of apoptotic cells starting from 120h was observed and reached about the same level for the three type of irradiation. These results were confirmed on both cell lines using TUNEL assay (data not shown).

Ceramide-dependent apoptotic pathway

To investigate whether ceramide is involved in high LET-induced apoptosis, this compound was quantified in both cell lines after low and high LET irradiation, using HPLC quantification (Figure 2). In the SCC61 p53-/- radiosensitive cells, an increase of ceramide level was observed from 24h following carbon irradiation. The ceramide production was time-dependent and occurred concomitantly with the induction of apoptosis.
In SQ20B p53-/-radioresistant cells, ceramide analysis showed a delayed increase starting from 120h after high and low LET exposure. In view of these results, a correlation could be established between the propensity of cells to undergo apoptosis and the radiation-induced ceramide production.

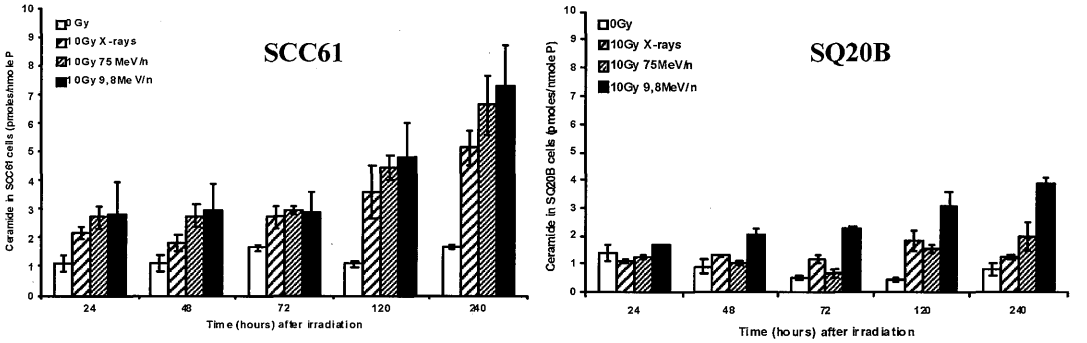

Figure 2 : Kinetics of ceramide production in SCC61 and SQ20B cells after high or low-LET irradiation.

To summarize, low and high LET irradiation induced apoptosis from an early stage in the radiosensitive SCC61 cells with levels being both LET- and time- dependent. Moreover, apoptosis seems to go through the p53-independent ceramide-dependent pathway. Conversely, only late apoptosis, but also ceramide-dependent, was detected in SQ20B cells following irradiation with a much lower percentage compared to SCC61 cells. Although both cell lines exhibited the same p53 status, two different pathways of cell death seem to be activated following carbon ion exposure.

Cell cycle distribution and expression of cell cycle associated proteins

We then investigated whether carbon ion irradiation could affect the distribution of SQ20B cells in the cell cycle.

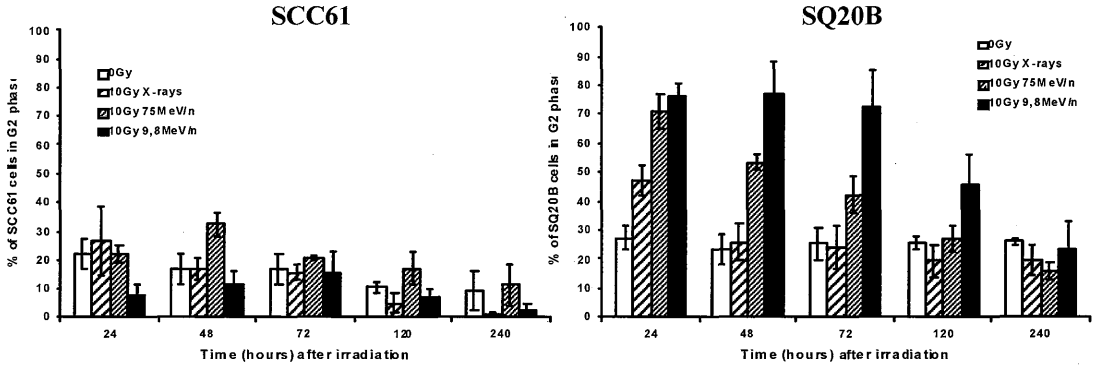

Figure 3 : Percentage of SCC61 and SQ20B cells in G2/M phase after high or low-LET irradiation.

A transient dose-dependent arrest in G2/M phase was measured in SQ20B cells at 24h following X-ray exposure (Figure 3). Irradiation with 75MeV/n carbon ions induced a more prolonged and pronounced increase in the G2/M phase arrest (24-72h) which concerned 71% of cells at 24h after 10Gy exposure. Irradiation with 9.8MeV/n carbon ions showed an even greater efficiency with a higher percentage of cells (83%) in the G2/M phase at 24h and an arrest persisting up to 120h. The analysis of the fraction of SQ20B cells in G1 revealed no delay or arrest (data not shown). The same experiments performed with SCC61 cells

showed no G1 or G2/M phase arrest, regardless of the radiation quality. Taken together, the proportion of cells in G2/M and the duration of the arrest increased with LET in SQ20B cells, whereas no arrest occurs in SCC61 cell line.

To gain insight into the molecular mechanisms underlying the inhibition of the cell cycle progression observed in SQ20B cells, we studied the expression of Chk1 and Chk2 proteins by western-blot analysis. Our results indicated that in SQ20B cells the phosphorylation of Chk1, but not Chk2 promoted the induction of G2/M arrest in SQ20B cells following irradiation. We also investigated the activation of the cyclin B1/Cdc2 complex and similarly to Chk1-P, the level of Cdc2-P increased in a LET-dependent manner during the 120h following irradiation and then declined to control levels (data not shown). Altogether, these results demonstrate that carbon ions induce higher levels of cell cycle inhibiting proteins than X-rays, resulting in a more prolonged and pronounced G2 arrest.

Senescence-associated-β-galactosidase activity

In the light of these results, we examined whether the growth inhibition of SQ20B cells could be related to a mechanism of senescence-like arrest. We therefore investigated the senescence-associated-β-galactosidase (SA-β-gal) activity at pH6, a specific marker of the different senescence processes. Figure 4 A,B shows enhanced β-gal activity in SQ20B cells, at 10 days following carbon ion irradiation.

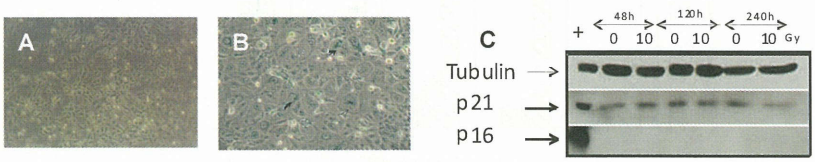

Figure 4: SQ20B cells stained for β-gal activity 10 days after 0Gy (A) and 10Gy (B) 9.8MeV/n carbon irradiation. Expression of p21 and p16 in SQ20B cells after9.8MeV/n carbon irradiation (C)

However, no induction or accumulation of senescence-related proteins (p21 or p16) was observed (Figure 4C). These observations suggest that the enhanced activity of β-gal detected in SQ20B was more a result of stress than an irreversible senescence-like arrest.

Cell death by mitotic catastrophe in SQ20B cells

To investigate the possible involvement of mitotic catastrophe following irradiation we studied the appearance of polyploid cells after irradiation.

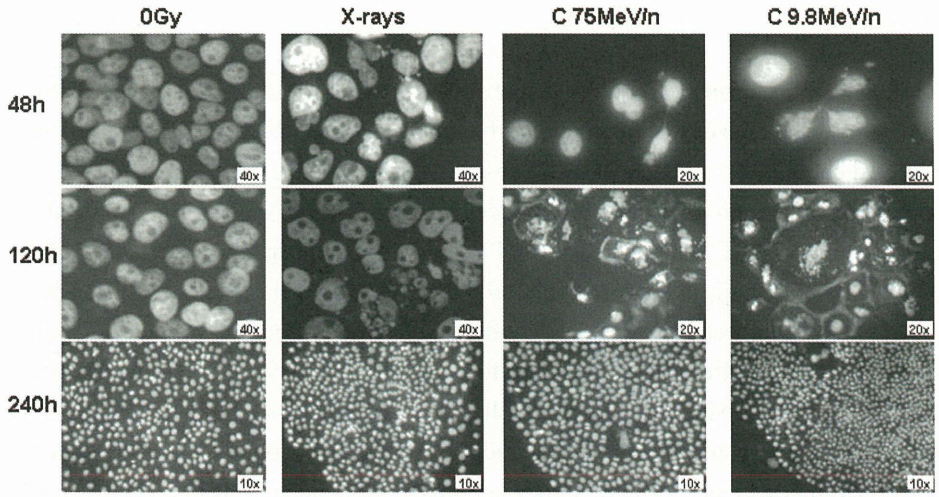

Figure 5 : Kinetics of the occurrence of polyploid SQ20B cells after irradiation with X-rays or carbon ions

Figure 5 shows, in SQ20B cells, the presence of fragmented or lobulated nuclei in association with micronuclei, characteristics consistent with mitotic catastrophe following 10Gy of carbon ion and X-ray irradiation. In addition, anaphase bridges were observed at 2 days for each condition of irradiation, indicating that the origin of these polyploid cells could be a failed redistribution of the chromosomes. It is noteworthy that X-rays induced a much lower percentage of anaphase bridges and aberrant cells than carbon ions. Induction of mitotic catastrophe was confirmed by the appearance of polyploid SQ20B cells observed by flow cytometry and by the activation of caspase-2 which was detected at 240h following X-ray and at 120 and 240h following carbon ion (data not shown). Notably, none of these morphological alterations was detected in SCC61 cells (data not shown).

Re-entry of SQ20B cells in the cell cycle after prolonged G2/M accumulation.

Although most of SQ20B cells underwent mitotic catastrophe followed by apoptosis, a subpopulation continued to proliferate. To evaluate this proliferation we performed BrdU-pulse labeling experiments following 10Gy of both types of irradiation (Figure 6).

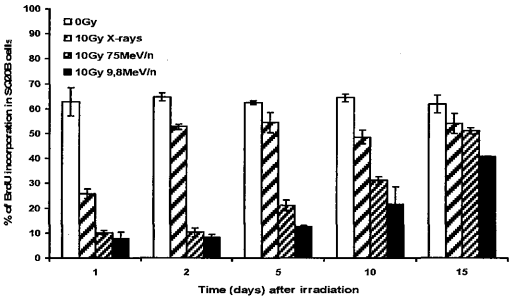

Figure 6 : BrdU pulse labeling in SQ20B cells after exposure to X-ray or carbon ion beams

Decreased proliferation of SQ20B cells was observed 24h after X-ray irradiation, followed by a proliferation closely similar to control cells. In contrast, after carbon ion exposure, a more prolonged and LET-dependent decrease in the number of labeled cells was detected consistent with the observed G2/M accumulation. However, from 2 days following X-ray or 10 days following carbon ion irradiation, the percentage of labeled SQ20B cells increased. In contrast, no significant proliferation recovery was evident in SCC61 cells (data not shown), consistent with the observation of early apoptosis after irradiation. These results demonstrate that even following irradiation with high doses of high-LET carbon ions, a fraction of SQ20B cells escape mitotic catastrophe and continue to proliferate.

Discussion

To assess the biological mechanisms potentially responsible for the high radioresistance of HNSCC tumors demonstrated by Mizoe *et al.* (11), we performed our study in two p53-mutated HNSCC cell lines with low or high radiosensitivity and compared the effects of the exposure to X-rays with carbon ion beams.

We first demonstrated that carbon ion irradiation induced a higher level of clonogenic cell death compared to X-rays. An increase in the RBE with increasing LET was detectable in both cell lines. However the radioresistant SQ20B cells systematically showed reduced sensitivity compared to the radiosensitive SCC61 cells. Suzuki *et al.* (13) also demonstrated a LET-dependent cell killing effect of carbon ions. Although the increase in efficiency of carbon ion irradiation compared to X-rays is well established, only a few studies have investigated the mechanisms underlying the observed cell death. Apoptosis has been described as a possible mechanism whereby heavy ions could overcome the radioresistance upon photon irradiation (14). Several studies have demonstrated that carbon ions may induce apoptosis independently of the p53 status (3,4). Here we have demonstrated that the pathway activated in response to high LET irradiation could be the

ceramide-dependent apoptotic pathway. These observations are in accordance with our previous studies which demonstrated that the sequence of events leading radiosensitive SCC61 cells to apoptosis in response to photons irradiation (8) initially involves ceramide production. In contrast, in the radioresistant SQ20B cell line a failure in ceramide production was correlated to a lack of apoptosis. In response to carbon irradiation the apoptotic cell death which goes through ceramide seems to be the main activated pathway in SCC61 cells. In contrast, SQ20B cells showed neither apoptosis nor ceramide production during the 72h following carbon ion or X-ray irradiation. The increase of sub-G1 cells which was associated to late apoptosis or to the end of mitotic catastrophe was observed only 120h after carbon ion exposure. However the percentage of SQ20B apoptotic cells was still much lower than for SCC61 cells.

Instead of early apoptosis a significant fraction of SQ20B cells responded to irradiation by undergoing a prolonged LET-dependent G2/M arrest. Our results are in agreement with Matsumura *et al.*, 2003 (15) who demonstrated that heavy-ions are more effective than X-rays in inducing G2 arrest.

The association of cell cycle arrest and senescence-like process with tumor cell growth inhibition in response to different stresses has been well documented. Benzina *et al.* (16) reported that fast neutrons combined to cisplatin induced a senescence-like cell cycle arrest rather than apoptosis in glioblastoma cells. Here we demonstrated an increase in SA-β-gal + SQ20B cells following irradiation. However, no accumulation of the p16 or p21 proteins responsible for the maintenance of an irreversible cell cycle arrest, was detected. Thus, the activation of SA-β-gal was related to cellular stress rather than a senescence-like cell cycle arrest (17).

A sustained cell cycle arrest may protect the cells from cytotoxicity induced by irradiation (18). High-LET irradiation is associated with more complex DNA damage due to higher local energy deposition. Thus, the LET-dependent prolonged cell cycle delay after carbon ion irradiation is consistent with the complex requirements for DNA repair. In SQ20B cells Chk1 activation was necessary for the establishment of this arrest. As a result, the subsequent activation of Cdc2/Cyclin B promoted the onset of mitosis in SQ20B cells, even though the repair of DNA could have been incomplete. The resulting profound effects on the behavior of the SQ20B cells induced several disturbances during mitosis, leading to anaphase bridges and multinucleated cells. These morphological features are typical of mitotic catastrophe (7). However, despite the specific morphology of the cells, mitotic catastrophe may represent a pre-stage of apoptosis. We have demonstrated that mitotic catastrophe occurred in SQ20B cells following carbon ion irradiation in a p53-independent manner through a caspase-2 pathway leading to a delay in apoptotic cell death, as described by Castedo *et al.* (19). Thus, increasing mitotic catastrophe is likely to be responsible for the high RBE values observed in SQ20B cells after carbon ion irradiation. However, despite the efficiency of carbon ions in inducing prolonged cell cycle arrest and after release, in inducing mitotic catastrophe, a subpopulation of SQ20B cells could escape mitotic catastrophe and re-enter the cell cycle. This observation may explain the potential local-regional recurrence observed among certain HNSCC patients treated by carbon hadrontherapy (11).

Conclusion

To our knowledge, for the first time different types of cell death have been investigated in response to carbon ion irradiation. We have demonstrated that this does not modify the type of cell death observed after X-ray exposure, but instead shows an increased effectiveness. Moreover, we have shown that two different p53-independent types of cell death were induced in two HNSCC cell lines with opposite radiosensitivity. In the light of our increased understanding of the cellular response of HNSCC cells to high-LET irradiation it is reasonable to postulate that associated adjuvant treatment forcing the tumor cells to enter apoptosis may improve the outcome of carbon hadrontherapy.

References

[1] Schulz-Ertner D, Tsujii H. Particle radiation therapy using proton and heavier ion beams. J Clin Oncol. 2007;25:953-964.

[2] Holgersson A, Jernberg AR, Persson LM et al. Low and high LET radiation-induced apoptosis in M059J and M059K cells. Int J Radiat Biol. 2003;79:611-621.

[3] Iwadate Y, Mizoe J, Osaka Y, et al. High linear energy transfer carbon radiation effectively kills cultured glioma cells with either mutant or wild-type p53. Int J Rad Oncol Biol Phys 2001;50:803-808.

[4] Takahashi A, Matsumoto H, Yuki K, et al. High-LET radiation enhanced apoptosis but not necrosis regardless of p53 status. Int J Radiat Oncol Biol Phys 2004;60:591-597.

[5] Tsuboi K, Moritake T, Tsuchida Y, Tokuuye K, et al. Cell cycle checkpoint and apoptosis induction in glioblastoma cells and fibroblasts irradiated with carbon beam. J Radiat Res 2007;48:317-325.

[6] Jones KR, Elmore LW, Jackson-Cook C, et al. p53-Dependent accelerated senescence induced by ionizing radiation in breast tumour cells. Int J Radiat Biol 2005;81:445-458.

[7] Ianzini F, Domann FE, Kosmacek EA, et al. Human glioblastoma cells transduced with a dominant negative p53 adenovirus construct undergo radiation-induced mitotic catastrophe. Radiat Res 2007;168:183-192.

[8] Alphonse G, Aloy MT, Broquet P, et al. Ceramide induces activation of the mitochondrial/caspases pathway in Jurkat and SCC61 cells sensitive to gamma-radiation but activation of this sequence is defective in radioresistant SQ20B cells. Int J Radiat Biol. 2002;78:821-835.

[9] Kolesnick R, Fuks Z. Radiation and ceramide-induced apoptosis. Oncogene. 2003;37:5897-5906.

[10] Schulz-Ertner D, Tsujii H. Particle radiation therapy using proton and heavier ion. J Clin Oncol 2007;25:953-964.

[11] Mizoe JE, Tsujii H, Kamada T, et al. Dose escalation study of carbon ion radiotherapy for locally advanced head-and-neck cancer. Int J Radiat Oncol Biol Phys. 2004;60:358-64.

[12] Beuve M, Alphonse G, Maalouf M, et al. Radiobiologic parameters and local effect model predictions for head-and-neck squamous cell carcinomas exposed to high linear energy transfer ions. Int J Radiat Oncol Biol Phys 2008;71:635-642.

[13] Suzuki M, Kase Y, Yamaguchi H, et al. Relative biological effectiveness for cell-killing effect on various human cell lines irradiated with heavy-ion medical accelerator in Chiba (HIMAC) carbon-ion beams. Int J Radiat Oncol Biol Phys 2000;48:241-250.

[14] Meijer AE, Jernberg AR, Heiden T, et al. Dose and time dependent apoptotic response in a human melanoma cell line exposed to accelerated boron ions at four different LET. Int J Radiat Biol 2005;81:261-272.

[15] Matsumura S, Matsumura T, Ozeki S, et al. Comparative analysis of G2 arrest after irradiation with 75 keV carbon-ion beams and 137Cs γ-rays in a human lymphoblastoid cell line Cancer Detect Prev 2003;27:222-228.

[16] Benzina S, Fischer B, Miternique-Grosse A, et al. Cell death induced in a human glioblastoma cell line by p(65)+Be neutrons combined with cisplatin. Life Sc i2006;79:513-518.

[17] Severino J, Allen RG, Balin S, et al. Is beta-galactosidase staining a marker of senescence in vitro and in vivo? Exp Cell Res 2000;257:162-171.

[18] Xiao Z, Chen Z, Gunasekera AH, et al. Chk1 mediates S and G2 arrests through Cdc25A degradation in response to DNA-damaging agents. J Biol Chem 2003;278:21767-21773.

[19] Castedo M, Perfettini JL, Roumier T, et al. Cell death by mitotic catastrophe: a molecular definition. Oncogene 2004;23:2825-2837.

The Mechanism behind the Effective Cell Killing by High LET Heavy Ion Irradiation

Ryuichi Okayasu, Takamitsu Kato, Akira Fujimori, Miho Noguchi, and Yoshihiro Fujii

Heavy-Ion Radiobiology Research Group, Research Center for Charged Particle Therapy,
National Institute of Radiological Sciences, Chiba, Japan
e-mail address: rokaysu@nirs.go.jp

Abstract

At the National Institute of Radiological Sciences (NIRS), over 4000 cancer patients have been treated by heavy ions with an impressive success rate. There are clinical, physical and biological factors behind this achievement, and in this presentation a few critical biological issues are discussed. Besides the physical advantage of the dose distribution of heavy ions, two important biological factors exist; one of them the inhibition of DNA double-strand break (DSB) repair by heavy ions and the other the reduced variation of cell survival levels throughout the cell cycle. The repair of DNA DSB was examined using constant field gel electrophoresis as well as gamma-H2AX assay, and both techniques clearly showed a significant inhibition of initial rejoining of DSBs induced by 70 keV/μm carbon ions. The degree of repair inhibition seems to be reflected in the radiation cell survival level. Using synchronized CHO cells, we investigated cell survival levels throughout the cell cycle with carbon ions, and the result was compared with that with X-rays. Our data indicated that much less variation in the cell survival level was observed when carbon ions were used to irradiate cells. Moreover, gene expression studies using a unique method developed at NIRS provided new insight into biological damage induced by heavy ions. These data together provide biological reasons for the successful outcome reported at the heavy ion facility at NIRS.

Introduction

It is generally believed that high linear energy transfer (LET) heavy ion radiation can induce a more complex type of DNA damage to cells, specifically DNA double-strand breaks (DSBs), than traditional X-rays or gamma-rays, and this, in turn, leads to a higher rate of killing of tumor cells when these lesions are not repaired [1-12]. As mentioned elsewhere, the physical dose distribution of heavy charged particles with the Bragg peak gives further advantage to treating tumor tissues more selectively and evade surrounding normal tissues.

Another important biological aspect of high LET heavy ion radiation is its reduced cell cycle dependency of cell survival rate. For mammalian cells in general, late S-phase cells are the most resistant, and cells in the mitotic phase are the most sensitive to low LET radiation sources [13]. In contrast, with high LET heavy ion radiation, the cell cycle responses seem much more modest. In 1975, using an accelerator available in Berkeley, Bird and Burkib [14] showed that the cell survival levels throughout the cell cycle phases are fairly similar, with no distinct dependency on the location of cells in the cell cycle. Although these data are very important and useful for heavy ion radiobiology, there have been almost no similarly repeated experiments using other heavy ion facilities. Recently, we have repeated the experiment with synchronized mammalian cells at the heavy ion medical accelerator (HIMAC) in Chiba, and some of the significant results are presented.

In this manuscript, data on DNA DSBs and their repair are presented first. Then some recent gene expression studies are described, followed by data on radio-sensitivity throughout the cell cycle with high LET irradiation.

Material and Methods

Cell survival and irradiation

Cells were irradiated with a Shimadzu Pantak HF-320 X-ray machine at a dose rate of 0.93 Gy/min. All heavy ion irradiations were performed at the heavy ion medical accelerator in Chiba (HIMAC) at the National Institute of Radiological Sciences (NIRS). We chose the LET value for carbon ions (290MeV/n, original energy) to be 70 keV/μm. Lucite absorbers (146 mm H_2O equivalent thickness) were used to obtain the desired LET value. Under this condition, about 50% of the original carbon beams remained (corresponding beam energy = ~ 40MeV/n). All cell survival experiments were performed using the conventional colony formation assay [15].

Cell synchronization

Synchronized cultures were obtained from exponentially growing cells by the technique of mitotic selection, using mechanical shake-off [14]. Throughout the shake-off procedure, pre-warmed medium was used to maintain the physiological temperature. The decanted suspension of selected cells was counted, and appropriate dilutions were made for plating cells for colony formation.

DNA DSB repair (constant field gel electrophoresis)

The method has been reported previously [16]. Immediately after irradiation (20 Gy) on ice, the medium was replaced with warm medium and cells were incubated in an incubator (37°C) for repair. At each repair point, cells were washed, trypsinized on ice for 20 min, and washed again in cold medium. The resulting cell pellets were embedded in 1% agarose (InCert agarose, FMC) at a density of 1.5 X 10^6 cells/ml, and placed on ice. These agarose samples were cut into plugs, and placed in lysis solution (TREVIGEN) containing proteinase K for 1 h on ice, and incubated for 24 h at 50°C. The plugs were equilibrated in TE buffer (SIGMA, pH 8.0), loaded on 0.6% SeaKem Gold agarose gels (Cambrex), and subjected to electrophoresis at 0.6 V/cm in 0.5 X TBE buffer for 36 h. The gel was stained with ethidium bromide and de-stained. The fluorescence intensities were measured with a UV transilluminator and a digital camera with an orange filter. NIH Image software was used for the analysis of DSB damage, and the fraction of released DSBs was calculated.

DNA DSB repair (H2AX)

The fixation and staining method for immunocytochemistry closely followed that previously described by K.Rothkamm and M.Löbrich [17]. For immunostaining, cells were cultured on flaskettes and synchronized into G1 phase by isoleucine deprivation as described above. After irradiation, cells were fixed in 4% paraformaldehyde for 15 min, washed 3 times in PBS for each 10 min, permeabilized for 5 min on ice in 0.2% Triton X-100, and sites that may have nonspecifically bounded the detecting antibody probe were blocked in PBS with 10% goat serum for 3 washes of 10 min each at room temperature. The flasks were then incubated with anti-γ-H2AX antibody (Trevigen) for 1 h, washed 3 times in PBS for 10 min each, and incubated with FITC-conjugated goat anti-rabbit secondary antibody (Sigma) for 1 h at 37°C. Cells were washed 4 times in PBS for 10 min each, and mounted by using Slow Fade (Molecular Probes) to reduce photobleaching during observation. Images of cells were obtained using an Olympus A70 fluorescence microscope equipped with an image analysis system. The processed images were stored and cells from these were later scored.

Gene Expression

Gene expressions were studied with the HiCEP method developed at NIRS, and the details are available from previous publications [18,19].

Results

Repair of DNA DSB is inhibited by 70 keV/μm carbon ion irradiation

We analyzed repair of DNA DSB using a gel-based assay. Fig.1 shows the results of DNA DSB rejoining kinetics in prostate cancer cells (DU145) irradiated with X-rays and 70 keV/μm carbon ions using constant field gel electrophoresis (CFGE) technique. The corresponding radiation cell survival levels are also shown in the figure.

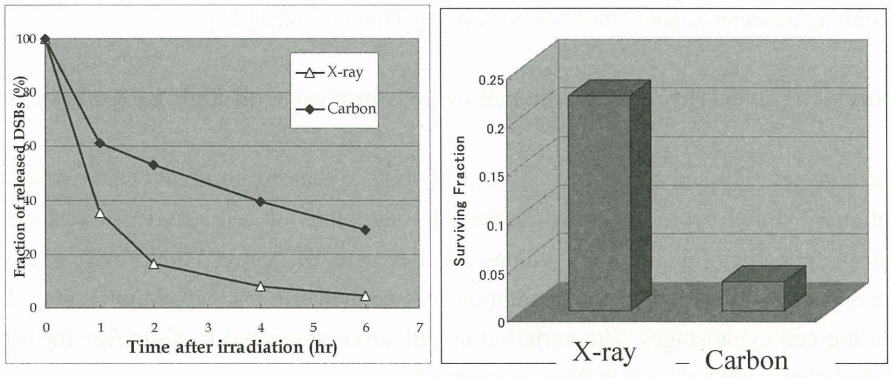

Fig.1. (Left) Comparison of DNA DSB repair kinetics in DU-145 tumor cells irradiated with X-rays and 70 KeV/μm carbon ions.
(Right) Cell survival levels (4 Gy) with corresponding irradiation sources are also provided.

The rejoining kinetics of DNA DSB with carbon ions was clearly impaired when compared to X-irradiation. The cell survival data with these two radiation sources seem to reflect the rejoining ability shown in this figure.

The gel assay we used above is useful; however, the radiation dose (e.g., 20 Gy) necessary for this assay is comparatively high and the data from the gel-assay cannot be compared with the cell survival data. Thus, we employed an immuno-staining focus assay to detect DSB repair. Fig. 2 shows the DSB appearance/disappearance kinetics using sensitive gamma-H2AX assay; the dose used here was 1 Gy for all radiation sources. As expected, the foci with X-irradiation disappeared quickly, while the foci with 70 keV/μm carbon ions disappeared much less efficiently. Moreover, the kinetics of foci appearance induced by 13 keV/μm carbon ions (the flat dose distribution part before the Bragg peak) behaved similarly to the kinetics obtained with X-rays.

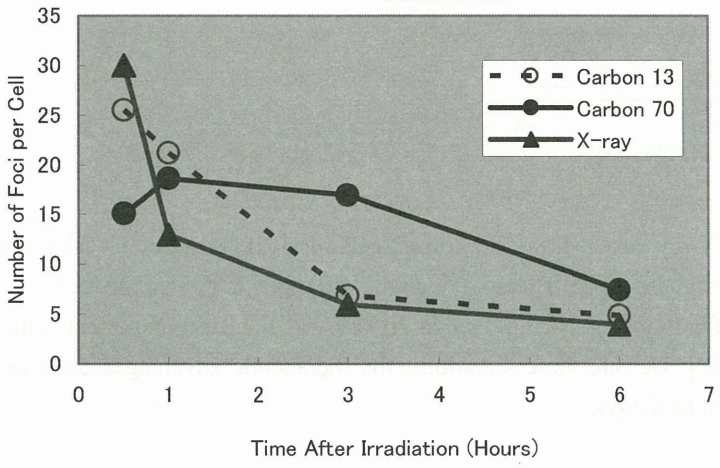

Fig. 2 Kinetics of gamma-H2AX foci appearance/disappearance in human cells irradiated with 1 Gy X-rays, 13 keV/μm and 70keV/μm carbon ions.

These useful data obtained at low doses reaffirmed the more severe biological outcome with high LET heavy ions. The DSB repair data were also shown to reflect the data at the chromosome level [e.g., 20].

Gene expression studies provide different patterns for high LET radiation

At NIRS, we have a unique system to detect gene expressions [18,19]. This sensitive method is called HiCEP (high coverage expression profiling) and was able to give us some new insights with high LET irradiation. Although variations in well-known genes for DNA damage responses were detected with high LET irradiation, we found some genes that are continually over-expressed only with high LET heavy ions, but not with low LET irradiation. ATF3 is one of these genes, and its significance is under investigation. In addition, we found a gene that was significantly down-regulated with both high and low LET irradiation, and it was identified as ASPM (abnormal spindle-like microcephaly associated gene) and has been partly characterized [21].

Variation in radiation cell survival levels throughout the cell cycle is modest with high LET heavy ion irradiation

Using synchronized Chinese hamster V79 cells, Bird and Burki [14] showed that the survival curve variation was found for X-rays as a function of cell cycle stages, while reduced variations of cell survival levels were found for heavy ion irradiation depending on the LET values. In the case of X-rays, there was a clear radio-resistant peak in the late S-phase. When carbon ion irradiation was applied (LET: 191 keV/μm), they did not find a variation throughout the cell cycle stages. The variation in cell survival seemed to disappear for high LET irradiation after LET reached about 200 keV/μm in their experiment.

We have performed a similar experiment with synchronized CHO cells using the HIMAC accelerator, and the cell survival data as a function of the cell cycle phases are shown in Fig.3. In order to better understand the tendency of the cell cycle effect, it is best to compare the data with 4 Gy X-rays and those with 2 Gy carbon ions due to a similar biological effectiveness. The variation for the carbon ions data appears less distinct throughout

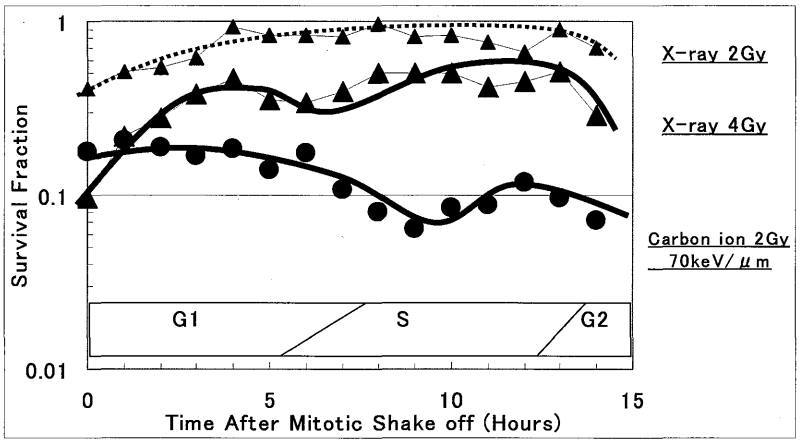

Fig. 3 Comparison of radiation cell survival levels in synchronized CHO cells irradiated with 2 Gy and 4 Gy X-rays, and 2 Gy 70 keV/μm carbon ions.

the cell cycle than that for X-rays. The X-ray curve shows the lowest cell survival at mitotic to G1 stages and tends to show a higher level toward the S-phase stage. There were slight variations in the carbon survival curve probably due to the mixed populations of carbon beams employed at 70 keV/μm; nucleus components other than carbon ions are included in the beam [22]. Despite these situations, the therapeutic advantages obtained with carbon beams are obvious when compared to X-rays.

Discussion

In this report, we have shown some of the critical biological characteristics associated with high LET heavy ion irradiation as compared with low LET irradiation. The repair of DNA DSB indicated clear evidence of inhibition of DSB rejoining in cells irradiated with high LET carbon ions, even at low radiation doses. It is significant that the cells irradiated with lower LET (13 keV/μm) carbon ions showed a tendency similar to

X-irradiated cells. This indicates that much less radiation damage can be expected with the flat part of dose distribution curve of carbon ion beams. This seems to give an advantage to carbon ion treatment, as tumor cells are targeted with the Bragg peak part of the beam.

Our recent data on the variation of cell survival levels throughout the cell cycle can give us further insight into high LET radiobiology. High LET radiation significantly reduces the variation in cell survival levels observed with low LET radiation. This gives another advantage to heavy ion therapy, as the radio-resistant peak at S-phase may not be a significant problem with high LET irradiation treatment. We have also extended our cell cycle related studies with DSB repair-defective mutants, and new understanding has been obtained with these studies (data not shown).

References

[1] Barendsen GW. Impairment of the proliferative capacity of human cells in culture by alpha-particles with differing linear-energy transfer. Int J Radiat Biol Relat Stud. Phys Chem Med 1964;15:453-466.

[2] Cox R, Thacker J, Goodhead DT, Munson RJ. Mutation and inactivation of mammalian cells by various ionizing radiations. Nature 1977; 267:425-427.

[3] Tobias CA, Blakely EA, Alpen EL, et al. Molecular and cellular radiobiology of heavy ions. Int J Radiat. Oncol Biol Phys. 1982; 8:2109-2120.

[4] Goodwin E, Blakely E, Ivery G, Tobias C. Repair and misrepair of heavy-ion-induced chromosomal damage. Adv. Space. Res. 1989; 9:83-89.

[5] Hendry JH. The slower cellular recovery after higher-LET irradiations, including neutrons, focuses on the quality of DNA breaks. Radiat. Res. 1991;128:111-113.

[6] Rydberg B, Lobrich M, Cooper PK. DNA double-strand breaks induced by high-energy neon and iron ions in human fibroblasts. I. Pulsed-field gel electrophoresis method. Radiat. Res. 1994;139:133-141.

[7] Frankenburg-Schwager M, Harbich R, Beckonert S, Frankenburg D. Half-life values for DNA double-strand break rejoining in yeast can vary by more than an order of magnitude depending on the irradiation conditions. Int. J. Radiat. Biol. 1994;66:543-547.

[8] Loucas BD, Geard CR. Kinetics of chromosome rejoining in normal human fibroblasts after exposure to low- and high-LET radiations. Radiat. Res. 1994;138, 352-360.

[9] Taucher-Scholz G, Heilmann J, Kraft G. Induction and rejoining of DNA double-strand breaks in CHO cells after heavy ion irradiation. Adv. Space. Res. 1996;18:83-92.

[10] Suzuki M, Kase Y, Kanai T, Ando K. Correlation between cell killing and residual chromatin breaks measured by PCC in six human cell lines irradiated with different radiation types. Int. J. Radiat. Biol. 2000; 76:1189-1196.

[11] Suzuki M, Piao C, Hall EJ, Hei TK. Cell killing and chromatid damage in primary human bronchial epithelial cells irradiated with accelerated 56Fe ions. Radiat. Res. 2001;155:432-439.

[12] George K, Wu H, Willingham V, Furusawa Y, Kawata T, Cucinotta FA. High- and low-LET induced chromosome damage in human lymphocytes: a time-course of aberrations in metaphase and interphase. Int. J. Radiat. Biol. 2001; 77:175-183.

[13] Hall EJ, Giaccia AJ. Radiobiology for the Radiologist. Lippincott Williams & Wilkins; 2005;6th edition.

[14] Bird RP, Burki HJ. Survival of synchronized Chinese hamster cells exposed to radiation of different linear-energy transfer. Int. J. Radiat. Biol. 1975;27:105-120.

[15] Okayasu R, Okada M, Okabe A, Noguchi M, Takakura K, Takahashi S. Repair of DNA damage induced by accelerated heavy ions in mammalian cells proficient and deficient in the non-homologous end-joining pathway. Radiat. Res. 2006;165:59-67.

[16] Hirayama R, Furusawa Y, Fukawa T, Ando K. Repair kinetics of DNA-DSB induced by X-rays or carbon

ions under oxic and hypoxic conditions. J. Radiat. Res. 2005;46:325-332.
[17] Rothkamm K, Löbrich M. Evidence for a lack of DNA double-strand break repair in human cells exposed to very low x-ray doses. Proc. Natl. Acad. Sci. U S A. 2003;100:5057-5062.
[18] Fukumura R, Takahashi H, Saito T, et al. A sensitive transcriptome analysis method that can detect unknown transcripts. Nucleic Acids Res. 2003; 31, e94.
[19] Fujimori A, Okayasu R, Ishihara H, et al. Extremely low-dose ionizing radiation upregulates CXC chemokines in normal human fibroblasts. Cancer Res. 2005;65: 10159-10163
[20] Sekine E, Okada M, Matsufuji N, Yu D, Furusawa Y, Okayasu R. High LET heavy ion induces lower numbers of initial chromosome breaks with minimal repair than low LET radiation in normal human cells. Mutat. Res. 2008;652:95-101.
[21] Fujimori A, Bing W, Suetomi K, et al. Ionizing radiation downregulates ASPM, a gene responsible for microcephaly in humans. Biochem. Biophy. Res. Commun. 2008;369:953-957.
[22] Matsufuji N, Fukumura A, Komori M, Kanai T, Kohno T. Influence of fragment reaction of relativistic heavy charged particles on heavy-ion radiotherapy. Phys. Med. Biol. 2003;48:1605-1623.

Biological Effectiveness of Mammalian Cells Exposed to Heavy Ion Beams

Yoshiya Furusawa

Research Center for Charged Particle Therapy, National Institute of Radiological Sciences, Chiba, Japan
e-mail address: furusawa@nirs.go.jp

Abstract

The LET-RBE spectra were investigated using cultured V79 cells by accelerated heavy ions. Cells were exposed to ^{3}He-, ^{12}C-, and ^{20}Ne-ion beams at HIMAC, the Medical Cyclotron at NIRS, and RRC at RIKEN with an LET ranging over approximately 10-500 keV/μm under aerobic conditions. Cell-survival curves were fitted by equations from the linear-quadratic model to obtain survival parameters, and the RBE values were analyzed as a function of LET. The RBE increased with LET, reaching a maximum at around 200 keV/μm, then decreased with a further increase in LET. Clear splits of the LET-RBE spectrum were found among ion-spices. The LET-RBE spectra were fitted by a newly contrived equation that including three parameters: L_p, A, and W. The parameters will indicate a LET that gives a maximum RBE, a related value to maximum RBE, and indicates the width of the peak of RBE, respectively. It is also found that the parameters can be defined as functions of atomic numbers of the accelerated ions. At a given LET, the RBE-value for lighter ions was higher than that for heavier ions at lower-LET region. The LET that gives maximum RBE shifts to higher LET for heavier-ions, and the maximum values of the peak of RBE decreased with the atomic number of the irradiated ions.

Introduction

The Heavy Ion Medical Accelerator in Chiba (HIMAC) was constructed at the National Institute of Radiological Sciences (NIRS), Chiba, Japan, in 1993 to perform advanced radiotherapy treatment of cancer[1], [2]. Clinical trials were also started using carbon-ion beams in June 1994, and over 3100 patients had been treated with HIMAC carbon-ion beams by 2007. For a requirement of pre-clinical radiobiological studies and the cooperative research projects in radiobiological field, a great numbers researchers visit HIMAC and huge number of data were obtained by researchers inside and outside NIRS including overseas. HIMAC is also available for scientific experiments, such as medical sciences, physics, radiation biology, and so on. The main subjects for radiobiological studies at HIMAC are studies concerning radiation therapy using heavy-ion beams. However results from the radiobiological studies are applicable for estimating radiobiological effects in a field of radiation protection study for the space, where the most biologically effective radiation is HZE beams.

The relative biological effectiveness (RBE) is one of the most important parameters in determining the biological effectiveness of heavy-ion beams. An accurate knowledge of the RBE was required at HIMAC when heavy-ion beam for cancer therapy will be started. RBE is roughly a simple function of LET, which is the rate of energy deposition in the linear dimension. However the detail and the suitable RBE for cancer therapy is not known, because there are big differences between low- and high-dose region, alternated by hypoxia, discrepancies among particles and by biological end-points. LET indicates the rate of energy deposition in the linear dimension of the absorbing material. There are differences in the radial energy deposition densities for beams of the same LET among accelerated ion species because of a difference in their electric charge and

velocity. This distribution of different track structures of the ionization density may produce different radiobiological effects on cells. However, there are few systematic biological data on the RBE and the LET of heavy ions, because it is usually difficult to expose many biological materials with the same exposure system under the same biological condition.

When we design a therapeutic ion beam, we must know biological effectiveness of the beam. However the LET and ion spices of the beam at defined depth in the body, the physical characteristics of the beam are very complex, because of the nuclear fragmentation of projectile ion and mixture of beams having different LETs to produce a spread-out Bragg peak. To know the RBE for those all ion spices at all radiation doses (or cell survival levels) and all LETs in the beam through biological experiments.

Only a data show here is cell killing on V79 cells as determined by a loss of colony-forming ability, and please see previous publication [5] for HSG cells that has used at HIMAC beam design. The data covers several ion-species, lighter-ions and heavier-ions than therapeutic carbon-ions. We will discuss the LET dependency of cell killing in an intermediate LET region (approximately 10-500 keV/μm) as well as the difference in the RBE spectra among the accelerated ion species. Also we will introduce a method to estimate biological effectiveness of heavy ions as a function of ion species and LETs. In addition, we will discuss possible method to estimate the biological effectiveness to all fragmented beams that have not measured biological experiments.

Experiments

1. Facility and Ion Beams

We exposed cells to ^{3}He-, ^{12}C-, and ^{20}Ne-ion beams. The exposures were carried out at the HIMAC, the medical cyclotron (NIRS-MC) at NIRS, and the ring cyclotron (RRC) facility at the Institute of Chemical and Physical Research (RIKN). The exposure systems at HIMAC, NIRS-MC and RRC were basically the same, and all the beam performance has confirmed by physics group of NIRS. An X-ray machine (Model Shinai-7, Shimadzu Co., Tokyo; 200 kVp, 20 mA, W-target, 0.5-mm aluminum + 0.5-mm copper filter) was used for obtaining the reference survival curves for RBE.

Dosimetry and LET determination at those facilities has previously reported[3][4][5]. Briefly, the dose rates of the beam were measured with a calibrated parallel-plate ionization chamber and/or a plastic scintillation counter at the sample position. A monitoring ionization chamber was placed upstream of the sample. The ratios between the monitor and the calibrated chamber were measured to determine the beam intensity at the sample position for the same ion. The exposure doses were automatically determined by a computer-aided irradiation system by integrating the output current from the monitor chamber.

The accelerated energies of beams used in our experiments were ranging from 12 MeV/u to 400 MeV/u. The LETs at the sample position were selected by changing the accelerated energy of the ion beam and adjusted by using an adequate thickness of aluminum or plastic (Lucite) absorbers[3]. For the experiment at higher-LET beams, we chose as possible as lower energy beam, however we also used some absorbers to select a LET values. Thus secondary ion beams generated in the absorbers cannot be avoided. The most affective ion in secondary beams at carbon experiments is a helium-ion with a LET of several keV/μm. The contribution of the absorbed dose from secondary ions was less than 2 %, as estimated from data obtained by a carbon 290 MeV/u carbon-ion beam near the end of its penetration[6][7]. For the other beams, there are no measurement of the fluence, dose, and LETs of secondary particles by a certain physical experiments. However we can roughly estimate the contribution of the dose from secondary beam by the dose at down stream of the penetration depth of each Bragg-peak. The values were less than 5% for all experiments. The dose would be smaller for beams having shorter penetration ranges than the estimated range.

TABLE 1. Ion Beams Used and possible LET

Ion	Energy in vacume (MeV/u)	LET_{min} # (keV/μm)	LET_{max} # (keV/μm)	Institute	Facility
^{3}He	6	28	90	NIRS	Cyclotron
^{4}He	150	2.2	50	NIRS	HIMAC
^{12}C	6	250	500	NIRS	Cyclotron
^{12}C	135	21	250	RIKEN	RRC
^{12}C	135/290/350/400	21/13/12/11	250	NIRS	HIMAC
^{20}Ne	135	58	400	RIKEN	RRC
^{20}Ne	135/230/400	58/41/30	400	NIRS	HIMAC

minimum LET for each beam, and possible maximum LET used for cell experiments.

2. Cell Culture and Survival Curve Fitting

Chinese hamster V79 cells cultured in Ham's F10 medium supplemented with 15% fetal bovine serum, 0.5 mg/ml Heart Infusion Broth (238400, Difco), and 100 U/ml penicillin and 100 μg/ml streptomycin was used. Cells were harvested by trypsinization, and seeded in dishes were cultured for about 1 day at 37°C in a 5% CO_2 incubator prior to exposure. After exposure, the cells were harvested by trypsinization, and re-suspended in a flesh medium. The numbers of cells in the suspension were counted by a particle counter, diluted with the medium, seeded in three 6-cm culture dishes at approximately 100 expected survivors per dish, and then incubated in an incubator for 6 days. The colonies in the dishes were fixed and stained. Colonies consisting of more than 50 cells were counted under a stereomicroscope as the number of viable cells. The plating efficiencies were greater than 80%. The α and β parameters were obtained from survival data plots by curve fitting using the LQ equation; $SF = \exp(-\alpha D - \beta D^2)$, by using computer programs. The D_{10} values were obtained from the α and β parameters from each survival data set.

Examples of survival curves were shown in Fig. 1. The curves for low-LET radiation showed a gentle curve with large shoulders. The curves become steeper and the shoulder was reduced with increasing of the LET. Gentle curves without shoulder were found at high-LET region. The survival curves for a lower-LET beam were well fitted by the LQ equation, and the survival curve parameters for X-rays; D_{10}, α, and β, were 7.07 Gy, 0.184 Gy^{-1}, and 0.0200 Gy^{-2}, respectively. When cells exposed to high-LET beams, data fitted well by the equation without the β term (or β = 0), because the curves were linear exponential. The curves were steepest and had no shoulder at LET 150 keV/μm or more, and the slope changed gradually with father increasing of the LET. Numerical data of survival parameters including other cell lines than V79 cells are reported previously [5] together with physical parameters of the beams (E, LET, LET_{100} and Z^{*2}/β^2). The RBE values were calculated as the ratio of the D_{10}s to that of X-rays. RBEs for different LET beams compared to X-rays were obtained for all the beams tested.

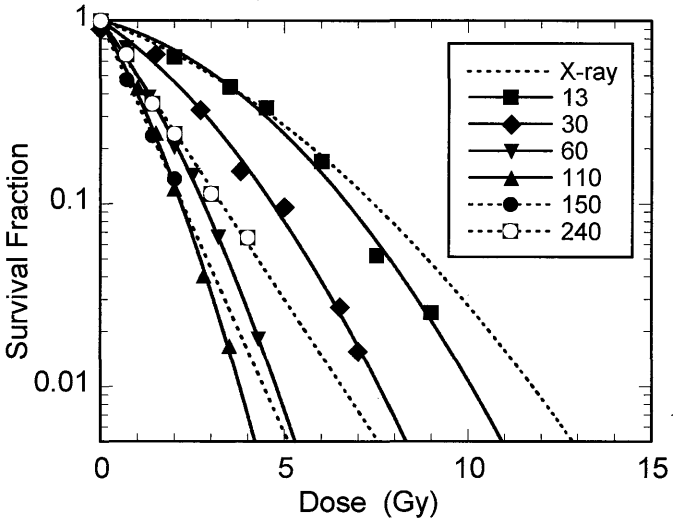

<Fig.1> Survival Curves for V79 Cells Exposed to Carbon Ions and X-rays. LET values of ion beams are indicated in the figure in keV/μm unit.

Analysis

1. Fitting of LET-RBE Curve

An experimental equation of LET-RBE relationships as a function of LET was investigated. The equation can be divided into two parts, and the relationship is expressed by using a composite function of the components. The first part (C1) describes a simple decreasing component of RBE with the LET, and the second part (C2) describes a peak of the RBE at a defined LET. The first part is expressed as;

$$C1_{(L)} = 1 / \mathrm{sqrt}\{(L/L_p)^2+Q/L+1\},$$

where L is the LET value of the ion-beam, L_0 is an LET that shows the inflection point of LET-RBE relationship, and Q is a parameter that defines the shape of the curve at inflection point. The second part is expressed as;

$$C2_{(L)} = A \exp\{ -\ln(L / L_p)^2 / W \},$$

where A is the maximum magnitude of the RBE, L_0 is the LET that gives maximum magnitude of the peak in the part, and the W is the width of the peak of RBE. The L_0 in C1 and C2 must be different parameter, but power of the C2 is major at around L_0. Also, Q can be negligible by the same reason. Here, we made the L_0 of the C1 and C2 to be the same and set Q = 0, to reduce the number of the parameters. Finally, here we used an equation;

$$RBE_{(L)} = 1 / \mathrm{sqrt}\{(L / L_p)^2 + 1\}+A \exp\{-\ln(L / L_p)^2 / W \},$$

to analyze the LET-RBE relationship. Calculations were performed by a fitting method using a computer program to minimize the weighted residuals.

The LET-RBE curves were determined using method described above for ^{3}He-, ^{12}C- and ^{20}Ne-ions with the LET ranging 18.6 - 90.8, 22.5 - 502, and 62.1 - 693 keV/μm, respectively, and the results were shown in Fig. 2. The LET-RBE spectra for all ion beams include ^{3}He-ion could be fitted with the fitting equation, and the values of the fitting parameters could be obtained.

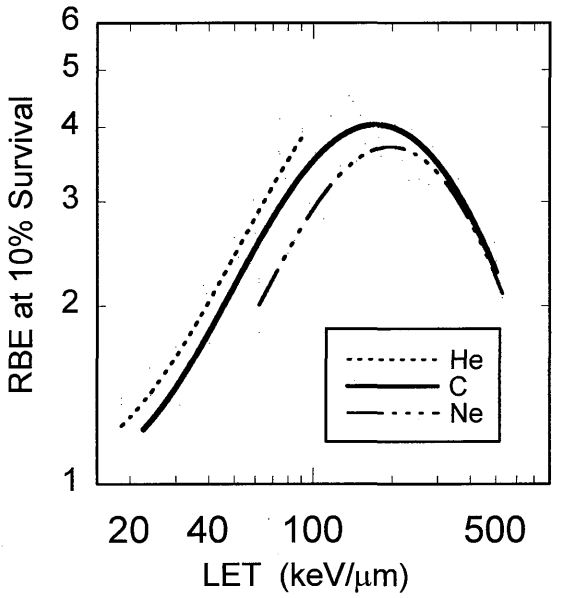

<Fig.2> Fitting of RBE as a Function of LET for V79 Cells Exposed to ^{3}He-, ^{12}C- and ^{20}Ne-Ion Beams (each data point not shown).

The spectra for those ions were different by the ion species especially in the low and middle LET range (<200 keV/μm), the RBEs showed different values for three different beams (^{3}He > ^{12}C > ^{20}Ne) at the same LET. The RBE spectra for ^{3}He-ion beams start to increase in a lower LET region compared to the other ion beams and reached a larger RBE (~ 4.0) at 90 keV/μm, but didn't showed a maxima. A peak RBE (3.56) was found at 88.3 keV/μm for a ^{3}He-ion beam by a similar experiment[8][9]. The depth-width of the Bragg peak for ^{3}He-ion beam is too narrow to expose a whole cell with a traversal having the same LET and the same dose rate. This means that the energy would be deposited at different LET and dose rates in a cell. The RBE may increase further more at higher LET of ^{3}He-ion, and it could be estimated to reach ~6 by the calculation. The maximum RBE values were found at around 200 keV/μm for ^{20}Ne-ion, and at around 150 keV/μm for ^{12}C-ion.

The difference in the RBE due to the ions is clear in lower-LET region up to 200 keV/μm (Fig. 2), where complete data sets for those three ions exist. For instance, the RBEs were, 3.3, 2.8 and 2.2 at 70 keV/μm for ^{3}He-, ^{12}C- and ^{20}Ne-ion, respectively. In the other word, the LET that gives 3.0 for the RBE of ^{3}He ions was 65 keV/μm, and that for ^{12}C- or ^{20}Ne-ion were at around 77 or 105 keV/μm. This means that to give the same radiobiological effectiveness for ^{12}C- and ^{20}Ne-ion beams to ^{3}He-ion beams, 1.2 or 1.6 times higher LET is required, respectively. There are considerable data[10][11][12] demonstrating such differences in the biological effectiveness of different ion species at the same LET. There is also a theoretical analysis[13] that predicts a difference between the LET-RBE spectra for different ions.

2. Fitting Parameters and Atomic Number

The LET-RBE relationships for ion-beams tested were plotted by a fitting method as described above. In general, the RBE increased with LET, showed peaks at around 100-200 keV/μm, and then decreased with LET. The LET-RBE spectra are different for the different ion spices. The LET-RBE curves are clearly different for the different ion beams. We thought that here must be a relationship between the parameters of the LET-RBE curves and atomic number of the accelerated ions, and the parameters Lp, A and W of LET-RBE curves were plotted as a function of atomic number of the ions (Fig. 3). The Lp increased and the A decreased exponentially with the increase of atomic number, and W was a constant. The relationship could be expressed as ;

Lp = 149•exp(0.0271•Z), with r = 0.985,
A = 583•exp(-0.0373•Z), with r = 0.997, and
W = 1.49.

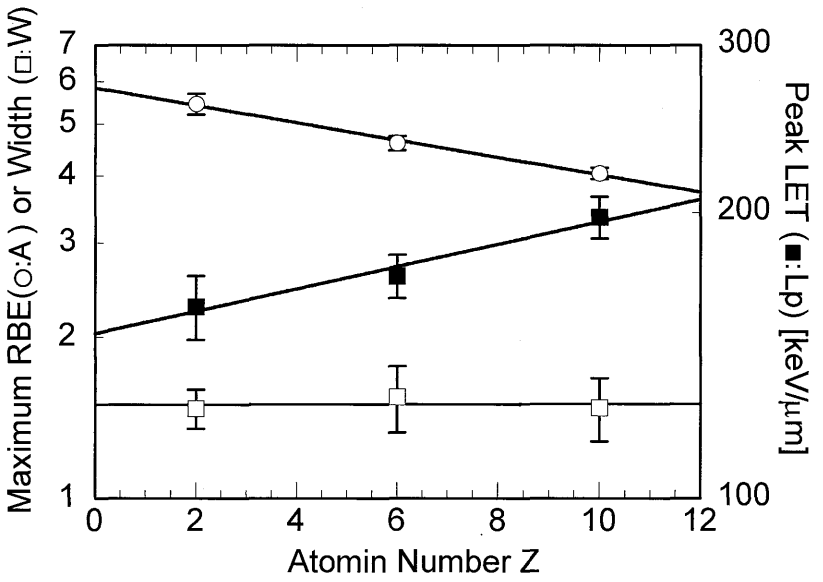

<Fig.3>. Parameters of LET-RBE Fitting Equation as a Function of Atomic Number of the Accelerated Ion (Z). The parameters are LET that gives the maximum RBE (L_p), amplitude (A) of the peak of RBE, and the width of the peak (W) of RBE.

Conclusion

We obtained LET-RBE spectra for killing of V79 cells exposed to different ion beams. At a given LET, the RBE-value for lighter ions was higher than that for heavier ions at lower-LET region. The LET-RBE relationship could fitted by a newly contrived equation that including three parameters; L_p, A, and W. It is also found that those parameters can be defined again as functions of atomic numbers of the accelerated ions. The LET of the maximum RBE (L_p) shifts to higher LET values for heavier-ions, amplitude (A) of the peak of RBE decreased with the atomic number of the irradiated ions, and the width of the peak (W) was a constant.

Using those parameters, we are possible to estimate RBEs to the beams at any LET and any ion spice that has not been measured the survival data biologically. Together with physical measurement of the fragmented beam i.e. components in total beam including atomic numbers and it's LET spectrum, we may possible to estimate total/average RBE of the beam. This means we may possible to estimate biological effectiveness to design further therapeutic beams with high accuracy.

Acknowledgement

We thank all staff members in the Division of Accelerator Physics and Engineering and the Division of Radiobiology and Biodosimetry at NIRS for their kind support during a part of this work. We thank the cyclotron crews at NIRS, and RIKEN for providing steady beams during the experiments. This investigation was partly supported by Special Coordination Funds of the Science Technology Agency, and the cooperative research with heavy-ion at HIMAC.

References

[1] H. Tsujii, J. Mizoe, T. Kamada, M. Baba, H. Tsuji, H. Kato, S. Kato, S. Yamada, S. Yasuda, T. Ohno, T. Yanagi, R. Imai, K. Kagei, H. Kato, R. Hara, A. Hasegawa, M. Nakajima, N. Sugane, N. Tamaki, R. Takagi, S. Kandatsu, K. Yoshikawa, R. Kishimoto and T. Miyamoto Clinical Results of Carbon Ion Radiotherapy at NIRS, J Radiat Res (Tokyo) 48 Suppl A (2007) A1-A13.

[2] M. Torikoshi, S. Minohara, N. Kanematsu, M. Komori, M. Kanazawa, K. Noda, N. Miyahara, H. Itoh, M. Endo and T. Kanai Irradiation System for HIMAC, J Radiat Res (Tokyo) 48 Suppl A (2007) A15-25.

[3] T. Kanai, T. Kohno, S. Minohara, M. Sudou, E. Takada, F. Soga, K. Kawachi and A. Fukumura Dosimetry and measured differential W values of air for heavy ions, Radiat Res 135 (1993) 293-301.

[4] T. Kanai, M. Endo, S. Minohara, N. Miyahara, H. Koyama-ito, H. Tomura, N. Matsufuji, Y. Futami, A. Fukumura, T. Hiraoka, Y. Furusawa, K. Ando, M. Suzuki, F. Soga and K. Kawachi Biophysical characteristics of HIMAC clinical irradiation system for heavy-ion radiation therapy, Int J Radiat Oncol Biol Phys 44 (1999) 201-210.

[5] Y. Furusawa, K. Fukutsu, M. Aoki, H. Itsukaichi, K. Eguchi-Kasai, H. Ohara, F. Yatagai, T. Kanai and K. Ando Inactivation of aerobic and hypoxic cells from three different cell lines by accelerated (3)He-, (12)C- and (20)Ne-ion beams, Radiat Res 154 (2000) 485-496.

[6] N. Matsufuji, A. Fukumura, M. Komori, T. Kanai and T. Kohno Influence of fragment reaction of relativistic heavy charged particles on heavy-ion radiotherapy, Phys Med Biol 48 (2003) 1605-1623.

[7] N. Matsufuji, M. Komori, H. Sasaki, K. Akiu, M. Ogawa, A. Fukumura, E. Urakabe, T. Inaniwa, T. Nishio, T. Kohno and T. Kanai Spatial fragment distribution from a therapeutic pencil-like carbon beam in water, Phys Med Biol 50 (2005) 3393-3403.

[8] M. Folkard, K.M. Prise, B. Vojnovic, H.C. Newman, M.J. Roper and B.D. Michael Inactivation of V79 cells by low-energy protons, deuterons and helium-3 ions, Int J Radiat Biol 69 (1996) 729-738.

[9] M. Belli, D.T. Goodhead, F. Ianzani, G. Simone and M.A. Tabocchini Direct comparison between protons and alpha-particles of the same LET: II. Mutation induction at the HPRT locus in V79 cells., International Journal of Radiation Biology 61 (1992) 625-629.

[10] E.A. Blakely, F.Q.H. Ngo, S.B. Curtis and C.A. Tobias Heavy-ion radiobiology: Cellular studies, in: J.T. Lett (Ed.), Advances in Radiation Biology, Academic Press, New York, 1984, pp. 295-389.

[11] G.W. Barendsen Response of cultured cells, tumors and normal tissues to radiations of different linear energy transfer, in: M. Ebert and A. Howard (Eds.), Current Topics in Radiation Research, North-Holland Publish Co., Amsterdam, 1968, pp. 293-356.

[12] H. Wulf, W. Kraft-Weyrather, H.G. Miltenburger, E.A. Blakely, C.A. Tobias and G. Kraft Heavy-ion effects on mammalian cells: Inactivation measurements with different cell lines, Radiation Research 8 (1985) S122-134.

[13] M. Scholz and G. Kraft Calculation of Heavy Ion Inactivation Probabilities Based on Track Structure, X Ray Sensitivity and Target Size, Radiation Protection Dosimetry 52 (1994) 29-33.

Modeling of the RBE: Difficulties and Needs for a New Model

Michaël Beuve

Université de Lyon, F-69622, Lyon, France; Université Lyon 1, Villeurbanne; CNRS/IN2P3, UMR5822, IPNL, LIRIS
e-mail address: mbeuve@liris.cnrs.fr

Abstract

The comparisons of LEM predictions with experimental data have pointed out that a good agreement could not be achieved for both low-LET and high-LET at a time. Recent improvements have been proposed leading to LEM II and then LEM III. However we have shown that the observed discrepancies arise from a contradiction between the basic postulates of the LEM and the stochastic nature of ionizing radiations. The development of alternative models, consistent with the physical and chemical properties of ionizing radiations, seems to be therefore necessary to improve the theoretical predictions.

Introduction

Cell survival to ionizing radiations is a relevant biological endpoint to plan radiotherapy and hadrontherapy treatments since it can be linked to the probability of tumor control. Generally, cell survival is estimated by *in-vitro* measurements of cell-survival curves, which draw the survival probability expressed as a function of the dose delivered by the irradiation facility (see Fig. (1)). To be integrated into a treatment planning system, experimental data have to be accurately reproduced by a model, which can predict survival values at any dose. Within conventional radiotherapy, survival is directly linked to the delivered dose. Consequently, an interpolation by a parametric function of the dose, for which the parameters are fitted to the experimental data, is convenient. Accordingly, the Linear–Quadratic Model (LQ) proposes a faithful representation with only two free parameters (α,β):

$$S(D) = e^{-\left(\alpha.D+\beta.D^2\right)} \qquad (1)$$

This model reproduces in particular the shoulder that can experimentally be observed (see Fig. (1)). In the field of radiotherapy with light ions (hadrontherapy), cell survival depends on dose, but also on ion species and ion energy. A Relative Biological Effectiveness (RBE) ratio was defined to qualify the biological effects of any radiation with regard to another radiation, in general to the *X-rays*. RBE of a given radiation is the ratio of the dose required with *X-rays* over the dose required with the given radiation to get the same biological effect.

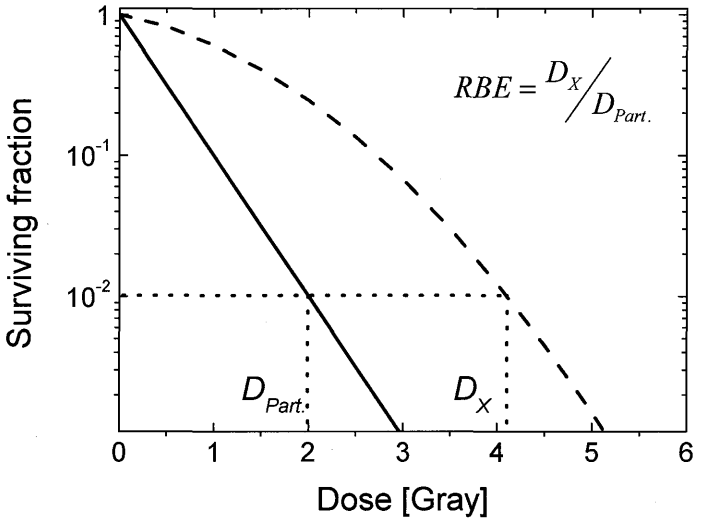

Figure 1: Definition of RBE: dashed line (resp. solid line) represents the fraction of cells that survive an *X-ray* (resp. light ion) irradiation versus the delivered dose. A shoulder shape is visible for the *X-ray* curve.

The complex behavior of ion-induced biological effects is attributed to the high level of heterogeneity (non-uniformity at microscopic scale) of the dose deposited in an ion track. Indeed, the density of ionized and excited molecules generated along the path can be huge. As a consequence ions may induce complex damages such like double strand breaks or clusters of damage sites in DNA. Such lesions are considered to be very difficult to repair for the cell and to be implied in cell death.

Two approaches are presently used for the planning of treatments by hadrontherapy with Carbon: the procedure used in the two Japanese centers for Hadrontherapy [1] and the Local Effect Model (LEM) used in GSI [2]. The LEM model has attracted a particular attention in Europe since it seems to be adapted to active beam system. Despite of an acceptable agreement between the LEM predictions and the experimental data, it has been pointed out that this agreement fails to cover, at a time, low- and high-LET domains. To improve the agreement between theory and experiments, several improvements to the LEM have been proposed leading to the LEM II and the LEM III. However we will show in this paper that the disagreement between experimental data and the LEM predictions are due to important failures in the LEM principles. Alternative models have therefore to be considered in the future.

The LEM is based on a description of track-structure through a radial dose to account for the heterogeneity of the energy deposition by swift ions. Radial dose is defined as the averaged local dose deposited by a single ion in an elementary volume expressed as a function of the distance between this volume and the ion trajectory. Radial dose includes ion-charge and ion-velocity parameters, and finally gave to the track-structure models the ability to predict important radiobiological features for ion irradiations. It is however an averaged quantity that neglects the stochastic nature of ionizing radiations.
After a brief description of the LEM, the paper will present a Monte-Carlo simulation of the dose deposited at a microscopic scale. It will then point out some important stochastic effects, in terms of dose heterogeneity and track overlapping, which are in contradiction with the LEM principles.

The LEM principles

To predict cell survival, the Local Effect Model (LEM) [3-4], considers that cell killing arises from the induction of lethal events by the ionizing radiation. Assuming that the distribution of lethal events obeys a Poisson distribution, the probability for the cell to survive reads:

$$S(D) = e^{-N_{lethal}(D)} \tag{2}$$

where $N_{lethal}(D)$ is the mean number of lethal events induced in the cell after a dose D. The first key assumption of the LEM is to consider lethal events as point-like events generated by the local dose deposited by the radiation. Thus, the number of lethal events in the cell is the summation of the local lethal events over the cell sensitive volume:

$$N_{lethal}(D) = \iiint_{Sensitive\,Volume} \rho_{lethal}(\boldsymbol{r})d\boldsymbol{r} \tag{3}$$

where the local density of lethal events is assumed to be a simple function of the local dose $d(\boldsymbol{r})$:

$$\rho_{lethal}(\mathbf{r}) = \rho_{lethal}(d(\mathbf{r})) \tag{4}$$

In the LEM, the local dose is calculated by cumulative effects, superimposing the local dose deposited by each ion, which is represented by the radial dose d_R:

$$d(\boldsymbol{r}) = \sum_i d_R(r_i) \tag{5}$$

where r_i is the radial distance of the point $\boldsymbol{r}$ to the trajectory of the i^{th} ion in the transversal plane to the beam axis.

The second key assumption of the LEM consists in extracting the relation between the density of lethal events and the local dose from survival measurements performed with *X-ray* radiation. Indeed, the local dose deposited by *X-ray* radiation is considered as uniform within the cell. Neglecting stochastic effects, it is therefore equal to the macroscopic dose D, which is delivered to the sample by the *X-ray* source:

$$d(\boldsymbol{r}) = D \tag{6}$$

Therefore for *X-ray* irradiation, Eq. (3) becomes simply:

$$N_{lethal}(D) \approx \rho_{lethal}(D).V_{sensitive} \tag{7}$$

According to Eq. (2), $N_{lethal}(D)$, and therefore $\rho_{lethal}(D)$, can be deduced from the measurement of cell survival $S_X(D)$ to *X-ray* irradiation (described by the α and β parameters) and from an estimation of the cell sensitive volume $V_{sensitive}$. This latter is assumed to be uniformly distributed over the cell nucleus. The diameter of the sensitive volume depends on the cell and ranges from 5-20 μm. An explicit expression for the average number of lethal events can thus be obtained as:

$$N_{lethal} = \iiint_{Sensitive\,Volume} \frac{-\ln S_X(d(r))}{V_{sensitive}} d\boldsymbol{r} \tag{8}$$

Practically, *an ion-impact configuration is randomly generated* for a dose D_{ion} with the following procedure 1°) the volume of interest containing the cell is defined large enough such like the energy deposited into the cell by any ion that does not impinge this "interest" volume is insignificant; 2°) the number of ion impacts is generated according a Poisson law for which the parameter, i.e. the mean number of impacts, corresponds to the delivered dose D_{ion}; 3°) the impact positions of each ion are generated randomly according to a uniform distribution.

For this configuration, the local dose is calculated by Eq. (5): for any point $\boldsymbol{r}$ of the sensitive volume and for any impinging ion i, it is possible to calculate the radial distance r_i and therefore the radial dose $d_R(r_i)$.

The average number of lethal events is then deduced from Eq. (8), which gives the probability $S(D_{ion})$ for the cell to survive a dose D_{ion} according to Eq. (2). This process has to be reiterated many times to reduce statistical fluctuations on the predicted survival. Following this protocol, the LEM can in principle predict cell survival to

any ion irradiation as soon as the cell sensitive volume and the cell survival to *X-rays* can be experimentally determined. However practically, a set of experimental data performed with ion irradiation is however required to fit a parameter [5] necessary to describe the curve of cell survival to *X-rays* at very high doses (>>10 Grays) since measurements cannot be performed at such doses.

As already mentioned in the introduction, radial dose is an averaged quantity, which therefore does not take fully into account the stochastic nature of ionizing radiations. To evaluate the impact of such an approximation, it seems relevant to simulate with a Monte Carlo simulation the local dose used in the LEM.

Material and methods

The calculation of dose (or energy) depositions into targets by Monte-Carlo simulation has ever been undertaken by various authors for other purposes [6-7] and with various methods. Here, we propose a method that matches with the integration of Eq. (8) into the LEM. Precisely, a water sample was divided into cubes (a cube mesh) whose size corresponds to the spatial extension of the lethal events for the LEM. The literature that describes the LEM does not fix the scale of locality. Instead lethal events are considered as point-like events and by using a radial dose the question can be averted. However to calculate a microscopic dose, i.e. the specific energy within microdosimetry terminology, the target extension has to be set. Lethal-event extension is necessarily larger than the atomic scale. It may be of the order of double-strand-break extension, which is typical less than 20 pairs of bases (~6 nm) [8-9]. One has also to consider that damage may be created by indirect actions. Therefore a damage site can be induced by a water radical produced elsewhere, and the diffusion distance is generally assumed to be of the order of few nanometers [8]. Finally, the mesh cube size was set to 10 nm to evaluate the stochastic effects in the LEM.

Our Monte-Carlo simulation consists in following the incident particles and all the produced electrons in the induced electronic cascades. The electrons are followed until their energy becomes lower than a cut-off energy set to 33 meV (300K). The result of the simulation is a spatial distribution of low-energy electrons, and ionized or excited water molecules. The dose deposited into a cube is calculated by summing the energy of all species in this cube at the end of the simulation. We would like to emphasize that the total stored energy represents about 85% of the energy transferred to the water sample directly by the radiation since a part of the energy is converted into target heating: below the threshold energy for water-molecule excitation and ionization, electrons lose their energy by phonon creation. Moreover, ionized molecules can be neutralized by electron capture and excited molecules can go back to ground state by non radiative processes.

For ions, all details of our simulation can be found in [10-11]. For *X-ray* irradiation, we simulated the irradiation by 1.3 MeV photons, which correspond to a major component of the spectrum that characterizes the *γ-rays* generated by a ^{60}Co source. At this energy, Compton interaction dominates and most of the photon interactions eject Compton electrons. The Compton-electron transport is simulated with the same code used [10-11] for ion irradiation. In both irradiation modalities, we applied to the irradiated sample periodical boundary conditions to avoid edge effects and to ensure equilibrium of charged particles. The sample was chosen either to mimic cell nucleus (10x10x10μm^3) or large enough to reduce statistical errors in histograms (50x50x10μm^3).

Results

Heterogeneities

We simulated the irradiation of a 50x50x10 μm^3 sample at a dose of 1 Gray with ^{60}Co *γ-rays*, H[10MeV] and C[10MeV/n] ions. The mesh cube size was set to 10 nm. The first observation we made is that most of the cubes do not receive any energy transfers, whatever the irradiation. More precisely, the probability for a cube to receive energy is 5.2 10^{-4} for ^{60}Co *γ-rays*, 3.7 10^{-4} for H[10MeV] and 2.0 10^{-4} for C[10MeV/n]. We can therefore conclude that, even for *X-ray* irradiation, the local dose is non-uniformly spread over the sample. Fig. (2) compares

histograms, which represent the probability for a cube to receive a given local dose, calculated for the three different projectiles. We observed that the distribution of local dose is broad. It varies from 10 Gray to a few 10^5 Grays, whatever the projectile. Below 10^4 Grays, the histograms are similar and reveals the strong heterogeneity, which is a common feature of all 3 radiations.

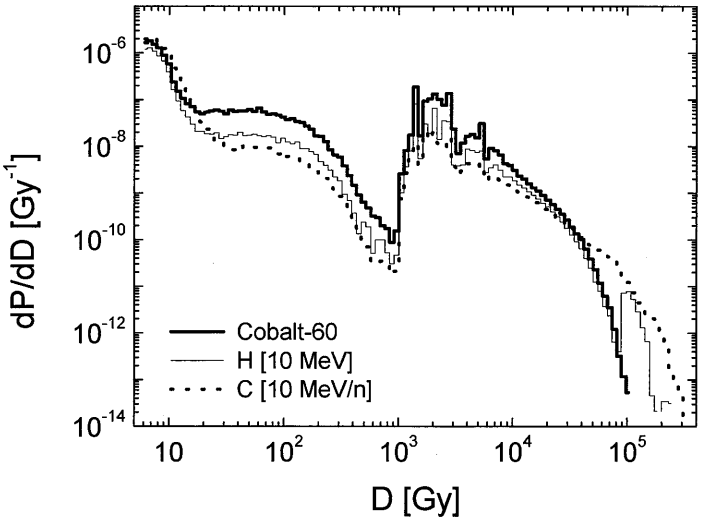

Figure 2: Histogram of local dose calculated for a water sample of 50x50x10 μm^3 irradiated at a dose of 1 Gray with a beam of ^{60}Co *γ-rays*, H[10MeV] and C[10MeV/n]. The mesh resolution is 10 nm.

From this analysis, we can conclude that local dose cannot be considered as uniform neither for ion irradiation nor for *X-ray* irradiation. Heterogeneities arise from the energy spectrum of elementary events and from the combination of events. Eq. (8), which links the averaged number of lethal events to the local dose in the LEM, is therefore questionable. Indeed, this latter expression is based on the assumption that fluctuations of local doses within a cell nucleus can be neglected for *X-ray* irradiation, while we have shown that they are actually huge. It is also important to emphasize that these heterogeneities, which are neglected for *X-rays*, are considered to be at the origin of the radiobiological efficiency of ions.

The contradiction between this LEM assumption and the stochastic nature of radiations could have been expected. Indeed the expression which links the density of lethal events to the cell survival to *X-rays* mixes two levels of scale:

$$\rho_{lethal}(d) = \frac{-\ln S_X(d)}{V_{sensitive}} \qquad (9)$$

The left-hand-side part of Eq. (9) refers to nanoscopic scale. The local lethal events correspond to the formation of complex damage such as DNA double strand breaks. At this scale, the local dose is deposited in less than 1ps. Instead the right-hand-side term refers to macroscopic scale. The dose is an average dose delivered within minutes. Moreover cell survival is an endpoint which cannot be considered with a scale downer than cell volume. More striking, local dose can easily overcome several millions of Grays in the track core of a high-LET ion. Therefore, to deduce the density of lethal events in this track core, one should in principle measure cell survival to a delivered X-ray dose larger than several millions of Grays!!! At such doses, the major death pathway is not the formation of local lethal event but instead cell vaporization.

Track overlapping

Track overlapping plays a significant role in the LEM predictions. In the LEM, track overlapping induces cell-killing with a higher efficiency than independent tracks would do. Indeed, due to the shoulder in the curves of

cell survival to *X-rays*, the local density of lethal events increases non-linearly with the local dose. As a consequence, the lethal effect induced by the superimposition of the local dose generated by two independent ion tracks is larger than the addition of their individual effects

$$\rho_{lethal}(d_1 + d_2) \geq \rho_{lethal}(d_1) + \rho_{lethal}(d_2) \qquad (10)$$

The left-hand-side part of this equation appears as high-order terms in delivered dose in Eq. (3) and, through Eq. (2), it is responsible for the apparition of shoulders in the LEM.

Generally speaking, the lower the LET is, the more significant the overlapping is. Indeed, for a fixed dose, the number of impacts increases as the LET decreases. Moreover, for an irradiation with ions of a given LET, decreasing ion velocity decreases the spatial extension of the tracks and therefore decreases the probability for overlapping.

From these considerations, one could understand why a shoulder can be observed for low-LET ions and why it disappears for ions at Bragg peak (low velocity and high LET).

To evaluate how stochastic effects might modify this overlapping scheme, we have simulated the local-dose deposition for *X-ray* irradiations with 1 Gray and 5 Grays (see Fig. (3)). At such doses and for *X-ray* irradiation, an effect of overlapping is expected to be significant since shoulders appear within this range of doses. Instead, we observe that both histograms are identical except for the factor of 5 in histogram amplitude, which corresponds to the dose ratio. In other words, at local scale, two incident particles cannot significantly contribute to the same local site. In fact, increasing the dose simply increases the number of hit cubes. We would like to stress that performing the same calculations with low-LET ions would give the same results.

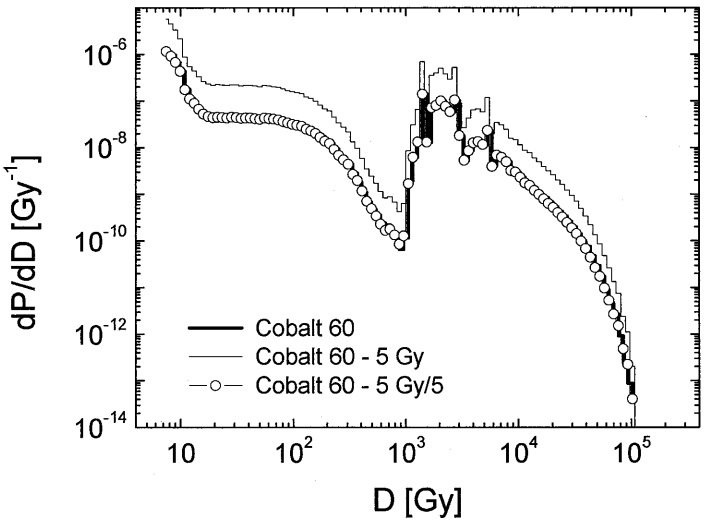

Figure 3: Histogram of local dose calculated for a sample of 10x10x10 μm^3 irradiated with a dose of 1 Gray and 5 Grays of ^{60}Co *γ-rays*. The mesh resolution is 10 nm. The curve labeled with "Cobalt 60-5Gy/5" represents the histogram calculated for 5 Grays and divided by a factor 5.

These observations can be mathematically written as

$$h_D(d_k) = h_1(d_k).D \quad \forall d_k \neq 0 \qquad (11)$$

where h_D (resp. h_1) is the histogram of local dose d_k for an irradiation dose of D (resp. 1 Gray). Such a relation can be conveniently inserted into Eq. (3) of the LEM after rewriting the latter:

$$N_{lethal} = \int_{d'} dd' \, \rho_{lethal}(d') \iiint_{SensitiveVolume} d\mathbf{r}\,\delta(d' - d(\mathbf{r})) \qquad (12)$$

The integration over the sensitive volume represents the volume associated to a local dose d':

$$\frac{d\mathbf{r}}{dd'} = \iiint_{Sensitive\,Volume} d\mathbf{r}\,\delta(d'-d(\mathbf{r})) \tag{13}$$

It is simply related to the histogram of local doses by normalization to the sensitive volume $V_{Sensitive}$:

$$h(d') = \frac{d\mathbf{r}}{dd'} \Big/ V_{Sensitive} \tag{14}$$

One gets then:

$$N_{lethal} = V_{Sensitive} \int_{d'} dd'\, \rho_{lethal}(d') h(d') \tag{15}$$

It is therefore possible to introduce Eq. (11) for a delivered dose D:

$$N_{lethal}(D) = V_{Sensitive} \cdot \int_{d'} dd'\, \rho_{lethal}(d') D.h_1(d') \tag{16}$$

Defining then a constant α by:

$$\alpha = N_{lethal}(D = 1\,Gy) \tag{17}$$

we can deduce from Eq. (2) that cell surviving fraction at a dose D obeys to:

$$S(D) = e^{-\alpha D} \tag{18}$$

This clearly shows that a pure local effect theory cannot predict shoulder in cell survival. This conclusion is robust: we have verified that Eq. (11), which is necessarily valid for cube length smaller than 10 nm, is still valid for cube length as large as 100 nm. All these conclusions raise questions on the physical meaning of the shoulders predicted by the LEM. The apparition of a shoulder in the LEM comes from the introduction of an averaged quantity, namely the radial dose, to represent the track structure. Indeed, as it is illustrated by Fig. (4), at the scale of local events, overlapping of tracks is actually very scarce for doses lower than 10 Grays. Superimposing radial dose comes down to superimpose events that occurred apart. Finally by superimposing averaged quantities, the LEM introduces *artificial non-local effects* and therefore artificial shoulders.

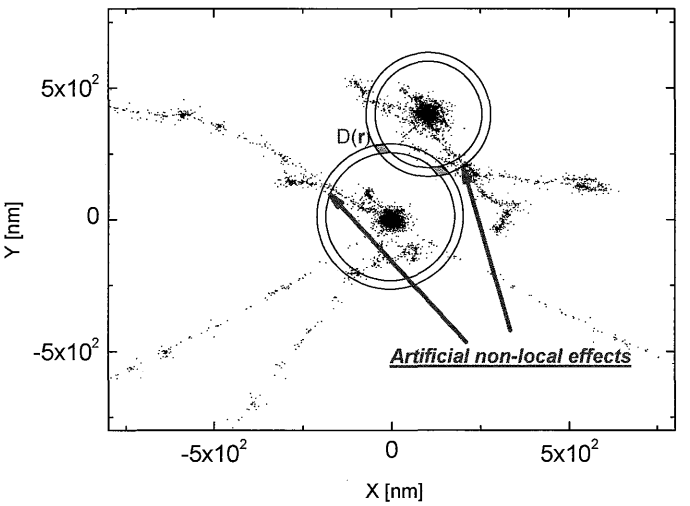

Figure 4: Overlapping of two ion tracks. The two couples of circles illustrate the calculation of local dose by superimposition of the radial dose. The two sets of points correspond to the projection of two track segments simulated by Monte-Carlo simulation.
The two arrows point to two clusters of events that are considered to superimpose in the framework of the LEM although they are clearly apart.

Conclusions

To get a better agreement with experimental data, the authors of the LEM have recently proposed some improvements to the LEM. However we have shown that the observed discrepancies arise from a contradiction between the basic postulates of the LEM and the stochastic nature of ionizing radiations. The relation between the density of local lethal events and the cell survival to *X-rays* is based on the incorrect assumption that the local dose is uniform for *X-rays*. Moreover the shoulder predicted by the LEM for low-LET ions is due to an artificial introduction of non local effects. The development of alternative models, consistent with the physical and chemical properties of ionizing radiations, seems to be necessary to improve the theoretical predictions.

Acknowledgements

This work has been supported by the INCa institute (Institut National Du Cancer) and CPER Hadronthérapie Rhône-Alpes.

References

[1] Kanai T, Furusawa Y, Fukutsu K, Itsukaichi H, Kasai K E & Ohara H Irradiation of mixed beam and design of spread-out Bragg peak for heavy-ion radiotherapy 1997 *Radiation-Research* 147(1), 78–85.]

[2] M. Krämer and M. Scholz, Treatment planning for heavy-ion radiotherapy: Calculation and optimization of biologically effective dose. *Physics in Medicine and Biology* 45, 3319-3330 (2000).

[3] M. Scholz and G. Kraft. Track structure and the calculation of biological effects of heavy charged particles. *Adv. Space. Res.*, 18(1/2):5–14, 1996.

[4] M. Scholz, A.M. Kellerer, W. Kraft-Weyrather, and G. Kraft. Computation of cell survival in heavy ion beams for therapy the model and its approximation. *Radiat. Environ. Biophys.*, 36:59–66, 1997.

[5] M. Beuve, G. Alphonse, M. Maalouf, A. Colliaux, P. Battiston-Montagne, P. Jalade, E. Balanzat, A. Demeyer, M. Bajard, and C. Rodriguez-Lafrasse. Radiobiologic parameters and local effect model predictions for head-and-neck squamous cell carcinomas exposed to high linear energy transfer ions. *Int. J. Rad. Onc. Bio. Phys.*, 71(2):635–42, Jun 2008.

[6] Nikjoo H, O'Neill P, Goodhead DT, Terrissol M. Computational modelling of low-energy electron-induced DNA damage by early physical and chemical events. *Int. J. Radiat. Biol.*, 71(5):467-83, May 1997.

[7] Champion C.; L'Hoir A.; Politis M.F.; Chetioui A.; Fayard B.; Touati A. Monte-Carlo simulation of ion track structure in water: ionization clusters and biological effectiveness, *Nucl. Instr. and Meth. in Phys. Res. Section B*, 146(1), 533-540(8), Dec. 1998.

[8] T. Elsasser and M. Scholz. Cluster effects within the loc al effect model. *Radiat. Res.*, 167(3):319–29, March 2007.

[9] M. Scholz and G. Kraft. The physical and radiobiological basis of the local effect model: a response to the commentary by r. katz. *Radiat. Res.*, 161:612 – 620, 2004.

[10] B. Gervais, M. Beuve, G. H. Olivera, and M. E. Galassi. Numerical simulation of multiple ionization and high LET effects in liquid water radiolysis. *Radiat. Phys. Chem.*, 75:493–513, April 2006.

[11] B. Gervais, M. Beuve, G. H. Olivera, M. E. Galassi, and R. D. Rivarola. Production of HO2 and O2 by multiple ionization in water radiolysis by swift carbon ions. *Chem. Phys. Lett.*, 410:330–334, July 2005.

The Current Status of the Treatment Delivery at HIMAC

Masami Torikoshi, Shinichi Minohara, Nobuyuki Kanematsu, Yumiko Ohno, Tadafusa Kumagae, Koji Noda, Takeshi Murakami, Mitsutaka Kanazawa, Eiichi Takada, Masahiro Endo, and Tatsuaki Kanai

Department of Accelerator and Medical Physics, National Institute of Radiological Sciences, Chiba, Japan
e-mail address: torikosi@nirs.go.jp

Abstract

A facility for radiation therapy with heavy ion beams, HIMAC, was completed in 1993 at the National Institute of Radiological Sciences in Chiba, Japan. Since starting clinical trials in 1994, about 15 years have passed. Approximately 10,000 sessions per year have been carried out by broad beam method, the favorite method of particle radiotherapy. During this period, we have seen many improvements and developments in the beam delivery system as well as the accelerator system, such as a method for respiratory-gated irradiation for correctly exposing organs moving with breathing to beams, a method for irradiating repeatedly a target with a thin layer field to improve the dose distribution, introduction of a multilayer ion-chamber into dosimetry to provide highly accurate dose measurement, applying a multi-leaf collimator with thin leaves, and so forth. A database system has been established to record and manage information concerning any trouble occurring in any of the systems of HIMAC. This database system is expected to prove useful not only for trouble-shooting but also for grasping and demonstrating the present status of the system.

1. Introduction

Heavy Ion Medical Accelerator in Chiba (HIMAC) is a complex of accelerator systems and treatment delivery systems; the accelerator systems consist of three ion sources, a cascade of two linear accelerators, two identical synchrotron accelerators and beam transport lines, and three treatment rooms with four beam ports (Room A: a vertical port, Room B: a vertical port and a horizontal port, and Room C: a horizontal port) [1]. It was completed in 1993, and clinical trials started a half year later, in 1994. Since beginning the clinical trials, HIMAC has experienced improvements and developments and introduction of higher-level functions based on high-level technologies.

Methods of treatment delivery have been developed and improved continuously since HIMAC completion. A respiration-gated irradiation method was started in 1996 for treating organs moving with breathing. This was realized based on a method for beam extraction/abortion in a short response time, which was developed with synchrotron accelerations [2, 3]. A system for the layer-stacking irradiation method was installed in 2000, and practical applications of this method started in 2003. It can be considered that this method is equivalent to a beam scanning method with a broad beam instead of a spot beam [4, 5]. Eye cancer treatment was begun with carbon beams in 2001 [6]; until then, eye cancers were treated with proton beams using a cyclotron accelerator of NIRS. The proton therapy for eye cancer was terminated at NIRS in 2004.

Devices, apparatuses and systems have also been developed and improved in order to obtain higher reliability and safety. A simulation room for patient pre-positioning was built in 1999 near the treatment rooms to check the geometrical relation of a patient with respect to the devices surrounding the couch. In the same year, a

multi-portal irradiation system was installed in Room C, which was equipped with a chair and a CT scanner, and the chair was equipped with an immobilization device. The CT scanner is set at the ceiling of the treatment room, and it vertically slides down when scanning a patient. Twelve patients were treated by the multi-portal method. However, no patient has been treated since then because no great advantage was found with this method, and patient positioning also takes a long time. Many developments in regard to dosimetry also took place. A multilayer ionization chamber was introduced into daily dosimetry in 2001 [7], greatly shortening the time of the daily dosimetry. Previously, daily dosimetry was carried out with a combination of a Farmer-type ionization chamber and a binary filter.

The number of patients receiving treatment has increased year by year. Range compensators designed for an individual treatment plan are indispensable. In some cases, more than six compensators are necessary for a single patient. Producing numbers of compensators is time-consuming and costly, and it represents a hurdle to shortening the interval between treatment planning and irradiation. A new method for manufacturing the compensator was developed. It is assembled by stacking thin plastic plates from which a shape is punched away, rather than drilling a polyethylene block using a numerically controlled machine. This process takes less than half an hour, while the conventional way took as long as eight hours in the case of the largest compensator. A multi-leaf collimator (MLC) is also an indispensable device for the broad beam method. The present MLC has leaves of 6.35 mm thickness and an aperture of 220 mm × 150 mm, which is narrower than the required area of 220 mm in diameter. An MLC with leaves of 2.35 mm thickness and an aperture of 220 mm in diameter was completed during R&D in 2006 and tested with carbon beams in 2007. The space between adjacent leaves is 0.15 mm. This thin-leaf MLC is able to make a fine shape in the aperture. Since, in the case of head and neck cancers, an aperture with fine shape is required in the collimator, patient collimators are manufactured and used for each individual treatment. The thin-leaf collimator is expected to be applicable for most cases, meaning that the patient collimators will become mostly unnecessary. This could lead not only to cost reduction but also shortened intervals between treatment planning and beginning of treatment. This technology has been used at the Gunma University Heavy Ion Medical Center, Maebashi, Japan, where the leaf thickness of the MLCs is a designed 3.35 mm.

Control systems are one of the targets to be improved. In particular, the software of control systems had latent problems, so-called "bugs", since the beginning of the operation. Usually, continuous effort and patient cooperation to eradicate these bugs in the software are required. The main workstation computers for the control systems were replaced in 2000, and the software was largely revised. However, along with the improvements, a lot of new bugs were also introduced with the software. A succession of minor revisions and a large-scale improvement of the software done in 2006 have successfully "exterminated" a considerable number of bugs. However, still now, diverse problems, caused by the software, although less frequent, are experienced in the control systems. At present, each treatment is allocated a beam port in the daily schedule. A new function introduced into the software is able to easily change the allocation of the beam port without measurement of the monitor unit (MU) of the individual patient when the scheduled beam port develops trouble due to various faults. This function is useful to adjust the load of each treatment room, that is, the number of sessions to be done can be averaged over the rooms. It should be noted that this function was realized based on the compatibility of all treatment rooms. The interface between computers and devices is always facing rapid changes in technology. We adopted a programmable logic controller (PLC), used as orthodox technology for industrial processes, as the interface device. It has been working stably without evident faults. However, it becomes a kind of a bottleneck when the computer in use has a faster processing speed, as the orthodox-type PLC does not accept very fast transmission. In other words, the interface system composed of PLC works stably and reliably as long as the processing speed is not as high as that of the latest computer. Since the irradiation system needs to control devices in the time scale of motion of the device that is in the order of ms or a few tens of ms, an interface system with a high speed processing ability is not necessary.

Highly precise irradiation in radiotherapy requires a highly advanced beam delivery system and technique of beam handling. A few examples are introduced as follows. The very fast beam abortion system that is called the RF knock-out method [3] was developed in 1996 to realize the respiratory-gated irradiation method. Another case is an AC power supplier that provides the bending magnets of the synchrotron accelerator with an electric current. The power supplier controls the amplitude of the current precisely to harmonize it with the acceleration patter by reducing the ripple of current to less than a few ppm, with the result that the amplitude of the intensity fluctuation of the extracted beam was reduced by an order of one or more. A dynamic correction quadrupole magnet installed in the synchrotron ring stabilized the beam orbit so that the beam extracted out of the synchrotron ring became stable [8]. Additionally, an automatic beam-tuning system was introduced in a high-energy beam transport control system [9].

Daily maintenance and activities of quality assurance are important to keep treatments safe and reliable. The immediate status of the system should be monitored to know the real-time condition. The easiest way to monitor the status is to see how frequently trouble occurs in the system. A database system has been brought into operation to manage the information on trouble occurring in HIMAC. This helps us recognize the present status qualitatively. In this article, we shortly report on the present status, how the treatment is carried out, and some topics regarding improvements and developments.

2. The present status of the treatment delivery system

2-1 Flow of treatment

Firstly, an immobilization device is formed for each patient in HIMAC, and then the patient is CT-scanned to obtain images to be used for treatment planning. It takes one or two days in most cases to design the treatment planning. As part of that, digital radiograph images (DRRs) are reconstructed for positioning the patient. The planning should be evaluated and approved at a meeting of the operators and specialists involved. Once it is approved, range compensators and collimators are manufactured. The patient, except one with prostate cancer, undergoes a treatment rehearsal the day before the first treatment. In the rehearsal, radiologists check the actual positioning in a room simulating a real treatment room, and X-ray images are taken that are used as reference images to be compared with X-ray images taken when actually positioning. In the case of prostate cancer, DRRs are used for positioning.

2-2 Dosimetry

In daily treatment, carbon beams with energy of 170, 290 and 400 MeV/u are used at the horizontal beam ports and 140, 290 and 350 MeV/u at the vertical beam ports. Both of the lowest energy beams are used only for eye treatments. Treatments using the same beam energy are collected together and carried out in sequence without changing the beam energy. When using a beam of a certain energy, dose monitors, two ion chambers, are calibrated by the multilayer ion chamber (MLIC) before treatment start as one of the quality assurance (QA) programs. We call this "*standard dosimetry*". For an individual treatment the calibration is also done at the field parameters specified in the treatment planning for the treatment, and this is called "*patient dosimetry*". The patient dosimetry is carried out only once before beginning the treatment. The MLIC is calibrated with a Markus chamber once a year in accordance with IAEA TRS-398 [10, 11]. The MLIC measures the depth-dose distribution (DDD) of the irradiation field, and DDD measurement provides information about the beam range as well as information on the calibration. Since the beam range depends on the beam energy, ion species, and whether an obstacle is in the beam path or not, the overall QA of the beam can be done simultaneously. The calibrated value of the standard dosimetry should be stable unless the irradiation system and/or accelerator system are in incorrect conditions. The changes in calibration values shown in Fig. 1 suggest that all the systems are performing in a stable manner.

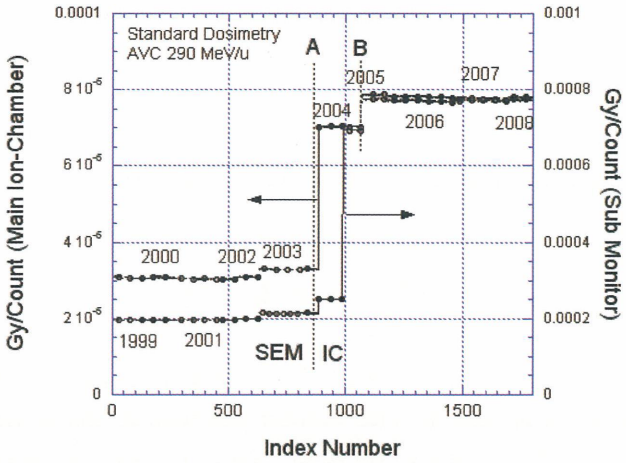

Fig.1 Calibration factors determined by standard dosimetry are plotted with respect to time (days). The factors indicate the long-term stability of the dose monitoring system. Changes in conditions of the standard dosimetry caused small jumps in the plots; the jumps at the beginning of 2004 were due to replacement of the ion-chamber and the secondary electro monitor with larger ion-chambers. A large jump occurring in the sub-monitor at the end of 2004 was caused by new calibration of the electronics (a current-frequency converter). The last jumps of 2005 were due to the change of a reference point to be calibrated: an entrance point was changed to a center of SOBP. The dose monitoring system has been working with the stability of less than 1% between jumps.

2-3 Irradiation for treatment

Treatments are carried out following a certain schedule. One treatment takes about 20 minutes, including positioning and irradiation. The patient is positioned manually so as to keep the patient safe even when with considerable couch moving. In the case of respiratory-gated irradiation, LED is put on the abdomen or back of the patient. The waveform of respiration, which is generated by motion of the LED, is superimposed on a TV display of X-rays. Radiologists can then know the right timing for taking an x-ray image, which needs to coincide with the timing of expiration. The waveform of respiration is shown in Fig.2. Irradiation for treatment of a static case takes less than a minute, and respiratory-gated irradiation is longer by only a factor of 1.5. The dose rate is more than 5 Gy/m in a clinical dose unit, and for eye treatment it is more than 14 Gy/m. Exposure takes place during a beam spill lasting about 1.5 s.

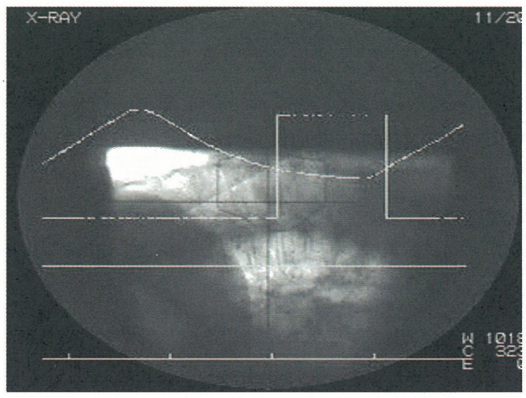

Fig.2 A waveform generated by motion of the body surface superimposed on the digitized fluoroscopic image is shown. The peak of the waveform corresponds to the timing of an inspiratory phase and the valley corresponds to an expiratory phase. As beam extraction is allowed in the expiratory phase, the logical signal reaches a high level during the period. The logical signal is used as a gate signal to control the RF-knockout system. Eventually the beam can be extracted from the synchrotron only during the period defined as the expiratory timing

The number of treatments is increasing year by year. The maximum number of sessions per day has reached 70, with the first treatment starting at 9:30 in the morning and the last ending around 18:00 on average. The patient dosimetry is performed after the last treatment. HIMAC provides beams for treatments four days a week, about 45 weeks a year. The unused weeks are dedicated to maintenance of HIMAC, which is done in August and March. Daily QA and device checks are being done daily before starting treatment.

3. Development of new irradiation methods and devices

3-1 Clinical use of layer-stacking irradiation method

By the broad beam method, the constant SOBP over the field results in an undesirable dose to normal tissue proximal to the target [12]. In cases of head & neck cancers and bone & soft tissue cancers such as those surrounded by critical organs or seated shallowly with a large volume, 100% of the prescribed dose is sometimes delivered to critical organs and/or a skin area by the conventional broad beam method. An improved method for avoiding irradiation of unwanted dose to normal tissue was proposed in 1983 [13], and a study was performed in 1996 - 1998 to examine its application feasibility at HIMAC [14]. In this method, a mini SOBP peak is produced using a short RGF. The full widths at 60% dose level of the peak dose are about 11.9, 12.8 and 15.9 mm for 290, 350 and 400 MeV/n, respectively. In irradiation, the mini peak is longitudinally swept in steps of 2.5 mm with changing thickness of RSF from the distal end of the target volume to the shallowest end, or in the opposite direction [15]. The compensator and MLC are also used as in the ordinary broad beam method, while the shape of the MLC varies as the mini peak moves from one slice to the next.

Through the process of layer-stacking, all device parameters for forming the field except for the thickness of a scatterer are changed at each step of the process. The MLC forms a lateral beam shape to agree with the cross-sectional shape of a certain slice of the target. Once the prescribed dose is delivered on the slice, a preset counter for the main ionization chamber interlocks the beam and gives a trigger signal to move the RSF and MLC and go to the next slice. The beam-on/off control is the same as that for the respiratory-gated irradiation. The interval from one slice to the next is about 100 ms or less. Each leaf of the MLC moves at a maximum speed of about 80 mm/s. All parameters (wobbling currents, scatterer index, WEL of RSF, leaf positions of MLC, irradiated dose and so forth) are recorded for every slice.

This method is applicable to organs moving due to breathing, by borrowing the technique of respiratory-gate irradiation. Simulation results showed that the field uniformity depended on the mini peak width and the target motion during the on-gate period [16]. When the target moves only within 2 mm during the irradiation, 100% dose of the prescribed dose is delivered to 95% of the target volume according to DVH. As the mini peak width becomes narrower for greater reduction of hot spots, the field uniformity deteriorates more. Besides, as the motion of the target becomes larger, the mini peak width should be larger to keep the field uniformity at a certain level. It is important, therefore, to optimize the overall dose distribution in accordance with the motion of the target.

3-2 Development of MLC with thin leaves

An MLC is an indispensable device for carrying out treatments effectively by the broad beam method. In brief, the MLC is a beam collimator with a flexible aperture that is controlled by a computer. The aperture with a wave-like shape is shown in Fig. 3 as an example. The MLC used at HIMAC has a maximum aperture of 220 mm × 150 mm and 23 pairs of leaves of 6.35 mm thickness. The leaves are not thin enough to create a cross-sectional shape of the field and satisfy the treatment requirements of such as head and neck cancers, which are surrounded by critical organs. In such a case, individual collimators are prepared with finer shape in the apertures to avoid critical organs from being exposed to unwanted beams. An MLC with thinner leaves has been developed that can replace the present MLC; the thickness of the leaf is 2.35 mm, the gap between adjacent leaves is 0.15 mm, and the maximum aperture is 220 mm in diameter, the maximum size of the available field.

The ability to block the beam is about 1% at the entrance region for a 400 MeV/u carbon beam, a value about twice that of the present MLC, as the total area contributed by the gaps between leaves is about 2.25 times larger than that of the present MLC.

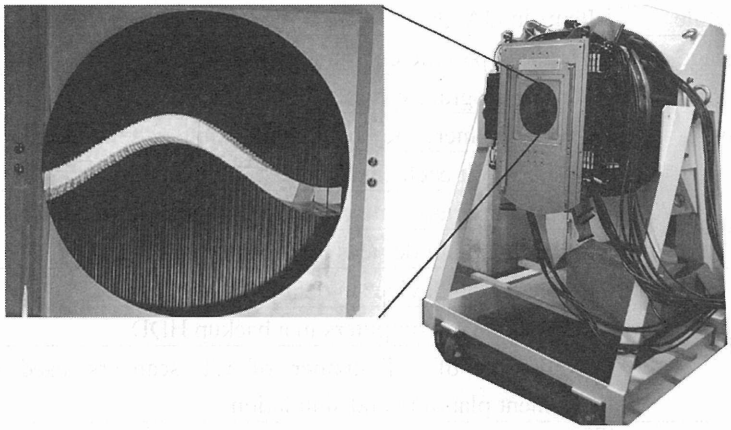

Fig.3 A multi-leaf collimator (MLC) on a test-stand and its aperture are shown. It was completed in 2006. The leaves are 2.35 mm thick and the gap between adjacent leaves is 0.15 mm. The maximum aperture is 220 mm in diameter. Each leaf moves at a speed of 13 mm/s at maximum. The diameter of the outer body is about 1 m. It was designed to replace the present MLC.

3-3 Development of laminated range compensator

Range compensators are also essential in the broad beam method. Usually, a few compensators are prepared for individual patients: the number of range compensators corresponds to the portal number. At present, polyethylene blocks are machined by a numerically controlled device to manufacture the range compensators, a time-consuming process that can take as long as eight hours. Then, cleaning and inspection takes about one hour. A new method for manufacturing range compensators, employing a punch technology, has been development. The compensator is assembled by lamination. Each plate is 3 mm thick, the distal end shape is punched out from the plate, and then the shape is inspected automatically. The plates are stacked up at the end stage of the process. The laminated block is manually tightened with bolts. This simple process has greatly shortened the manufacturing time, as punching and stacking takes half an hour or less. It is expected to enable us to optimize treatment planning again just before treatment. Considering the combination of the thin leaf MLC and the laminated range compensators, the interval between treatment planning and the beginning of treatment will be much shorter.

3-4 QA activity and the present status of the irradiation system

As is well known, QA is one of the most important activities for maintaining safety and reliability in radiotherapy. The items to be looked after in a QA program (Table 1) should follow this schedule: daily, weekly, every half-year, annually, and every few years. In spite of that, however, subtle faults, errors such as in software, and human errors are still inevitable. Recently, a database was introduced for managing the information on trouble occurring in all systems of HIMAC and its measures. The information has been qualitatively recorded since 1999, while prior to that only partial information was recorded. Change in the number of events including serious ones that caused the irradiation system to develop trouble, subtle faults/errors, and human errors in operation is shown in Fig.4a, in comparison with the change in the number of patients. In Fig.4b, normalized numbers of events classified into a few causes are shown. In particular, the number of events occurring due to hardware, such as devices, electronics, cables, screws and so forth, has increased since 2002. It seems most likely that the irradiation system itself is in a status of aging.

Table 1 Main items in QA/QC in the irradiation system of HIMAC

Schedule	Items in QA/QC
At usage	Checking parameters for setting devices
Daily	X-ray radiography system
	Checking emergency buttons including patient call
	Dosimetry at each energy level
Weekly	Saving important data of server system in a backup HDD
	Inspecting main devices by eye
Half-year	Inspecting all devices in detail
	Saving data of computers in a backup HDD
	Calibration of CT-number of CT scanners used in treatment planning and simulation
Annually	Alignment of devices on a beamline
	Calibration of a reference monitor and MLICs
A few years	Calibration of electronics such as thermometer, etc.

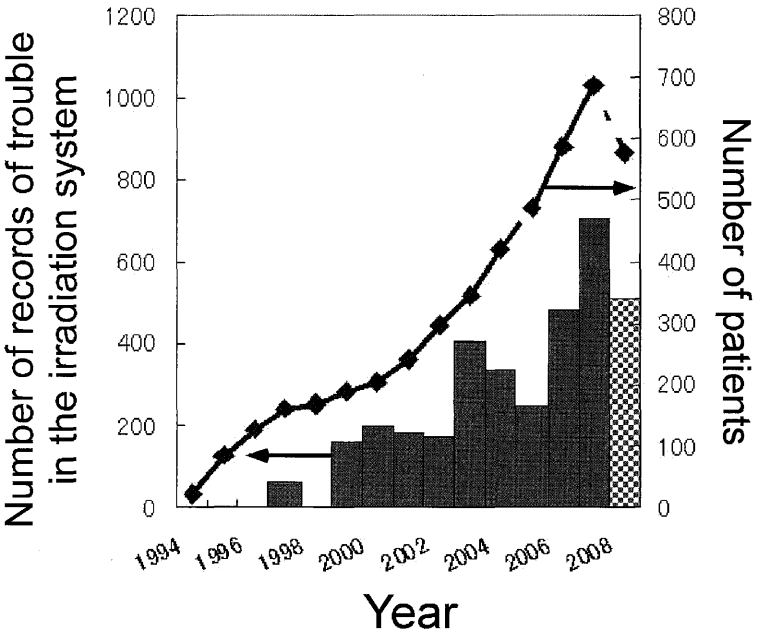

Fig.4a The number of recorded items regarding trouble occurring in the irradiation system is compared with the number of patients. Overall, the former increased as the latter increased.

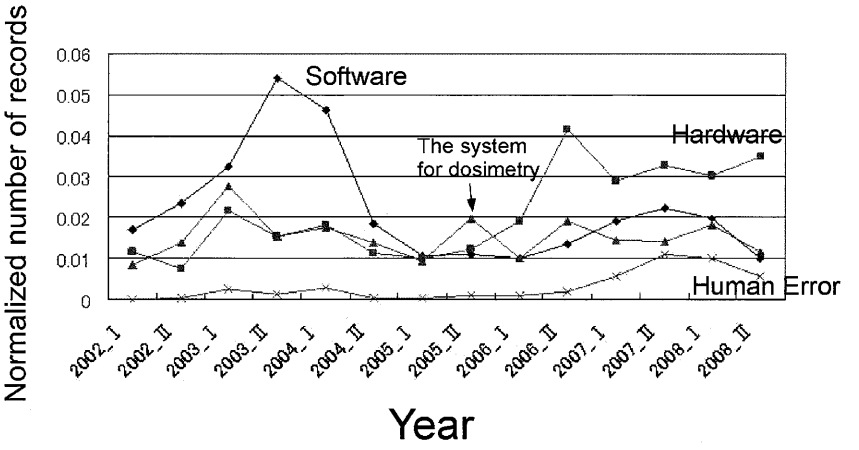

Fig.4b The causes of trouble are classified into software, hardware, the system for dosimetry and human error. Each number is divided by the number of treatments, which is called the normalized number, meaning the incidence of a fault due to a specific cause. It is notable that the incidence of faults caused by hardware increased year by year, the incidences of events caused by software and the dosimetry system are constant overall, while there is a large hump in software around 2004, thought to be caused by "bugs" introduced by a large software revision in 2003. A small hump also appears in the incidence of human error in 2008, probably because a few new operators were introduced into the system.

Some events cause serious trouble or failure to the system. Serious failure is defined as follows: interruption of the treatment or requiring more than an hour to restore. The number of serious events occurring since April 2007 stands at 30. During this period, the number of sessions done in the three treatment rooms was about 16,000, so this means an incidence of less than 0.2%, occurring every 11 days on average. In other words, the number of events occurring in the period was 1218, and about 2% of these could be could be categorized as serious failure.

4. Summary

It can be concluded that, overall, the carbon radiotherapy at HIMAC has been proceeding well since the beginning of the first clinical trial. On the one hand, HIMAC itself and the method of irradiation have undergone many developments and improvements, and in this sense HIMAC is continuously evolving. On the other hand, almost fifteen years have passed, and it is considered that the systems have begun showing indications of aging; steady practice of the QA/QC program has been maintaining the safety and reliability of the treatments and the daily performance of the systems. Based on these efforts, 70 treatments per day can be carried out without serious failure. From the point of view of technology, the broad beam method is now one of the most matured and reliable methods in particle radiotherapy, its systems and control are to some extent simple, and the dosimetry is reliable because its technology can be borrowed from conventional radiotherapy. This situation is somewhere different from the scanning method, and it is easily applicable to respiratory-gated irradiation. Needless to say, the total reliability of particle radiotherapy is based on the stable and reliable operation of the accelerators.

Acknowledgement

We would like to express out greatest thanks to the members of Accelerator Engineering Co. for their faithful and devoted efforts.

References

[1] Yamada, S., Takada, E., Kohno, T., and Noda, K. (1995) Construction, Commissioning and Pre-clinical Studies of Heavy Ion Medical Accelerator in Chiba (HIMAC). In: HIMAC report. NIRS Publication NIRS-M-109:HIMAC-009.

[2] Minohara, S., Kanai, T., Endo, M., Noda, K., and Kanazawa, M. (2000) Respiratory gated irradiation system for heavy-ion radiotherapy. Int. J. Radiat. Oncol. Biol. Phys. 47:1097-1103.

[3] Noda, K., Kanazawa, M., Itano, A., Takada, E., Torikoshi, M., Araki, N., Yoshizawa, J., Sato, K., Yamada, S., Ogawa, H., Itoh, H., Noda, A., Tomizawa, M., and Yoshizawa, M. (1996) Slow beam extraction by a transverse RF field with AM and FM. Nucl. Instrum. Meth. A 374: 269-277.

[4] Kanematsu, N., Endo, M., Futami, Y., Kanai, T., Asakura, H., Oka, H., and Yusa, K. (2002) Treatment planning for the layer-stacking irradiation system for three-dimensional conformal heavy-ion radiotherapy. Med. Phys. 29: 2823-2829.

[5] Kanai, T, Kawachi, K, Matsuzawa, H., and Inada, T. (1983) Broad beam three-dimensional irradiation for proton radiotherapy. Med. Phys. 10: 344-346.

[6] Tsuji, H., Ishikawa, H., Yanagi, T., Hirasawa, N., Kamada, T., Mizoe, J., Kanai, T., Tsujii, H., and Ohnishi, Y. (2007) Carbon-ion radiotherapy for locally advanced or unfavorably located choroidal melanoma: a phase I/II dose escalation study. Int. J. Radiat. Oncol. Biol. Phys. 67: 857-862

[7] Shimbo, M., Urakabe, E., Futami, Y., Yusa, K., Yamashita,, H., Matsufuji, N., Akagi, T., Higashi, A., and Kanai, T.(2000) Development of a multi-layer ion chamber for measurement of depth dose distributions of heavy-ion therapeutic beam for individual patients. Nippon Acta Radiologica 60:274-279 (in Japanese)

[8] Furukawa, T., Torikoshia, M., Noda, K., Sato, S., Katsumata, M., Shiraishi, T., Shimojyu, T., Kanaia, T., Takada, E. and Yamada, S. (2006) Development toward turn-key beam delivery for therapeutic operation at HIAMC. Proceedings of EPAC 2006, Edinburgh, Scotland 2325-2328

[9] Torikoshi, M., Noda, K., Takada, E., Tsubuku, H., Kai, S. and Katsumata, T. (1999) Development of automatic tuning for high energy beamline at HIMAC. Proceedings of the 1999 PAC1999, U.S.A., New York 1309-1312.

[10] Kanai, T. (2000) Heavy-ion radiotherapy In: Proc. of Atomic and Molecular Data and Their Applications. Eds. Berrington, K. A. and Bell, K. L. pp.25-35.

[11] IAEA, Absorbed dose determination in external beam radiotherapy (2000) In: Technical Report Series 398, IAEA, Vienna.

[12] Kanematsu, N., Endo, M., Futami, Y., Kanai, T., Asakura, H., Oka, H., and Yusa, K. (2002) Treatment planning for the layer-stacking irradiation system for three-dimensional conformal heavy-ion radiotherapy. Med. Phys. 29: 2823-2829.

[13] Kanai, T, Kawachi, K, Matsuzawa, H., and Inada, T. (1983) Broad beam three-dimensional irradiation for proton radiotherapy. Med. Phys. 10: 344-346.

[14] Futami, Y., Kanai, T., Fujita, M., Tomura, H., Higashi, A., Matsufuji, N., Miyahara, N., Endo, M., and Kawachi, K. (1999) Broad-beam three-dimensional irradiation system for heavy-ion radiotherapy at HIMAC, Nucl. Instrum. Method. A430:143-153.

[15] Schaffner, B., Kanai, T., Futami, Y., Shimbo, M., and Urakabe, E. (2000) Gidre filter design and optimization for the broad-beam three-dimensional irradiation system for heavy-ion radiotherapy. Med. Phys. 27:716-724.

[16] Komori, M., Kanematsu, N., Minohara, S., and Kanai, T. (2004) Effect of respiratory motion on dose uniformity with layer-stacking irradiation system. Jpn. J. Med. Phys. 24:105-106 (in Japanese)

New Treatment-Facility Project at HIMAC

Koji Noda, Takuji Furukawa, Taku Inaniwa, Yoshiyuki Iwata, Tatsuaki Kanai, Mitsutaka Kanazawa, Nobuyuki Kanematsu, Atsushi Kitagawa, Shinichi Minohara, Shinichiro Mori, Takeshi Murakami, Masayuki Muramatsu, Shinji Sato, Toshiyuki Shirai, Eiichi Takada, Yuka Takei, Masami Torikoshi

Research Center for Charged Particle Therapy, National Institute of Radiological Sciences, Chiba, Japan
e-mail address:noda_k@nirs.go.jp

Abstract

The first clinical trial with carbon beams generated from HIMAC was conducted in June 1994. The total number of patients treated was in excess of 4,000 as of June 2008. The impressive advance of carbon-ion therapy using HIMAC has been supported by high-reliability operation and by the development of accelerator technology. Based on more than ten years of experience with HIMAC, we have proposed a new treatment facility for the further development of therapy with HIMAC. The new facility, as an extension of the existing one, has been designed, and the related R&D work has been carried out. The following descriptions give a summary account of the design study and the related R&D work for this new treatment facility at HIMAC.

1. Introduction

Heavy-ion beams are very suitable for the treatment of deeply seated cancer because of an excellent physical-dose distribution and high-LET characteristics around the Bragg peak. Therefore, NIRS decided to carry out heavy-ion cancer therapy with HIMAC [1]. The first clinical trial of cancer treatment with carbon beams was conducted in June 1994. The total number of patients treated until June 2008 was more than 4,000. Based on more than ten years of experience with HIMAC, we have proposed a new treatment facility toward adaptive cancer therapy [2] with heavy ions, making the one-day treatment of lung cancer possible. Further, the new treatment facility should accurately treat a fixed target, a moving target with breathing and/or a target near a critical organ. For these purposes, a 3D-scanning method with a pencil beam is employed in the new treatment facility. A phase-controlled rescanning (PCR) method [3] has been proposed and studied, especially for treating a moving target. A rotating gantry with the PCR method [4] is also employed in order to reduce the patient's load, such as face-downward position during patient positioning, and to increase treatment accuracy for a tumor near a critical organ through multi-field optimization [5]. In addition, we have designed the beam-delivery system, the rotating gantry system, the treatment flow including patient positioning and the facility planning. The related R&D work has also been carried out with HIMAC since 2006. We review the design study and the related R&D work for the new treatment facility at HIMAC.

2. Design consideration

In HIMAC treatments, we have observed shrinkage of the target size as well as a change in its shape during the entire treatment. In order to keep the sophisticated conformations of the dose distributions even in such cases, it has been required that treatment planning is carried out just before each fractional irradiation, which we

call adaptive therapy. For this purpose, 3D scanning with a pencil beam should be employed, because it does not use any bolus and patient collimators, which take a long time to be manufactured. It is also well-known that 3D scanning has brought about a high treatment accuracy in the case of a fixed target [6]. However, this method has not yet been applied to treating a moving target with breathing in practical use. Therefore, we have developed the PCR method to treat a moving target, as mentioned in 3.1.

A ^{12}C beam is mainly used for treatments that have been carried out in the existing HIMAC treatment. Different ion species will also be employed for the further development of HIMAC therapy. Thus, the maximum ion energy is designed to be 430 MeV/n in both the horizontal and vertical beam-delivery systems, in order to obtain more than the residual range of 30 cm in a ^{12}C beam and more than that of 22 cm in an ^{16}O beam. The maximum lateral field and SOBP sizes are 25 cm × 25 cm and 15 cm, respectively, in order to cover almost all treatments with HIMAC [7]. On the other hand, the rotating gantry system employs a maximum energy of 400 MeV/n, a maximum lateral field of 15 cm × 15 cm, and a maximum SOBP size of 15 cm in order to downsize the gantry. Further, positron-emission beams, such as ^{11}C and ^{15}O, will be used to verify the irradiation area and their ranges in a patient's body. At HIMAC, R&D work has been carried out in order to obtain positron-emission beams accelerated directly through the HIMAC accelerator [8], instead of using the projectile-fragmentation method.

The new treatment facility is connected with the upper synchrotron at HIMAC. In the treatment hall, placed underground of the facility, three treatment rooms are prepared in order to treat more than the present number of patients with the HIMAC treatment. Two of the treatment rooms are equipped with both horizontal and vertical beam-delivery systems, and the other one is equipped with a rotating gantry. Two treatment-simulation rooms are also equipped for patient positioning as a rehearsal, and for observing any change in the target size and shape during the entire treatment period with an X-ray CT. Furthermore, there are six rooms devoted to patient preparation before irradiation. A schematic view of the new treatment facility is shown in Fig. 1.

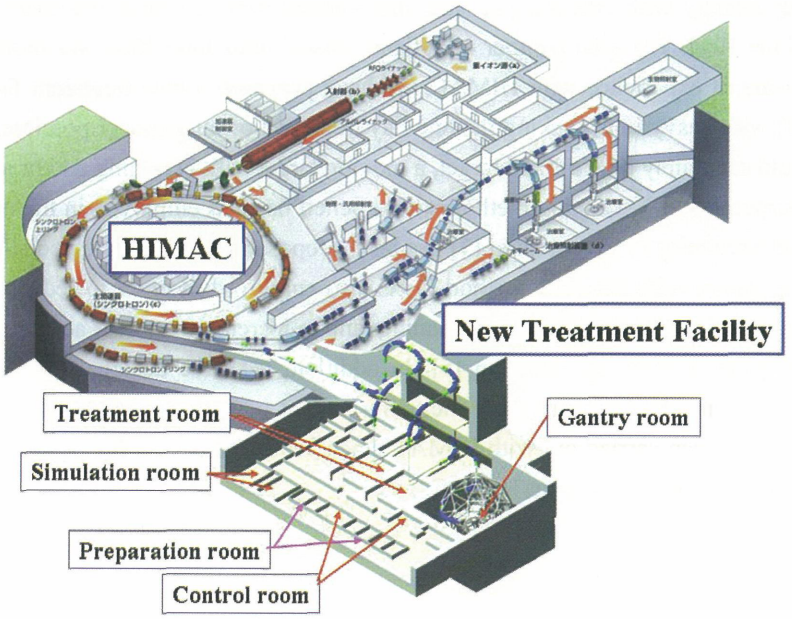

Fig. 1. Schematic view of the new treatment facility and the present HIMAC.

3. Design study and R&D work

3.1 Development of the HIMAC accelerator

The beam intensity from the HIMAC synchrotron has been increased in order to complete one fractional irradiation with one cycle of synchrotron operation. In this case, the efficiency of the gated irradiation will be increased by extending the flattop duration, which will save considerable irradiation time. In order to increase the beam intensity, we have thus carried out a tune survey during beam injection. As a result, it was found that the 3rd-order coupling resonance caused beam loss. This resonance was corrected by four sextupole magnets, and the beam lifetime was increased by more than 5 times. Further, we tried multi-harmonics operation of the RF acceleration system in order to suppress the space-charge effect after bunching. This operation increased the acceleration efficiency by around 40% [9]. Consequently, around 2×10^{10} carbon ions can be accelerated to the final energy. This intensity is sufficiently high to irradiate almost all tumors treated with HIMAC when using the 3D-scanning method with a beam-utilization efficiency of more than 90%. The extended flattop operation was successfully tested at the HIMAC synchrotron. In the scanning experiment described in 3.4, the flattop duration was successfully extended to around 25 s from 2 s used in routine operation, as shown in Fig. 2. Further, the beam profiles during an extraction duration of 100 s were measured by a multi-wire proportional counter in the high-energy beam-transport line. From the results of an analysis of the measurement, it was estimated that both the position and the size for the extraction duration of 100 s were stabilized within ±0.5 mm at the iso-center.

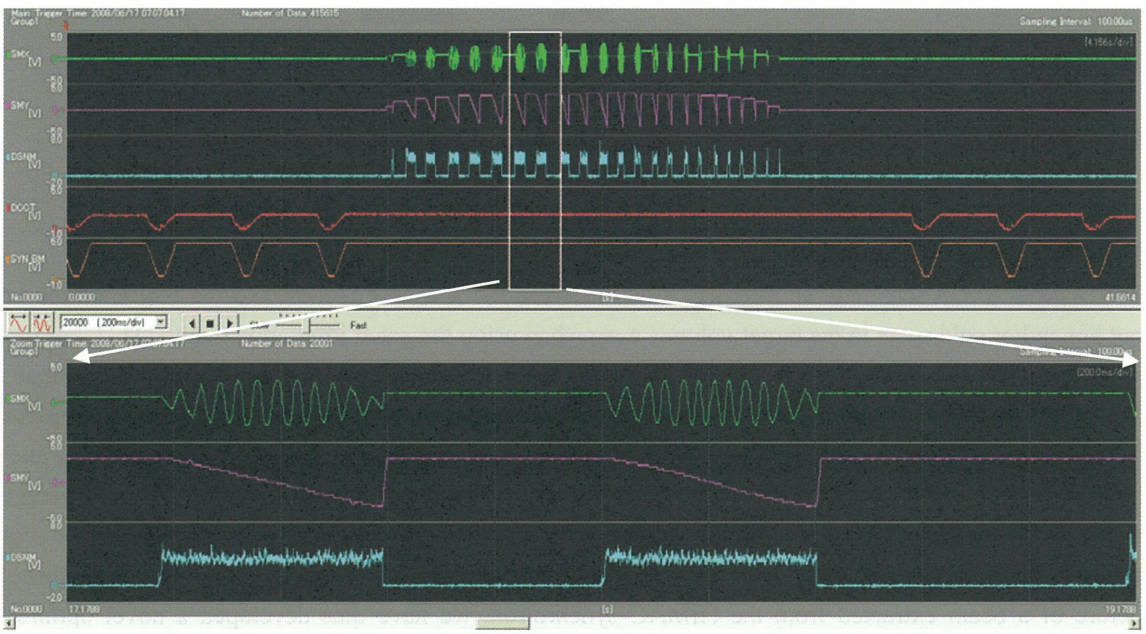

Fig. 2. (a) The extended FT operation. From upper trace, Current of X and Y scanning magnet, the extracted beam current. The full span is 145 s. (b) Enlarged figure of (a).

3.2 Design of beam-delivery system

Both the horizontal and vertical beam-delivery systems consist of a pair of scanning magnets, dose monitors, a ridge filter and a range shifter. The total length of the beam-delivery system is around 9 m. The beam-scanning speed is designed to be 100 mm/ms for fast scanning. Two dose monitors, which are parallel-plate ionization chambers with an effective area of 250 mm^2, are used for dose management. The beam position and size are monitored by multi-wire proportional counters. Considering the slice thickness, the Bragg peak is slightly

spread out by a mini ridge filter. The range shifter is utilized to change the slice in the target. Thus, the range shifter should be as close as possible to the iso-center in order to avoid any change of the beam size by multiple scattering through the range shifter. Ref. [3] describes its design in detail and the beam-delivery system is shown in Fig. 3. In order to verify the proposed 3D-scanning method, a test bench of the beam delivery system with 3D-scanning method has been constructed in the physics experimental hall at HIMAC.

In the present design, the rotating gantry employs a pencil-beam raster scanning, which is identical to the one used for the horizontal and vertical beam-delivery systems. It is important for the gantry design to avoid any change in beam size in accordance with the rotation angle. Thus, we will adapt a compensation method of asymmetric phase-space distribution [10]. This method is based on multiple scattering by a thin foil placed at the position with optimum beam-optical parameters in the beam-transport line. Further, the final dipole magnet is divided into 30-degree and 60-degree magnets, and two scanners are placed between the two magnets in order to extend the effective length from the scanners to the iso-center. The total weight of the gantry system is around 350 tons.

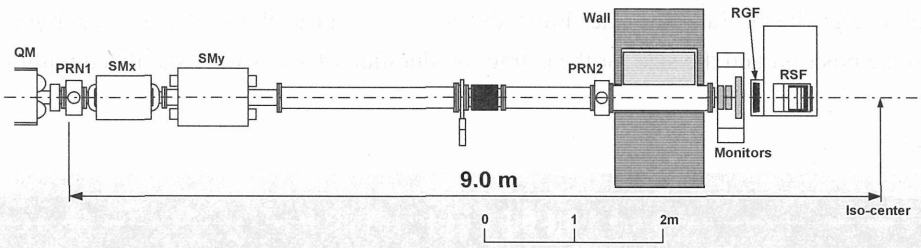

Fig. 3. Test bench of beam-delivery system

3.3 Verification of PCR method

In 3D pencil-beam scanning, an interplay effect between the scanning motion and the target motion brings about hot and/or cold spots in the target volume, even when using the gated irradiation method [11], because the sizes of the distal and lateral dose profiles of the pencil beam are comparable to the residual motion range. The PCR method, therefore, which is combined with the rescanning technique and gated irradiation, is employed in order to avoid producing hot/cold spots. In the PCR method, rescanning on a slice is completed during one gate generated in the respiration period of the patient's breathing. Since the moving target position is averaged in both the lateral and distal directions, the hot and/or cold spots are not produced. The rescanning method requires a relatively large number of scans, which cause a relatively long irradiation time. Based on the uniform time structure of a beam extracted from the HIMAC synchrotron, we have thus developed a novel optimization technique for fast scanning in order to shorten the irradiation time, in which extra exposure during the transition of each spot is taken into account [12]. The result of a simulation study showed that the PCR method provided a feasible solution in which a dynamic beam-intensity control technique [13] based on the RF-KO slow extraction method [14] plays an important role for adequately controlling the phase correlation under a relatively small number of rescanning procedures. In the PCR method, it is noted that the irradiation time for each depth slice should be adjusted to be within 1-2 s of the respiration gate duration. Consequently, we obtained a feasible solution for a moving target irradiation by fast raster-scanning method with rescanning and gating functions.

3.4 Scanning experiment

Since 3D-scanning is one of the key technologies for the PCR method, we carried out a fast raster-scanning experiment by using the HIMAC spot-scanning test line [15]. The irradiation control system was slightly

modified so as to be capable of raster scanning irradiation instead of spot scanning irradiation. At the present stage, we have adapted the measured dose response of the pencil beam with an energy of 350 MeV/n, corresponding to a 22-cm range in water. The beam size at the entrance and the width of the Gaussian-shaped mini-peak were 3.5 and 4 mm at one standard deviation, respectively. The validity of the beam model and the optimization calculation had already been verified experimentally [12]. Using the dynamic intensity control system, the beam intensity was kept almost constant during irradiation. In the experiment, a spherical target of 4 cm in diameter was irradiated so as to produce a uniform physical dose field. The measured dose distributions were in good agreement with the calculation result at different penetration depths.

4. Summary

At the HIMAC accelerator complex, beam studies were carried out especially for increasing the irradiation accuracy and treatment efficiency. As a result, we were able to upgrade the performance of the HIMAC accelerator complex. Based on this upgrade, we have proposed a new project for further development of heavy-ion therapy with HIMAC, entailing the construction of a new treatment facility. The new treatment facility has three treatment rooms: two rooms are equipped with horizontal and vertical beam-delivery systems equipped with a 3D pencil-beam scanning capability, and the other with a rotating gantry with a 3D pencil-beam scanning capability. The beam-scanning irradiation method uses the PCR method with a fast scanning performance. These developments have made continuous successful progress since 2006.

References

[1] Y. Hirao et al., Nucl. Phys. A 538, 541c–550c (1992).

[2] K. J. Halverson et al., Int. J. Radiat. Oncol. Bio. Phys. 21:1327-1336 (1991).

[3] T. Furukawa, T. Inaniwa, S. Sato, T. Tomitani, T. Minohara, K. Noda, T. Kanai, Med. Phys. 34 (3), 1085-1097 (2007).

[4] T. Furukawa, T. Inaniwa, S. Sato, Y. Iwata, S. Minohara, K. Noda, T. Kanai, in these proceedings.

[5] A. Lomax, Phys. Med. Biol. 44:1219-1226 (1999).

[6] Th. Haberer, W. Becher, D. Schardt, G. Kraft, Nucl. Instrum. Meth. A 330, (1993) 296-305.

[7] K. Noda et al., J. Rad. Res., 48 (2007) A43-A54.

[8] S. Hojo, T. Honma, Y. Sakamoto, S. Yamada, Nucl. Instrum. Meth. B 240 (2005) 75.

[9] C. Ohomori et al., Nucl. Instrum. Meth. A 547 (2005) 251.

[10] T. Furukawa and K. Noda, Nucl. Instrum. Meth. A 565 (2006) 430.

[11] S. Minohara, T. Kanai, M. Endo, K. Noda and M. Kanazawa: Int. J. Rad. Oncol. Bio. Phys. 2000;47:1097-1103.

[12] T. Inaniwa, T. Furukawa, T. Tomitani, S. Sato, K. Noda, T. Kanai, Med. Phys. 34 (8) 3302-3311 (2007).

[13] S. Sato, T. Furukawa, K. Noda, Nucl. Instrum. Meth. A 574, (2007) 226-231.

[14] K. Noda et al., Nucl. Instrum. Meth. A 374 (1996) 269.

[15] E. Urakabe et al., Jpn. J. Appl. Phys. 40 (2001) 254.

Cryogenic Gantry: Which Problems Remain to be Solved

François A. Kircher

CEA, Irfu, SACM, Centre de Saclay, 91191 Gif sur Yvette, France
e-mail address: francois.kircher@cea.fr

Abstract

This paper describes the main results of a preliminary design study made about the possible use of cryogenics rotating gantries for 400 MeV carbon ion beams. Assuming an active scanning mode, the main challenge is the 90 d° superconducting bending magnet located at the exit of the gantry. The main conclusion of the study is that no technical impossibility has been found, and that the construction and tests of a full scale model of this magnet would strongly confirm the interest of such a solution.

Introduction

If rotating gantries are now widely used inside proton therapy centers, it is not the same for the few ion therapy centers now built or under construction. In Europe, only the precursor Heidelberg ion therapy center has one. This gantry is using conventional magnets and this technology has shown its limits for 400 MeV carbon ions of high magnetic rigidity.

As superconductivity is now widely used for medical applications, MRI magnets being the best example, a preliminary study was done by several French laboratories (CEA, IN2P3), in collaboration with the Etoile project, to look at the possibility to use superconducting magnets in such gantries. The main results of this study are summarized in this paper.

Basic requirements for the beam delivery system

These requirements were formulated by the medical specialists:

- active beam scanning
- irradiation area of 200*200 mm^2
- beam diameter at the tumor: from 4 to 10 mm
- rotation of the gantry of 360 d°, with an accuracy of ± 0.012 d°
- during the rotation, the beam isocenter at the tumor must stay within a 1 cm radius sphere
- maximum penetration depth of the carbon ions of 280 mm, which corresponds to the ion energy of 410 MeV/nucleon and a maximum magnetic rigidity of 6.45 T.m
- variation of the beam particle energy corresponding to 30 slices distant of 4 mm, with a slice every 1.5 sec.

This corresponds to a maximum change of field of 0.9 T in 45 sec, i.e. a field variation of 0.02 T/sec.

Cryogenic gantry design

The design of the cryogenic gantry which has resulted from the study is shown on Fig. 1. Some minor adjustments will still be possible after the detailed study of the beam transport optics.

All magnets, except the main 90 d° bending magnet, are conventional:

- 2 pairs of quadrupole doublet and one quadruplet for the beam focalization
- 2 bending dipoles, with a deviation of 45 d° each
- 2 scanner magnets placed upstream to the last bending magnet, to reduce the dimensions of the whole system.

The superconducting 90 d° bending magnet has the following parameters:

- central orbit radius of 2 m, corresponding to a central field of 3.17 T for 400 MeV carbon ions
- integral field homogeneity of a few 10^{-3} inside the irradiation area for the full range of the magnetic field variation
- a total weight around 20 t

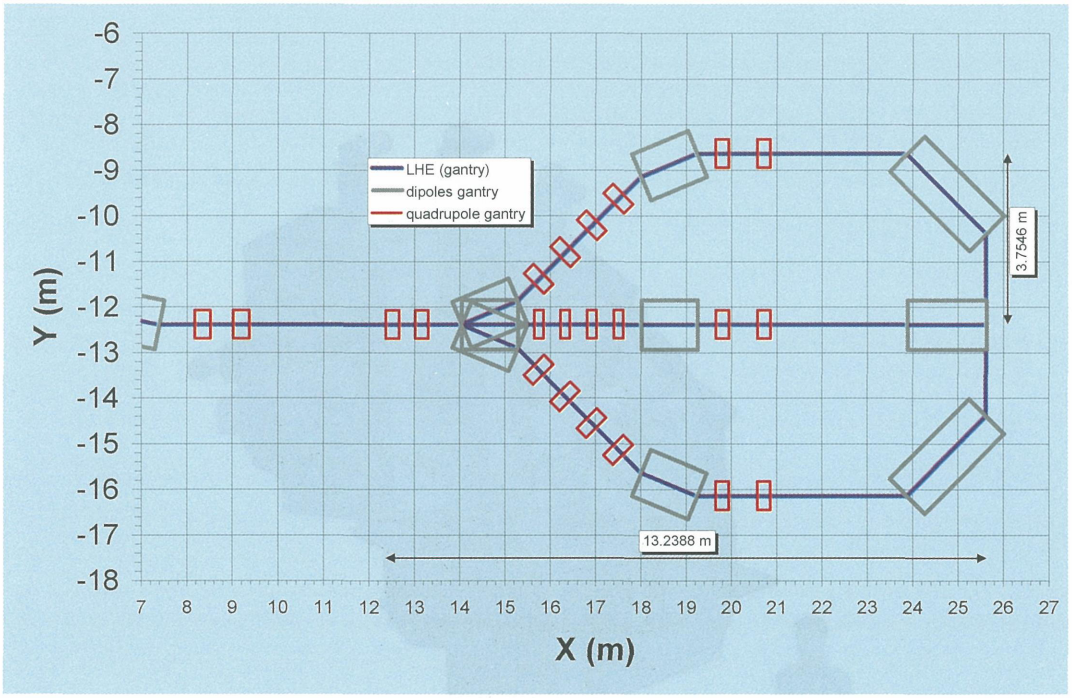

Fig. 1: Design of the cryogenic gantry (shown at 3 different angular positions)

The general structure of the cryogenic gantry is similar to a conventional one, but of course smaller and lighter. Assuming an accuracy of ± 1 mm in the positioning, the comparison of the parameters of the two gantries is given in Tab. 1.

Tab. 1: comparison of the parameters of two gantries for 400 MeV carbon ions

Parameter	Conventional gantry	Cryogenic gantry
Length (m)	20	14
Overall diameter (m)	12	8
Weight (t)	600	210

Technical solutions for the 90 d° superconducting bending magnet

This magnet is the technical innovation of the cryogenic gantry. It uses proved technical solutions, with safety margins adapted to its specific use

1. Coil

The coil is made of several winding using NbTi as superconductor. The shape of the coils, bent on 90d°, is quite unusual, but has already been produced for other applications, such as compact superconducting synchrotrons. Recently, the feasibility of winding such coils has been shown [1].

The control of the effect of the end profilers of a superconducting magnet is not as easy as with a conventional magnet, where the rotation angle of the iron pole faces can be accurately machined. Consequently, this point still needs to be studied in more details. Even if the use of magnetic iron is to be avoided as much as possible to reduce the weight of the magnet, some local iron shimming can be envisaged to cope with this effect. Note that this effect on the beam optics during the rotation of the gantry is more important with a beam extracted from a synchrotron than from a cyclotron, because of the large difference of emittance in both directions in the first case. A general view of the magnet inside its cryostat is given in Fig. 2.

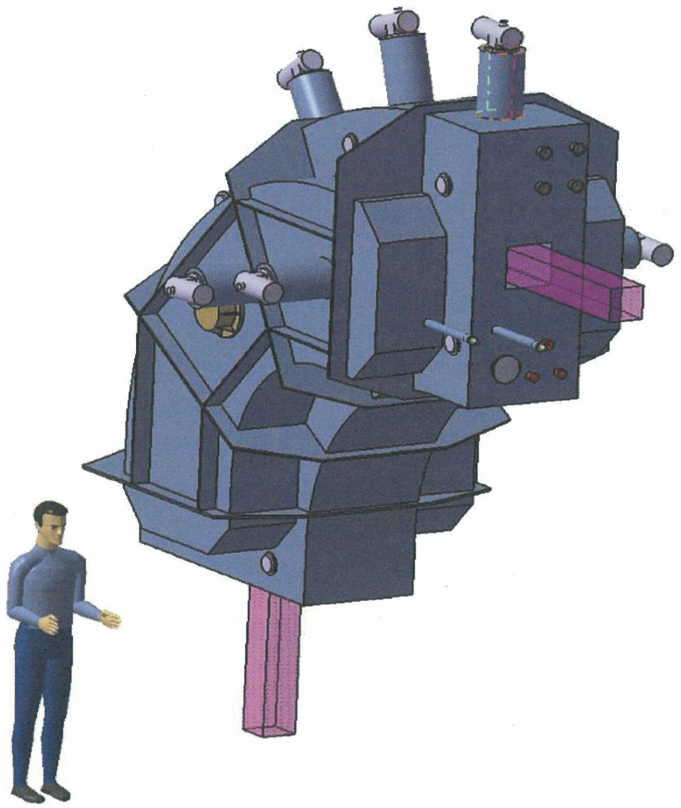

Fig. 2: General view of the superconducting 90 d° bending magnet

2. Superconductor

Niobium-titanium is used as basic superconductor. The conductor consists of a cable made of several strands, embedded in a copper matrix. Inside the strands, the superconducting material is divided into very fine filaments, as in other accelerator magnets, to reduce the losses when the magnetic field is varied. Enough superconductor is

put to get a safety margin in temperature when operating the magnet. The copper is used to minimize the temperature of the magnet in case of quench (loss of the superconducting state).

3. Cooling

Both the cooling from room temperature to 4.5 K and then the keeping of the magnet at a temperature of 4.5 K during operation are done using cryocoolers, this means just by thermal conduction, avoiding the use of any cryogenic fluid. With the cryogenic power of presently available cryocoolers, the cooling time from room temperature to 4.5 K is estimated to 14 days, and the recovery after a quench in about 2 days. Liquid nitrogen and liquid helium can be used to speed up the cooling from room temperature if necessary. It has been experimentally demonstrated that the efficiency of the cryocoolers has almost no dependence with its position during a 360 d° rotation.

All together, the cryogenic losses in operation are estimated at around 7 W at 4.5 K.

Conclusions

Our preliminary design study of a cryogenic gantry has not shown any technical impossibility. As this stage, some points are still to be looked at in more details, such as the optimization of the magnetic structure of the superconducting 90 d° bending magnet with respect to the beam optics. All the techniques which are foreseen for the construction of the superconducting magnet such as niobium-titanium superconductor with fine filaments to reduce the losses, bent coils, use of cryocoolers..., have already been used before, but neither together for such an application. So this is the real challenge.

The use of superconductivity for the main 90 d° bending magnet enables to reduce the dimensions of the cryogenic gantry by about 30% in length and diameter, and its weight by a factor of about 3, compared to a conventional gantry.

The project seems interesting enough to have discussions going on with the company IBA to collaborate in the detailed design, construction and tests of a full scale model.

References

[1] Farinon S, et al. The Winding Method and Model of Superconducting Bending Dipole for Hadrontherapy. IEEE Trans. on Applied Supercond. 2004; 14: 585-588

New Methods of Real-time Control Imaging for Ion Therapy

D. Dauvergne[1*], M. Battaglia[1], G. Montarou[2], E. Testa[1]

[1]*IPNL, Université de Lyon, F-69003 Lyon; Université Lyon 1 and IN2P3/CNRS, UMR 5822, F-69622 Villeurbanne, France*

[2]*LPC Clermont-Ferrand, IN2P3, Université Blaise Pascal, Clermont-Ferrand, France*

[*] *e-mail address:d.dauvergne@ipnl.in2p3.fr*

Abstract

We present the ongoing studies aiming at providing a real-time control of the dose distribution during ion therapy. These studies are undertaken in the frame of the National and Rhône-Alpes Regional Research Programs for Hadontherapy. We aim at implementing combined modalities for real-time quality control of the deposited dose for future therapy centers. Several modalities are under development within this research program. Improvements on Positron Emission Tomography (PET) can be obtained by means of Time of Flight, using fast scintillators or resistive plate chambers, with dedicated readout and electronics. The in-bream prompt gamma imaging looks very promising in view of recent preliminary results, provided Time of Flight is used to discriminate gamma from neutrons and scattered particles. A collimated detection setup or a Compton camera is envisaged. Prompt emission of light charged particles like protons is also discussed.

Introduction

The main distinctive characteristic of ion-therapy, as compared to conventional radiotherapy, is the highly non-uniform profile of dose deposition inside the irradiated body. The dose increases gradually along the ion path to reach a steep maximum at the Bragg peak. Beyond this point, the longitudinal dose drops down quite abruptly, since only a small flux of secondary particles contribute to it. The lateral dose distribution is also quite narrow. Indeed, the transverse dispersion comes mostly from multiple scattering of the charged projectiles before stopping.

Therefore, *in vivo* 3D-imaging of the dose is of utmost importance for quality control during patient treatment, and drives a diversified R&D program which includes a variety of techniques. The uncertainty on the location of the Bragg peak in the patient may be large, as much as 1 cm in some cases, due to the stoichiometric calibration of the CT images used in treatment planning, as well as to possible morphologic changes occuring between CT and treatment and during the treatment itself, such as patient mispositioning tumour shrinkage, weight change and organ motion. Since no primary radiation emerges from the patient, *in vivo* imaging must be performed exploiting secondary radiations. To be useful, such radiation must emerge from the patient, *i.e.* to have a weak interaction probability, and be correlated to the primary beam dose distribution. This information on the electromagnetic energy deposition (the LET) can be extracted from hadronic interactions [1,2,3].

A significant effort has been already deployed to address these issues and several techniques have been proposed and tested. The present paper reviews the various developments underway on the on-line beam dose deposition imaging that are performed within the Rhône-Alpes Regional Program for Research in Hadrontherapy, with the motivation of providing new methods for quality control in future therapy centers like ETOILE in Lyon. These developments include improvement of in-beam Positron Emission Tomography (IBPET) by means of time of flight, in-beam imaging by prompt gamma-rays and secondary charged particles.

Positron Emission Tomography

So far the only operating control system available during ion therapy is PET, which is based on the observation of the radiation from radioisotopes formed in the nuclei fragmentation process, namely the annihilation of β^+ particles into two photons [3,4,5,6,7]. The main β^+ radioactive isotopes formed during proton or carbon irradiation are ^{11}C, ^{15}O and ^{10}C, with respective half-lives of 20 min, 2 min and 20 s. The suitability of various light ion beams for PET imaging has been studied at GSI and HIMAC [8,9,10]. Although only the target nuclei undergo fragmentation during proton therapy, the absolute rate of β^+ emission induced during a treatment is higher by a factor of 3-5 for proton than for carbon irradiation, where also projectile fragmentation occurs, due to the larger fluence of protons required to provide the same effective dose.

The relatively short radioisotope lifetimes cited above make IBPET very attractive. This is the solution that was promoted by Enghardt *et al.* [11] with the dual-head PET BASTEI (Beta Activity Measurements at the Therapy with Energetic Ions) that has been installed at the GSI pilot project and has demonstrated its ability to provide a control of neck and head irradiations with carbon ions. The IBPET was used at GSI until 2008, whereas most of PET devices used in ion-therapy centers are offline, which necessitates the transport of the patient immediately after the treatment. However, the relatively low induced activities [12] require the acquisition of PET data for about 10 minutes or more, which limits considerably the patient flow in routine clinical environment in the case of IBPET. In addition, the integration of an IBPET device into a treatment site has to be arranged as a limited angle scanner, in order to avoid interference with the patient positioning. This causes artefacts in the reconstructed β^+ activity distributions which partly destroy the relationship between dose and activity. Moreover, over such a period of acquisition time, the metabolism causes a wash-out of the radioactive nuclei, which blurs the image of the implanted radioactive isotopes [13]. The low statistics problem could be circumvented by using radioactive ^{11}C ion beams instead of stable ions which, in addition, provide additional therapeutic dose after implantation due to the projectile radioactivity [14]. Tomitani *et al* have studied the biologic lifetime, *i.e.* the metabolic wash-out, of the implanted radio-elements in clinical conditions with rabbits. They reported that more than 50% of the β+ activity is lost within 4 minutes or less, depending on the tissue irradiated [15].

Improvements of IBPET involve mainly the use of TOF between the two detected gammas. Indeed, during heavy ion treatments, a considerable amount of activity is coming from outside the field of view of the IBPET camera. An accuracy below 200 ps FWHM would reduce considerably the region of interest to a size of the same order as the tumor volume, and therefore decrease the number of background events registered. An important issue of PET imaging is the computer procedure needed to reconstruct an image and extract information about the deposited dose [16,17]. A significant gain on the reconstruction time could be obtained by increasing the coincidence accuracy by means of TOF between the two detected photons. This increase in image processing speed arises from the possibility to calculate at once the point of positron annihilation as soon as the coordinates of the hit detectors and the TOF information are known. Such an algorithm needs to process one single iteration through the collected data, unlike standard iterative reconstruction algorithms. Thus this would also reduce limited solid angle artifacts and open the way to quantitative imaging.

Lanthanum halide ($LaBr_3$) scintillating crystals can in principle reach such 10^{-11}s time resolution. For the readout of the scintillating material, two alternatives could be explored: fast, position-sensitive photomultipliers having sub-ns rise times, or the recently developed solid state Silicon PhotoMultiplier (SiPM). The SiPMs operate in the Geiger mode due to the avalanche nature of their signal, and they have a fast response time with nominal resolution of 50 ps or better. Unlike photomultipliers, SiPMs are not sensitive to magnetic fields, which makes them candidates for use in a multimodal TOF-PET – MRI. But they have not been used in large systems to date.

Prompt gamma imaging

Since the probability for prompt gamma emission is expected to be of the same order as that for fragmentation, gamma imaging may be regarded as a competitive technique to provide real-time information about the local dose [18,19,20] both for proton and carbon ion therapy.

Prompt gamma-rays are emitted by excited fragments with sufficiently small decay times so that the largest part of the photons are emitted in flight, keeping somewhat the information on the nuclear fragmentation location.

However, measuring prompt gamma during a therapy treatment is not straightforward, since a major source of background arises from the emission of other secondary species like neutrons and light fragments, and also from Compton scattering of photons emitted in all directions. In particular, neutrons have a high multiplicity and high scattering probability in surrounding materials, and they may not be correlated to the ion path. Therefore, various alternatives are offered to provide selective information about the prompt gamma emission profile.

1. Collimated gamma-camera

The first one consists in a selective collimation and shielding. This method was followed by Min *et al* [18] during proton irradiation of a water phantom target. Using a scanning system based on a thick lead and paraffin collimator, the authors could demonstrate that the gamma emission profile keeps correlated with the proton range in water up to projectile incident energy of 200 MeV. However, the limited solid angle imposed by the heavy and oversized collimation setup may prevent this method from being operated in a clinical environment.

2. Time Of Flight-gamma camera with beam tagging

In order to improve the detection efficiency and the background rejection, our group proposed a prompt gamma detection method [19,21] which uses time of flight information to discriminate between photons and massive particles. Indeed, massive particles and scattered radiations in the surrounding materials are delayed before reaching the photon detector, as compared to direct photons. The concept was tested on a carbon ion beam at GANIL, taking advantage of the pulsed structure of the incident beam, 1 ns pulse each 80 ns. Figure 1 shows a 2D-spectrum of the energy detected by a collimated scintillator as a function of TOF for a ^{13}C ion beam

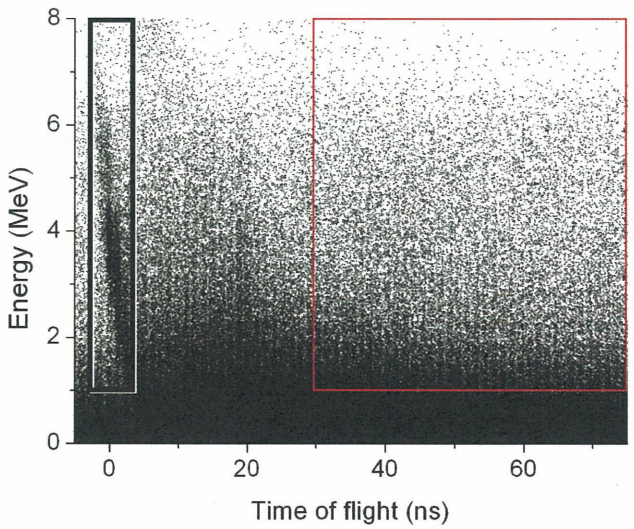

Figure 1. Two-dimensional spectrum of the γ-equivalent energy deposited in the NaI(Tl) detector as a function of the time of flight. The collimated scintillator aims at a location at the middle of the ion path (detection angle θ=90°) for a 74 MeV/u carbon ion beam inside a PMMA target. The left rectangle corresponds to a selection of prompt γ-rays, and the right one to a neutron selection [21].

energy of 74 MeV/u impinging a thick PMMA target. The detector was located at 90° from the beam axis, at a distance of 60 cm from the target, with a narrow collimation slit (2 mm). The detected prompt gamma photons appear as a vertical band at short TOF values (the small drift with energy is due to electronics artifacts). However they account for only a minor fraction of the detected particles, which are dominated by neutrons.

The feasibility of the method is shown in Figure 2 which gives the longitudinal profile of the measured rates corresponding to the selections of prompt gammas only and of neutrons, above a given energy threshold, corresponding to the selection cuts highlighted in Figure 1. A photography of the irradiated sample shows clearly the beam range by means of the visible damage in the target. The Bragg peak corresponds to the sharp defect accumulation at the end of the range. The photon profile is well correlated to the ion range, whereas that for neutrons steadily increases with depth. Further studies performed at higher beam energies at GSI confirm that the correlation between prompt gamma yields and dose profile is preserved for carbon ions with longer ranges (in this case, the TOF was triggered by a thin scintillator intercepting the low intensity beam). This makes the proposed method feasible for the typical energies of carbon ion therapy.

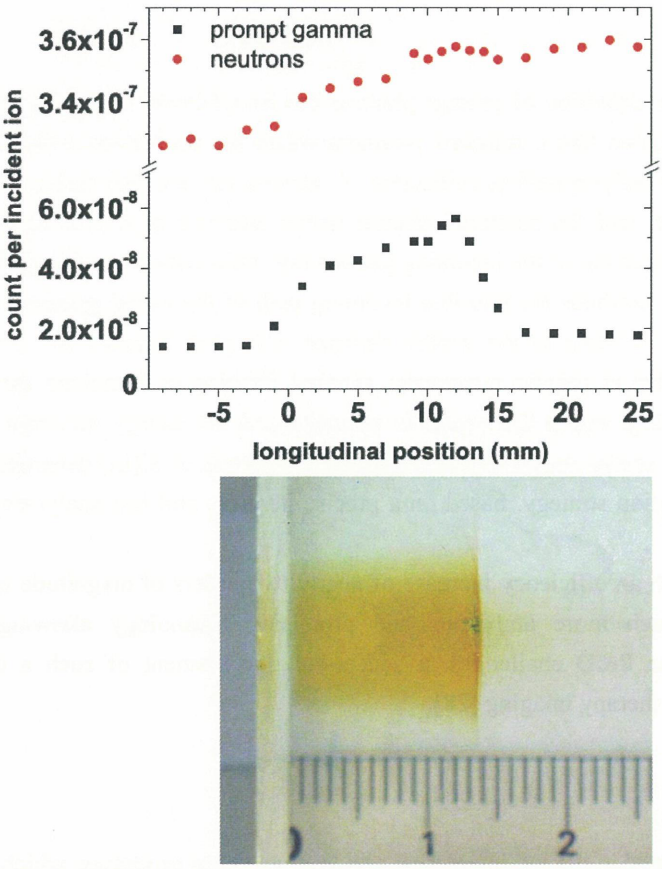

Figure 2: Detection rates as a function of the longitudinal position z obtained for the two different selections on the time of flight TOF and the energy deposited E in the detector indicated in Figure 1: photon selection (squares) and neutron selection (circles) [19]. Bottom: picture of the irradiated PMMA target.

The absolute photon yields measured are encouraging in view of designing a real-time control device during therapy. Although the solid angle of the collimated detector was small in these experiments, one can extrapolate the observed yields in view of a more efficient detection device. By increasing the solid angle by two orders of magnitude or more – which is made possible by minimizing the passive shielding against neutrons - enough contrast between the irradiated and non-irradiated zones should be observed within a few seconds exposure, thus allowing a real-time control during patient treatments. These feasibility studies are combined with GEANT 4

simulations which, in a first step, provide direct comparison with theoretical models, and, in a second step, will help for designing an optimized detection setup.

A 2D-transverse position information on the incoming ions is required to complete the longitudinal profile. The incident beam tagging, in both time and transverse position, requires the development of a fast position-sensitive detector, with a count rate capability of 10^8 ions/s and 1 ns time resolution. A prototype, consisting in a scintillating fibers hodoscope read out by flat-panel PMs, is under development at IPN Lyon. Since scintillating fibers are affected by radiation damage on the intense primary beam, an alternative technology under consideration consists in polycrystalline diamond detectors, produced by Chemical Vapor Deposition (CVD) [22,23,24]. Such detectors exhibit quite good radiation tolerance. Diamond detectors can be obtained with large area, 1 ns or less timing resolution, and with x and y segmentation in order to cope with the high count rate and provide position information in an event by event mode.

Although 3D-data are recorded by this method, the limited statistics imposed by the collimation may restrict the quantitative imaging to 1D or 2D projections. Nevertheless, this represents a considerable breakthrough in the quality control for ion-therapy, since this information is not yet available.

3. Compton camera

A considerable improvement in the detection of prompt photons can be achieved with a Compton Camera. The system can be considered to function like a standard γ-camera where the performance-limiting absorbing collimator is replaced by an electronically-operating collimator. A gamma ray emitted undergoes a Compton scattering in a first (scatter) detector, and the scattered photon which interacts in a secondary (absorption) detector conveys information on the direction of the incoming gamma ray. Information on energy deposition and interaction position in these detectors confines the possible incoming path of the initial gamma ray to lie on a cone, whose apex is the interaction position in the scatter detector. Compton cameras are currently under development worldwide, for application in gamma astronomy, medical imaging or homeland security [25,26]. For the case of prompt gamma imaging, where the source is extended and the energy spectrum is broad, the position and energy resolutions of the scatter detector are the key issues. A stack of Si(Li) detectors is envisaged [27]. In parallel, a specific reconstruction strategy, based on a precise iterative and fast analytic reconstruction algorithm, is under development.

The Compton camera solution, with an efficiency increase of nearly two orders of magnitude compared to a collimated gamma-camera, is a much more ambitious and promising technology allowing online real 3D-imaging of the dose. Beyond the R&D challenges, a successful development of such a device would represent a major breakthrough in ion therapy imaging [28].

Charged Particle Imaging

The analysis of charged particles, created in the ion interaction and fragmentation processes, which emerge from the patient offer a potential complementary opportunity to determine the points of interaction of the primary beam. The principle, which resembles that of vertex identification in fixed target particle physics experiments, is to reconstruct the trajectories of the particles emerging form the interactions by a precise charged particle hodoscope and extrapolate them back to their production point. The intercept of the trajectory of individual particle with the line of flight of the incoming ion, has been proposed in the context of the CNAO-sponsored AQUA quality assurance program and should provide a determination of the point of interaction with a resolution of a few mm, limited by multiple scattering and the effect of secondary interactions. Further, the possibility to use multiple particle tracks produced at the same interaction points would open the way to a real vertex reconstruction, intrinsically able to give a three-dimensional measurement of the point of interaction with accuracies of the order of 1 mm. A program of simulation validation using data for the secondary proton yield

and energy spectra and of secondary proton tracking and vertexing is currently being carried out jointly by IPN Lyon and TERA. In a second phase, a demonstration of the 3D reconstruction capabilities of these methods on a carbon ion beam using a small scale charged particle tracker and calorimeter is envisaged.

Conclusion

A diversified research program on online dose monitoring during ion therapy is currently ongoing, supported by the Rhône Alpes Regional Program for Research in Hadrontherapy. The program is carried out in the perspective of providing advanced and combined solutions for the treatment quality insurance to the ETOILE ion therapy, which is expected to treat the first patients by late 2012. These studies are also supported by CNRS-GDR MI2B. They are part of the European project ENVISION proposed by the ENLIGHT++ research network in the frame of the FP7.

References

[1] Schardt D, Schall I, Geissel H *et al.* Nuclear fragmentation of high-energy heavy-ion beams in water. Adv. Space Res. 1996;17: 87-94.

[2] Inaniwa T, Kohno T, Tomitani T *et al.* Experimental determination of particle range and dose distribution in thick targets through fragmentation reactions of stable heavy ions. Phys. Med. Biol. 2006; 51:4129-4146.

[3] Matsufuji N, Fukumura A, Komori M *et al.* Influence of fragment reaction of relativistic heavy charged particles on heavy-ion radiotherapy, Phys. Med. Biol. 2003; 48: 3393-3403.

[4] Enghardt W, Crespo P, Fiedler F et al., Charged hadron tumour therapy monitoring by means of PET Nucl. Instrum. Methods Phys. Res. A, 2004, 525, 284-288.

[5] Parodi K, Bortfeld T, Enghardt W *et al.* PET imaging for treatment verification of ion therapy: Implementation and experience at GSI Darmstadt and MGH Boston. Nucl. Instrum. and Meth. A. 2008; 591: 282-286.

[6] Solevi P, Study of an in-beam PET system for CNAO, the National Centre for Oncological Hadrontherapy. 2007; PhD thesis, University of Milano.

[7] Nishio T, Miyatake A, Inoue K *et al*, Experimental verification of proton beam monitoring in a human body by use of activity image of positron-emitting nuclei generated by nuclear fragmentation reaction. Radiol Phys Technol. 2008; 1:44–54

[8] Iseki Y, Mizuno H, Futami Y, Positron camera for range verification of heavy-ion radiotherapy, Nucl. Instrum. Methods. Phys. Res. A 2003;515: 840-849

[9] Pawelke J, Enghardt W, Haberer T *et al.* In-beam PET imaging for the control of heavy-ion tumour therapy. IEEE Trans. Nucl. Sci. 1997;44:1492-1498.

[10] Inaniwa T, Tomitani T, Kohno T and Kanai T, Quantitative comparison of suitability of various beams for range monitoring with induced β+ activity in hadron therapy. Phys. Med. Biol. 2005; 50: 1131-1145.

[11] Enghardt W, Debus J, Haberer T *et al.* The application of PET to quality assurance of heavy-ion tumor therapy. Strahlenther Onkol. 1999; 175-S2: 33-36.

[12] Enghardt W, Parodi K, Crespo P *et al.*, Dose Quantification from In-Beam Positron Emission Tomography, Rad. Oncol. 2004; 73:S96-98

[13] Fiedler F, Priegnitz M, Jülich R *et al.*, In-beam PET measurements of biological half-lives of ^{12}C irradiation induced β^+-activity. Acta Oncol. 2008; 47:1077-1086.

[14] Kitagawa A, Furusawa Y, Kanai T et al, Medical application of radioactive nuclear beams at HIMAC. Rev. Sci. Instrum. 2006;77:03C105

[15] Tomitani T, Pawelke J, Kanazawa M *et al*, Washout studies of 11C in rabbit thigh muscle implanted by secondary beams of HIMAC. Phys. Med. Biol. 2003; 48:875-889.

[16] Inaniwa T, Kohno T, Yamagata F *et al.* Maximum likelihood estimation of proton irradiated field and deposited dose distribution. Med. Phys. 2007; 34:1684-1692.

[17] Shakirin G, Crespo P, Enghardt W, A Method for System Matrix Construction and Processing for Reconstruction of In-Beam PET Data. IEEE Trans. Nucl. Sci. 2007;54:1710.

[18] Min C H, Kim C H, Youn M Y, Kim J W, Prompt gamma measurements for locating the dose falloff region in the proton therapy. Appl. Phys. Lett. 2006;89:183517.

[19] Testa E, Bajard M, Chevallier M et al., Monitoring the Bragg peak location of 73 MeV/u carbon ions by means of prompt gamma-ray measurements. Applied Physics Letters, 2008, 93, 093506

[20] Polf J C, Peterson S, Ciangaru G *et al.,* Prompt gamma-ray emission from biological tissues during proton irradiation: a preliminary study. Phys. Med. Biol. 2009; 54 :731–743

[21] Testa E, Bajard M, Chevallier M et al., Dose profile monitoring with carbon ions by means of prompt-gamma measurements. To be published in Nuclear Instruments and Methods B. Preprint available online at http://hal.archives-ouvertes.fr/hal-00283936/fr/

[22] Descamps C, Tromson D, Tranchant N *et al.* Clinical studies of optimised single crystal and polycrystalline diamonds for radiotherapy dosimetry. Radiation Measurements 2008; 43: 933-938.

[23] Bergonzo P, Brambilla A, Tromson D *et al.* Diamond as a tool for synchrotron radiation monitoring: beam position, profile, and temporal distribution. Diamond and Related Materials 2000; 9: 960.

[24] Rebisz M, Alternative methods for heavy-ion therapy dosimetry. Thesis, Heidelberg, 2007.

[25] Tanimori T, Hattori K, Kabuki S *et al.* Advanced Compton Camera with the ability in electron tracking based on Micro Pixel Gas Detector for Medical Imaging Nuclear Science Symposium Conference Record, 2006. IEEE 2006; 6:3870–3874.

[26] Protic D, Hull EL, Krings T, Vetter K. Large volume Si(Li) orthogonal strip detectors for Compton effect - based instruments. IEEE Trans. Nucl. Sci. 2005; 52:3181-3185.

[27] Walenta AH, Brill AB, Castoldi A *et al.* Vertex determination in a stack of Si-drift Detectors for High Resolution Gamma-ray Imaging. IEEE Trans. Nucl. Sci. 2005; 52:1434-1438

[28] Feng Y, Baciak J, Haghighat A, A Design of Compton Cameras for Imaging Gamma Emission in Proton Therapy, 50th AAPM Annual Meeting, July 27-31, 2008, Houston, Texas, 2008. Available online: http://www.aapm.org/meetings/amos2/pdf/35-9435-45230-12.pdf (29.09.2008)

Analysis of Moving Target

Shinichiro Mori, Nobuyuki Kanematsu, Taku Inaniwa, Hiroshi Asakura, Suguru Dobashi, Motoki Kumagai, Shinichi Minohara, Takeshi Yanagi, Tohru Okada, Riwa Kishimoto, Susumu Kandatsu, Shigeru Yamada, Hirotoshi Kato, Masayuki Baba, Hiroshi Tsuji, Tadashi Kamada

Research Center for Charged Particle Therapy, National Institute of Radiological Sciences, Chiba, Japan
e-mail address: shinshin@nirs.go.jp

Abstract

Purpose: Organ movement due to respiration may change the run of a charged particle beam that can result in degradation of dose conformation to the target. We introduced our approaches to quantitatively assessing potential problems in treatment planning due to organ movement by using four-dimensional CT (4DCT) data.
Methods and Materials: Several tens of inpatients with lung, pancreas or prostate cancer underwent 4DCT acquisition under free breathing conditions using a 256 multi-slice CT in cine mode. Gross tumor volume (GTV) displacement was evaluated as a function of the respiratory phase and calculated internal target volume (ITV). Using these results, passive 4D dose distributions were conducted.
Results: 4DCT images with the 256 multi-slice CT improved the evaluation of tumor displacement without 4DCT artifacts that were observed using the conventional multi-slice CT. Respiratory-induced GTV displacement between peak exhalation and inhalation was 7 mm, 7 mm and 15 mm for the upper, middle and lower lobes, respectively, for lung cases, 9 mm for pancreas cases, and less than 1 mm for prostate cases. Adding intrafractional motion into the treatment planning, the prescribed dose can be given to the targets at all respiratory phases sufficiently (no under-dose to the target).
Conclusions: By allowing accurate determination of the margin using 4DCT, quantitative analysis of GTV displacement provides useful information for treatment planning.

Introduction

Respiratory-induced intrafractional organ motion has been investigated using a variety of methods, including fluoroscopy, ultrasound (US), MRI, CT and PET, in thoracic, abdominal and pelvic sites. An understanding of intrafractional motion characteristics in charged particle treatment planning is useful for determining the internal margin and optimizing beam parameters (beam angle, gating window etc.), because degradation of image quality due to respiratory motion affects treatment planning and delivery of the treatment beam. Moreover, organ positional and geometric variations results in degraded treatment accuracy in two ways, first by moving the tumor out of the beam field, and second by altering the water-equivalent length (= WEL) from the skin surface to the tumor[1-9]. These effects could be observed in degraded dose conformation of charged particle treatment (scattered and scanned beams) as well as photon beam treatment. Quantification of organ motion using a single 2-dimensional projection image, however, limits the information of out-of-plane motion, rotation or deformation during breathing that can be captured. This is because tumors moving under respiration do not behave consistently, but rather move in different paths during inhalation and exhalation in a hysteresis-like manner. In the thoracic and abdominal regions, recently introduced CT scanners can acquire respiratory-correlated images

(four-dimensional CT: 4DCT), thus allowing the direct observation of several points (3D) of movement.

We have been developing respiratory-gated pencil-beam scanning treatment by extending the capability of the existing HIMAC (Heavy-Ion Medical Accelerator in Chiba) facility[10]. Respiratory-gated scanning should consider multiple time axes such as respiration (period, amplitude), beam irradiation, and accelerators. Because pencil-beam scanning irradiation is more sensitive to intrafractional motions than is conventional broad-beam irradiation, WEL variation should be minimized by consideration of intrafractional motion, including reproducibility of the respiratory amplitude.

Here, we introduced our approaches for a moving target in carbon ion beam radiotherapy.

Volumetric Cine Imaging for Treatment Planning

The helical scan method permits continuous CT scanning with simultaneous table movement and the successful acquisition of volumetric data, and is now used routinely for therapeutic applications in most hospitals. Radiotherapy under free breathing as well as respiratory gating requires clear determination of the internal target volume (ITV). Since the images are obtained at different absolute time axes for each slice position, the acquisition of time-based information is limited. To enable the incorporation of organ motion directly (volumetric CT data as a function of respiratory phase), the 4DCT scan method has been developed. 4DCT scanning is performed in the cine mode, which operates the scanner without couch movement using respiratory signals from surrogate systems to obtain all respiratory phases in each couch position. Then, it moves the couch to the next position and sorts CT images at the same respiratory phase. The 4DCT function is now integrated into commercial CT scanners, and many hospitals presently use it for radiotherapy planning. However, the 4DCT image obtained by multi-slice CT includes the same respiratory phase, although the time stamp is incoherent in each couch position. The respiratory pattern is not always the same in each respiratory cycle such as phase shift and phase drift etc[11-13]. Furthermore, the respiratory pattern could possibly vary in irregularly breathing patients. As a result, these conditions might induce image artifacts, where a slice at a given position may have anatomical inconsistencies. Our institute developed a 256 multi-slice CT, which employs a 12.8-cm wide cylindrical 2D detector system built into the frame of a conventional 16 multi-slice CT (Aquilion, Toshiba Medical Systems)[14] (Fig. 1a). Within this 12.8-cm system, the 256 multi-slice CT obtains volumetric cine CT data without resorting to the respiratory phase (Fig. 1b). We introduced the quality of 4DCT images obtained with conventional multi-slice CT and suggested improvements of image quality using 256 multi-slice CT.

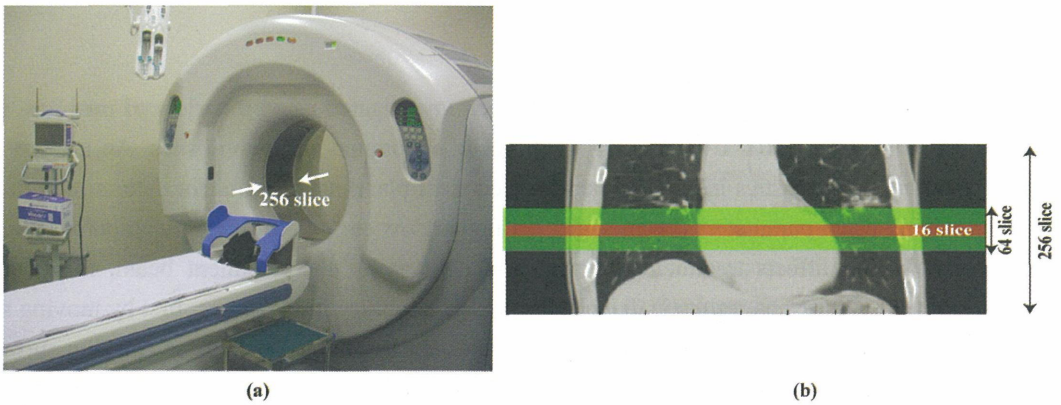

Figure 1. (a) 256 multi-slice CT scanner, (b) Scan range in a single rotation for 16, 64 and 256 multi-slice CT.

4DCT abdominal images obtained with 4 multi-slice CT are shown at the respective phases in Figure 2. The 4DCT image at peak exhalation shows the accurate anatomical shape and does not include significant banding

artifact (Fig. 2a). However, the anatomical shapes in 4DCT are degraded at mid-inhalation (Fig, 2b) and peak inhalation (Fig. 2c). These geometrical errors are due to resorting errors in 4DCT using conventional multi-slice CT. Since the resorting process in 4DCT acquisition is based on the respiratory phase, the respiratory amplitude is not always the same during 4DCT acquisition. The different amplitude in each slice was not capable of precisely visualizing the geometrical shape, therefore degrading image quality and hampering quantitative analysis, possibly affecting dose distribution. That is to say, a fundamental problem with 4DCT is that the images obtained by conventional multi-slice CT need to be resorted in the same respiratory phase, because even the latest commercially available multi-slice CT scanners obtain less than 4 cm in a single rotation. As a result, images in patients with low reproducibility of respiratory motion or irregular breathing may be subject to image sorting errors and degraded image quality. The 4DCT acquisition method using the conventional multi-slice CT, therefore, provides improved image quality compared to the helical CT scan method, which is not a quantitative method.

On the other hand, the 256 multi-slice CT captured high spatiotemporal volumetric data without any artifacts, as shown in Figure 3. Volumetric CT data can be acquired at a vertical distance of 12.8 cm, with both the respiratory phase and amplitude aligned in all slices. The 256 multi-slice CT shows that the anatomical shape is not so deformed in each respiratory phase in this patient [15].

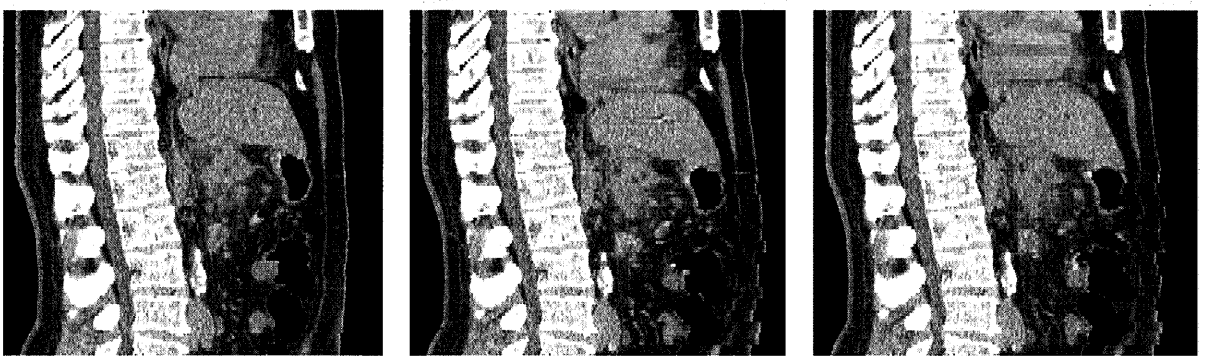

(a) Peak exhalation (b) Mid-inhalation (c) Peak inhalation

Figure 2. 4DCT sagittal images obtained by 4 multi-slice CT scanner (data provided by Massachusetts General Hospital, MA). (a) Peak exhalation (b) Mid-inhalation (c) Peak inhalation. Image quality degradation was due to inconsistencies of respiratory amplitude.

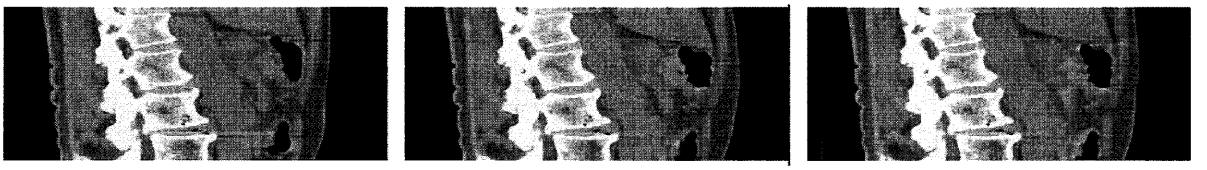

(a) Peak exhalation (b) Mid-inhalation (c) Peak inhalation

Figure 3. 4DCT coronal images obtained with 256 multi-slice CT scanner. (a) Peak exhalation (b) Mid-inhalation (c) Peak inhalation

Quantification of Intrafractional Motion

We quantified organ motions due to respiration in thoracic, abdominal, and pelvic sites as a function of time using the 256 multi-slice CT or 16 multi-slice CT (12 of 28 lung cases only). Subjects were selected randomly from a group of inpatients in our hospital. Patients were fixed on the patient bed with immobilization, as routinely used in treatment. After several minutes rest in a supine position on the CT bed, all 4DCT acquisitions were performed under free breathing, with patient respiration monitored by the respiratory sensing system, which

consists of a position-sensitive detector sensor and an infrared-emitting light termed an "active" marker. This system is routinely used for gated irradiation and CT acquisition during heavy ion radiotherapy at our institution. To accurately monitor patient respiration, the output signal is transferred to the ECG signal input connector in the CT console and recorded with the projection data. The respiratory signal therefore corresponds to the projection data without a time delay. Scan conditions were slice collimation of 256 x 0.5 mm or 128 x 1.0 mm, 0.5 s in a single rotation and scan time of less than 6 s to obtain one respiratory cycle without patient couch movement. The respiratory cycle was subdivided into 10 phases, with T0 as peak inhalation and T50 as peak exhalation.

Gross tumor volume (GTV) was manually contoured on the CT data set at peak exhalation by a certified radiation oncologist. GTV contours at other phases were calculated by deformable registration, following which the oncologist checked the contour curves at each phase. Center of mass (COM) was calculated by using the GTV contours.

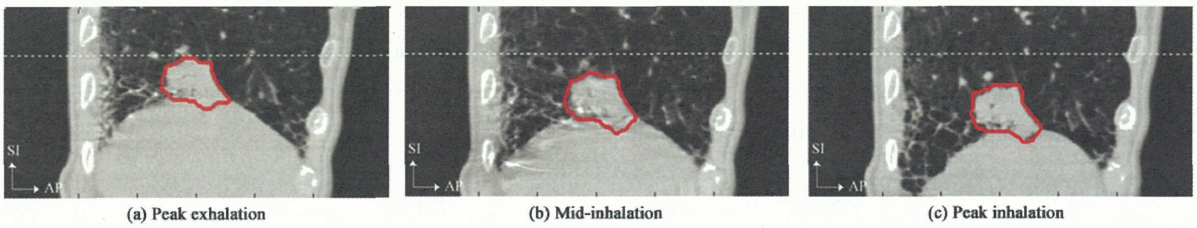

Figure 4 Lung sagittal images at (a) peak exhalation, (b) mid-inhalation and (c) peak inhalation. Red line shows GTV.

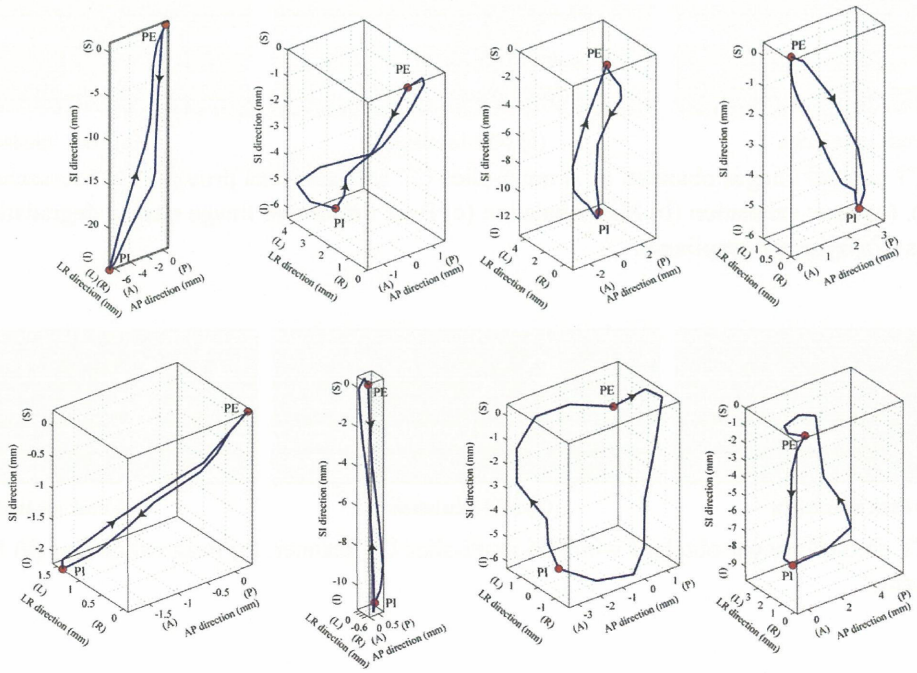

Figure 5. GTV-COM displacements for 8 cases without immobilization. Respiratory cycle and distance between peak-exhalation and –inhalation are shown in parentheses.

A total of 28 lung patients (including 14 patients without immobilization) participated in the 4DCT study. Volumetric cine imaging of the lung satisfactorily obtained continuous movement of the tumor in the sagittal section (Fig. 4). Motion artifacts due to breathing were frozen by a temporal resolution of 250 ms, allowing the

tumor shape to be evaluated accurately. Moreover, thin slice thickness and short total acquisition time helped determine target margins without 4DCT artifacts. The tumor was near the diaphragm and its displacement was approximate 2 cm at maximum. 3D visualization of GTV-COM displacement as a function of respiratory phase in other lung patients is shown in Figure 5. GTV-COM trajectory in a single respiratory cycle of the 4DCT revealed that most tumors show hysteresis-like behavior.

For patients without immobilization, average GTV-COM displacement relative to that at peak exhalation was 1.9 mm (range 0.2-5.4 mm) in the left-right, 4.0 mm (range 0.7-6.8 mm) in the anterior-posterior, and 10.3 mm (range 2.5-24.7 mm) in the superior-inferior directions, while GTV-COM displacement with immobilization was 1.4 mm (range 0.5-2.3 mm) in the left-right, 2.2 mm (range 0.8-4.7 mm) in the anterior-posterior, and 6.6 mm (range 1.6-21.8 mm) in the superior-inferior direction (Table 1). Use of immobilization can still reduce GTV displacement due to respiration and is a useful complement to current charged particle beam treatment.

Since the gantry beam port for our current treatment system in our center has not yet been installed, two fixed beam ports (horizontal and vertical directions) are being used. The range of beam angle selection was expanded by rotating the patient couch. To avoid patient positional variation by doing this and keeping patient setup accuracy, the patient is fixed tightly by immobilization. The carbon ion beam is delivered to the target with four beam angles from the gantry angles, which were selected from the ipsilateral rather than the contralateral side of the tumor, consisting of two pairs at an orthogonal beam angle, with one beam of each pair tilted 40° to minimize beam overshoot overlap regions (e.g. 340° and 70° with tilting the patient couch -20°, and 20° and 110° with tilting the patient couch +20°). Therefore, the use of immobilization is mandatory for the current carbon ion beam treatment to increase treatment accuracy, and attaching immobilization is not painful for patients.

Table 1 Average GTV-COM displacement for lung patients.

Direction	GTV-COM displacement (mm)			
	No immobilization		Immobilization	
	Mean	(Range)	Mean	(Range)
Left-right	1.9	(0.2-5.4)	1.4	(0.5-2.3)
Anterior-posterior	4.0	(0.7-6.8)	2.2	(0.8-4.7)
Superior-inferior	10.3	(2.5-24.7)	6.6	(1.6-21.8)

For pancreas cases, six inpatients with pancreatic tumor were evaluated. 3D-visualized GTV and the magnitude of geometrical variation from peak exhalation as a function of respiratory phase were calculated by using the pancreas 4DCT data sets shown in Figure 5. GTV-COM in the patient illustrated moved 0.8 mm/0.7 mm (left/right side), 0.5 mm/0.4 mm (anterior/posterior side) and 0 mm/8.2 mm (superior/inferior side) in a single respiratory cycle (respiratory-ungated phase), and 0.5 mm/0.7 mm (left/right side), 0.4 mm/0 mm (anterior/posterior side) and 0 mm/2.6 mm (superior/inferior side) in the 30% duty cycle around the exhalation (respiratory-gated phase). GTV-COM moved in the inferior direction, mainly due to intrafractional respiratory motion. GTV deformation due to respiration was observed, but its magnitude was not so large.

For all six patients, average COM displacement for the ungated phase relative to that at peak exhalation was 0.7 mm in both left and right directions, and 2.5 mm in the anterior, 0.1 mm in the posterior, and 8.9 mm in the inferior directions. In contrast, average COM displacement in the gated phase was minimized to 0.9 mm in the anterior and 2.6 mm in the inferior direction, and close to 0.0 mm in the other directions.

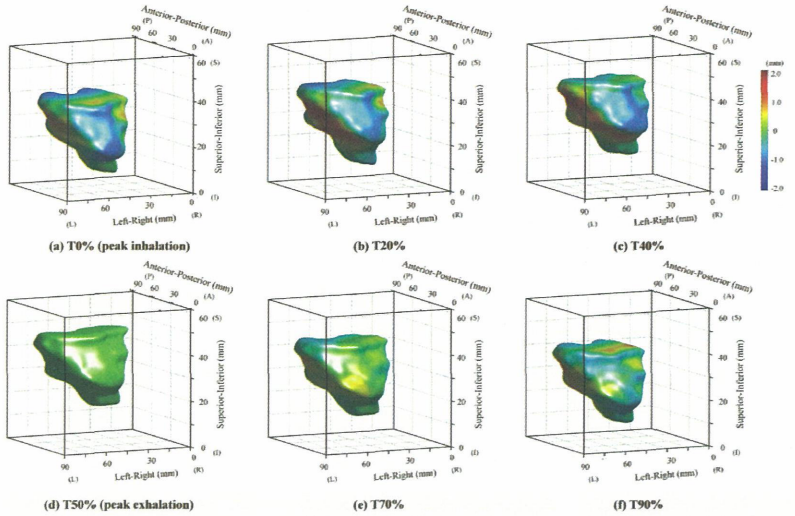

Figure 5. 3D-visualized GTV and the magnitude of geometrical variation from peak exhalation as a function of respiratory phase. (a) T0 (peak inhalation), (b) T20, (c) T40, (d) T50 (peak exhalation), (e) T70 and (f) T90.

With regard to prostate cases, twenty inpatients exhibited prostate displacement as a function of respiratory phase. Less than 1 mm of prostate COM moved in the superior, inferior and posterior directions mainly due to intrafractional respiratory motion. We have not yet compared prostate movements with and without immobilization, although these small displacements might be affected by immobilizing the patients as seen in the lung cases.

Dose Variation Due To Intrafractional Motion

Treatment planning for charged particle beams is similar in process to the planning of external photon beam treatment. A treatment plan is designed, typically employing beams from several angles; beam weights are adjusted to adequately cover the target volume while honoring the dose constraints of normal tissues. A major difference with charged particle beam therapy is the design of the compensating boli to account for range variations, with the goal of stopping the charged particle beam at the distal surface of the target from each beam direction. If intrafractional motion results in unacceptable range variations or in unacceptable irradiation of distal normal tissues, over- or under-dosing would be caused. Especially, the magnitude of over- or under-dosing could be emphasized in lung cases due to density changes by replacing between the lower density of lung and solid tumor density.

For passive beam treatment, we have already developed a design of compensating bolus by providing for stoppage of the charged particle beam at the distal edge of the clinical target volume (CTV) at each respiratory phase by taking into account intrafractional respiratory motion [2]. By doing this, the prescribed dose can be given to the targets at all respiratory phases sufficiently (no under-dose to the target), although small over-dose to the tissues could be caused when a solid tumor and tissues are moving.

We calculated two passive beam treatment strategies (conventional method and layer-stacking method [16]) by using 4DCT data sets in respiratory ungated treatment and compared the accumulated dose distributions including deformable registration. The layer-stacking method may be positioned between the conventional method and scanning method. The compensating bolus is designed to cover a 90% dose to CTVs at each respiratory phase, and then it is applied to 4DCT data sets to calculate dose distribution. The accumulated dose distribution was calculated by registering the carbon ion beam distribution at the respective phases to peak-exhalation (T50) by applying deformable registration, which calculates transformation maps that were then

applied to the contours to transform them from the other respiratory phases except peak exhalation to peak exhalation. A single beam angle of 160° was selected. For the layer-stacking method, we calculated two scenarios; synchronized with and without respiratory motion and each layer painting dose.

The carbon ion beam dose distributions by layer-stacking method minimized excessive dose to normal tissues rather than that by conventional method, but over 90% dose was given to CTV (Figs. 6a and 6b). As described above, over- and under-dosing was caused by replacing solid tumor due to respiration at each respiratory phase, but these dose variations are averaged in the accumulated dose (marked as arrows in Fig. 6). However, the dose distribution without synchronized respiratory motion and dose painting in each layer degraded the dose uniformity (Fig. 6c). This problem could be seen in the scanning method under free breathing conditions. Now we are developing 4D treatment planning for the layer-stacking and active beam methods to overcome the above problem.

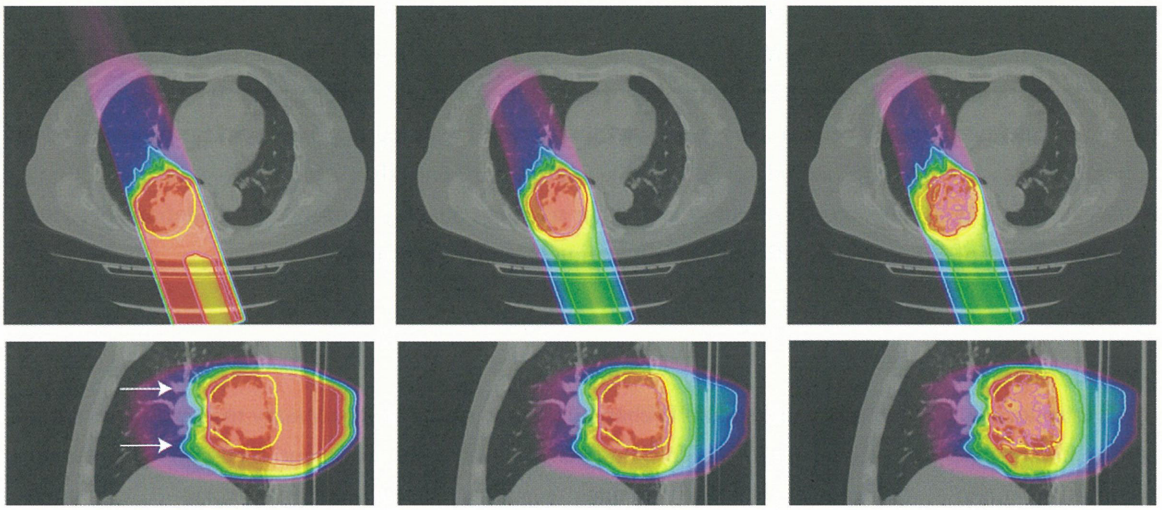

Figure 6. Accumulated carbon ion beam dose distribution with a beam angle of 160° for ungated treatment. (a) Conventional passive beam method. (b) Layer-stacking method with synchronized respiratory cycle and dose painting in each layer. (c) Layer-stacking method without synchronized respiratory cycle and dose painting in each layer. Yellow line shows CTV at peak exhalation. Pink, red, green and light blue lines are 95, 90, 50, 30 % isodose.

Other Topics

1. Real-time target monitoring

As described above, 256 multi-slice CT has the ability to overcome some of the limitations of 4DCT using conventional multi-slice CT. The problem, however, is that neither provides insights into how variable patients' breathing is during the few minutes of treatment time. Current 4DCT scans acquire only a single respiratory cycle, so that, as a result, the patient's respiratory cycle and tumor position are not reproducible for all respiratory activity during treatment. On the other hand, however, the respiratory pattern may result in inconsistencies especially in patients with irregular breathing (e.g. phase shift / drift). Phase shift induces inconsistencies between external respiratory signals and internal target movements, and their magnitudes are reported to be less than 1 second [11-13]. These inconsistencies between planning 4DCT and beam irradiation are liable to degrade treatment accuracy. One solution for minimizing these problems is to use a respiratory coaching system [17, 18]. To observe the tumor position more accurately, the respiratory pattern, which is not captured during the imaging for planning 4DCT, should be monitored. Several investigators have adopted tumor tracking using a dynamic flat panel

detector (FPD) [18-20]. Although using the FPD would be useful for determining the respiratory gated beam on time using an implanted fiducial marker, tracking errors could be caused when the implanted marker moves over the bone structure.

2. Development of 4D visualizing tools

Although investigators have reported on 4D imaging techniques to incorporate organ motion directly into radiotherapy, the uncertainty range in 4D treatment has not yet been fully explored. Widely available commercial treatment planning systems remain basically 3D in nature and output beam parameters at a specific respiratory phase only. Despite the need for quantitative information about the function of the respiratory phase, beam overshoot or undershoot dose has not been fully evaluated. A 4D range variation analysis tool (Aqualyzer) has been developed to characterize and quantify penetration of a charged particle beam during respiration[21]. Because the Aqualyzer quantifies range variation as a function of time and visualizes in beam's-eye-view (BEV) for passive beam treatment using essentially 4DCT data, Aqualyzer is useful for the rapid assessment of range variations in treatment and in determining the optimum beam angle and respiratory gating window. Also, Aqualyzer calculates the 4D carbon ion beam dose distribution including the time axis. Software-based 4D dose evaluation takes a long time, including deformable registration, and also, especially, scanning 4D calculation should consider a dual time axis (respiratory and beam scanning phases). Improving calculation speed will allow faster assessment of 4D dose, and GPU-based calculation is being integrated.

Conclusions

We introduced the NIRS approaches to a 4D charged particle study. It is necessary to quantify uncertainties for each treatment planning process and provide solutions for increasing treatment accuracy. At present, we are investigating and developing carbon beam scanning treatment including the time axis (intrafractional/interfractional), although there are still many problems that need to be resolved for its clinical application. We are convinced, however, that our approach to moving targets in charged particle therapy will be a decisive factor in overcoming these problems and in improving treatment using the scanning irradiation method.

References

[1] Mori S, Chen GT, Endo M. Effects of intrafractional motion on water equivalent pathlength in respiratory-gated heavy charged particle beam radiotherapy. Int J Radiat Oncol Biol Phys 2007;69:308-317.

[2] Mori S, Wolfgang J, Lu HM, et al. Quantitative assessment of range fluctuations in charged particle lung irradiation. Int J Radiat Oncol Biol Phys 2008;70:253-261.

[3] Lattanzi J, McNeeley S, Pinover W, et al. A comparison of daily CT localization to a daily ultrasound-based system in prostate cancer. Int J Radiat Oncol Biol Phys 1999;43:719-725.

[4] Hong L, Goitein M, Bucciolini M, et al. A pencil beam algorithm for proton dose calculations. Phys Med Biol 1996;41:1305-1330.

[5] Seiler PG, Blattmann H, Kirsch S, et al. A novel tracking technique for the continuous precise measurement of tumour positions in conformal radiotherapy. Phys Med Biol 2000;45:N103-110.

[6] Roach M, 3rd, Faillace-Akazawa P, Malfatti C, et al. Prostate volumes defined by magnetic resonance imaging and computerized tomographic scans for three-dimensional conformal radiotherapy. Int J Radiat Oncol Biol Phys 1996;35:1011-1018.

[7] Britton KR, Starkschall G, Tucker SL, et al. Assessment of gross tumor volume regression and motion changes during radiotherapy for non-small-cell lung cancer as measured by four-dimensional computed tomography. Int J Radiat Oncol Biol Phys 2007.

[8] Seppenwoolde Y, Shirato H, Kitamura K, et al. Precise and real-time measurement of 3D tumor motion in lung due to breathing and heartbeat, measured during radiotherapy. Int J Radiat Oncol Biol Phys 2002;53:822-834.

[9] Chen QS, Weinhous MS, Deibel FC, et al. Fluoroscopic study of tumor motion due to breathing: facilitating precise radiation therapy for lung cancer patients. Med Phys 2001;28:1850-1856.

[10] Noda K, Furukawa T, Fujisawa T, et al. New accelerator facility for carbon-ion cancer-therapy. J Radiat Res (Tokyo) 2007;48 Suppl A:A43-54.

[11] Guckenberger M, Wilbert J, Meyer J, et al. Is a single respiratory correlated 4D-CT study sufficient for evaluation of breathing motion? Int J Radiat Oncol Biol Phys 2007;67:1352-1359.

[12] Tsunashima Y, Sakae T, Shioyama Y, et al. Correlation between the respiratory waveform measured using a respiratory sensor and 3D tumor motion in gated radiotherapy. Int J Radiat Oncol Biol Phys 2004;60:951-958.

[13] Korreman SS, Juhler-Nottrup T, Boyer AL. Respiratory gated beam delivery cannot facilitate margin reduction, unless combined with respiratory correlated image guidance. Radiother Oncol 2007.

[14] Endo M, Mori S, Tsunoo T, et al. Development and performance evaluation of the first model of 4D CT-scanner. IEEE Trans. Nucl. Sci 2003;50:1667-1671.

[15] Mori S, Baba M, Yashiro T, et al. Volumetric cine imaging for four-dimensional radiation therapy planning using the second model of the 256-detector row CT-scanner: Initial experience in lung cancer. Euro J Radiol 2006;57:71-73.

[16] Kanematsu N, Endo M, Futami Y, et al. Treatment planning for the layer-stacking irradiation system for three-dimensional conformal heavy-ion radiotherapy. Med Phys 2002;29:2823-2829.

[17] George R, Chung TD, Vedam SS, et al. Audio-visual biofeedback for respiratory-gated radiotherapy: impact of audio instruction and audio-visual biofeedback on respiratory-gated radiotherapy. Int J Radiat Oncol Biol Phys 2006;65:924-933.

[18] Neicu T, Berbeco R, Wolfgang J, et al. Synchronized moving aperture radiation therapy (SMART): improvement of breathing pattern reproducibility using respiratory coaching. Phys Med Biol 2006;51:617-636.

[19] Sharp GC, Lu HM, Trofimov A, et al. Assessing residual motion for gated proton-beam radiotherapy. J Radiat Res (Tokyo) 2007;48 Suppl A:A55-59.

[20] Murphy MJ. Tracking moving organs in real time. Semin Radiat Oncol 2004;14:91-100.

[21] Mori S, Chen GT. Quantification and visualization of charged particle range variations. Int J Radiat Oncol Biol Phys 2008;72:268-277.

Carbon Therapy Facility at Gunma University Heavy-ion Medical Center

Satoru Yamada, Ken Yusa, Mutsumi Tashiro and Kota Torikai

Heavy-ion Medical Center, Gunma University, Maebashi, Japan
e-mail address: satoru@showa.gunma-u.ac.jp

Abstract

A new carbon therapy facility is under construction at Gunma-University Heavy-Ion Medial Center, GHMC. The main accelerator is a slow-cycling synchrotron with an average diameter of around 20 m, and it accelerates carbon ions up to an energy range from 140 to 400 MeV per nucleon. We have four treatment rooms in the new facility, three of which will have a fixed horizontal beam line, both fixed horizontal and fixed vertical beam lines, and a fixed vertical beam line, respectively. The fourth room will be used for developmental studies for advanced irradiation techniques. The number of patients treated in the facility is expected to be around 800 per year. The design details of the facility are based on design and R&D studies performed at the National Institute of Radiological Sciences. Construction will be completed by the end of FY2008, and beam tests are scheduled for 2009.

1. Introduction

In Japan, more than 300,000 patients succumb to cancer every year, with the number increasing rapidly year by year. Protecting the public against the spread of cancer is of the highest priority. The National Institute of Radiological Sciences (NIRS) decided to construct a high-energy heavy ion therapy facility, HIMAC [1], for this purpose. Clinical trials were initiated with carbon beams in 1994. Accumulating the clinical results of more than 4,000 patients, it has been made clear that carbon therapy is greatly effective in the fight against human cancers [2]. High construction and operation costs of a therapy facility, however, are the big obstacles in the growth of carbon therapy. Design and R&D studies have been carried out at NIRS to obtain a cost-effective design for such a therapy facility. Gunma University has been collaborating with these studies since 2004. A new facility under construction at Maebashi will be the first demonstration facility of these developmental studies.

In the design process, the following are considered to be important. Only high-energy carbon ions will be used in the facility to reduce the size and cost of the apparatus. Beam characteristics should cover the clinical beam characteristics of HIMAC. Our final goal is to establish a cost-effective design of a carbon therapy facility in a hospital environment.

Our project is financially supported by the Japanese Government and local governments of Gunma Prefecture, Maebashi City, Takasaki City, and many other cities in Gunma Prefecture.

2. Major specifications of the facility

Major specifications of the facility were determined on the basis of the statistics of clinical treatments at HIMAC. It was decided to accelerate only carbon ions in the new therapy facility, with a maximum energy established at 400 MeV/u. This energy ensures a 25-cm residual range in water and, for example, carbon ions

can penetrate a human body and reach the prostate through a patient's pelvis. Another important requirement of the new facility is to have two orthogonal beam lines directed toward the same isocenter. This beam line configuration is required in order to realize sequential beam irradiation from different directions with single positioning of a patient. A fast beam course and energy switching are also required for the same purpose. The major specifications of the facility are summarized in Table 1. The layout of the new facility is shown in Fig.1. The main building of the facility is about 65 m × 45 m, completed at the end of October 2008. An outside view of the new building is shown in Fig. 2.

Table 1. Major specifications of the therapy facility

Items	Contents
Ion Species	Carbon ions only
Range	25 cm max. in water (400 MeV/u)
Field Size	15 cm × 15 cm max.
Dose Rate	5 GyE/min. (1.2×10^9 pps)
Treatment Rooms	3 (H, V, H&V)
	No rotational gantries
Fourth Room	Prepared for future developments
Irradiation Techniques	Respiration Gated
	Single & Spiral Wobbling Methods
	Layer-Stacking Method

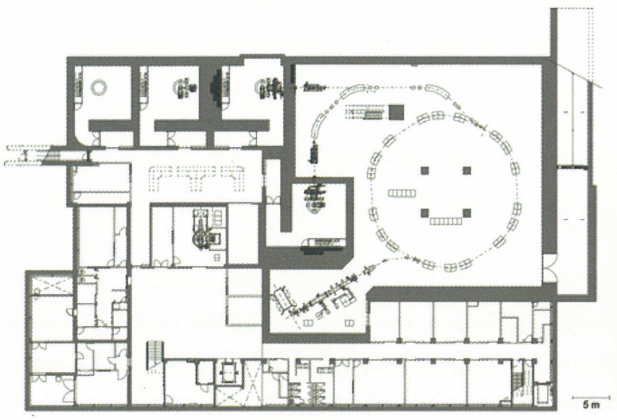

Fig.1 Plan view of the facility.

Fig. 2. Outside view of the facility

3. Accelerator system

The accelerator of the facility consists of an Electron Cyclotron Resonance (ECR) type ion source, a Radio-Frequency Quadrupole (RFQ) linac, an Interdigital-H (IH) linac with Alternating Phase Focusing (APF) structure and a synchrotron ring followed by a high-energy beam transport system. C^{4+} ions will be produced by the ECR source and pass through a thin carbon foil installed downstream of the IH linac. An output energy of the linac is determined at 4 MeV/u so that more than 90% of C^{4+} ions are converted to fully stripped ions. An averaged diameter of the synchrotron is about 20 m and will accelerate C^{6+} ions up to 400 MeV/u.

3.1. Ion source

In the ECR source, permanent magnets are adopted to generate magnetic fields both for sexta-pole and mirror fields [3], [4]. Based on experimental studies with a conventional 10 GHz ECR source at HIMAC, the field distribution of the mirror magnet is designed so that a charge distribution of carbon ions is optimized at 4+. A

microwave source with traveling wave-type power tube was adopted, with a frequency range and maximum power of 9.75 – 10.25 GHz and 650 W, respectively. By tuning the microwave frequency, power level and bias disc potential, we obtained more than 300 e μ A C^{4+} ions stably at an extraction voltage of 30 kV. The normalized beam emittance was about 1 π mm·mrad as expected. An example of charge spectra is shown in Fig. 3. A photograph of the ECR source in the new facility is shown in Fig. 4.

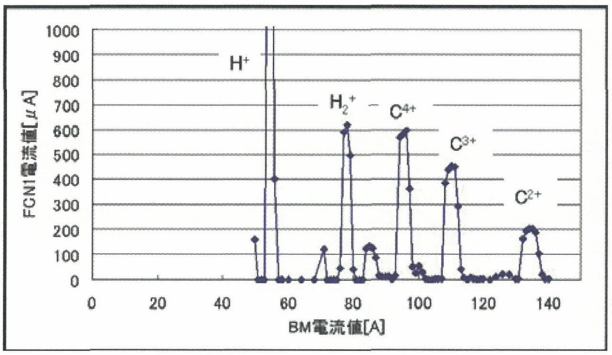

Fig.3. An example of charge spectra

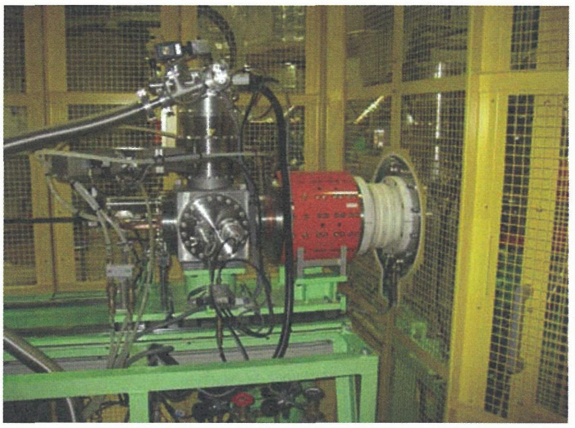

Fig. 4. ECR source installed at the new facility

3.2. Linac system

A linac system is composed of a conventional four-vane type RFQ linac and an interdigital-H type linac with alternating-phase focusing (APF) structure [5], [6]. The RFQ accelerates carbon ions from 10 to 600 keV/u, and the output energy of the APF-IH linac is 4 MeV/u. Since both linacs need no extra focusing element in the linac cavities, the tuning procedure of the linac system is very simple and easy. The operation frequency is chosen to be 200 MHz, and the cavity diameter is about 35 cm for both linacs. Cavity lengths are 2.4 m for RFQ and 3.4 m for IH. The estimated rf power is about 100 kW for RFQ and 400 kW for IH. The peak surface field in the cavity is kept at a rather low value of 23.6 MV/m (1.6 Kilpatrick) to avoid sparking problems. A 50 μg/cm^2 thick carbon foil stripper is installed at the output of the IH linac. A stripping efficiency of C^{4+} to C^{6+} was estimated to be better than 90% [7].

In the design process of the APF-IH linac, a three-dimensional field calculation code, Microwave Studio, was very powerful for obtaining resonant frequency, gap voltage distribution, etc. Only one model cavity was made to check the validity of the computer code before constructing a full-scale model at NIRS. With the full-scale model, beam tests have been performed at NIRS, and the measured values of energy, energy spread, and beam emittance of the accelerated beam reproduced the design values quite accurately. The transmission efficiency through the linac system was also good, as expected.

The injector linac in the new building is shown in Fig. 5, together with the ECR source on the right. Major specifications of the linacs are listed in Table 2.

Table 2. Specifications of the linac system

Items	RFQ	APF-IH
q/A	1/3	1/3
Frequency, MHz	200	200
Input/Output Energy, MeV/u	0.01/0.6	0.6/4.0
Inside Diameter of Tank, cm	~ 35	~ 35
Tank Length, m	2.4	3.4
Max. Surface Field, MV/m	23.6 (1.6 Kilp.)	23.6 (1.6 Kilp.)
RF Power	~ 100	~ 400

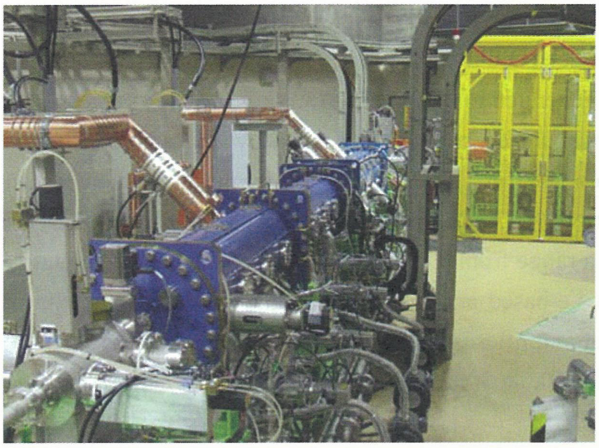

Fig. 5. Injector in the new facility

Fig. 6. Synchrotron ring under construction

3.3. Synchrotron

The synchrotron has a conventional FODO type lattice structure and accelerates fully stripped carbon ions from 4 up to 400 MeV/u [8], [9]. The circumference of the ring is 63.3 m and the average diameter is about 20 m. The bending field changes from 0.13 to 1.48 T. There are 18 bending magnets in the ring, each of which is about 6 t, making the total weight over 100 t.

Horizontal and vertical tunes are designed to vary from (1.775, 1.198) to (1.73, 1.218) and (1.68, 1.235) at injection, acceleration and extraction stages, respectively. The momentum compaction factor is around 0.33, and errors in the bending field may affect rather strongly the beam orbit in the ring. The drift of the bending field should be less than 5×10^{-4} at the flat top. The tune spread due to space charge effects is estimated to be around -0.07 in the vertical direction at injection.

Table 3. Major specifications of the synchrotron

Items	Contents
Ion Species	C^{6+}
Injection Energy	4 MeV/u
Extraction Energy	140 ~ 400 MeV/u
Beam Current	1.3×10^9 pps max.
Repetition	1/3 Hz, typical
Circumference	63.3 m
Bending Field	0.13 ~ 1.48 T
Acceptance	
Momentum	± 0.3%
Horizontal/Vertical	250/26 π mm·mrad
Injection Method	Multiturn
Extraction Method	Slow, 1/3 resonance
RF System	
Frequency Range	0.87 ~ 6.77
Harmonic Number	2
Acceleration Voltage	2 kV max.
Estimated Power	~ 7 kW

A typical excitation pattern of the synchrotron field is the flat base, smoothing, flat top and total period of 0.05, 0.05, 1.6 and 3.0 sec., respectively. The value of dB/dt is designed to be 2.148 T/s. Ions not extracted during the flat top will be decelerated to reduce unwanted radiation generated in the synchrotron ring.

The injection and extraction methods are conventional multiturn injection and slow extraction using 1/3 resonance, respectively. Acceptances of the synchrotron ring are 26 and 250 π mm·mrad for vertical and horizontal directions. During 25 turns of multiturn injection of 57.1 μs, 5.1×10^9 carbon ions will be injected in the synchrotron ring. Acceleration rf frequency varies in a range from 0.88 to 6.77 MHz with a harmonic number of two. A single-gap acceleration cavity is loaded with Fe-based amorphous cores and generates a maximum voltage of 2 kV. The maximum output power of the power amplifier is 8 kW.

The major specifications of the synchrotron are listed in Table 3, and a photograph of the synchrotron ring is shown in Fig. 6.

4. Beam delivery system

The wobbler method was adopted for our beam delivery system based on more than 10 years experience at HIMAC. In order to improve the beam efficiency in a large irradiation field size, we adopted a spiral wobbler technique [10]. By single wobbler technique, the beam size is required to satisfy a definite relation with the radius of the circular wobbling orbit at an isocenter. In the spiral wobbling scheme, however, the amplitude of AC currents of the wobbler magnets is modulated properly, and the beam spot size can be much smaller than that of a simple wobbling scheme. It takes less than 1 sec. to form uniform dose distribution when the frequency of the wobbler field and amplitude modulation are 80 and 30 Hz, respectively. In Fig. 7, the principle of the spiral wobbler method is shown schematically in comparison with the single wobbler method.

The distance between the iso-center and the final beam transport element of the bending magnet was chosen to be 9 m. We can make a maximum 15 cm × 15 cm irradiation field with a dose distribution error better than ±2.5%.

The layer-stacking irradiation technique developed at NIRS [11] will be adopted. This technique is considered to be effective for reducing an unwanted high-dose area in front of the target by controlling precisely the multilieaf collimator during stacking irradiation.

A horizontal beam delivery system is installed in treatment rooms A and B, whereas a vertical system is installed in rooms B and C. Treatment room D is empty at the beginning stage, and a scanning irradiation technique with a sharp pencil beam will be developed in this room.

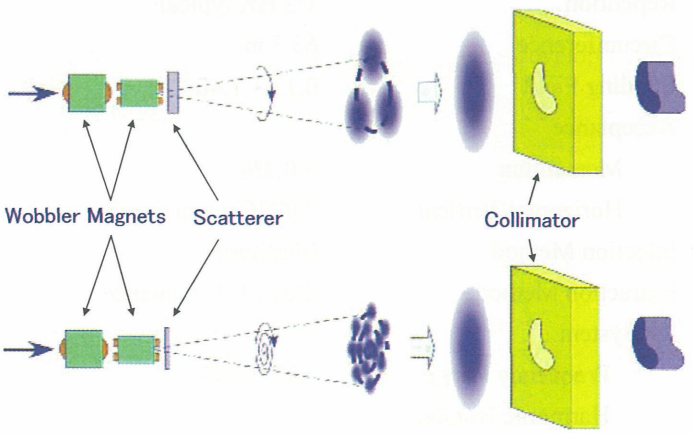

Fig. 7. Single wobbler method (top), and spiral wobbler method (bottom)

5. Construction schedule

Construction of our facility started in February 2007. After completion of the new building, major apparatuses have been installed in the building until the end of 2008. Beam tests started with the ECR source, and high power tests of the injector linacs have also been initiated. Beam tests of the whole accelerator system will be carried out during the coming autumn. The first treatment of a patient is scheduled in March 2010. By 2017, we expect the total number of treatments to reach its final level of 800 per year.

6. Acknowledgements

Design and R&D studies have been performed under the strong initiative of the HIMAC group at NIRS. The authors give their sincere thanks to Drs. T. Kanai, K. Noda and other members of the HIMAC group.

References

[1] Y. Hirao, et al. Heavy Ion Synchrotron for Medical Use – HIMAC project at NIRS, Japan, Nucl. Phys. A538, 541c, 1992.

[2] H. Tsujii, J. Mizoe, T. Kamada, et al. Clinical Results of Carbon Ion Radiotherapy at NIRS, J. Radiat. Res., 48, A1, 2007.

[3] M. Muramatsu, A. Kitagawa, Y. Sakamoto, et al. Compact ECR ion source with permanent magnets for carbon therapy. Rev. Sci. Instr., 75(5), 1925, 2004.

[4] M. Muramatsu, A. Kitagawa, S. Sato, et al., Development of a compact electron-cyclotron-resonance ion source for high-energy carbon-ion therapy, Rev. Sci. Instr. 76, 113304, 2005.

[5] Y. Iwata, S. Yamada, T. Murakami, et al. Nucl. Instr. & Meth. in Phys. Res., A569, 685, 2006.

[6] Y. Iwata, S. Yamada, T. Murakami, et al. Performance of a compact injector for heavy ion medical accelerator, Nucl. Instr. & Meth. in Phys. Res., A572, 1007, 2007.

[7] Y. Sato, T. Miyoshi, T. Muramatsu, et al., Penetration of 4.3 and 6.0 MeV/u highly charged heavy ions through carbon foils, Nucl. Instr. & Meth. in Phys. Res., B225, 439, 2004.

[8] K. Noda, K., T. Furukawa, Y. Iwata, et al. Design of carbon therapy facility based on 10 years experience at HIMAC, Nucl. Instr. & Meth. in Phys. Res., A562, 1038, 2006.

[9] K. Noda, T. Furukawa, T. Fujisawa, et al. New Accelerator Facility for Carbon-Ion Cancer-Therapy, J. Rad. Res., 48, Suppl. A, A43, 2007.

[10] M. Komori, T. Furukawa, T. Kanai and K. Noda, Optimization of Spiral-Wobbler System for Heavy-Ion Radiotherapy, Jpn. J. Appl. Phys. 43, 6463, 2004.

[11] T. Kanai, et al. Commissioning of a conformal irradiation system for heavy-ion radiotherapy using a layer-stacking method, Med. Phys. 33, 2989, 2006.

NIRS

National Institute of Radiological Sciences
Education and International Cooperation Section
4-9-1 Anagawa, Inage-ku, Chiba 263-8555, Japan
e-mail: kokusai@nirs.go.jp
Tel: +81-43-206-3025
Fax: +81-43-206-4061

GCS ETOILE

Centre national d' Hadronthérapie par ions Carbone
60, avenue Rockefeller, 69008 - Lyon, France
e-mail: comm@centre-etoile.org
Tel : 33 (0) 4 72 78 89 20
Fax : 33 (0) 4 78 76 06 43

Scientific Secretariat